FTL **FLEET TECHNOLOGY LIMITED**

92-01260/

MATERIALS TECHNOLOGY CENTRE 3728C.FR

STUDY OF WIDE PLATE TESTING OF STRUCTURAL STEELS FOR ARCTIC SHIPS

Final Report

By

L. Malik, B.A. Graville, M. Tomin and S.R. Bala

VOLUME I: MAIN REPORT

Work on the project was conducted under the auspices
of the Canada Centre for Mineral and Metallurgical Technology,
Canadian Coast Guard (Northern) and Panel for Energy R and D (PERD).

DSS Contract Serial No. : 23440-9-9014/01-SQ

DSS File No. : 003SQ-23440-9-9014

CANMET Project No. : 9-9014

Scientific Authority : Dr. W.R. Tyson

MICROMEDIA
51pp

Date: May 1991

TEAM

The work described in this report and its appendices was performed by a team comprising the following principals:

L. Malik	Fleet Technology Limited
B. A. Graville	Graville Associates Inc.
S.R. Bala	Welding Institute of Canada
M. Tomin	Reltec Advisory Services Inc.

During the course of the investigation, numerous useful discussions were held with Dr. W. Tyson (Metals Technology Laboratories) and Mr. John McCallum (previously at Canadian Coast Guard-Northern), and the authors are grateful for the same.

The experimental assistance of other staff at Fleet Technology Limited and the Welding Institute of Canada is also acknowledged.

EXECUTIVE SUMMARY

The toughness specifications for structural steels for ship construction have been evolving over the last forty years. The impetus for this comes from occasional but well publicized ship failures, as well as from developments in material fracture toughness assessment and in strategies for fracture control in welded structures. With prospects of increasing navigation in the Canadian Arctic, the potential for environmental damage in case of a serious failure, remote location and colder temperatures, Canadian Coast Guard has the mandate to develop design standards and steel specifications that would render such an event highly unlikely. Consequently, the Canadian Coast Guard, in conjunction with the marine industry, has over the last decade or so, developed the Canadian Arctic Safety and Pollution Prevention Regulations (CASPPR), of which the steel toughness specifications are an integral part.

The CASPPR specifications for minimum steel toughness were derived from the NKK approach which was developed in the late seventies, for ocean going vessels (design temperature 0°C), and which is consistent with the toughness requirements in various Classification Society Rules. The basis of the NKK approach is to prevent brittle fracture initiation from an ≈250mm long crack in the steel, and toughness requirements are derived from quasistatic fracture mechanics tests and their empirical correlation with the commonly specified Charpy Vee Notch toughness.

The primary objective of the investigation reported here and an earlier comparison study has been to provide verification for the minimum steel toughness requirements specified in CASPPR. The latter involved fracture toughness assessment of several steels at a more realistic intermediate loading rate, using relatively small specimens, and its correlation with conventional test (Charpy, Pellini's drop weight) results. In the current program, larger scale wide plate tests were conducted to verify the NKK fracture toughness - Charpy toughness correlation and to assess the validity of the more recently developed failure analysis diagram for assessing fracture toughness requirement in the elastic plastic regime.

The wide plate and smaller scale fracture toughness results indicated that they are consistent with the NKK correlation, and that the failure analysis diagram provided a conservative assessment of flaws or fracture toughness requirements. On the basis of this evidence, it is concluded that the toughness specifications in CASPPR are reasonable and adequate.

It should be added that in very recent years, it has been considered desirable for fracture control plans to incorporate 'short crack arrest' capability in the base material as well. At present, it is not an explicit criterion in CASPPR or any other Classification Society Rules. A series of short crack arrest tests, on base material and heat affected zone, have also been conducted in this program and results obtained suggest that the next step in the evolution of toughness requirements in CASPPR and International Classification Society Rules should take the short crack arrest capability aspects into consideration.

SOMMAIRE

Les spécifications de la ténacité pour les aciers pour la construction des navires a beaucoup évolué au cours des dernières quarante années. Le changement des spécifications est du à la publicité produite lorsque des navire font défaillances, aux développements de la mesure de la résistance à la rupture et aux stratégies pour le contrôle de rupture pour des structure soudées. Une augmentation du nombre de navires circulant dans l'Arctique Canadien est prévue. Le potentiel existe d' endommager l'environnement par une rupture sérieuse dans un endroit isolé et à température froide. La Garde Côtière Canadienne a pour but d'établir des standards de calcul et des spécifications d'acier qui rendraient la probabilité d'un tel évènement minime. La Garde Côtière Canadienne, alliée avec l'industrie marine a développé au cours des derniers dix ans le Règlement sur la prévention de la pollution des eaux arctiques par les navire (RPPEAN). Ce document contient en part les spécifications pour la ténacité de l'acier.

Les spécifications incluses dans RPPEAN pour la ténacité minimal de l'acier, furent dérivées en utilisant l'approche NKK qui fut développée vers la fin des années soixante-dix pour des navires océaniques (température de conception 0° C), et qui sont en accord avec les exigences requises par diverses Sociétés de Classification Réglementaire. La base de l'approche NKK est la prévention de l'initiation d'une rupture fragile d'une fissure de longueur ≈ 250mm dans l'acier. Les exigences de la ténacité furent dérivées de tests de rupture mécanique quasistatique et leur corrélation empirique communément spécifiée par des essais de résilience.

L'objet primaire de cette investigation et des études précédentes fut de vérifier les valeurs de ténacités minimales de l'acier spécifiées par RPPEAN. Les études précédentes avaient recours à l'évaluation de la ténacité de rupture de plusieurs aciers à une vitesse de sollicitation intermédiaire plus réel, utilisant des échantillons relativement petits, et leur corrélation avec les résultats de tests conventionnels (Charpy, Pellini's Drop Weight). Dans le programme tests actuels, des essais sur de larges plaques furent faits pour vérifier la corrélation entre la ténacité de rupture NKK et Charpy, et pour évaluer la validité de l'analyse de diagramme de défaillance développé pour la ténacité de rupture requise pour le régime élastique plastique.

Les résultats de la ténacité à la rupture pour de larges plaques et celles d'échelles plus petites sont en accord avec la corrélation NKK et indiquent que le diagramme d'analyse de défaillance donne une évaluation conservatrice pour les défauts ou pour la ténacité de rupture requise. Basé sur cette évidence, il est conclu que les spécifications de la ténacité dans RPPEAN sont raisonnable et adéquates.

Récemment, on a considéré d'incorporation la capacité de l'arrêt de courtes fissures dans le matériel de base pour les plans de contrôle de fissures. A présent, ce n'est pas un critère explicite dans les règlements de RPPEAN ou de n'importe quel autre Société de Classification Réglementaire. Une série de tests sur l'arrêt de courte fissure fut faite lors de ce programme. Les résultats obtenues suggèrent que la prochaine étape dans l'évolution sur les exigences de la ténacité pour RPPEAN et les Sociétés de Classification Réglementaire serait de prendre en considération les aspects de l'arrêt de court fissure.

TABLE OF CONTENTS

VOLUME I

Page

PROJECT TEAM/ACKNOWLEDGEMENTS (ii)

EXECUTIVE SUMMARY (iii)

1.0 INTRODUCTION 1

1.1 The NKK Approach 2

2.0 INVESTIGATION AND RESULTS 4

3.0 INVESTIGATION AND RESULTS 5

3.1 Test Steel and Its Characterization 5
3.2 Characterization of the Heat Affected Zone (HAZ) 5
3.3 Wide Plate Tests 6
3.4 Short Crack Arrest Tests 7

4.0 DISCUSSION AND ANALYSIS 9

4.1 Wide Plate Tests 9
4.2 Short Crack Arrest Tests 13

5.0 SIGNIFICANCE OF THE RESULTS WITH RESPECT TO CASPPR 16

6.0 CONCLUDING SUMMARY 18

7.0 REFERENCES 19

TABLES AND FIGURES

ANNEX Estimates of Crack Arrest Toughness Based on SCA Test Results

TABLE OF CONTENTS (cont'd)

VOLUME II

APPENDIX A Characterization Report

APPENDIX B Welding Institute of Canada Wide Plate Report

APPENDIX C Short Crack Arrest (SCA) Test Development and Detailed Procedures and Results

APPENDIX D Reltec Wide Plate Report

1.0 INTRODUCTION

Over the last decade or so, the Canadian Coast Guard, in discussion with the marine industry's representatives, has been engaged in developing structural steel toughness requirements for arctic class ships. These requirements were developed on the basis of arctic navigation experience and found to be consistent[1,] with the NKK approach[2] for specifying minimum steel toughness requirements for ocean-going vessels (design temperature of 0°C). Consequently, the toughness requirements formulated for the Arctic Class ships were incorporated in Canadian Arctic Safety and Pollution Prevention Regulations (CASPPR).

The underlying basis of the NKK approach is the empirical correlation between the Charpy Vee Notch (CVN) energy transition temperature of a steel and its minimum anticipated fracture toughness. The correlation was developed during the seventies, using wide plate tests containing 80mm long machined notches. In order to provide further support for the CASPPR steel toughness requirements, the main objective of the current program was to verify the wide plate fracture behaviour of a steel in relation to its CVN toughness.

The aim of the NKK approach is to prevent brittle fracture initiation from cracks which may be up to 250mm long, and have their crack tips residing in the base material. It has also been demonstrated[1,2] that steel toughness requirements so formulated would also be adequate to prevent unstable fracture initiation from short cracks that have their tip in the base material but under the influence of yield level weld tensile residual stresses.

Traditionally, the fracture control plan for ships also incorporates crack arrestors. Crack arrest approaches to fracture control are based on the assumption that crack initiation at some point ought to be assumed and that the material should have adequate toughness to arrest a fast running crack. The question arises as to what size of crack needs to be arrested which has led to various criteria for crack arrest being proposed. A "long" crack arrest criterion may be established on the basis that a brittle fracture could initiate in a plate (for example in a storage tank) and propagate completely across the plate before encountering an adjacent plate. The criterion would require the latter plate to have adequate toughness to arrest the long crack in the first plate.

Another criterion might be based on the assumption that fracture initiation could occur at a small brittle region (say, an arc strike) and cause a small 'pop-in'. The criterion would require the surrounding material to have enough toughness to arrest the pop-in at say a stress equal to the yield stress, i.e. a pop-in arrest criterion. A third criterion might assume that initiation occurs in a weld or from an attachment and a crack propagates a short distance over a region where residual stresses are high. Surrounding material would be required to have enough toughness to arrest the short crack in a region outside the residual stress zone. This 'short crack' arrest approach has been studied by Tanaka et al[3] and a test method developed to evaluate the crack arrest toughness under such conditions.

Although crack arrest is not an explicit criterion in the CASPPR regulations, it was decided to conduct a limited number of short crack arrest tests, focusing on the base material, and heat affected zone therein.

In order to provide the background data to support the larger wide plate and short crack arrest test results, several of the small scale conventional tests were also carried out.

1.1 The NKK Approach

This approach was formulated by the Japanese Classification Society NKK (Nippon Kaiji Kyokai) in 1979 and is based on wide plate (centre-notched tension) test results for ships steels[2,4].

The suitability of a steel for any particular location or structural member of the ship structure is judged in two stages. First, its minimum fracture toughness, K_c, is estimated from the CVN specification (a certain minimum number of Joules at a specified temperature). Next, it is compared to the fracture toughness requirement for that location based on design conditions (service and residual stresses, service temperature and assumed allowable crack lengths). The steps involved in calculating the minimum anticipated fracture toughness can be summarized as follows:

Step 1: Estimate an absorbed energy transition temperature T_E (°C) corresponding to 50% fibrous fracture, from minimum specified CVN absorbed energy (E_T in kg.m) at the test temperature T_t using the equation

$$E_T = \frac{1}{\sqrt{2\pi}} \int_{-\infty}^{T_t - T_E} \exp\left\{-\frac{1}{2}\left(\frac{T_t - T_E}{20}\right)^2\right\} dT_t$$

Step 2: Estimate the brittle fracture initiation temperature T_i (°C) as a function of the energy transition temperature (T_E), the steel thickness (t, mm) and yield strength (σ_y, kg mm^{-2}) as follows:

$$T_i = (0.00321\sigma_y + 0.391)(T_E + 273) + 2.74\sqrt{t} - 278.59$$

This equation had been established based on wide plate tests with a centre machined notch 80mm in length, and an applied stress of $0.5\sigma_y$.

Step 3: Estimate the fracture toughness (K_c - blunt notch in kg mm$^{-3/2}$) of the steel using the expressions:

$$K_c = K_o \exp\{-k_o/(T + 273)\}$$

where k_o = 562K (experimentally obtained material constant)

$$K_o = 0.177\sigma_y \exp\{562/(273 + T_i)\} \text{ (in kgmm}^{-3/2}\text{)}$$

Step 4: Estimate the fracture toughness (K_{cf} - fatigue sharpened notch) based on the experimentally established relationship:

$$K_{cf} = 0.68\ K_c$$

The procedures outlined above thus can be used to generate a table giving the minimum anticipated value for fracture toughness of steel plates for hull use as a function of its strength, thickness, CVN specification and temperature, and this is shown in Table 1 as reproduced from Reference 4.

For steel selection, these values need to be compared with the minimum fracture toughness needed based on the design parameters, and can be represented by the equation:

$$K_{cf(required)} = (\alpha + ß)\ \sigma_y\sqrt{\pi a}$$

where 2a, the maximum allowable through thickness crack length, is assumed to be 250mm (for base material); α is the design stress as a fraction of the yield strength σ_y (also called the coefficient of utilization) and ß is the magnitude of the residual (and reaction) stresses as a function of σ_y. The crack is assumed to reside in a weld longitudinal residual stress field perpendicular to the plane of the flaw; and for this situation, ß is assumed to be 0.6.

Once the thickness and coefficient of utilization are established for a structural member, it is then straight forward to calculate $K_{cf(required)}$ and then select a steel grade using the data in Table I.

2.0 OBJECTIVES

The objectives of the program, in view of the background presented in the previous section, were:

(i) to validate the structural steel toughness requirements in CASPPR Schedule 3 from the point of view of resistance to brittle fracture initiation from long fatigue cracks;

(ii) to develop short crack arrest testing capability, and to establish the stress/temperature transition for arrest of short running cracks. Since the test is a go/no go type of test with each result being classified as fracture or arrest, the arrest transition must be determined by bracketing using multiple specimens.

3.0 INVESTIGATION AND RESULTS

3.1 Test Steel and Its Characterization

The base material procured for the program was a 25mm thick, control rolled steel. Its detailed characterization is reported in Appendix A. Based on the steel processing route, its chemistry, tensile and Charpy vee notch properties (at various temperatures), the steel is closest to ABS Grade DH36. The actual steel properties and the minimum grade requirements are reported in Table II.

The crack tip opening displacement (CTOD) toughness of the steel was determined following the British Standard 5762-79, using both .15mm wide saw notches (representing the notches in the wide plate tests) and fatigue precracks according to the conventional practice. The data at the four test temperatures for the wide plate tests are summarized in Table III.

The table also includes the square root of the ratio of average CTOD values obtained using the two notches, and represents the fracture toughness ratio, when it is expressed in terms of K_c (MPa√m or equivalent units). The ratio is seen to be 0.73 to 0.94, whereas the NKK work uses a value of 0.68. It is conceivable that in the Japanese wide plate tests, the notches were significantly more 'blunt' than the 0.15mm wide saw notch used in the present investigation.

From the point of view of crack arrest toughness of the steel, Compact Crack Arrest (CCA) tests as per ASTM E1221 were carried out at various temperatures (the fracture path in all specimens was perpendicular to the rolling direction), and the results obtained are shown in Figure 1. At -20°C, which is slightly below the steels' NDT temperature, the plain strain compact crack arrest toughness is seen to be about 60 MPa√m or greater. However, it should be noted that in a companion study[5] wherein the CCA behaviour of several steels was examined, the lower bound value at the NDT temperature was 46 MPa√m.

3.2 Characterization of the Heat Affected Zone (HAZ)

Welds for HAZ characterization and for HAZ short crack arrests were made, transverse to the rolling direction, using the submerged arc welding process. The 25mm thick plate was welded in two passes using heat input of ≈5 kJ/mm, typical of shipyard practice. The heat affected zone obtained was reasonably straight as seen in a typical cross-section of the weld shown in Figure 2.

The heat affected zone was characterized in terms of its NDT temperature (ASTM E208) and its compact crack arrest toughness (ASTM E1221). While detailed procedures and results are included in Appendix A, it is sufficient to note that the profile of the notch in the brittle bead had to be changed from square bottom to a vee shape in order to get the fractures in the HAZ in the NDT specimens. The NDT temperature was thus determined to be -15°C, which is similar to the -10°C to -15°C obtained for the base material.

The compact crack arrest tests for the HAZ were carried out at 0°C, -20°C or -40°C, however none of the 19 specimens tested satisfied all the validity requirements of ASTM E1221. The most frequent cause was insufficient crack jump at the initiation event; some specimens also showed tunnelling and/or crack deviation into the base material. In four specimens, the crack followed the HAZ all the way; unfortunately, the remaining unfractured ligament was smaller than the minimum requirements. All the same, it is believed that results from these four specimens represent the upper bound compact crack arrest toughness of the HAZ examined. These four data points are plotted in Figure 3, and it is estimated from these that at the NDT temperature, the compact crack arrest toughness of the HAZ is 57 MPa√m at most.

3.3 Wide Plate Tests

Four wide plate tests were conducted, using the 4000 ton test rig at the Welding Institute of Canada. Each specimen was nominally 945mm wide, and contained an approximately 250mm long crack at its centre. The cracks, introduced by a power saw and then extended to the final length using .15mm thick saw blade, were transverse to the rolling direction and the loading axis.

Each test was instrumented with thermocouples, twelve strain gauges, and six clip gauges in order to provide data regarding the fracture stresses and crack tip opening displacements.

While the thermocouple and strain gauge locations were the same for all four tests, those for the clip gauges changed. In test 1 (at -75°C), it was intended to obtain CTOD values by triangulation and so none of the clip gauges was placed at the crack tips. In fact, two of the clip gauges were located at or close to the mid-crack length. In the subsequent tests, two (test 2 at -40°C) to four (tests 3 and 4 at -20°C and -55°C respectively) clip gauges were placed at the crack tip, and the remaining ones for triangulation were no more than 50mm from the crack tip.

From the point of view of analysis of wide plate tests, the relevant results are summarized in Table IV. It should be noted that the gross fracture stress was calculated from both the jack pressure and the strain gauge readings, and there was some discrepancy (of the order of 5%) between the two, the former being higher. Detailed experimental results are included in Appendix B, however, in the following discussion, the gross fracture stress values used are based on the jack pressure.

The increase in measured (average) CTOD with applied stress in the four wide plate tests is shown in Figure 4.

3.4 Short Crack Arrest Tests

In the present work, the design by Tanaka[3] could not be used directly because of space limitations in the WIC wide plate testing rig. Considerable development was therefore needed during the test program and details of this are reported separately in Appendix C. The test essentially involved a ≈1200mm X 500mm plate, with rolling direction and loading axis being perpendicular to the 1200mm dimension. For HAZ testing, the welds were parallel to the 500mm dimension. A small, compact tension type of crack starter plate, made from a brittle steel (AISI 1040 or 1060 steel) is welded onto the test steel using hard, brittle weld deposit. When the crack starter plate is loaded independently using a jack, a brittle, fast running crack is injected into the test plate, and depending on the test temperature and stress applied to the test plate, the injected crack may be arrested or propagate all the way and fracture the plate.

The overall program provided for only six short crack arrest tests on parent metal and six for the heat affected zone. Because of this rather limited number of tests, a coarse bracketing procedure was necessary to define the position of the crack arrest transition. To define the position unambiguously, a minimum of four valid results would be required for parent material and four for heat affected zone. A review of other work on short crack arrest methods also suggested that a coarse bracketing technique was needed. A temperature bracket of 20°C was therefore selected with a view to obtaining a fracture and an arrest at temperatures 20°C apart at each of two stress levels. The temperatures were selected by reference to the Nil Ductility Transition Temperature (NDTT) as determined from drop weight testing (-15 to -10°C for the base metal and -15°C for the HAZ). The likely position of the arrest transition was estimated from reference to the Pellini diagram and to other short crack arrest results in the literature.

The two stress levels selected were the minimum specified yield strength of the material (350 MPa) and 75% of this (263 MPa). Lower values than this were not considered to be likely to lead to fractures since evidence from other published short crack arrest results suggested stresses over 200 MPa were needed to sustain propagation from the crack starter. Since the measured (upper) yield of the plate was 401 MPa at room temperature, the stress levels planned corresponded to 87% and 65% of actual yield respectively.

Based on this information, a decision tree for conducting the tests was drawn up and is shown in Figure 5. In practice, a number of difficulties were experienced with the crack starter and this planned sequence could not be followed completely. Nevertheless, the results obtained did suggest that the test conditions initially selected correctly bracketed the arrest transition.

Readings from strain gauges mounted on the test plates were used to determine the actual holding stresses. These were somewhat below the planned levels, particularly at the higher level. The actual values are used in all subsequent analyses.

For base metal tests, complete fractures were obtained in two tests, one at -15°C for the lower stress (262 MPa) and one at +5°C for the upper stress (311 MPa). At -15°C, the fracture was brittle with typical chevron markings and small shear lips of about 1mm width on each side. At +5°C, the fracture was again brittle with slightly larger shear lips being 2-3mm on one side and about 1mm on the other side. The central section of the fracture was brittle with typical chevron markings and the full section of the specimen fractured. This result confirmed the adequacy of the overall design of the test since no arrests took place at a point beyond the grooved section. Thus once the crack had extended beyond this point, there was sufficient energy to ensure complete fracture of the test plate.

For the heat affected zone tests, similar results were obtained with two specimens showing complete fracture, one at -15°C (246 MPa) and the other at +5°C (322 MPa). Again the fractures were brittle with no obvious shear lips at either temperature. Most of the fracture followed the heat affected zone emerging at the toe of the weld. The results confirmed that the welding procedure and placement of crack starter were successful in allowing the crack to run in the HAZ along the length of the weld.

None of the other tests showed fracture of the ligament region and therefore no tests showing crack arrest at the end of the grooved region were obtained. Some of the remaining tests showed divergence of the crack in the starter plate and a full discussion of the problems associated with crack starting is given in Appendix C. For base metal tests, two tests showed straight cracks in the starter plate which arrested on entering the test plate. These are considered valid tests although fracture of the ligament did not occur. In the heat affected zone tests, three tests showed arrest of the starter crack on entering the test plate. In test 9, a large brittle weld had been placed at the base of the crack starter plate and arrest occurred here. It is possible that the heat affected zone of the attachment weld contributed to arrest in these tests but the drop weight data and the two tests that fractured suggest that the heat affected zone had very similar properties to the parent plate.

Thus the arrest of the starter crack on entering the plate is representative of arrest by the parent material. It is concluded therefore that these tests are valid arrests controlled by parent material toughness and therefore can be used in conjunction with the fractured test results to bracket the arrest transition. A summary of the results is given in Table V. Since the grooved ligament region did not fracture in the arrest tests, the transition established does not correspond to a crack arrest of a 120mm crack but something somewhat smaller.

4.0 ANALYSIS AND DISCUSSION

4.1 Wide Plate Tests

As mentioned before, one of the objectives of the small scale quasistatic CTOD, and the larger scale wide plate tests was to verify the minimum anticipated fracture toughness of the steel, derived from the NKK approach. The latter (for sharp, fatigue like cracks) is plotted in Figure 6 against the reciprocal of the test temperature (in °K) for grades DH36 and EH36. These particular grades are selected since the test steel in the project is closest to grade DH36, and since the actual CVN toughness of the test steel meets the grade EH36 requirements.

The actual fracture toughness of the steel may be computed from CTOD values (fatigue sharpened specimens) or the wide plate test results. The CTOD value, δ, and fracture toughness, K, are related by the following expression:

$$K = \sqrt{m \cdot \sigma_y \cdot E \cdot \delta} \qquad (1)$$

where σ_y is the yield strength, E is Young's modulus and m is a constant. At the four test temperatures for the wide plate tests, the steel showed brittle plain strain behaviour and for such situations, the constant m in Equation (1) above is taken to be 2.

The fracture toughness values calculated from CTOD are shown in Table VI, and also included in Figure 6, in relation to the minimum anticipated values by the NKK approach.

Similarly, the nominal fracture toughness, K_σ, may be computed from the wide plate test results, assuming linear elastic behaviour. Thus

$$K = f\left(2\frac{a}{W}\right)\sigma \cdot \sqrt{\pi a} \qquad (2)$$

where 2a = through thickness crack length
W = plate width
f(2a/W) = finite plate width correction = 1.046 for the wide plate dimension used.
σ = gross fracture stress

The fracture toughness values so calculated are shown in Table VII, and are once again shown in Figure 6 in relation to the minimum expected toughness based on the NKK correlations.

It is obvious that most of the data points lie within the band defined by the NKK lines for Grade DH36 and EH36 steel. Since the test steel meets the CVN requirements for EH36 grade, the NKK minimum anticipated fracture toughness would seem to be slightly non-conservative.

However, it should not be "completely" surprising that the fracture toughness values computed from CTOD are below the EH36 line since the constraint in the three point bend CTOD specimens is considerably higher than that in the wide plate tests used in Japan. This is also obvious from the fact that the CTOD values measured in the wide plate tests are substantially larger than the 3 point bend CTOD values (see Table III and IV).

Similarly, the 'linear elastic' or the nominal fracture toughness values computed from the wide plate test would indicate at first glance that the NKK line is nonconservative, especially since the wide plate tests had a relatively blunt crack tip (.15mm saw blade) and the NKK lines are for sharp cracks. However, it is apparent from the calculated 'net section stress' that in three of the wide plate tests, it exceeded the steel's yield strength at the test temperature (Figure 7), and that the fracture stress is being controlled by the plastic flow behaviour of the steel. It is likely that if the a/W ratio for the wide plate tests was smaller, then higher gross fracture stress and therefore higher nominal fracture toughness values would have been obtained.

Notwithstanding the above, the presence of net section yielding in some of the wide plate tests means that elastic-plastic fracture mechanics methodology should be employed to analyze the results. One of these is based on the strip yield model, and in the context of the wide plate program, two aspects can be investigated.

First, the calculated CTOD from collapse modified strip yield model[6] can be compared with the measured CTOD as a function of stress, in the wide plate tests[7]. The calculated CTOD, δ, is given by:

$$\delta = \frac{8 \cdot \sigma_{pc}^{2} \cdot \bar{a}}{\pi \cdot \sigma_{y} \cdot E} \ln \sec\left(\frac{\pi \sigma}{2 \sigma_{pc}}\right) \qquad (3)$$

where σ_{pc} = far field plastical collapse stress
σ_y = yield strength
$\bar{a}$ = effective crack depth
E = Young's modulus
σ = far field applied stress

The calculated CTOD values at -75°C and -20°C, for the wide plate test geometry (ignoring the finite plate width correction) are superimposed on the measured ones in Figure 8. Those at -55°C and -40°C are not shown but lie within the band defined by the calculated CTOD curves at -75°C and -20°C. Keeping in mind the normal scatter observed in experimental measurements, the calculated curve coincides reasonably well with the experiment based CTOD values for wide plate tests at -20°C, -40°C and -55°C. At -75°C, however, the measured CTOD values are considerably larger than the calculated ones. This apparent discrepancy is believed to be due to the large crack length over which the "triangulation" approach was applied for this test. The opening of the crack faces under applied stress is not linear along its length; instead it is like an arc of a circle and the application of the triangulation principle then overestimates the CTOD. If this factor is taken into account, then the average CTOD at fracture at 214 MPa would be ≈0.6mm rather than 0.827mm shown in Table IV. However, even with this correction, the CTOD value is substantially higher than that predicted by the strip yield model and the precise reason for this discrepancy is not known.

Secondly, the applicability of the failure analysis diagram for engineering critical assessment can be evaluated based on the wide plate test results. The failure analysis diagram is shown in Figure 9. The ordinate in this diagram, $\sqrt{\delta_r}$, in the absence of residual and bending stresses, is given by

$$\sqrt{\delta_r} = \sqrt{\frac{\delta_I}{\delta_{mat}}}$$

$$= \frac{\sigma\sqrt{\pi a}}{\sqrt{m \cdot \sigma_y \cdot E \cdot \delta_{mat}}} \cdot f\left(\frac{2a}{W}\right)$$

where σ is the gross fracture stress
δ_{mat} is materials' CTOD toughness

and other parameters have been defined earlier.

The abscissa in the failure assessment diagram, S_r, is given by

$$S_r = \frac{\sigma_n}{\sigma_f}$$

where σ_n is the net section stress = $\sigma(1 - 2a/W)$
and σ_f is the flow stress as defined earlier.

The calculated data points for the four wide plate tests are shown in relation to the failure assessment diagram in Figure 9, and are observed to be outside the locus defined by the assessment line, i.e. all wide plate tests failed at stresses higher than those predicted by the failure assessment diagram. One can therefore conclude that the FAD offers a viable approach for defect assessment in situations involving crack tip plasticity.

4.2 Short Crack Arrest Test

The original fracture diagram developed by Pellini[8] shows a crack arrest curve indexed to the NDTT. The crack arrest curve is intended to represent long crack arrest and was originally derived from crack arrest tests such as the Robertson and Esso test. In subsequent work[9], another crack arrest curve for very thick sections was proposed. In Figure 10, the present results are shown plotted on the fracture analysis diagram together with the original crack arrest curve using an NDTT at -15°C as the index. The bars on the points representing fracture show the uncertainty in the stress assuming the complete crack starter load contributed to the stress intensity at the end of the grooved section when the crack propagated. Both parent material and heat affected zone results are plotted in the diagram. The results confirm that the short crack arrest transition lies to the left and above the original full crack arrest curve.

In the revised Pellini diagram[9], the crack arrest transition was predicted from fracture mechanics and was a function of thickness. This is shown in Figure 11 where a straight line is drawn between the L criterion (loss of plane strain constraint) and the YC (yield) criterion for 25mm thickness. The present results corresponding to fracture lie to the left of this line although those at +5°C are very close to it. Since the upper part of the line should correspond to elastic/plastic fracture in which large shear lips should be evident, the present results at 5°C where very small shear lips occurred suggests the line is not conservative. The line, however, is made more conservative if it is shifted 5°C higher to correspond with the upper estimate of NDTT (-10°C). The position of the Pellini line is very sensitive to the exact choice of reference toughness curve, i.e. the assumed increase in plane strain toughness with temperature that is used. Pellini used a reference curve somewhat higher than the ASME reference curve and this point is discussed in more detail later. The present results do suggest that even at 20° above the NDTT (i.e. at 5°C), the toughness is not rising rapidly.

In the Tanaka crack arrest test, the ligament is supposed to crack and the arrest even occur at the end of the grooved section. Because the crack would arrest with a known length under a known stress, fracture mechanics analysis may be used to provide an estimate of K_{ca}, the crack arrest toughness. Unfortunately in the present experiments, none of the tests showed cracking through the ligament and therefore K_{ca} cannot be determined directly from the results. Nevertheless, it is possible to obtain estimates of the likely values by consideration of all the results and compatibility among them. For example, in the tests that fractured completely, it is known that the fracture toughness must have been below a specific amount for the crack to propagate beyond the end of the grooved area. Based on the behaviour of drop weight tests at the NDTT, the likely dynamic toughness at that temperature may also be determined. Furthermore, it may be assumed that the stress intensity at the tip of the crack entering the test plate from the crack starter is proportional to the applied stress on the main test specimen, since the geometry of the crack starter is roughly the same in all tests. Based on these considerations, an upper and lower limit to the possible range of toughness values has been estimated. Since identical fracture results were obtained for base metal and for HAZ, the estimates apply to both regions. Full details of the calculations are shown in Appendix E. The results of the analysis are summarized in Table VIII.

Based on the above considerations, it has also been possible to estimate the effective size of the starter crack at the point at which it entered the main test plate and where arrest took place. The depth of an equivalent edge (surface) crack was found to be in the range 9.5 to 15.1mm. This value is significantly smaller than the crack run length in the crack starter plate and confirms the difficulty of getting this crack to enter the test plate. Part of this may result from the rather short attachment weld (40mm). Since the crack driving force comes from elastic unloading of the starter plate, the short weld effectively 'shields' the main plate from this unloading. The main plate does not 'see' the full length of the starter crack but a shorter crack.

The results obtained in the program, therefore, correspond to crack arrest at a rather short crack compared to the 120mm originally intended. Nevertheless, the transfer of a running crack from a secondary plate into a main plate is a situation of practical significance since this may occur in ships and the present results are therefore of considerable interest. Indeed, the difficulty of achieving crack arrest of cracks 120mm suggests the shorter crack arrest (~20mm) may be a more useful criterion.

The values of K_{ca} for the base metal may be compared with those found by Tanaka et al, and the present results are plotted with Tanaka's data in Figure 12. The lower estimate coincides almost exactly with the ASME reference curve and the upper estimate is slightly above Tanaka's lower bound curve. Overall, the present results appear to agree quite well with the previous published results.

The results may also be compared with the values of K_{Ia} determined from compact crack arrest tests (CCA). Although some CCA tests were technically invalid, they have been included. Results are shown in Figure 13 where it is seen that CCA K_{Ia} values lie substantially above the K_{ca} values from the SCA tests. This is to be expected since the K_{ca} values were indexed to the dynamic initiation toughness (K_{Id}) at the NDTT estimated from previous equations[10]. In that previous work, it was shown that K_{Ia} (CCA data) usually lies above K_{Id}. If the K_{ca} values are indexed to K_{Ia} at the NDTT as shown in Table IX, the K_{Ia} and K_{ca} (upper estimate) values agree very closely. The conclusion is that the rate of increase of toughness above the NDTT measured in the compact crack arrest test is the same as the upper limit estimated from short crack arrest tests. It must be pointed out that values above +5°C are extrapolated values since no fractures occurred at 20°C. It is likely that the toughness at 20°C increases more rapidly than predicted because of loss of plane strain constraint but there was no direct proof.

Using the upper and lower estimates of fracture toughness, critical crack sizes for arrest may be determined as a function of stress and temperature. The calculation assumes a through crack and the results are plotted in Figures 14 and 15 for the upper and lower bound estimates of toughness. There is reasonable agreement between the curves using the upper bound toughness and those proposed in the revised Pellini diagram. This is shown again in Figure 16 with the curves for various defect sizes drawn in. In the Pellini diagram, the present results correspond to crack arrest of a surface crack about 20mm deep.

The short crack arrest tests showed that complete brittle fractures may occur at stresses below yield at temperatures well above the nil-ductility transition temperature under slow loading conditions if initiation occurs in a brittle region. Two tests at +5°C, which is 20°C above the NDTT, fractured completely at a stress about 82 to 85% of the yield strength. In contrast, the conventional wide plate tests (initiation tests) required net section stresses exceeding yield even at -55°C. Nevertheless, the results were in agreement with the original Fracture Analysis Diagram which is indexed to the NDTT determined from (dynamic) drop weight tests. But the results also suggested that the revised Pellini diagram in which the crack arrest curve is based on fracture mechanics considerations, is not conservative. The position of the crack arrest curve as determined by the Pellini method is very sensitive to the choice of plane strain toughness reference curve. Pellini[9] felt that the ASME reference curve was too conservative and therefore selected a curve with toughness increasing more rapidly with temperature.

The plane strain toughness chosen corresponds to the dynamic initiation toughness. Analysis of data in the literature[10] has shown that dynamic toughness can be related to dynamic yield strength and temperature over a wide range of temperatures extending well above NDTT. Using the best fit line to this data, rather than Pellini's reference curve, the crack arrest line has been determined using Pellini's method. This is shown in Figure 17 together with the original. It is clear that the change of reference toughness curve has resulted in a very large shift of the estimated crack arrest curve, well beyond the position in the original fracture analysis diagram. This sensitivity to the choice of reference curve is a serious limitation of the revised Pellini diagram.

The CASPPR regulations are based on prevention of initiation from large fatigue cracks. There is no criterion for crack arrest. The present results of SCA tests do not, therefore, relate directly to the CASPPR requirements. They do show, however, that if a large defect resided in a high stress brittle region, complete fracture could result.

Crack arrest is an explicit fracture criterion in the S473 toughness requirements. For 'good crack arrest', the requirement is that a running crack should be arrested at 60% specified minimum yield strength. For a thickness less than 26mm, this requires no-break performance in the drop weight test at T-10°C where T is the toughness design temperature (i.e. crack arrest at 5°C above the NDTT). Thus in the present steel (NDTT = -15 to -10°C) crack arrest is expected at -10° to =5°C for a stress of 210 MPa. Test #11 (HAZ) did not fracture at -5°C and 243 MPa and tests #13 (HAZ) and 5B (BM) did not fracture at +5°C. Thus the test results were consistent with the requirements of S473. Crack size is not explicitly discussed in S473 although it is apparent from the present results that the requirements would only provide for arrest of rather small cracks.

5.0 SIGNIFICANCE OF THE RESULTS WITH RESPECT TO CASPPR

The fracture criterion used in CASPPR (1) is that the steel should have sufficient fracture toughness to prevent brittle fracture initiation from 250 mm long cracks, assuming that residual and long range reaction stresses together do not exceed $0.2\sigma_y$. In comparison, the NKK approach conservatively assumes that these could be as high as $0.6\sigma_y$ (2).

Both these approaches ignore the "intermediate" loading rates that the midship region in ships are subjected to, and instead estimate the minimum fracture toughness of the steel at a static loading rate, following the NKK correlation[2]. Calculations using these approaches indicate that applied stresses in the range 70 to 90% of the yield strength could be tolerated without initiating brittle fracture from 250 mm long cracks.

An alternate approach is to assess the fracture toughness of steel at an appropriate intermediate loading rate. This indeed was done in a companion study[5] wherein it was also suggested that 0.1 mm intermediate loading rate CTOD should be adequate to prevent brittle fracture initiation from 250 mm long cracks, assuming that service stresses, and residual and reaction stresses do not exceed $0.4\sigma_y$ and $0.2\sigma_y$, respectively.

It was concluded in this study that both (NKK and Intermediate Loading Rate) approaches lead to similar CVN requirements for hot rolled and normalized steels, such steels being used more often for shipbuilding.

This agreement between the two approaches is considered coincidental in that the NKK approach overestimates the fracture toughness of the steel but at the same time assumes high values for the service stresses, and the residual and reaction stresses.

However, for the thermomechanically treated steels, the agreement between the two approaches was poorer, and it seemed that the CVN requirements arrived at by the NKK approach could be non-conservative. Further, it was concluded that toughness specifications, in terms of the NDT temperature would have more uniform application.

Notwithstanding the above, one of the thermomechanically treated steels was used in the wide plate test program. The static fracture toughness of the steel calculated from the fatigue sharpened three point bend CTOD specimens is reasonably close to the minimum predicted by the NKK approach, keeping in mind the higher constraint of the CTOD specimens. Similarly, the nominal fracture toughness estimated from the wide plate tests is close to the NKK minimum. This agreement is though fortuitous to some extent because of the net section yielding in three of the tests.

A more important observation, however, is that in spite of the net section yielding in the wide plate tests at -55°C or higher test temperatures, the gross fracture stress is more than 80% of the room temperature yield strength. The maximum value of applied and residual stresses in the midship region is believed to be $0.6\sigma_y$ in comparison.

The wide plate results therefore are consistent with the minimum anticipated static fracture toughness of steels based on the NKK approach, and provide support for the CASPPR requirements, keeping in mind there are several factors contributing to the conservatism in the requirements:

(i) the previous study[5] on relationship between intermediate loading rate toughness and conventional properties, utilized the highly constrained 3 point bend CTOD specimen and a loading rate that is at the upper limit of rates conceivable in the midship region;

(ii) the brittle fracture initiation criterion assumes principal stresses perpendicular to the crack plane, and uniform in nature, as is the case in the wide plate tests. In most ship structural situations, the cracks can be oriented at a smaller angle to the principal stress [1], and they would often propagate in a stress field of negative gradient.

(iii) the analysis in the present as well as the companion study[5] has been deterministic and 'lower bound' in nature, i.e. it incorporates high stresses, toughness at minimum design temperature, and a large flaw. The probability of all three events occurring at the same time is generally low.

(iv) finally, the approaches used to develop the toughness specifications do not take into account the inherent structural redundancy in the ship structures. It has been demonstrated by Tomin et al[1] that the presence of stiffeners reduces the probability of fracture initiation by one to two orders of magnitude.

It is therefore concluded that the CASPPR requirements for structural steel toughness are reasonable and adequate.

Looking at the future enhancements in standards and codes, the outputs from these programs indicates that toughness specifications based on the NDT temperature may have a more universal application. It should be one of the goals in further enhancements of standards to include a fracture criterion based on capability of arresting short cracks, as has already been done in CSA Standard S473 on Fixed Steel Offshore Structures. It is recognized that such steps cannot be taken in isolation, and it requires further debate and consensus development amongst the various organizations dealing with structural steel standards for ships.

6.0 CONCLUDING SUMMARY

The present program has focused on wide plate testing, and short crack arrest capability of a structural steel. These relatively large scale tests have been supported by various smaller, conventional tests, and in conjunction with a previous companion study, it is concluded that:

(i) the wide plate test results obtained in the program are consistent with the minimum fracture toughness predicted by the NKK empirical approach.

The results also demonstrate the usefulness of the failure analysis diagram in proposed revisions to PD6493 for assessing defects or predicting failure stresses in situations involving crack tip plasticity.

(ii) the CASPPR steel specifications, in terms of Charpy vee notch toughness, are adequate and reasonable.

(iii) the results relating to correlation between fracture toughness and quality assurance test results (CVN, NDT temperature) should be discussed further in the international community in order to explore and confirm if NDT temperature based specification would have universal applicability.

(iv) in the long term, the fracture control plan should include a fracture criterion based on a short crack arrest capability of the steel as well; the results obtained in the program, and precedence in the form of CSA Standard S473 on Fixed Steel Offshore Structures, would be of assistance in this regard.

7.0 REFERENCES

[1] Tomin, M., "CASPPR Subcommittee Report, Ch. 7, "Steel Selection", RELTEC Report to CCG, January 1989.

[2] Nippon Kaiji Kyokai Document submitted to IACS, "Minimum Service Temperature of Hull Structural Steels", July 1979.

[3] Tanaka, K., Sato, M., and Ishikawa, T., "Short Crack Arrest Concepts", International Symposium on Fracture-Safe Designs for Large Storage Tanks, The Welding Institute, 1986, pp.125-135.

[4] Yajima, H. and Tada, M., "Materials Selection for Hull Steel Plates Based on Fracture Toughness", Technical Review published by Nagasaki Technical Institute, Mitsubishi Heavy Industries Ltd., Feb. 1981, p.52.

[5] Malik, L. and Tomin, M., "Evaluation of Toughness of Conventional Ship Steels at Intermediate Loading Rate, and Its Implications", Fleet Technology Limited Report to CANMET, January 1991.

[6] Garwood, S.J. et al, "Crack Tip Opening Displacement (CTOD) Methods for Fracture Assessments: Proposal for Revision to BSI PD6493", The Welding Institute Member Report 3711/1988.

[7] Anderson, T.L. et al, "The Use of CTOD Methods in Fitness For Purpose Analysis", presented at the Workshop on CTOD Methodology, GKSS Research Centre, Geeshacht, April 1988.

[8] Pellini, W.S., "Principles of Fracture-Safe Design "Welding Journal Research Supplement (Part 1), March, pp.91-s to 109-s and (Part 2) April, pp.147-s to 162-s, 1971.

[9] Pellini, W.S., "Guidelines for Fracture-Safe and Fatigue-Reliable Design of Steel Structures", The Welding Institute, 1983.

[10] Graville, B.A., "Crack Arrest Requirements for Arctic Structures", DSS Contract 23440-8-9190/01-SQ CANMET, 1989.

[11] Tomin, M. et al, "Fracture Control for Arctic Structures - A Model for Analyzing Structural Details", DnV Report to MTL-CANMET (1988).

TABLES AND FIGURES

Table I: Minimum K_c Values of Steel Plates for Hull Use based on NKK Calculations

(unit : kg, $\overline{mm}$/mm²)

Steel	Grade	Temp. (°C)	Thickness (mm) 10	15	20	25	30	35	40	45	50
Mild steel	A	0	548	534	507	482	471	459	448	438	428
		−10	507	493	469	446	435	425	415	405	396
		−20	466	453	431	410	400	390	381	372	364
		−30	425	414	393	374	365	356	348	340	332
		−40	385	375	356	339	330	323	315	308	301
		−50	345	336	320	304	297	290	283	276	270
	B	0	628	594	578	548	534	520	507	482	471
		−10	581	549	534	507	493	481	469	446	435
		−20	534	505	491	466	453	442	431	410	400
		−30	487	461	448	425	414	403	393	374	365
		−40	441	417	406	385	375	365	356	339	330
		−50	396	374	364	345	336	328	320	304	297
	D	0	727	685	646	628	611	578	563	548	534
		−10	672	633	597	581	565	534	520	507	493
		−20	618	582	549	534	519	491	478	466	453
		−30	564	531	501	487	473	448	436	425	414
		−40	511	481	454	441	429	406	395	385	375
		−50	458	432	407	396	385	364	355	345	336
	E	0	1 168	1 084	1 009	974	941	880	851	824	798
		−10	1 080	1 003	933	901	870	814	787	762	738
		−20	993	922	858	828	800	748	723	700	678
		−30	906	841	783	756	730	682	660	639	619
		−40	820	762	709	684	661	618	598	579	560
		−50	736	684	636	614	593	554	536	519	503
50kg/mm² class high-tensile steel ($\sigma_y \leq$ 32kg/mm²)	AH	0	711	676	643	627	598	584	571	558	545
		−10	653	625	595	580	553	540	528	516	504
		−20	605	574	546	533	508	496	485	474	463
		−30	552	524	499	487	464	453	443	433	423
		−40	500	475	452	441	420	410	401	392	383
		−50	448	426	405	395	377	368	360	352	344
	DH	0	913	887	837	792	770	750	730	711	693
		−10	844	820	774	732	712	694	675	658	641
		−20	776	753	711	673	655	637	621	605	589
		−30	708	688	649	614	598	582	566	552	538
		−40	641	623	588	556	541	527	513	500	487
		−50	575	559	528	499	486	473	460	448	437
	EH	0	1 255	1 173	1 135	1 064	1 031	999	969	941	913
		−10	1 160	1 085	1 049	984	953	924	896	870	844
		−20	1 066	997	964	904	876	849	824	799	776
		−30	973	910	880	825	800	775	752	729	708
		−40	881	824	797	747	724	702	681	661	641
		−50	791	739	715	671	650	630	611	593	575

Table II: Test Steel Properties

Characteristics	Test Steel	Min. Requirements for DH 36
Lower Yield Strength	373	355
Upper Yield Strength (at Room Temperature) (MPa)	401	
CVN Energy (J) @ -20°C		
Long.	71	34
Trans.	32	23
34J (Long) Transition Temperature	≤-40°C	-20°C
NDT Temp. (°C) (E208)	-10° to -15°	No requirement

Table III: CTOD toughness of the test steel* (Quasistatic Loading Rate)

Test Temp. °C	Avg. CTOD (mm)		Ratio $\sqrt{(A/B)}$
	.15mm Saw Notch (A)	Fatigue Precrack (B)	
-20°	0.3314	0.2950	0.94
-40°	0.3298	0.2625	0.90
-55°	0.2145	0.1220	0.75
-75°	0.1175	0.0633	0.73

* All specimens had their longitudinal axes parallel to the steel rolling direction.

Table IV: Wide Plate Test Results

Test Temp. °C	Gross Stress at Fracture MPa	Average CTOD at Fracture in the WP tests (mm)
-75	214	0.827
-55	348	1.040
-40	322	0.945
-20	336	1.230

Table V: Summary of Short Crack Arrest Test Results

Test #	Location	Temp., °C	Stress MPa	Result
1	BM	-15	262	Complete fracture
2	"	+5	256	Invalid (arrest in weld metal)
3	"	+5	312	Invalid (crack divergence)
4	"	+5	311	Complete fracture
5	"	+5	237	Arrest of starter crack (5B)
6	"	+20	315	Invalid (no starter crack)
7	"	+5	240	Invalid (crack divergence)
8	"	+20	326	Arrest of starter crack
9	HAZ	+20	312	Arrest of starter crack
10	"	+5	322	Complete fracture
11	"	-5	243	Arrest of starter crack
12	"	-15	246	Complete fracture
13	"	+5	244	Arrest of starter crack

Table VI: Steel Fracture Toughness Based on CTOD Values

Test Temp. (°C)	Avg. CTOD (mm)	Yield Strength* (MPa)	Fracture Toughness "K" (MPa √m)
-75	.0633	432	106.4
-55	0.122	414	144.6
-40	0.2625	400	208.5
-20	0.295	388	217.7

* From Appendix A

Table VII: Steel Fracture Toughness Based on Wide Plate Test Results (Linear Elastic assumption)

Test Temp. °C	Gross Fracture Stress (MPa)	Nominal Fracture Toughness (MPa √m)	Net Section Stress at Fracture
-75	214	140	291
-55	348	227*	473
-40	322	211*	438
-20	336	220*	457

* (Net section yielding occurred in these tests)

Table VIII: Summary of Estimates of Crack Arrest Toughness

Temp. °C	Estimate of K_{ca} (MPa $\sqrt{m}$)	
	Upper	Lower
-15	43.3	43.3
-5	55.1	46.5
+5	70	49.9
20	101*	55.6

* Extrapolated value, since no fracture was obtained at 20°C, the actual K_{ca} could be much higher.

Table IX: Comparison of SCA Results with CCA Results

Temp. °C	K_{Ia} (avg. of CCA tests) MPa$\sqrt{m}$	Upper estimate of K_{Ia} (from SCA tests) Indexed to K_{Ia} from CCA test at NDTT*
-20	63.6	
-15	-	65
-5	-	83
0	98.3	-
5	-	105
18	147	-
20	-	152

* Since CCA tests were not done at -15°C (NDTT) the value of K_{Ia} = 65 has been obtained by interpolating from the value K_{Ia} = 63.6 at -20°C.

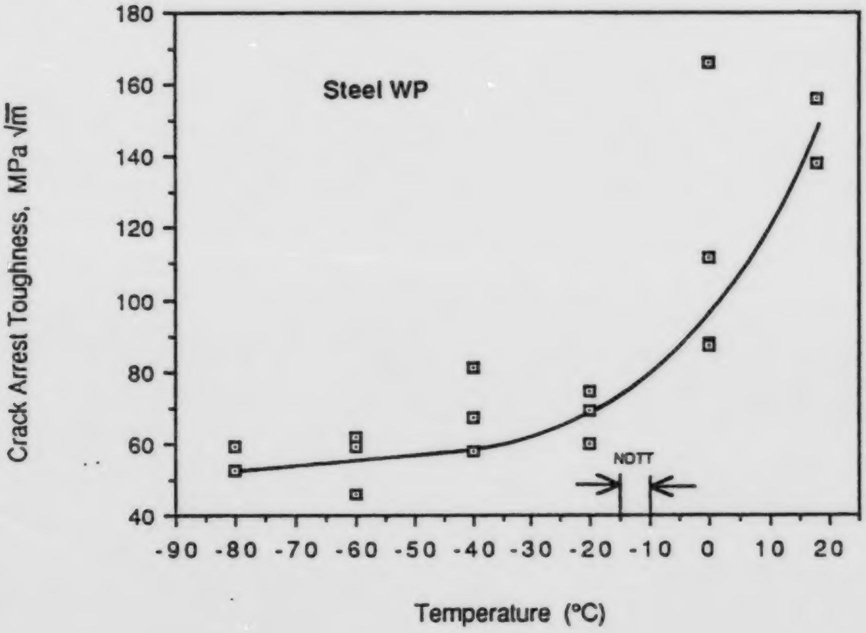

Figure 1: Compact crack arrest toughness of steel WP at various temperatures

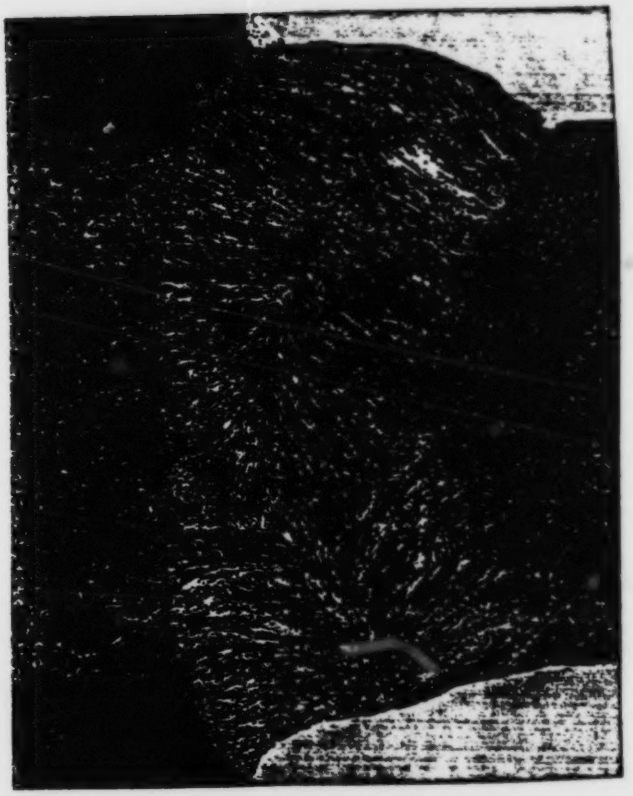

Figure 2: Cross section from the butt weld made using the finalized procedure (Neg. 12073) (Photomacrograph also shows the bars used to avoid the nail head shape.)

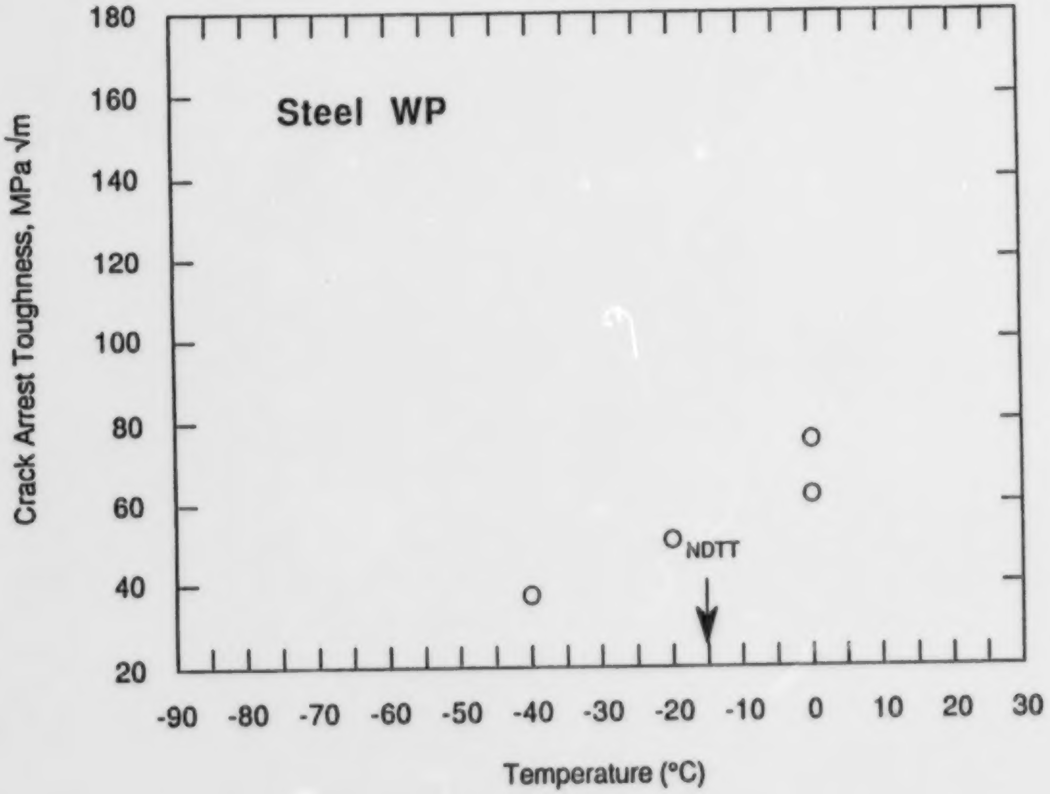

Figure 3: Compact crack arrest toughness of the HAZ in the steel WP, based on specimens with insufficient remaining ligament only

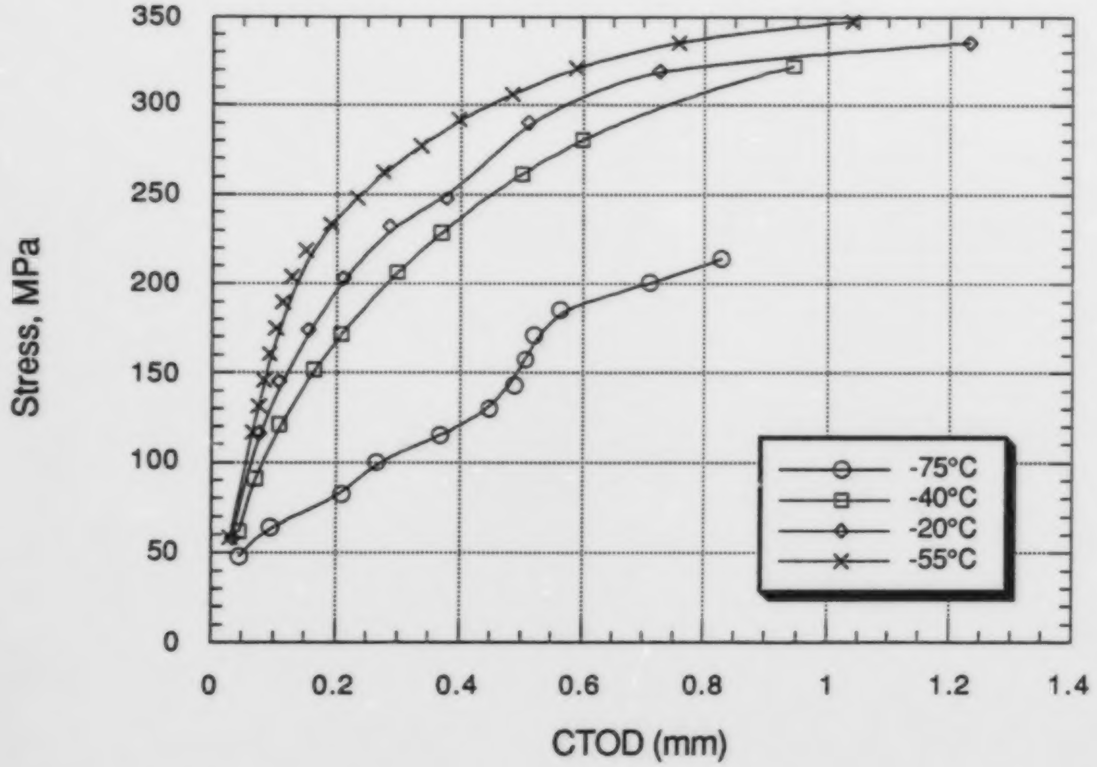

Figure 4: Crack tip opening displacements in the wide plate tests calculated from clip gauge outputs

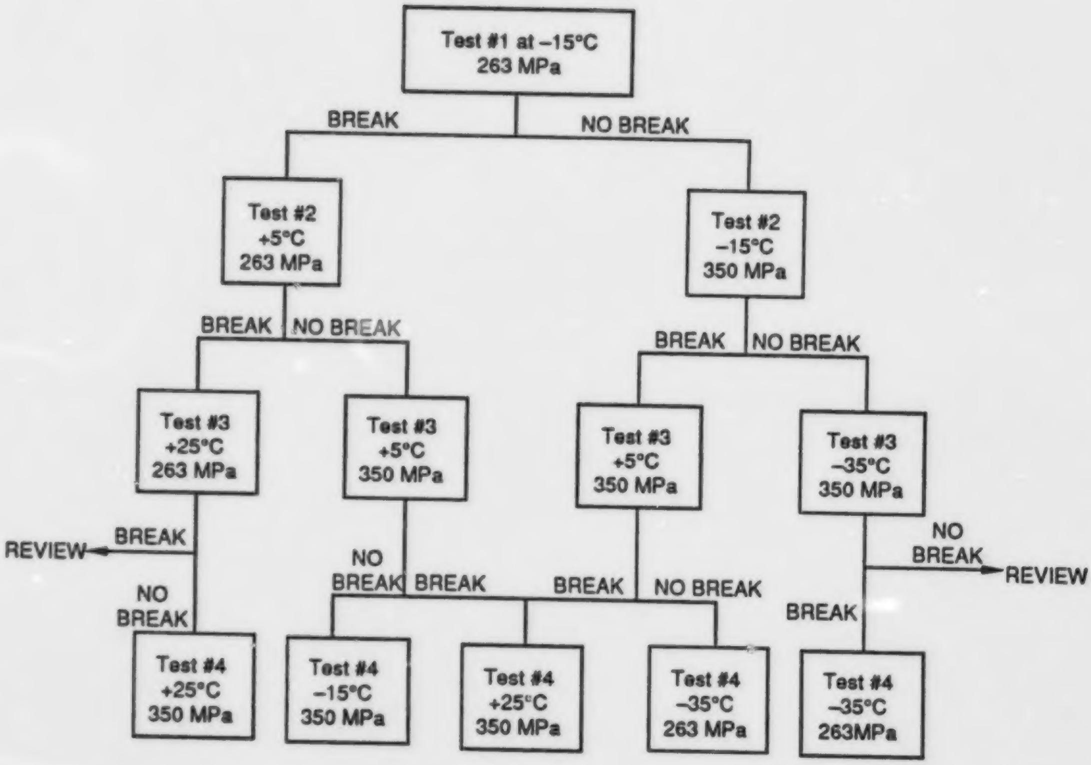
Test #1 at –15°C
263 MPa
BREAK
NO BREAK
Test #2
+5°C
263 MPa
Test #2
–15°C
350 MPa
BREAK
NO BREAK
BREAK
NO BREAK
Test #3
+25°C
263 MPa
Test #3
+5°C
350 MPa
Test #3
+5°C
350 MPa
Test #3
–35°C
350 MPa
REVIEW
BREAK
NO
BREAK
NO
BREAK
BREAK
BREAK
NO BREAK
NO
BREAK
REVIEW
BREAK
Test #4
+25°C
350 MPa
Test #4
–15°C
350 MPa
Test #4
+25°C
350 MPa
Test #4
–35°C
263 MPa
Test #4
–35°C
263MPa

Figure 5: Test sequence for base material short crack arrest tests.

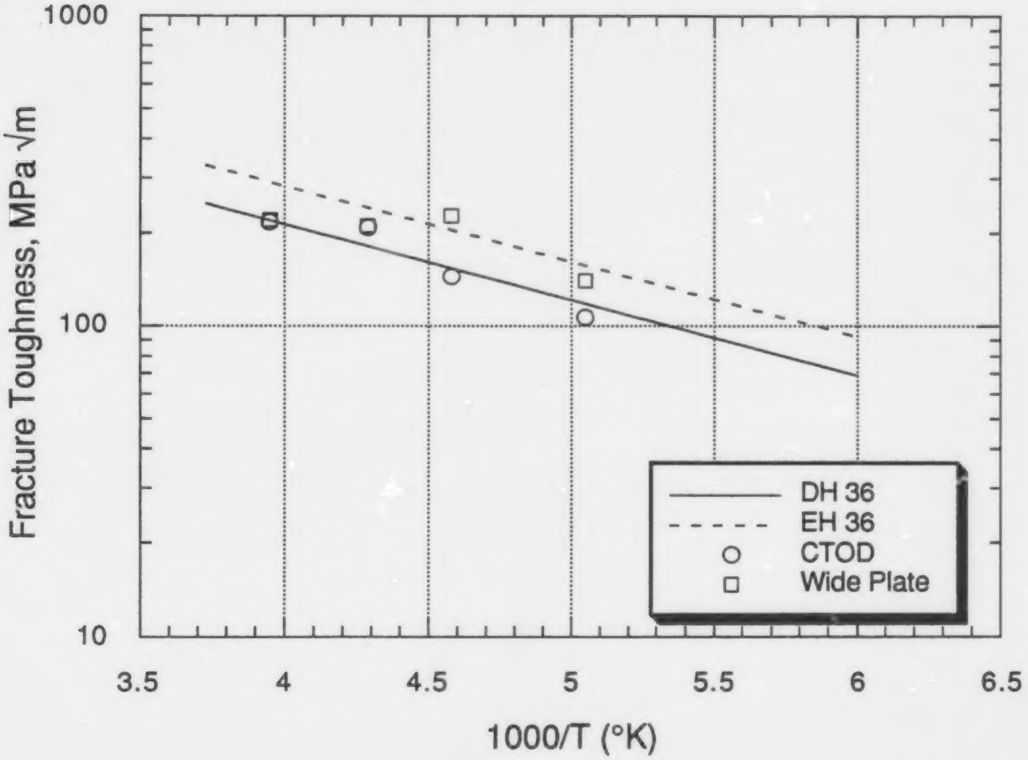

Figure 6: Test steel fracture toughness calculated from CTOD data (fatigue sharpened) and wide plate tests, compared to the minimum anticipated toughness (NKK) for Grades DH36 and EH36

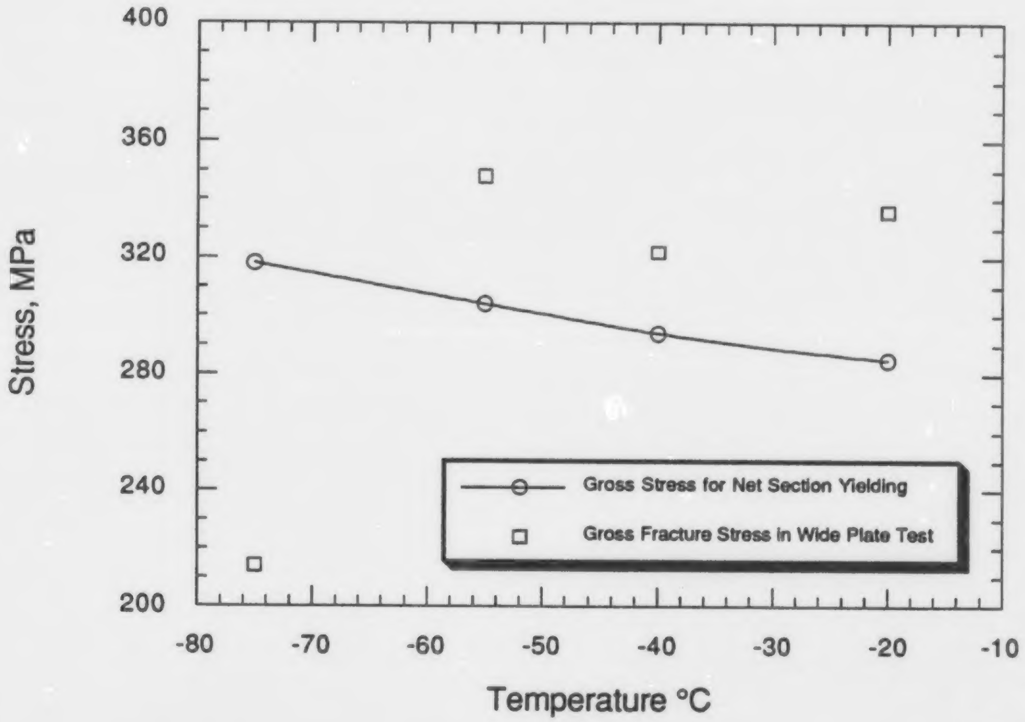

Figure 7: Gross fracture stress in the wide plate tests in relation to the gross stress required for net section yielding

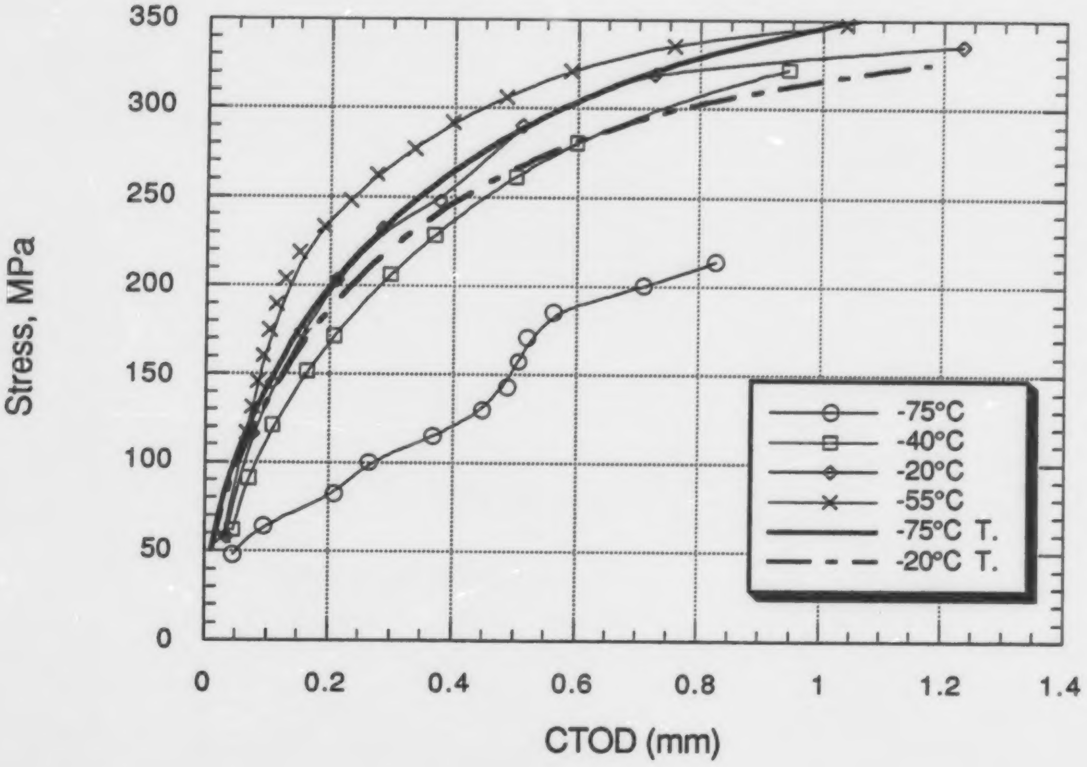

Figure 8: CTOD calculated from the strip yield model (-75°CT and -20°CT) compared to those calculated from clip gauge measurement in wide plate tests

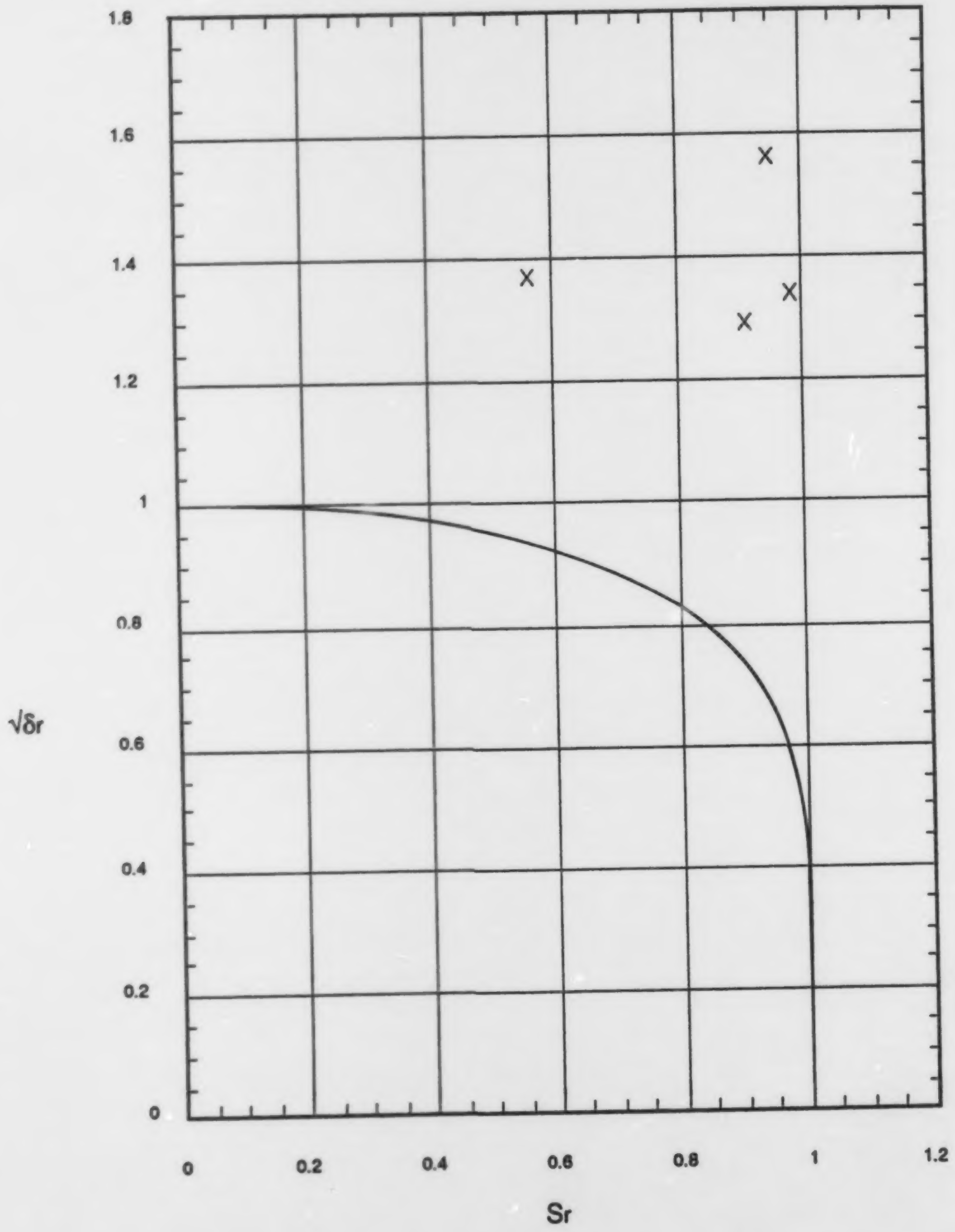

Figure 9: The locus of the failure assessment line, and the wide plate test results

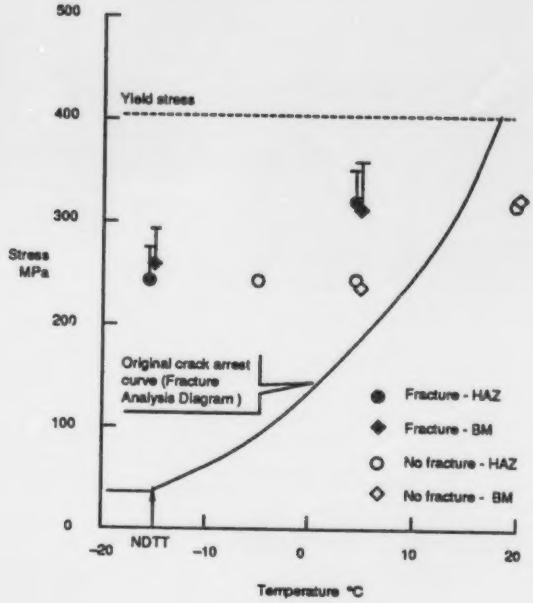

Figure 10: Results of short crack arrest tests plotted on Fracture Analysis Diagram

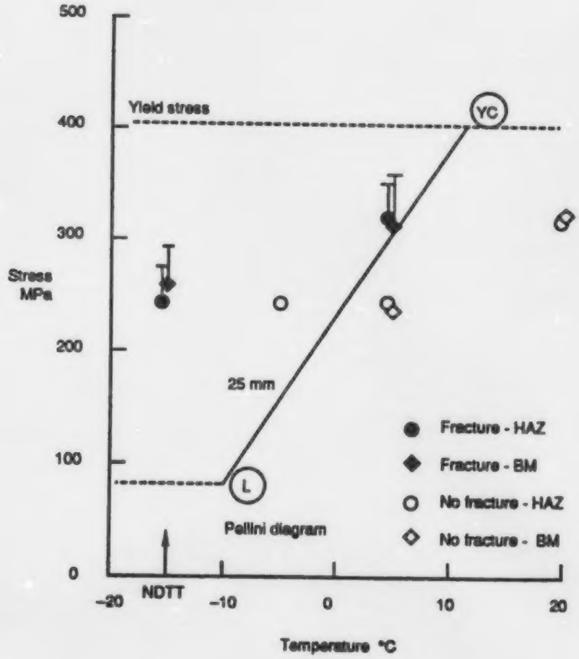

Figure 11: Results of short crack arrest tests plotted on Pellini Diagram

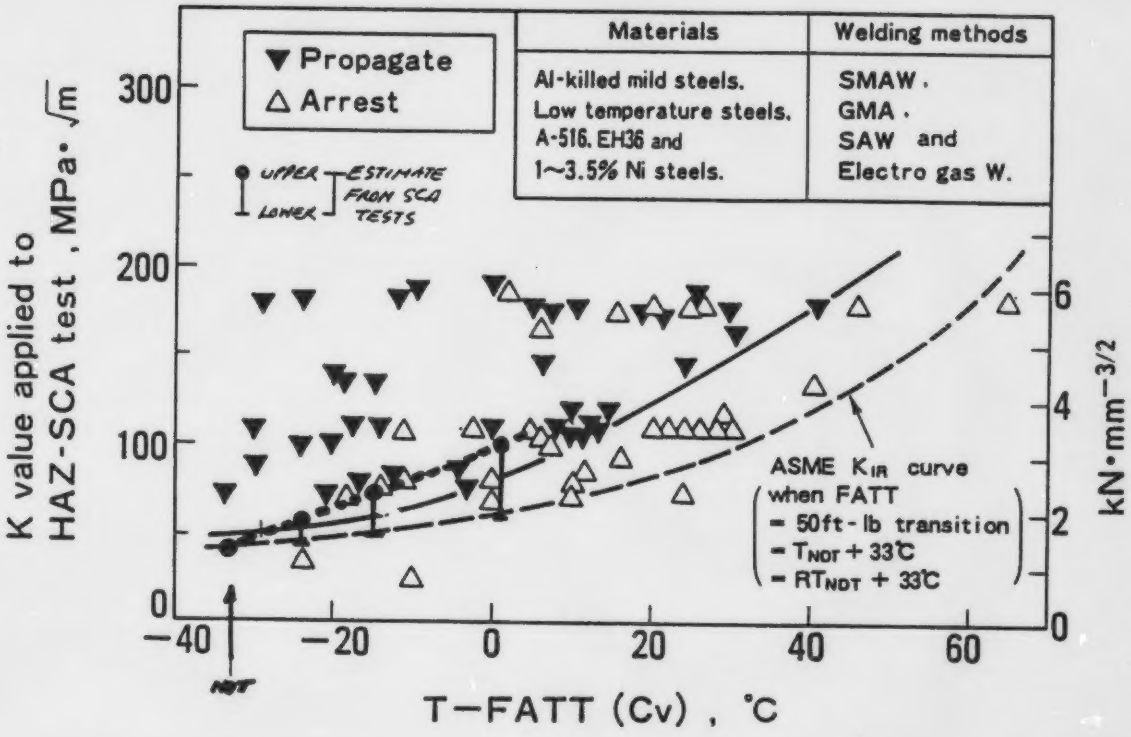

Figure 12: Crack arrest toughness estimated from SCA results compared with Tanaka's data

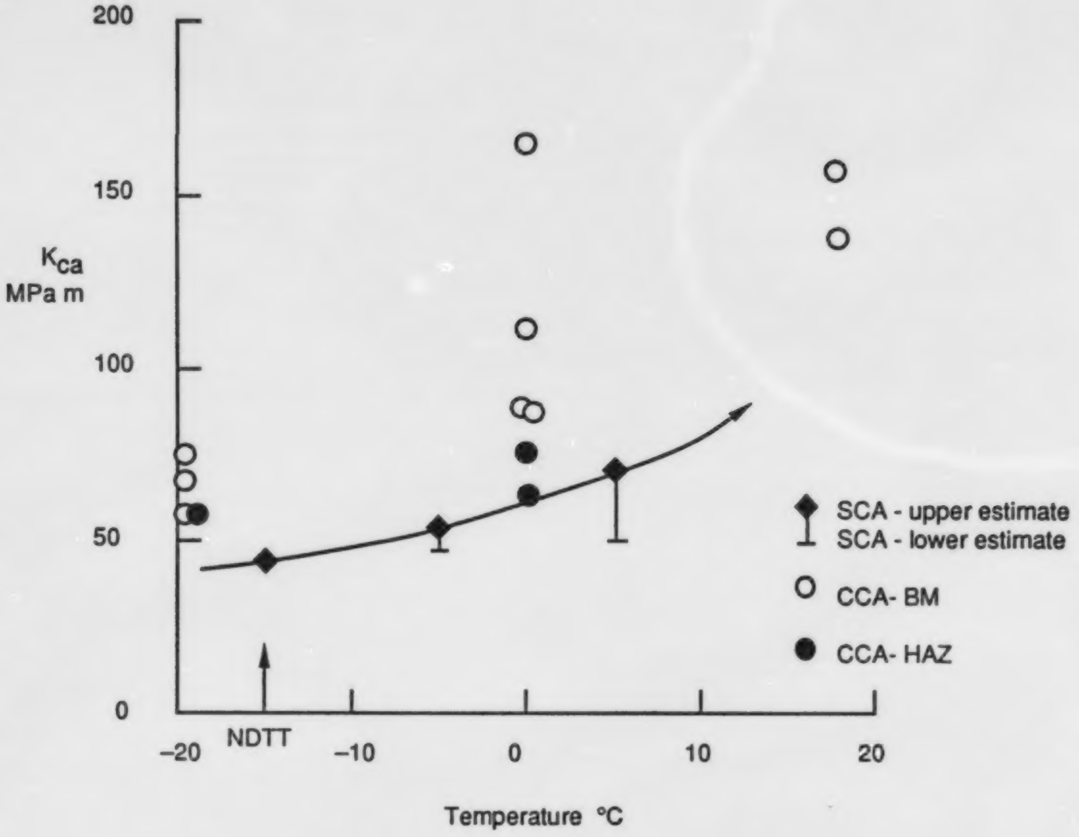

Figure 13: Toughness from SCA tests compared with K_{Ia} from CCA tests

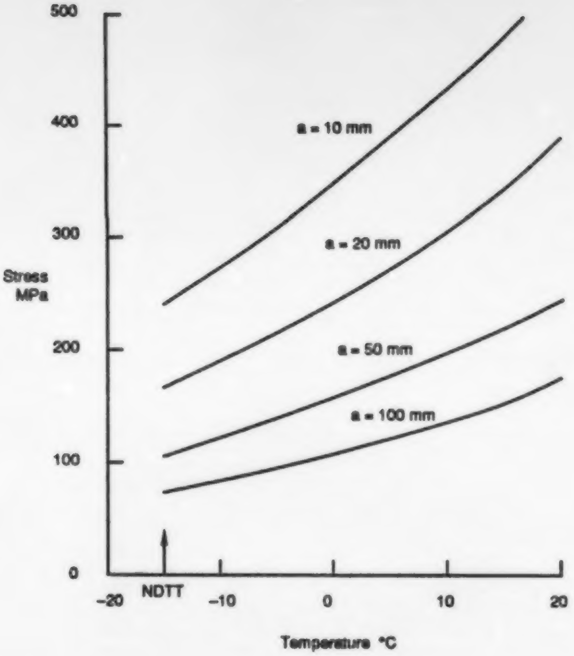

Figure 14: Critical crack sizes for arrest based on upper estimate of toughness

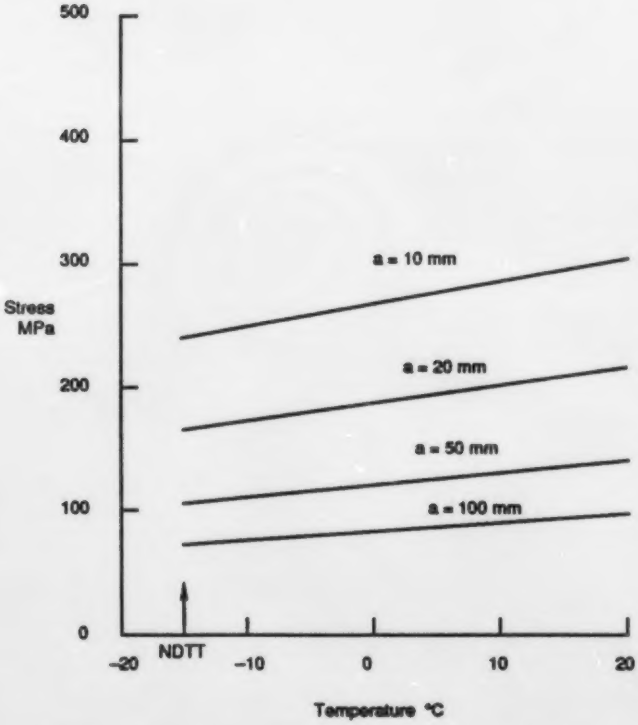

Figure 15: Critical crack sizes for arrest based on lower estimate of toughness

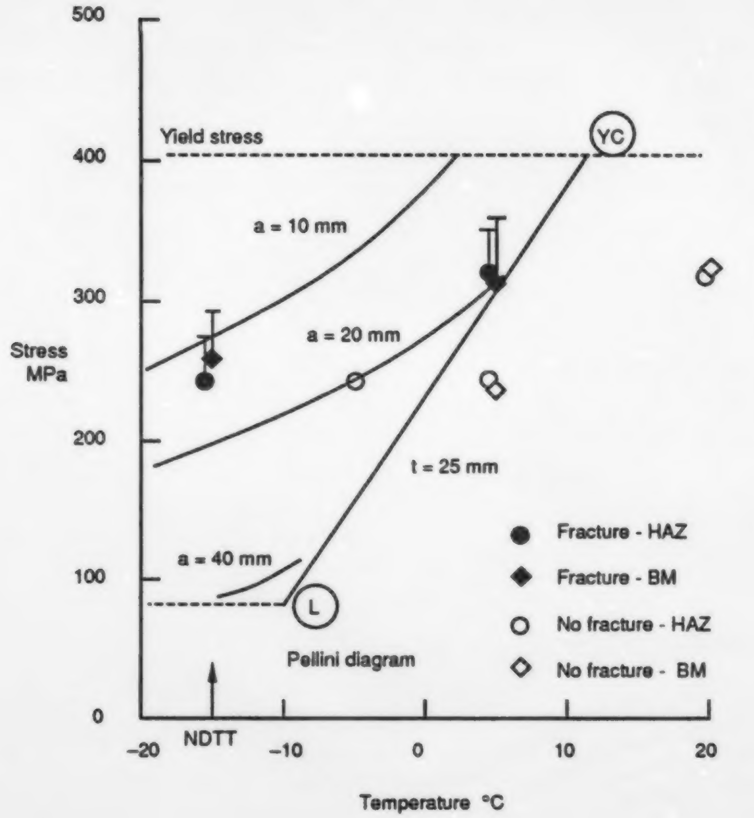

Figure 16: SCA test data compared with critical crack size estimates from Pellini diagram

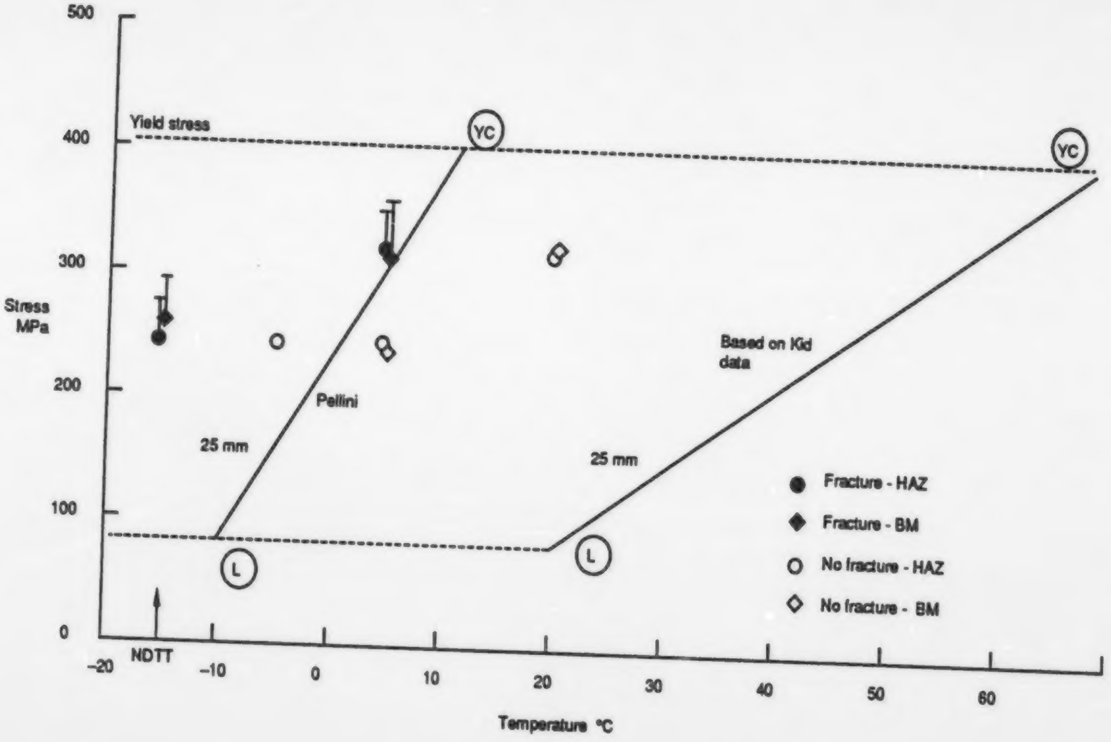

Figure 17: Shift of crack arrest line in Pellini diagram when based on a modified K_{Id} reference curve

ANNEX

ESTIMATES OF CRACK ARREST TOUGHNESS BASED ON SCA TEST RESULTS

ANNEX

Estimates of Crack Arrest Toughness Based on SCA Test Results

1. Max. K_{ca} at −15°C = 109 MPa√m (Test 12) (assuming 2a = 120 mm)
   Max. K_{ca} at +5°C = 138 MPa√m (Test 4)

2. Estimate of minimum toughness based on equation for average K_{Id} for older steels (Figure 13 in Ref. 10).

$$\log\left[\frac{K_{Id}}{\sigma_d}\times 10^3\right] = 0.004\,\Delta T + 1.864$$

RT strength = 401 MPa (Fleet report Table III)

$$\sigma_{yd} = 401 + \frac{1850-401}{T_{°K}\times 16.1\times 10^{-3}} - 157$$

T°C	σ_d MPa	ΔT °C	$\log\left[\frac{K}{\sigma_d}\times 10^3\right]$	$\frac{K}{\sigma_d}\times 10^3$	K_{Id} MPa√m
−15	592.8	0	1.864	73.11	43.3
−5	579.8	10	1.904	80.17	46.5
5	567.7	20	1.944	87.9	49.9
20	551	35	2.004	100.9	55.6

3. Assume K_{Id} is the crack arrest toughness at NDTT. Assume also K_{Id} is the lower bound of K_{ca}. Assume the upper bound increases with temperature in the form:

$$\log\left[\frac{K_{ca}}{\sigma_{yd}}\times 10^3\right] = \beta\Delta T + 1.864$$

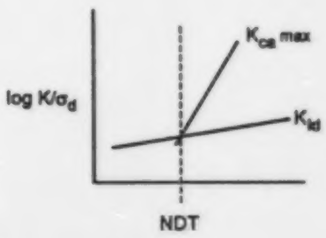

Determine maximum β from maximum K_{ca} at

+5°C = 138 MPa√m

$$\log\left[\frac{138}{567.7}\times 10^3\right] = \beta\times 20 + 1.864 \quad \therefore 20\beta = 2.3858 - 1.864$$

$$\beta = 0.02609$$

Calculate β and K_{ca} values for various max. K_{ca} values at 5°C less than 138 MPa√m.

Temp.°C	σ_d	K_{Id} (min. K_{ca})	K_{ca} (max.)	K_{ca} (max.)	K_{ca} (max.)
–15	592.8	43.3	43.3	43.3	43.3
–5	579.8	46.5	77.3	55.1	53.1
+5	567.7	49.9	138	70	65
+20	551	55.6	330	100.6	88.3
		$\beta =$	0.02609	0.01135	0.009745

4. Assume that the crack starter condition is represented by:

$$K = \alpha \times \sigma \qquad (\sigma \text{ is applied stress in main plate})$$

From tests which fractured find minimum possible values of α using K_{Id} as the minimum toughness:

–15°C	245 MPa	$K_{Id} = 43.3$	min. $\alpha = 0.177$
+5°C	315 MPa	$K_{Id} = 49.9$	min. $\alpha = 0.158$

Using various values of K_{ca} as maximum toughness, find min. α (from fractured tests) and max. α (from non-fractured tests):

	NF		F		NF		F		NF		F		NF		F	
Temp.	K_{ca}	max. α	K_{ca}	min. α	K_{ca}	max. α	K_{ca}	min. α	K_{ca}	max. α	K_{ca}	min. α	K_{Id}	max. α	K_{Id}	min. α
–15°C	43.3	—	43.3	0.177	43.3	—	43.3	0.177	43.3	—	43.3	0.177	43.3	—	43.3	0.177
–5	77.3	0.32	77.3	—	55.1	0.225	55.1	—	53.1	0.217	53.1	—	46.5	0.19	46.5	—
+5	138	0.563	138	0.438	70	0.286	70	0.222	65	0.265	65	0.206	49.9	0.20	49.9	0.158
20	330	1.05	330	—	101	0.32	101	—	88.3	0.28	88.3	—	55.6	0.177	55.6	—
	①				②				③				④			

In ①, the highest minimum α exceeds the lowest max. α and is therefore not admissible.
In ③, the highest min. α is below the lowest max. α and is permitted.
In ②, the highest min. α is about equal to the lowest max. α so this represents the maximum K_{ca} values.
In ④, the highest min. α is about equal to lowest max. α so this represents lowest K_c values.

5. Summary:

	Highest likely K_{ca} values		Lowest K_{ca} ($=K_{Id}$)	
Temp.°C	α	K_{ca}	α	K_{ca}
–15	0.223	43.3	0.177	43.3
–5		55.1		46.5
+5		70.0		49.9
20		101		55.6

All based on K_{Id} being the toughness at NDTT.

6. Crack starter characteristic crack size.
Assume crack enters test plate at elliptical surface crack.

$$\therefore\ K = 1.2\,\sigma\sqrt{\pi\frac{a}{Q}} \quad \therefore\ \alpha = 1.12 \times \sqrt{\pi\frac{a}{Q}} \quad Q = 1.2$$

$$\text{For } \alpha = 0.223, \quad a = \frac{1.2}{\pi}\left(\frac{0.223}{1.12}\right)^2 \times 1\,000 = 15.1\text{ mm}$$

$$\text{For } \alpha = 0.177, \quad a = \frac{1.2}{\pi}\left(\frac{0.177}{1.12}\right)^2 \times 1\,000 = 9.5\text{ mm}$$

This suggests the attachment weld acts as a bit of a barrier (residual stresses?) and much of the K due to the initial crack run in the starter plate is lost. The above values are quite reasonable when compared to other estimates.

Volume

2

FLEET TECHNOLOGY LIMITED

MATERIALS TECHNOLOGY CENTRE 3728C.FR

STUDY OF WIDE PLATE TESTING OF STRUCTURAL STEELS FOR ARCTIC SHIPS

Final Report

By

L. Malik, B.A. Graville, M. Tomin and S.R. Bala

VOLUME II: APPENDICES

Work on the project was conducted under the auspices of the Canada Centre for Mineral and Metallurgical Technology, Canadian Coast Guard (Northern) and Panel for Energy R and D (PERD).

DSS Contract Serial No. : 23440-9-9014/01-SQ
DSS File No. : 003SQ-23440-9-9014
CANMET Project No. : 9-9014
Scientific Authority : Dr. W.R. Tyson

MICROMEDIA

Date: September 1991

326 pp

TABLE OF CONTENTS (CONT'D.)

VOLUME II

APPENDIX A: Characterization of the Steel and Heat-affected Zone used in the Project.

APPENDIX B: Wide Plate Tests - Procedures and Results.

APPENDIX C: Short Crack Arrest (SCA) Test Development and Detailed Procedures and Results.

APPENDIX D: Wide Plate Tests - Analysis of Results.

APPENDIX A

CHARACTERIZATION OF THE STEEL AND HEAT-AFFECTED ZONE USED IN THE PROJECT

FLEET TECHNOLOGY LIMITED E93728C

CHARACTERIZATION OF THE STEEL AND HEAT AFFECTED ZONE USED IN THE WIDE PLATE PROJECT

(Tasks 2, 7, 10, and 11)

April 1991

Submitted to:

Project Manager
"Study of Wide Plate Testing of Structural Steels for Arctic Ships"

Submitted by:

FLEET TECHNOLOGY LIMITED
311 Legget Drive
Kanata, Ontario, K2K 1Z8

TABLE OF CONTENTS

		Page
1.0	INTRODUCTION	1
2.0	STEEL PROCUREMENT	1
3.	TEST PROCEDURES AND RESULTS	2
	3.1 Blanking of Plates for Various Specimens	2
	3.2 Tests on Base Material	2
	3.3 Heat Affected Zone Testing	6
4.0	DISCUSSION AND SUMMARY	9
5.0	REFERENCES	10

TABLES AND FIGURES

1.0 INTRODUCTION

The main component of the program consisted of four wide plate tests with the objective of providing support for the Structural Steel Toughness Requirements in CASPRR Schedule 3. In addition, the contract required development of a short crack arrest (SCA) test procedure, based on the Tanaka approach[1], and then performing such tests on the base material selected for the program, and on heat affected zone of a two pass full penetration weld in the steel plate.

To support analysis of the results obtained from the larger wide plate and SCA tests, appropriate smaller scale tests were also carried out at Fleet Technology Limited. The test procedures employed and the results obtained are described in this report.

2.0 STEEL PROCUREMENT

Algoma Steel was approached to obtain sufficient quantity of steel for the project. The main requirements were that the steel be equivalent to ship Grade DH36 (25mm thick) and that its Charpy Vee Notch (CVN) toughness be reasonably close to the minimum specified (34J @ -20°C). After conducting CVN tests on several plates, Algoma Steel decided to control roll a slab, and provide the requested amount of steel (3 plates, each 3.66m X 2.44m).

The chemical analyses of the steel, given in the mill test report, and as obtained independently in this program, are given in Table I. Normally, 25mm thick, Grade DH36 steel containing Nb or V is normalized. However, control rolling is allowed as a substitute if testing of individual plates confirms that the CVN specifications are met. The CVN and tensile test results obtained at Algoma Steel are given in Table II. The minimum requirements for Grade DH36 ship steel are: min. 355 MPa yield; min. 34J CVN absorbed energy in the longitudinal orientation and 23J in the transverse orientation, at -20°C.

For identification of the steel and machined specimens, it was given the identification code "WP".

3.0 TEST PROCEDURES AND RESULTS

3.1 Blanking of Plates for Various Specimens

Blanks for all large scale tests (wide plate, and short crack arrest tests) were removed such that the artificially introduced flaws, and their propagation path would be perpendicular to the rolling direction.

The scheme for cutting of the plates is shown in Figure 1. The material for the wide plate, CTOD, CVN, and tensile tests was removed from one plate (Figure 1(a)). The material for short crack arrest tests (base material) was obtained from the second plate (Figure 1(b)). The NDT temperature was determined for both these plates. Also, the blanks for compact crack arrest tests on base material were removed from both the plates.

For preparing the short crack arrest and compact crack arrest test specimens for HAZ evaluations, most of the material used was from the second plate.

The third plate was used for making two HAZ SCA specimens, and for making two smaller welds for in-house evaluations at the Metals Technology Laboratories (Figure 1(c)).

In extracting the small test specimens, care was taken to ensure that flame cut regions were discarded and did not influence the test results.

3.2 Tests on Base Material

(i) Tensile Tests

Eight tensile specimens, 12.5mm diameter and 50mm in gauge length were removed from the quarter thickness location and tested at temperatures selected for the wide plate tests. The cross-head rate was 0.053 mm/s giving a strain rate of $\approx 10^{-3} s^{-1}$. The results obtained are summarized in Table III. The minimum requirements at room temperature (20°C) are easily met. Also, the yield strength increases, as expected, with decrease in test temperature.

(ii) Metallography

The base material microstructure was examined on a thickness face, parallel to the rolling direction. As seen in Figure 2, the steel has a relatively fine ferritic grain size, measured to be ASTM No. 7 to 8. Finer grain sizes lead to improved notch toughness.

Vickers hardness traverse (10 kg load), across the plate thickness, was also conducted. The hardness was uniform through the thickness, the average value being 172 HV_{10}.

(iii) Charpy Vee Notch Tests

Several standard size CVN specimens (10mm X 10mm X 55mm) were machined such that their axes were located at the quarter thickness position of the steel plate. The specimens were removed from both the longitudinal and transverse orientations, and then tested at various temperatures, in accordance with ASTM A370, to obtain the transition curves. The data obtained are shown in Table IV, and the transition curves are shown in Figure 3.

The toughness values at -20°C are similar to those reported in the mill test report, and meet the minimum requirements fore DH36 grade of steel. Thus, in the longitudinal direction, the average absorbed energy at -20°C is 89J (minimum 34J required) and the 34J transition temperature is ≤ -40°C. Similarly, in the transverse orientation, the average absorbed energy at -20°C is 31J (23J minimum required) and the 23J transition temperature is ≈ -32°C.

(iv) Nil-Ductility Transition (NDT) Temperature

Following the procedures outlined in ASTM E208, size P2 specimens (≈130mm X 50mm X 19mm) were machined from the first two steel plates in such a way that they retained one of the original plate surfaces. The long dimension of the specimens was parallel to the rolling direction. Lincoln Wearweld electrodes were used to deposit the brittle beads, their hardness being typically HRC45.

The drop weight energy used was 350J consistent with the steel's yield strength.

The NDT temperature established from 6 to 8 specimens was -15°C for the first plate, and -10°C for the second plate.

(v) CTOD Tests

Several BX2B CTOD specimens were machined from the steel such that their long axes were parallel to the rolling direction. The specimens were machine notched and two types of "precracks" were used - fatigue precrack following British Standard 5762 on CTOD testing, and a 'saw notch' made with a saw blade ground down to 0.15mm thickness. The non-standard 'saw notch' tests were carried out since the four wide plate tests performed in the program would employ such a notch.

All specimens had an a/W ratio ≈0.5, and for the fatigue precracked samples, the peak stress intensity factor for the final 1mm length of the precrack did not exceed 22 MPa√m. The specimens were allowed to soak for at least 10 minutes at the selected test temperature before commencement of the test.

The CTOD results obtained are summarized in Tables V and VI for the saw notched and fatigue precracked specimens, respectively, and also plotted in Figure 4.

It is evident that the CTOD values vary over a relatively large range, especially in the temperature range -55° to -20°C. Overall, while the CTOD values increase with temperature, this becomes prominent at temperatures above -20°C, and there seems to be a plateau in the temperature range -40° to -20°C.

From the data, it is possible to compare the CTOD values obtained by a 'sawed notched' and by a 'fatigue precrack'. Thus,

Test Temp. (°C)	Avg. CTOD Saw Notch, mm (CTOD_N)	Avg. CTOD Fatigue Precrack, mm (CTOD_F)	SQRT. Ratio ($\text{CTOD}_F/\text{CTOD}_N$)
-20	0.3314	0.2950	0.94
-40	0.3218	0.2625	0.90
-55	0.2145	0.1220	0.75
-75	0.1175	0.0633	0.73

The above data suggests that the nature of the precrack (sawed notch or fatigue precrack) has the greatest influence on results in the lower shelf region. With increase in test temperature towards the upper shelf region, 'saw notch' CTOD values tend to approach those obtained with a fatigue precrack.

In the NKK approach[2] to develop CVN toughness requirements for ship steels, this ratio is suggested to be 0.68 at the specified CVN test temperature. Based on the table above, a value of 0.68 should give a lower bound value for fracture toughness in the presence of a sharp crack.

CTOD tests were also carried out at MTL at an intermediate loading rate (cross head speed = 34.8mm/s, $\dot{K} = 6538$ MPa$\sqrt{m}$) using fatigue precracked specimens[3]. The data is summarized in Table VII, and plotted in Figure 5, along with the quasistatic results. The 0.1mm CTOD transition temperature has increased by about 46°C due to the higher loading rate.

(vi) Compact Crack Arrest (CCA) Tests

The test for determining the crack arrest toughness of steels using compact specimens loaded by means of a split pin and a wedge was initially developed by Ripling and Crosley[4]. After round-robin testing on three structural steels[5], the test procedures were incorporated into an ASTM Standard in 1988[6].

In the present program, the dimensions of the specimen and test procedures conformed to ASTM E1221. The dimensions of the specimens tested are shown in Figure 6. All specimens were extracted such that the intended fracture plane in the specimens was the same as for the wide plate and short crack arrest tests, i.e. perpendicular to the rolling direction.

Specimen preparation involved squaring of the blank specimen, followed by machining of the deep through thickness groove and the circular hole for seating the split pin and wedge for loading during the test. A brittle weld bead was then deposited at the root of the deep grooves using Lincoln Wearweld electrodes. A 3mm deep, ≃0.4mm wide notch was electro-discharge machined into the weld bead, leaving nominally 4mm of the brittle weld bead. The brittle fracture of this ligament when the specimen is loaded in steps by the split pin-wedge arrangement, endeavours to inject a fast running crack into the test material. The energy required to initiate the crack in the brittle weld bead and the test material, and the distance it propagates into the test material due to energy dissipation are then used to calculate the plain strain compact toughness of the material. (The specimen is side-grooved before conducting the test in order to facilitate crack propagation in the plane, and to provide plain strain conditions.) The crack propagation distance into the test material was measured after heat tinting the specimen at 250°C for 1 hour.

The results of the tests conducted at various temperatures are shown in Table VIII, as well as in Figure 7.

The effect of higher temperatures in increasing the crack arrest toughness is quite evident, especially above the NDT temperature, and the trend is similar to that obtained by Ripling and Crossley (see Figure 8), although the values obtained in this study are lower.

3.3 Heat Affected Zone Testing

(i) Welding of Panels

The main objective of this task was to make welded panels for assessing the "short crack arrest (SCA)" behaviour of heat affected zone in the steel being investigated.

The welding procedures developed for making these panels is given in Table IX, and it had the objectives of:

(a) employing a relatively high heat input, two pass welding procedure, typical of shipyard practice for machine (mechanized submerged arc) welds;

(b) producing a relatively straight HAZ, compared to those normally associated with double vee welds in order to facilitate testing and analysis of results; this was achieved by selecting a machined groove of the design shown in Table X and by using a bar at the top to reduce the extent of capping pass nail head.

A typical cross-section of the weld is shown in Figure 9.

The welding consumables used were:

Lincoln LA75 wire (5mm diameter)
Lincoln 880M flux

The wire contains nominally 1% nickel and supplier's technical literature indicates that weld metal toughness should at least meet the requirement of 40J at -50°C in the as-welded condition (using the standard test procedure outlined in CSA Standard W48.6).

All welds were made perpendicular to the rolling direction so that the fracture path in the HAZ would also be perpendicular to the rolling direction, as was the case with the wide plate and compact crack arrest tests in the base material.

Six panels, ≈500mm (parallel to weld) X 1200mm were welded and shipped to the Welding Institute of Canada for short crack arrest testing.

In addition, narrower (≈225mm wide) panels were welded to extract 'HAZ' compact crack arrest and NDT specimens.

(ii) NDT Tests

Eight oversized NDT blanks were machined from the narrow weld panel, and macro-etched to delineate the fusion boundary. A line was then scribed on the top surface, ≈.25 to .5mm from the fusion line, into the heat affected zone, to guide the placement of the machined notch in the brittle bead. The NDT temperature obtained was -40°C, which was unexpected in light of the parent steel properties and the high weld heat input. The tested NDT specimens were then sectioned, and it was observed that in all cases, the crack had initiated from the corner of the flat bottomed notch that was above the weld metal rather than the heat affected zone (see for example, Figure 10(a)). The NDT temperature measured (-40°C) is therefore applicable to the weld metal rather than the heat affected zone.

It was decided to prepare an additional six specimens, wherein the standard ASTM E208 procedure was modified in one respect, viz., the machined notch had a 'vee' profile rather than a square one. Otherwise, the procedure followed was the same as described before. The NDT temperature obtained now was -15°C. Once again, the specimens were sectioned to ascertain the crack path, and two of these are shown in Figures 10(b) and (c). It is observed that at -15°C (break in the NDT test) the crack initiated and propagated through reheated (by the brittle bead) HAZ into the original submerged arc HAZ. At -10°C, on the other hand, the crack was arrested within the HAZ reheated by the brittle bead.

For the purposes of this investigation, the NDT temperature of the HAZ can be considered as -15°C, which is similar to that for the base material (-10° to -15°C).

(iii) Compact Crack Arrest Tests

The procedures for machining the blanks and testing were the same as outlined earlier, with one difference - oversized blanks were machined and squared first and the front and back ends (thickness faces) macro-etched to locate the HAZ. Vertical lines through the coarse grain HAZ at approximately half thickness location were scribed as shown in Figure 11. These two lines on the front and back end were joined on the top and bottom faces, which then defined the centre plane of the specimen which should contain the EDM notch in the brittle weld bead, and side grooves.

The results obtained are summarized in Table X, and unfortunately, these show that none of them are strictly valid in terms of ASTM E1221 requirements. The three main reasons for these invalidities are:

(a) insufficient crack jump;
(b) tunnelling of the crack and/or deviation into the base material;
(c) insufficient remaining ligament at crack arrest.

The 'insufficient crack jump' situation was encountered at all the three test temperatures. In its extreme form, there was no crack jump at all in several specimens tested at 0°C - a temperature higher than the NDT temperature of both the base material and the heat affected zone. Thus, Figure 12 shows the fracture surfaces of three tested samples wherein the crack jump is insufficient. Selected specimens which showed insufficient crack jump were sectioned ≈5 to 7mm below the brittle weld bead to check the placement of the side groove (mid-plane) with respect to the fusion boundary and these are shown in Figure 13. Except for specimen 2 tested at -20°C, the plane defined by the side grooves is in the heat affected zone, quite close to the fusion boundary.

Examples of specimens wherein the crack tunnelled, usually into the base material, are shown in Figure 14. The cross-sections from these specimens are shown in Figure 15. The placement of side grooves and mid-plane are seen to be quite accurate again, and in fact in specimen 11, the crack jump follows the coarse grain heat affected region to begin with. However, soon thereafter, it tunnels into base material as confirmed in Figure 15(c).

The third case, wherein the remaining ligament is insufficient, is shown in Figure 16. The crack paths near initiation and near crack arrest are shown in Figure 17 for these specimens. It is clear that the crack was able to follow the heat affected zone all the way, and then get arrested rather close to the back end of the specimen. The two requirements that the standard specifies in this regard are:

$$W - A_a > 0.15\,W$$

i.e. remaining ligament > 24.75mm (i)

and $W - A_a > (K_a/\sigma_{yd})^2$ (ii)

where K_a = crack arrest toughness
and σ_{yd} = the dynamic yield strength,

usually taken to be ≈200 MPa higher than the static yield strength.

Specimens 6, 18 (0°C), 13 (-20°C), and 9 (-40°C) all meet the second requirement above but not the first one - the remaining ligament being 12 to 16mm rather than the 24.75 minimum required.

Keeping this limitation in mind, it is believed that the results from these four specimens represent the upper bound compact crack arrest toughness of the heat affected zone examined. These four data points are plotted in Figure 18, and comparing this with Figure 8, it seems that the compact crack arrest toughness of the HAZ is lower than that of the base material.

4.0 DISCUSSION AND SUMMARY

The toughness properties of the steel used for the wide plate and short crack arrest tests, and of a weld heat affected zone in the steel have been established. The tests conducted included Charpy Vee Notch, drop weight test to determine the NDT temperature, crack tip opening displacement test (with saw notch, or fatigue precrack), and compact crack arrest tests for the base material, and NDT and compact crack arrest tests for the heat affected zone.

Performing various tests for the base material was straight forward and acceptable results were obtained, however evaluation of heat affected zone is more complex, partly because the heat affected zone/fusion boundary profile, and partly due to the specific test procedures.

Thus, in the test to establish the NDT temperature, a vee notch in the brittle bead had to be employed instead of a square bottom slot specified in ASTM E208. In the nineteen compact crack arrest tests conducted, all were invalid following the various requirements in ASTM E208. It is noted that the number of cycles required for crack jump frequently exceeded 5 - the upper limit for crack initiation suggested in ASTM E1221, even though the HAZ arrest toughness seems to be lower than that of the base material. It is conceivable that the thermal cycle due to the brittle bead changes the properties of the test HAZ making it more difficult to achieve the minimum crack jump requirements. A relatively 'finer grain HAZ' under the side groove may be another complicating factor.

5.0 REFERENCES

[1] Tanaka, K. et al, "Short Crack Arrest (SCA) Concepts", International Symposium on Fracture Safe Designs for Large Storage Tanks, The Welding Institute (UK), 1986.

[2] Nippon Kaiji Document submitted to IACS, "Minimum Service Temperature of Hull Structural Steels", July 1979.

[3] Malik, L. and Tomin, M., "Evaluation of Toughness of Conventional Shipbuilding Steels at Intermediate Loading Rates, and Its Implications", Report submitted by Fleet Technology to MTL and CCG(N), January 1991.

[4] Ripling, E.J. and Crosley, P.B., "Crack Arrest Fracture Toughness of a Structural Steel (A36)", Welding Journal, March 1982, Vol. 61, No.3, p. 655.

[5] Barker, D.B., "A Report on the Round Robin Program Conducted to Evaluate the Proposed ASTM Test Method for Determining the Crack Arrest Fracture Toughness, K_{1a}, of Ferritic Material", NUREG/CR-4996, University of Maryland, January 1988.

[6] ASTM E1221-1988, "Standard Test Method for Determining Plane Strain Crack Arrest Fracture Toughness, $K_{(a)}$, of Ferritic Steel".

[7] Remzi, E.M., "Crack Arrest Test Methods and Properties of Structural Steels", TWI Members Report 282/1985, August 1985.

TABLES AND FIGURES

TABLE I: Chemical Analysis of the Steel (wt %)

	C	Mn	Si	P	S	Cr	Ni	Cu	Al	V	Nb	N ppm
Mill Test Report	0.17	1.07	0.23	0.015	0.009	0.13	0.10	0.20	0.043	0.055	<0.01	
Check	0.18	1.07	0.22	0.018	0.012	0.10	0.09	0.16	0.042	0.040	<0.01	66

TABLE II: Tensile Properties and Charpy Vee Notch Toughness of the Steel (WP)
(As Reported in the Mill Test Report)

	First Plate	Second Plate
Yield Strength (MPa)	412	423
Tensile Strength (MPa)	568	571
% Elongation in 50mm	28	28
CVN Absorbed Energy at -20°C	99, 107, 89 (Longitudinal) 28, 34, 33 (Transverse)	91, 77, 75 33, 26, 34

TABLE III: Tensile Properties of the Steel WP

Temp. (°C)	Specimen Orientation	Lower Yield Strength (MPa)	Upper Yield Strength (MPa)	Ultimate Tensile Strength	% Elongation
20	Longitudinal	373	401	543	31.0
	Transverse	376	386	544	29.0
-20	Longitudinal	388	391	576	33.5
	Transverse	390	413	576	35.0
-40	Longitudinal	400	455	586	31.5
	Transverse	391	433	572	32.0
-75	Longitudinal	432	482	623	33.5
	Transverse	443	460	622	35.0

TABLE IV: Charpy Vee Notch Test Results for the Steel WP

TRANSVERSE			
Test Temp. (°C)	Absorbed Energy, J	Lat. Expansion (mm)	% Shear
20	65	1.20	60
20	80	1.50	80
10	60	1.18	40
10	61	1.25	50
0	49	1.05	40
0	57	1.25	50
-10	41	0.93	30
-20	38	0.80	30
-20	34	0.75	30
-20	23	0.58	20
-30	34	0.65	20
-40	9	0.20	10
-40	26	0.53	20
-40	20	0.55	20
-40	26	0.55	10
-50	22	0.43	10
-60	8	0.20	10
-60	18	0.38	10
-60	14	0.33	5
-70	12	0.30	0
-80	3	0.18	0
-80	7	0.23	0

LONGITUDINAL			
Test Temp (°C)	Absorbed Energy, J	Lat. Expansion (mm)	% Shear
20	136	2.00	80
20	129	2.20	NB
0	122	1.68	60
0	123	1.78	60
0	129	1.70	70
0	126	1.68	60
-20	85	1.50	30
-20	58	1.00	20
-20	84	1.33	40
-20	56	0.88	30
-20	73	1.25	30
-40	70	1.25	30
-40	66	1.15	30
-40	78	1.38	20
-40	68	1.08	20
-50	14	0.33	0
-50	35	0.30	10
-50	16	0.30	0
-60	30	0.63	10
-60	14	0.30	0
-60	18	0.40	0
-60	24	0.53	0
-60	19	0.33	0
-60	9	0.25	0
-70	9	0.28	0
-70	11	0.23	0
-70	9	0.25	0
-70	14	0.40	0
-80	8	0.23	0
-80	9	0.25	0

TABLE V: CTOD Results for the Steel WP (0.15mm Wide Notch)

Sample	Temp. (°C)	a/w	B (mm)	W (mm)	CTOD (mm)	Mode of Failure
L13	10	0.467	26.14	50.78	1.06	m
L27		0.467	26.17	50.71	1.20	m
L6	0	0.469	26.11	50.79	1.23	m
L29	-15	0.452	26.22	50.82	0.92	u
L22		0.455	26.23	50.76	0.72	u
L46	-20	0.487	26.2	50.75	0.54	c
L52		0.480	26.16	50.78	0.13	c
L49		0.477	26.20	50.71	0.30	c
L45		0.483	26.03	50.76	0.30	c
L54		0.484	26.09	50.75	0.40	c
L1	-25	0.46	26.14	50.75	0.38	u
L31		0.475	26.25	50.80	0.46	c
L53		0.492	26.12	50.84	0.49	c
L55		0.482	26.14	50.70	0.44	c
L21	-35	0.480	26.21	50.74	0.45	c
L10		0.476	26.23	50.69	0.50	u
L40		0.479	26.02	50.81	0.27	c
L48	-40	0.482	26.42	50.89	0.46	c
L36		0.487	26.27	50.76	0.43	c
L41		0.484	26.27	50.88	0.39	c
L43		0.479	26.09	50.75	0.21	c
L70		0.479	26.14	50.22	0.13	c
L35	-45	0.475	26.11	50.76	0.21	c
L19	-55	0.478	26.13	50.73	0.16	c
L11		0.480	26.23	50.85	0.17	c
L69		0.478	26.02	50.74	0.10	c
L71		0.490	26.07	50.80	0.43	c
L33	-75	0.474	26.25	50.74	0.13	c
L4		0.481	26.15	50.73	0.09	c
L47		0.485	26.40	50.69	0.21	c
L42		0.481	26.28	50.85	0.10	c
L38			24.65	49.10	0.06	c
L24	-90	0.453	26.27	50.75	0.08	c

TABLE VI: CTOD Results for the Steel WP (Fatigue Precrack)

Sample	Temp. (°C)	a/W	B (mm)	W (mm)	Yield Strength (MPa)	CTOD (mm)	Mode of Failure	Validity Check	Invalidity Code*	Stable Crack Growth (mm)
L8	-5		26.13	50.75	390	.878	u	VALID		1.52, 2.10, .61
L34	-5		26.20	50.66	390	1.009	m	VALID		
L2	-5		26.11	50.76	390	.678	u	VALID		.56, .98, .62
L44	-20	.515	26.05	50.84	395	.091	c	VALID		
L50	-20	.496	26.09	50.86	395	.151	c	VALID		
L39	-20	.548	26.04	50.58	395	.165	c	VALID		
L51	-20	.528	26.21	50.74	395	.956	u	VALID		
L3	-20	.534	26.16	50.74	395	.117	c	VALID		.96, 1.59, 1.15
L5	-40	.509	26.11	50.83	420	.357	u	VALID		.09, .12, .24
L18	-40	.507	26.13	50.77	420	.247	c	VALID		
L20	-40	.507	26.23	50.76	420	.199	c	VALID		
L32	-40	.489	26.22	50.78	420	.275	u	VALID		
L23	-40	.526	26.21	50.80	420	.153	c	VALID		.11, .17, .13
L25	-40	.506	26.06	50.66	420	.344	u	VALID		.23, .21, .16
L26	-55	.564	26.17	50.78	435	.101	c	INVALID	5	
L7	-55	.564	26.11	50.70	435	.129	c	INVALID	5	
L28	-55	.508	26.15	50.63	435	.095	c	VALID		
L16	-55	.499	26.17	50.74	435	.064	c	VALID		
L17	-55	.501	26.07	50.85	435	.247	u	VALID		
L9	-55	.519	26.03	50.80	435	.096	c	VALID		.07, .19, .20
I12	-75	.520	26.17	50.73	454	.071	c	VALID		
I15	-75	.512	26.15	50.82	454	.056	c	VALID		
I14	-75	.517	26.21	50.70	454	.063	c	VALID		

*Invalidity Codes:

1 K_f exceeds max. limit
2 Max. difference between a_o1 and $a_o3 > 5\%W$
3 $a_{max} - a_{min} > 10\%W$
4 Minimum fatigue crack length < 1.25mm or 2.5%W
5 a_o/W ratio not between 0.45 and 0.55
6 Slope of crack plane > 10°
7 Multinucleation effect present
8 a/W ratio not between 0.15 and 0.7

TABLE VII: CTOD Toughness of the Steel at an Intermediate Loading Rate (from Ref. 2; Tests Conducted at MTL)

Test Temp. (°C)	CTOD (mm)
40	1.194
20	0.336, 0.380, 1.159
10	0.240, 0.415, 0.183
0	0.126, 0.113
-20	0.027, 0.076
-40	0.096

TABLE VIII: Results of Compact Crack Arrest Tests for the Steel WP (ASTM E1221)

Temp (°C)	Specimen	Cycles to Failure	Initiation Stress Intensity, (MPA√m)	Crack Arrest Toughness, (MPa√m)	Validity Check	Invalidity Code*
0	CCA2	6	186.2	165.9	INVALID	
-40	CCA3	2	109.5	58.2	VALID	2
-20	CCA4	2	116.6	69.0	VALID	
0	CCA5	3	148.6	87.7	VALID	
-40	CCA6	1	117.1	66.9	VALID	
-20	CCA7	2	111.7	74.6	VALID	
-40	CCA9	1	117.9	81.4	VALID	
-60	CCA10	1	90.1	46.3	VALID	
-60	CCA11	1	109.2	59.4	VALID	
-60	CCA12	1	94.1	61.8	VALID	
0	CCA13	6	235.7	87.0	INVALID	1, 2
18	CCA14	6	269.4	156.2	INVALID	2
18	CCA15	6	272.2	137.9	INVALID	2
-20	CCA16	2	128.2	59.8	VALID	
0	CCA17	6	182.8	111.5	VALID	
-80	CCA18	1	82.8	52.3	VALID	
-80	CCA19	1	81.7	59.3	VALID	

*Invalidity Codes

1 $W-A_a>0.15W$
2 $W-A_a>(Ka/YS_d)$^2
3 $B>(K_a/YS_d)$^2
4 $A_a-A_o>2N$
5 $A_a-A_o>(K_a/YS_d)$^2

FTL FLEET TECHNOLOGY LIMITED

TABLE IX: Welding Procedure Data Sheet

Project No: 3728C
Specimen No:

Material Specification:
Welding Process: SAW
Manual or Machine: Machine
Position of Welding: 1G
Filler Metal Brand Name: LA75-880M Flux Dia. = 5 mm
Filler Metal Classification:
Shielding Gas: Flow Rate:
Nozzle Orifice Size:
Single or Multipass: Multipass (2 pass)
Single or Multiple Arc: Single
Heat Input Requirement (E): ~ 5 kJ/mm
Preheat Temperature: Take away moisture from bar
Interpass Temperature: --
Preheat Method: --

(Indicate material thickness on drawing)

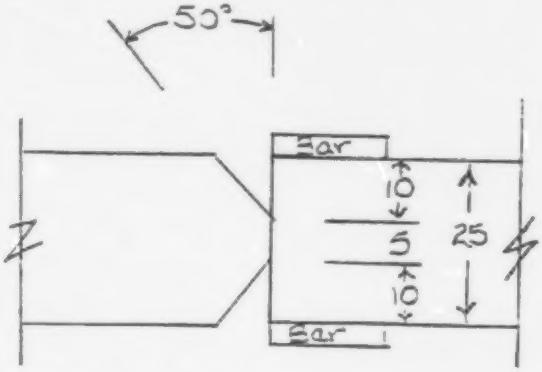

Joint Preparation

Weld Size	Side	Layer	Pass No.	Amps		WFS		Volts		Travel Speed (s)		E.S.O. mm					
				I	Dial	mm/min	Dial	V	Dial	mm/min	Dial						
	1	1	1	780-805		1245		36		305		31					
	2	1	1	1020-1050		1702		38		381		31					
																$E = \frac{I \times V \times 60}{S}$	

Procedure Notes:
① Objective is to obtain a straight HAZ
② with little distortion
③
④
⑤
⑥
⑦

Procedure Application Notes:
①
②
③
④
⑤
⑥
⑦

Date: September 1990
Welders Name: L. Thompson
Inspected By:
Procedure By:

TABLE X: Results of Compact Crack Arrest Tests for HAZ

Temp. (°C)	Spec. No.	Cycles to Failure	Initiation Stress Intensity Factor (MPa√m)	Crack Arrest Toughness (MPa√m)	Validity Check	Invalidity Code*	Comment
0	4	9	--	--	Invalid	4	No crack jump
	5	5	--	--	Invalid	4	No crack jump
	6	9	200.2	62.0	Invalid	1	Insuff.remaining ligament(16mm instead of 25mm min.)
	10	8	--	--	Invalid	4	No crack jump
	11	7	--	--	Invalid	4	Insuff. crack jump; out of plane tunnelled crack front
	18	5	--	--	Invalid	4	No crack jump
	19	8	223.5	75.6	Invalid	1	Insuff. remaining ligament(12mm instead of 25mm min)
-20	1	2	101.4	85.3	Invalid	4	Insufficient crack jump
	2	1	100.6	91.4	Invalid	4	Insufficient crack jump
	3	3	133.6	--	Invalid	--	Crack tunnelled into base material
	13	8	151.6	50.9	Invalid	1	Insuff. remaining ligament(14mm instead of 25mm min)
	16	2	107.4	87.6	Invalid	4	Insufficient crack jump
	17	7	196.8	--	Invalid	4	No crack jump
-40	7	1	78.7	65.5	Invalid	4	Insufficient crack jump
	8	2	96.2	--	Invalid	--	Crack deviated into base material
	9	5	156.0	37.4	Invalid	1	Insuff. remaining ligament(14mm instead of 25mm min)
	12	1	97.6	78.6	Invalid	4	Insufficient crack jump
	14	1	87.7	74.8	Invalid	4	Insufficient crack jump
	15	1	87.9	--	Invalid	4	Insufficient crack jump; deviation into base material

*Invalidity Codes

1 $W-A_a>0.15W$
2 $W-A_a>(Ka/YS_d)^2$
3 $B>(K_a/YS_d)^2$
4 $A_a-A_o>2N$
5 $A_a-A_o>(K_a/YS_d)^2$

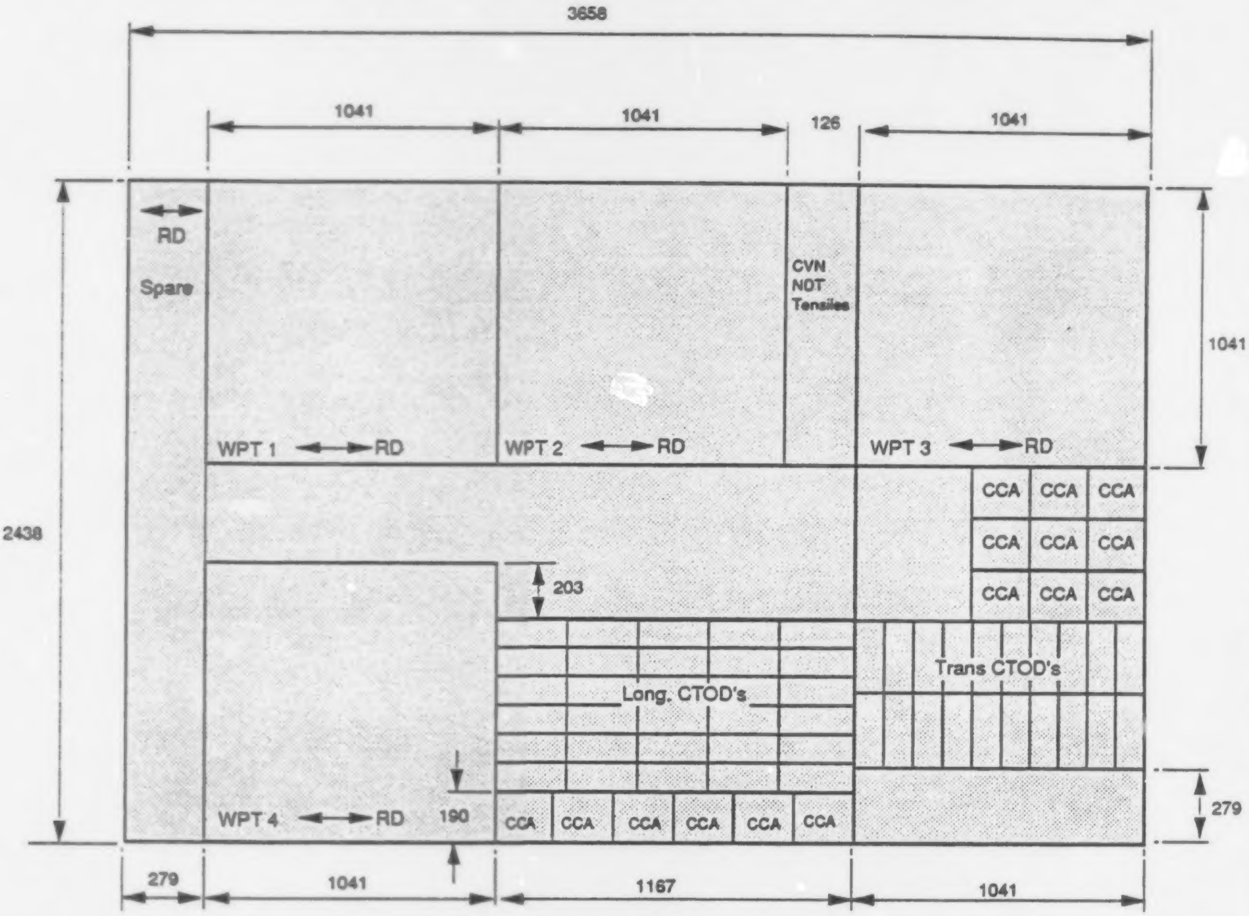
3658
1041
1041
126
1041
RD
Spare
CVN
NDT
Tensiles
1041
WPT 1 RD
WPT 2 RD
WPT 3 RD
2438
CCA CCA CCA
CCA CCA CCA
CCA CCA CCA
203
Trans CTOD's
Long. CTOD's
279
WPT 4 RD
190
CCA CCA CCA CCA CCA CCA
279
1041
1167
1041

Figure 1 (a): Plate 1 Blanking Scheme for extracting Specimens for Base Material Tests (WPT - Wide Plate Tests; CCA - Compact Crack Arrest Tests). *(all dimensions in mm)*

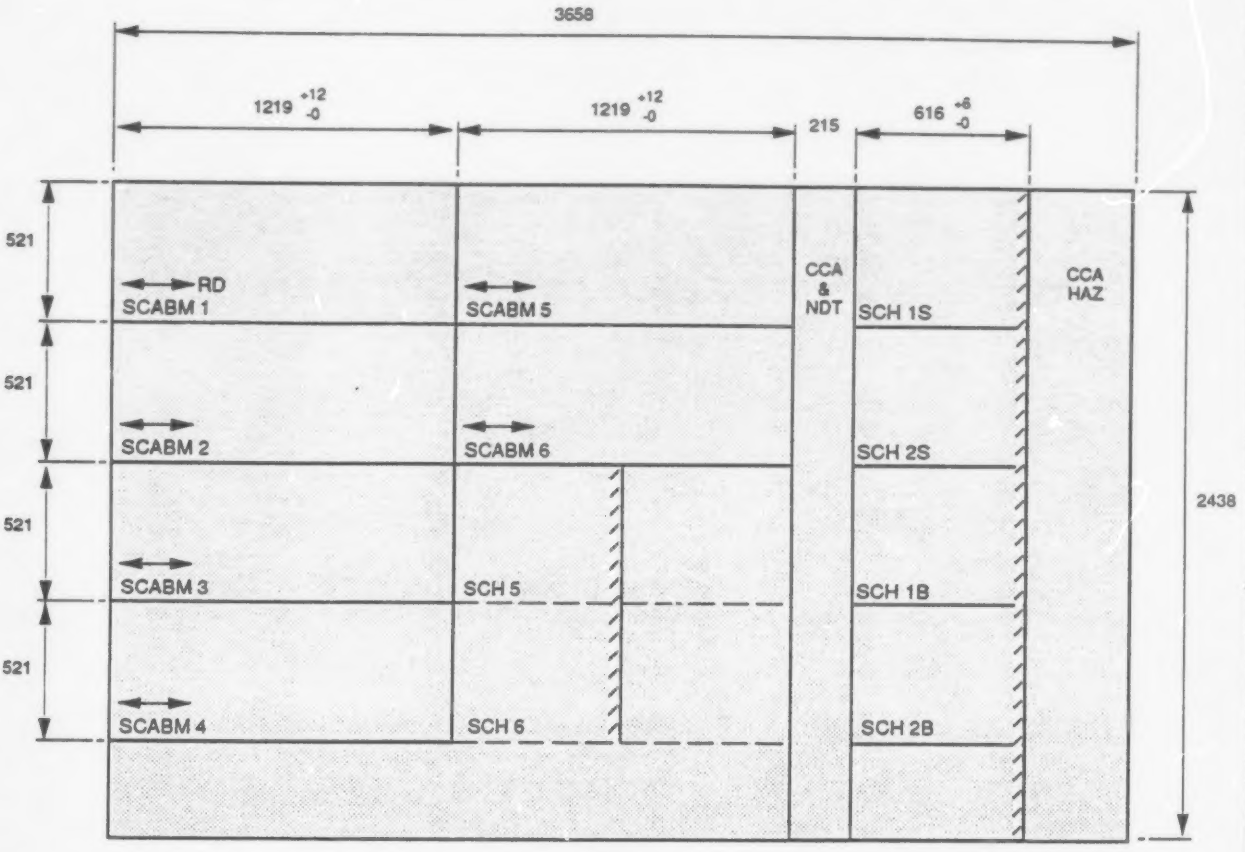
3658
1219 +12 -0
1219 +12 -0
215
616 +6 -0
521
521
521
521
2438
RD
SCABM 1
SCABM 2
SCABM 3
SCABM 4
SCABM 5
SCABM 6
SCH 5
SCH 6
CCA & NDT
SCH 1S
SCH 2S
SCH 1B
SCH 2B
CCA HAZ

Figure 1 (b): Plate 2 Blanking Scheme (SCABM → Short Crack Arrest Test, Base Material; SCH → Short Crack Arrest Test, HAZ; S indicates Straight Side HAZ; B Indicates Bevel Side HAZ; CCA → Compact Crack Arrest Test for Base Material)

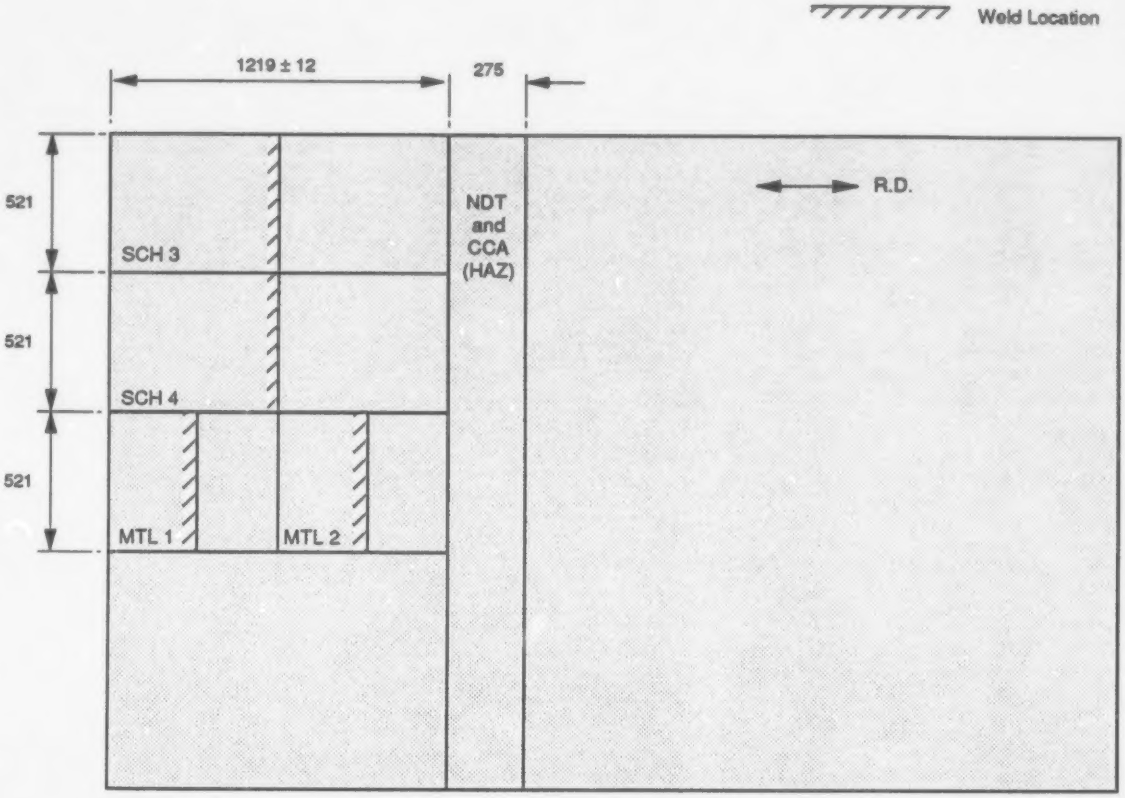
Weld Location
1219 ± 12
275
R.D.
521
521
521
SCH 3
SCH 4
MTL 1
MTL 2
NDT
and
CCA
(HAZ)

Figure 1 (c): Plate 3 Blanking Scheme (SCH → Short Crack Arrest Test, HAZ; MTL → Smaller Welds for MTL for HAZ Characterization)

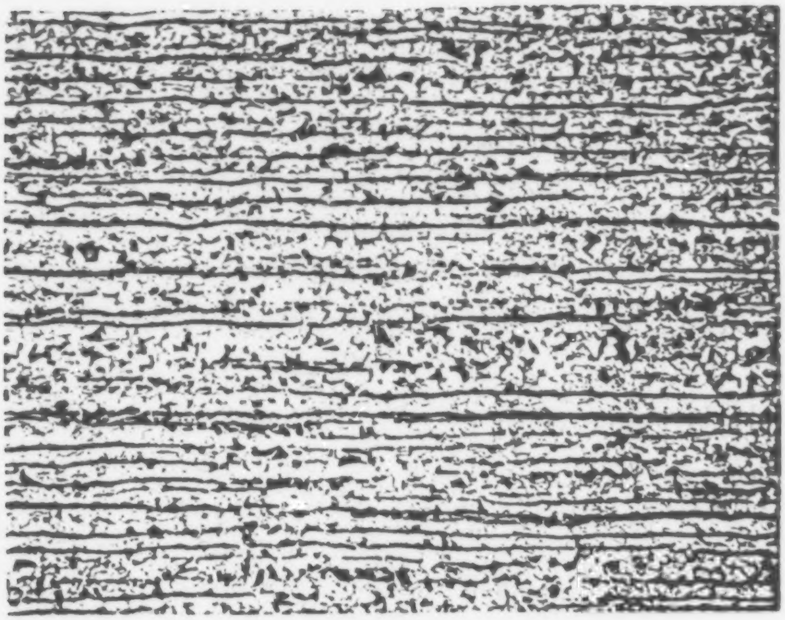

Figure 2: **The microstructure of the steel investigated in the program (Neg. 11905, X100)**

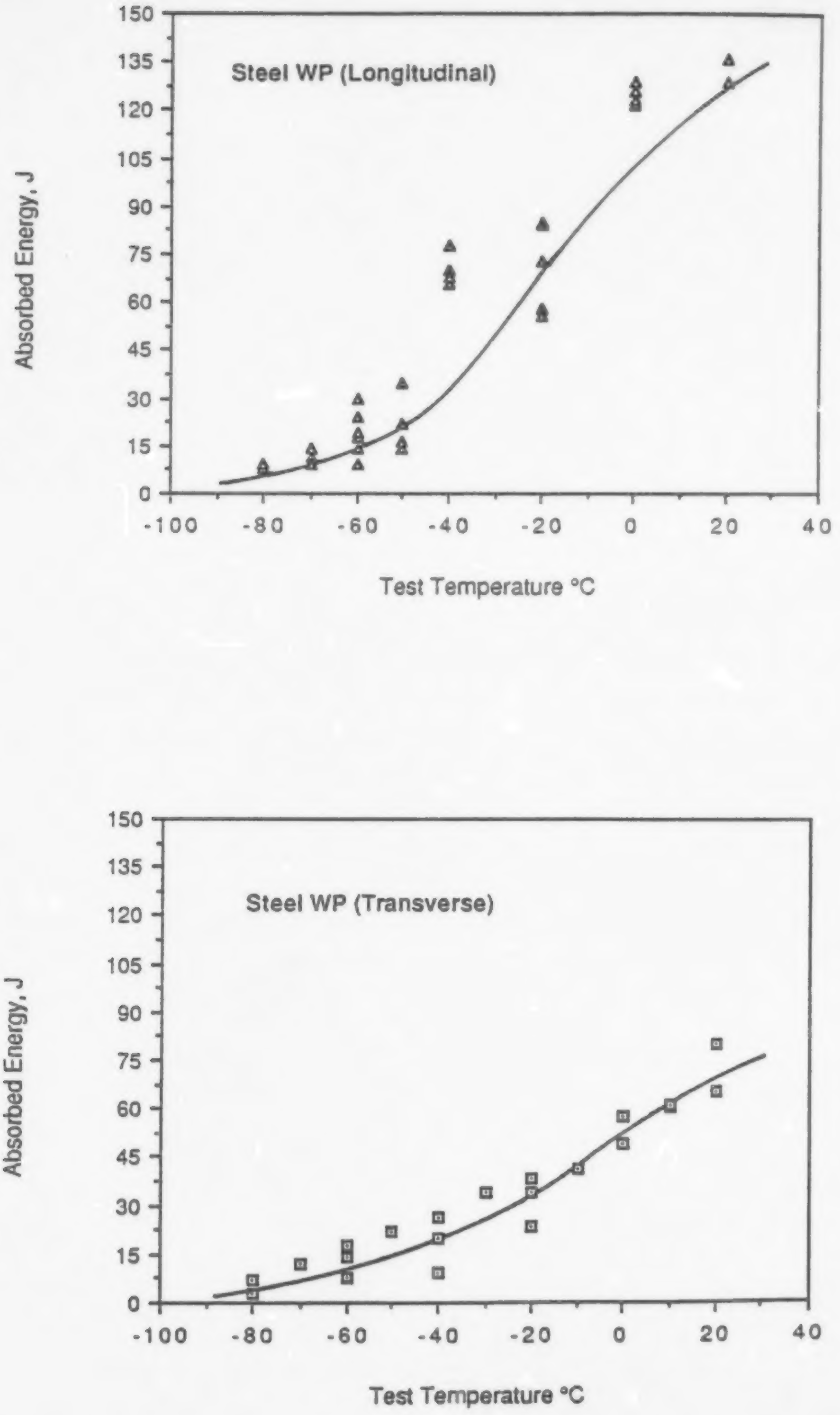

Figure 3: CVN transition curves for the Steel WP

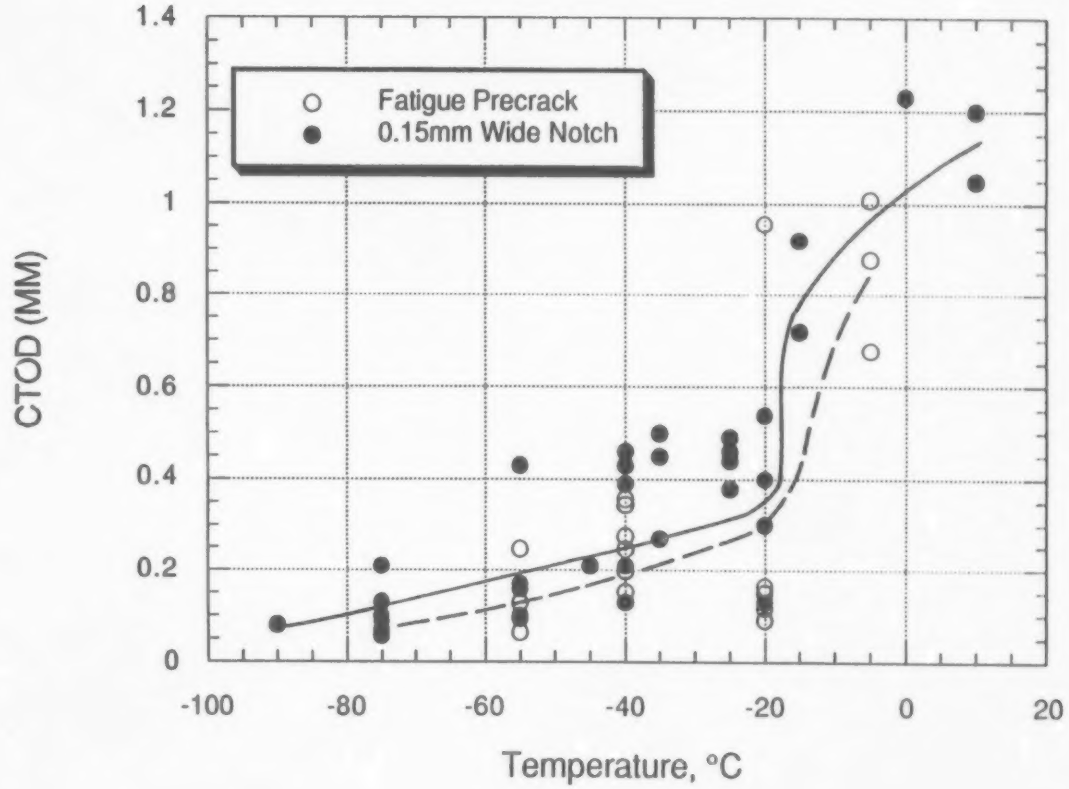

Figure 4: CTOD transition curves for the Steel WP, using 0.15mm wide saw notch or a fatigue precrack

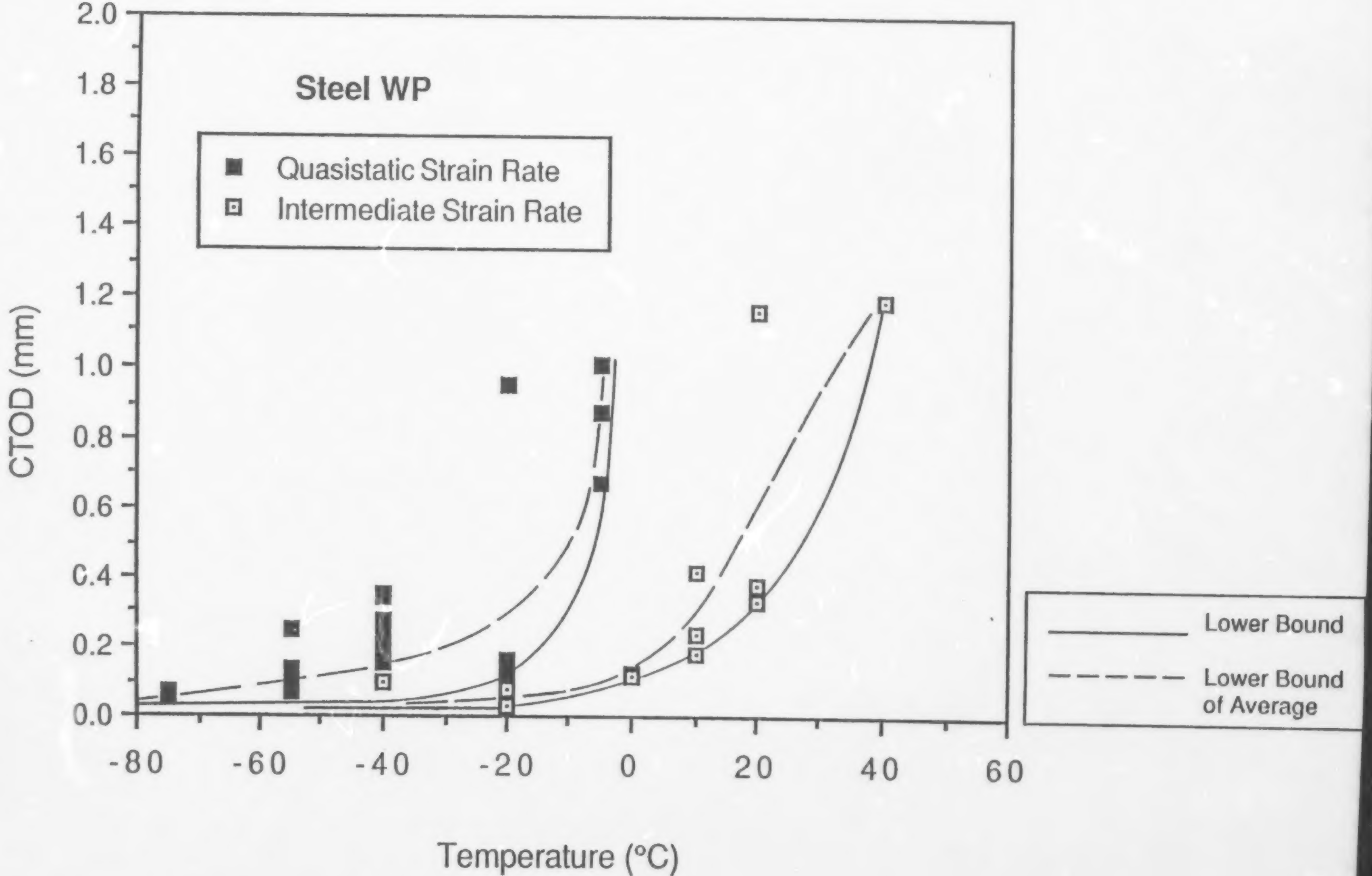

Figure 5: CTOD transition curves for the Steel WP at quasistatic and intermediate loading rates - specimen with fatigue precrack (from Ref. 2)

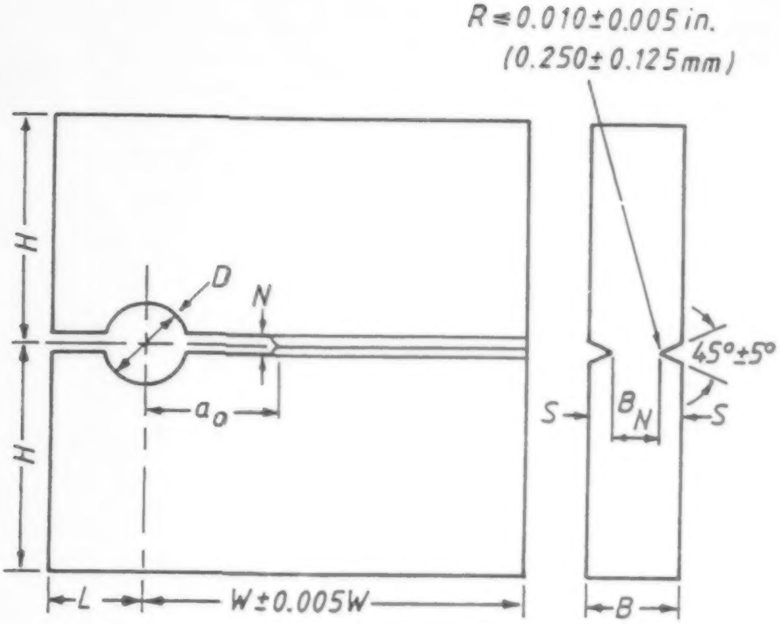
R ≤ 0.010±0.005 in.
(0.250± 0.125 mm)
H
H
D
N
a_0
45°±5°
S
B_N
S
L
W±0.005W
B

$H = 0.6\,W \pm 0.005W$

$S = (B - B_N)/2 \pm 0.01B$

$N \leq W/10$

$0.15W \leq L \leq 0.25W$

$0.30W \leq a_0 \leq 0.40W$

$0.125W \pm 0.005W \leq D \leq 0.250W \pm 0.005W$

B	W	H	N	L	D	S	a_o
25	165.0	99.0	12.7	33.0	31.5	3.175	57.9

Figure 6: **Dimension of the crack arrest specimens used in the investigation (reproduced from Ref. 6)**

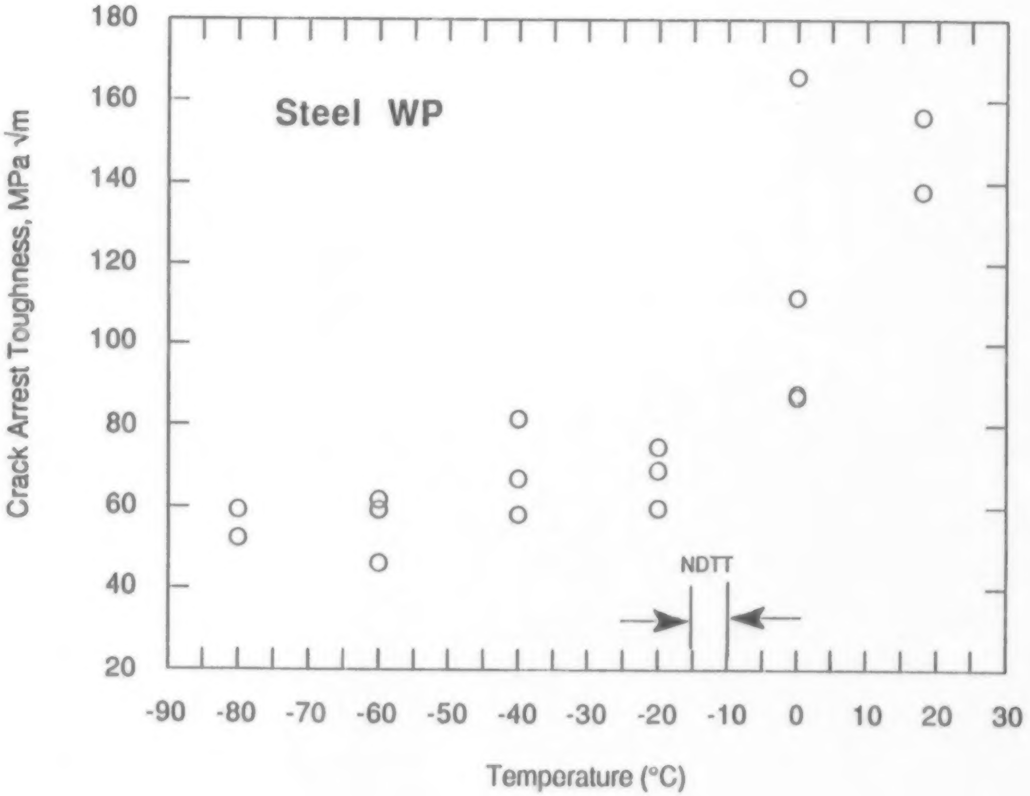

Figure 7: Compact Crack Arrest Toughness of Steel WP at Various Temperatures

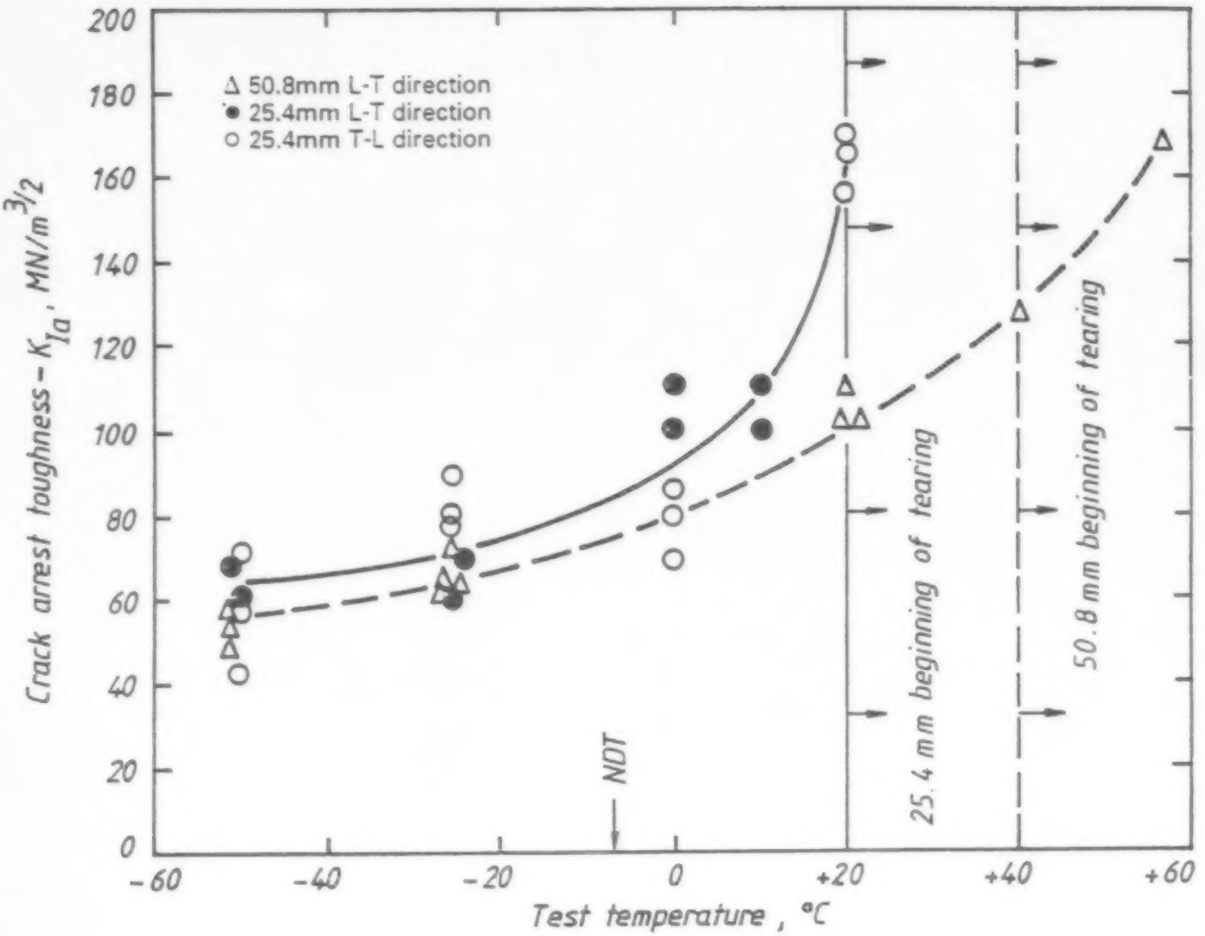

Figure 8: Effect of test temperature on the crack arrest toughness of A36 steel (reproduced from Ref. 6)

Figure 9: Cross-section from the weld made using the finalized procedure (Neg. 12073)

(a)

(b)

(c)

Figure 10: Longitudinal cross-sections at the centre of brittle beads in NDT specimens.

(a) square notch, tested at -40°C (Neg. 12757)
(b) Vee notch, tested at -15°C (Neg. 12756)
(c) Vee notch, tested at -10°C (Neg. 12755)

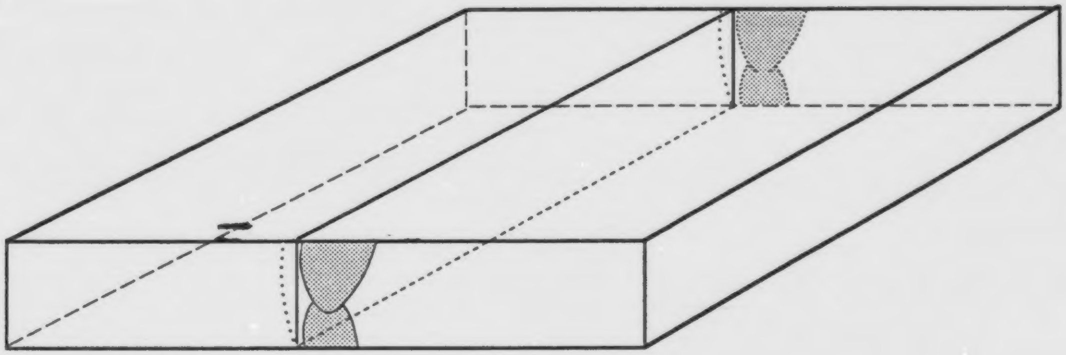

Figure 11: Locating the Mid-frame for the HAZ CCA Specimen

1 cm
#15, (-40°C)
1 cm
#8, (-40°C)
1 cm
#2, (-20°C)

Figure 12: **Insufficient crack jump in HAZ CCA specimens (Neg. 12672, 12670 and 12667)**

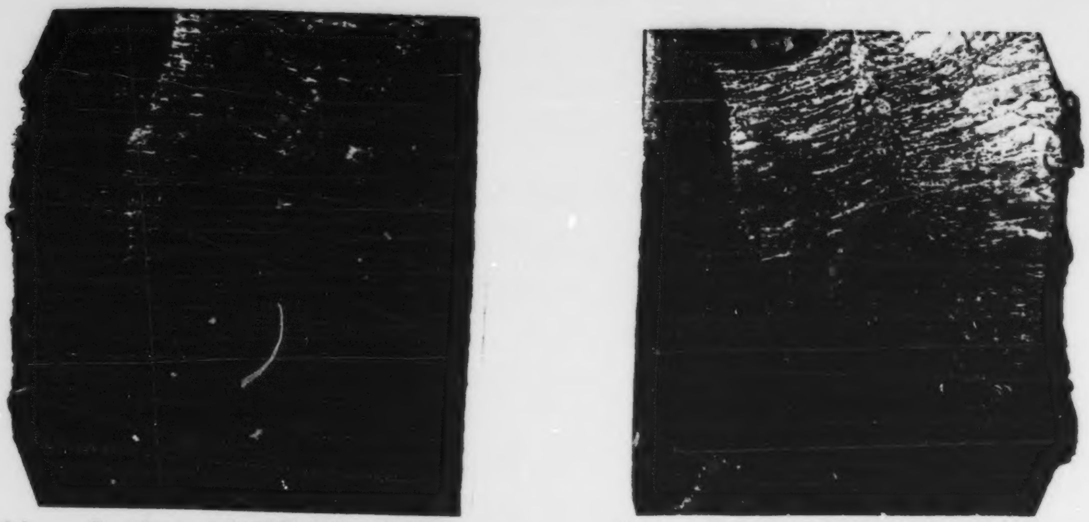

(a) Specimen 2 (-20°C) (Neg. 12677)   (b) Specimen 4 (0°C) (Neg. 12683)

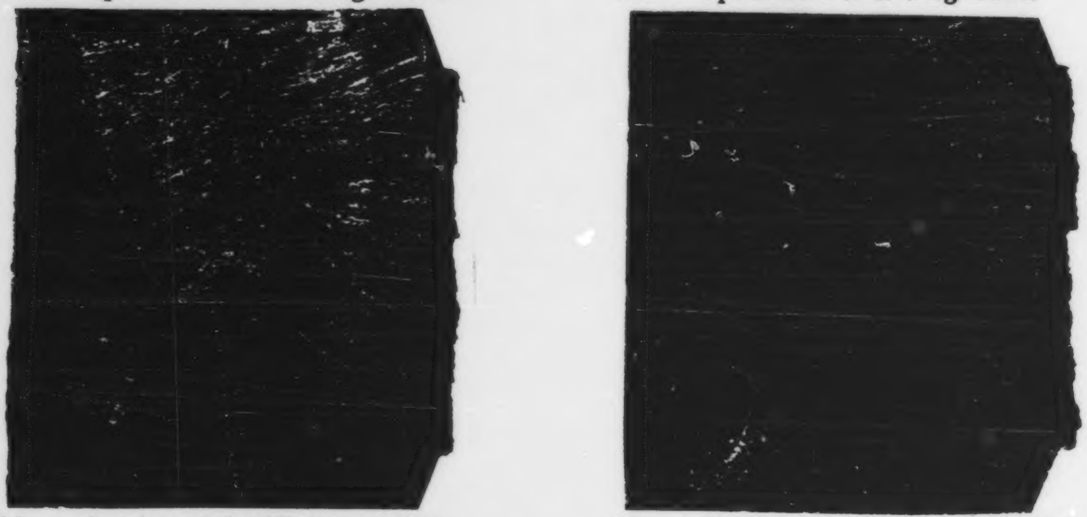

(c) Specimen 7 (-40°C) (Neg. 12681)   (d) Specimen 8 (-40°C) (Neg. 12675)

(e) Specimen 12 (-40°C) (Neg. 12690)   (f) Specimen 17 (-20°C) (Neg. 12685)

Figure 13: The injected crack path, ≈5 to 7mm from the brittle weld bead in specimens showing insufficient crack jump (Mag. X3.3)

1 cm
#3, (-20°C)
1 cm
#11, (0°C)

Figure 14: Crack tunnelling in HAZ CCA Specimens 3 and 11 (Neg. 12668, 12674)

(a) Specimen 3 (-20°C) 5-7mm from the brittle bead (Neg. 12678)

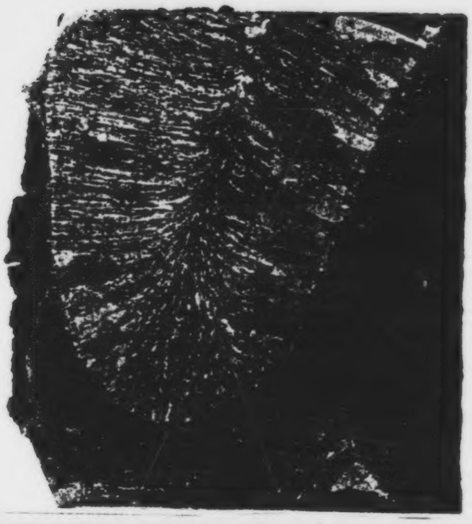

(b) Specimen 11 (0°C) 5-7mm from the brittle bead (Neg. 12682)

Specimen 11 (0°C) Section through the tunnelled portion of the crack (Neg. 12689)

Figure 15: The crack path in HAZ CCA specimens showing tunnelling (Mag. X3.3)

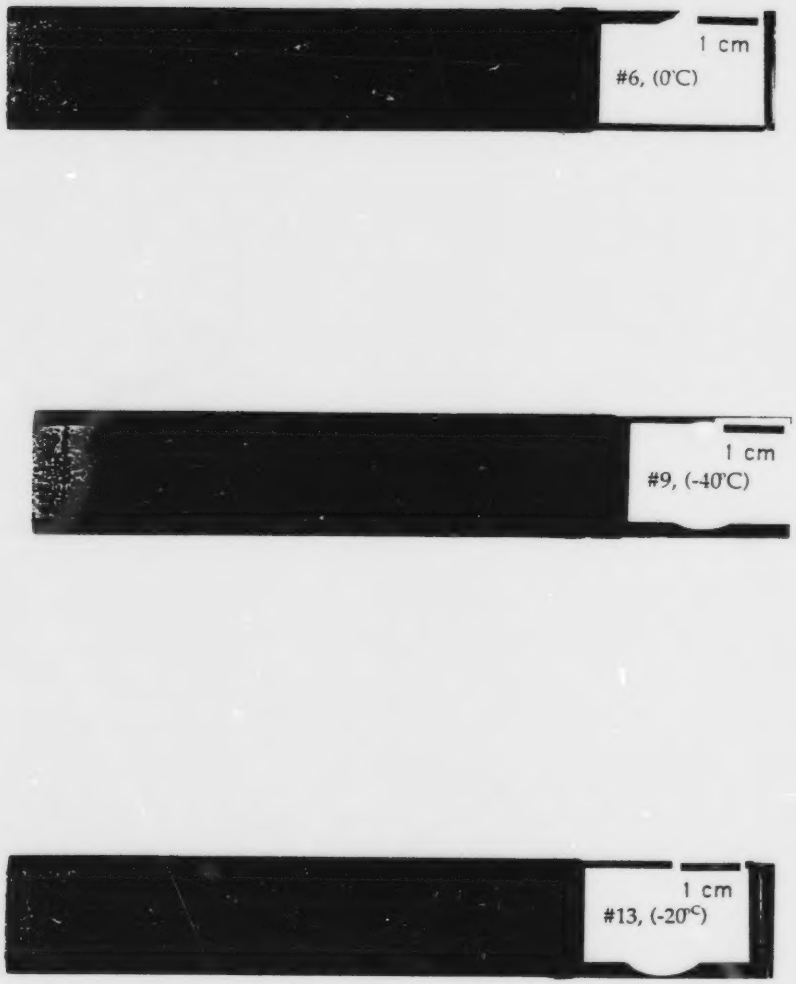
1 cm
#6, (0°C)
1 cm
#9, (-40°C)
1 cm
#13, (-20°C)

Figure 16: HAZ CCA specimens showing insufficient remaining ligament (Negs. 12673, 12671 and 12669)

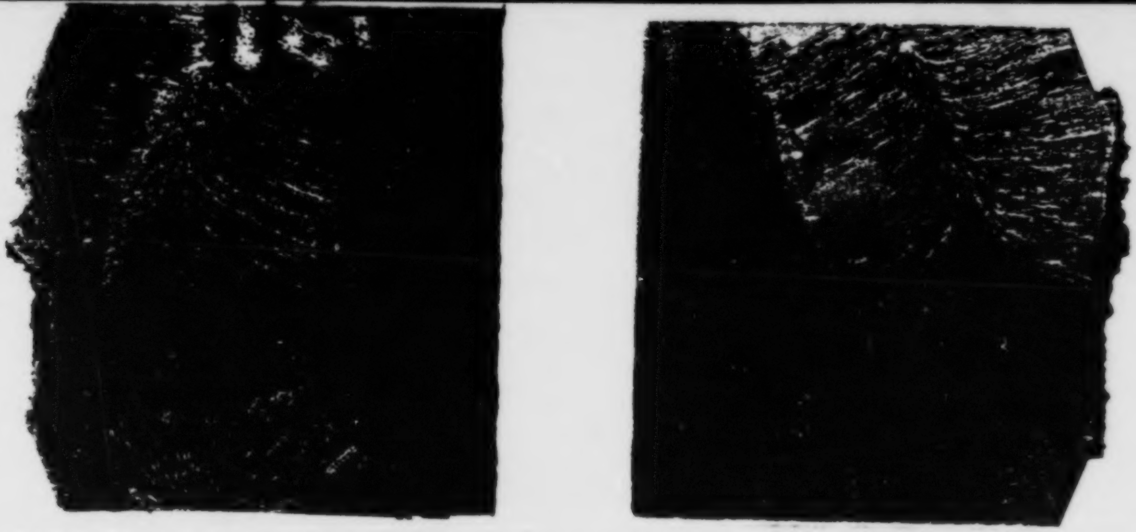

(a) Specimen 6 (0°C) (Neg. 12679) (b) Specimen 6 (0°C) (Neg. 12687)

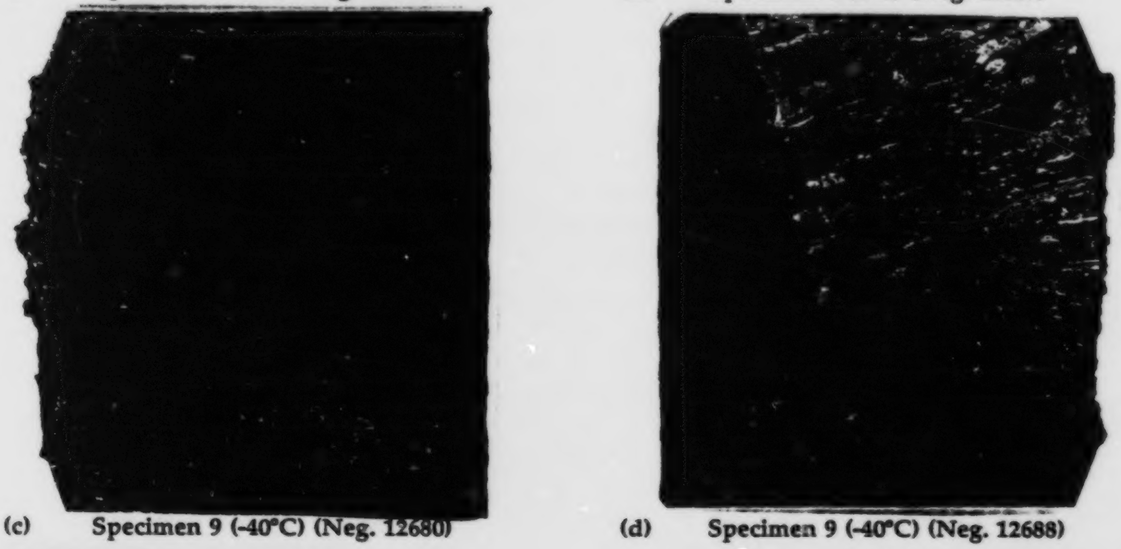

(c) Specimen 9 (-40°C) (Neg. 12680) (d) Specimen 9 (-40°C) (Neg. 12688)

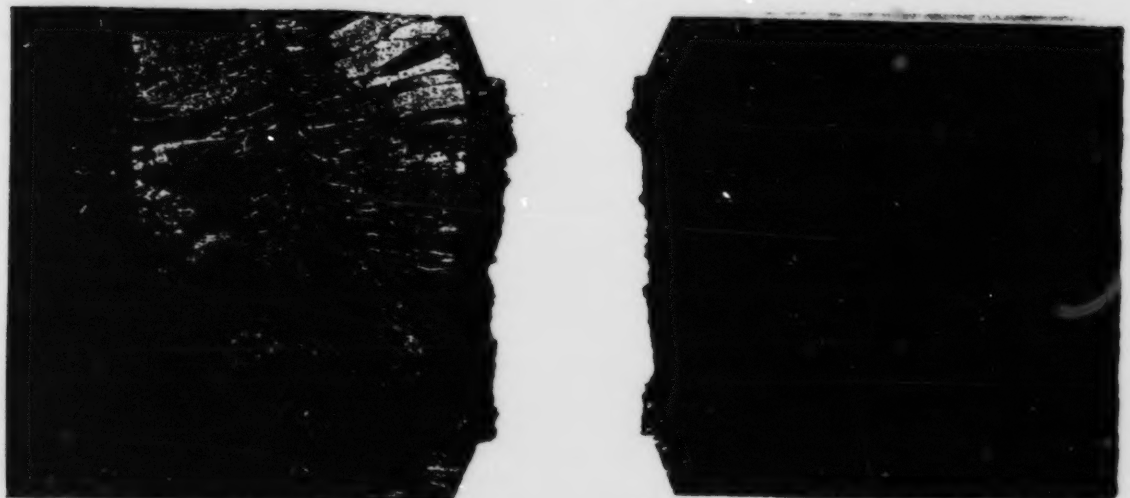

(e) Specimen 13 (-20°C) (Neg. 12684) (f) Specimen 13 (-20°C) (Neg. 12691)

Near Initiation Near Arrest

Figure 17: Crack path near initiation and near arrest in HA CCA specimens 6, 9 and 13 (Mag. X3.3)

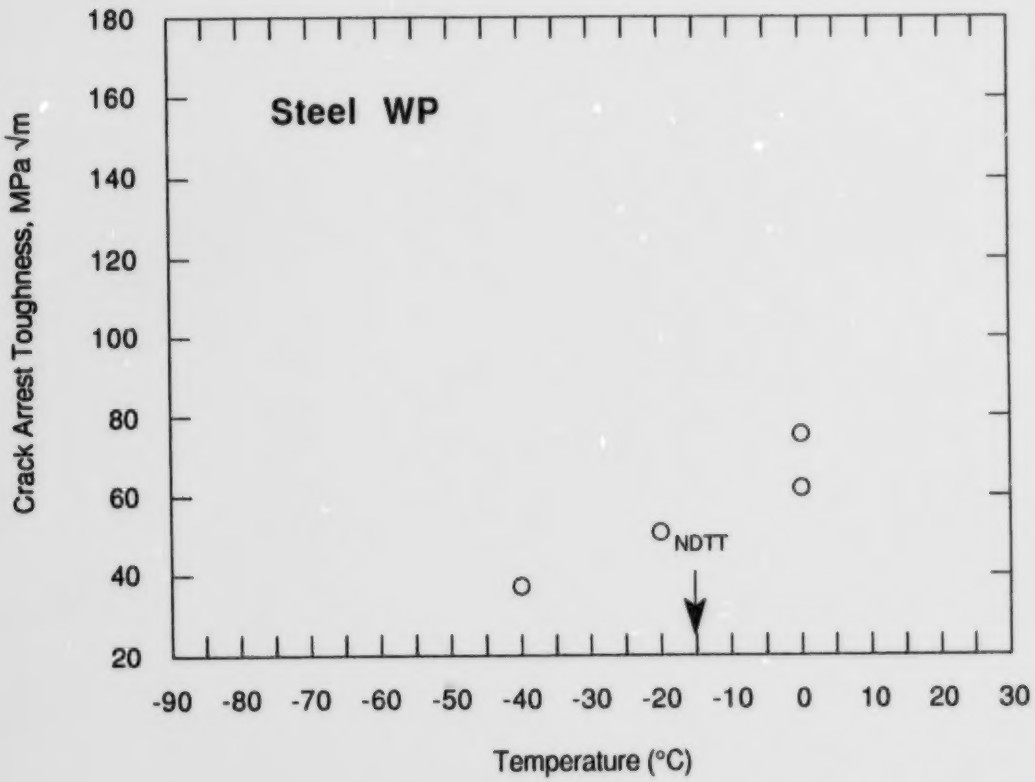

Figure 18: Compact Crack Arrest Toughness of the HAZ in the Steel WP, Based on Specimens with Insufficient Remaining Ligament Only

APPENDIX B

WIDE PLATE TESTS - PROCEDURES AND RESULTS.

WELDING INSTITUTE OF CANADA
INSTITUT DE SOUDAGE DU CANADA

STUDY OF WIDE PLATE TESTING OF STRUCTURAL STEELS FOR ARCTIC SHIPS

TASK 4

Welding Institute of Canada Report RC 391/1/1990

Final Report to Task 4
Fleet Technology Limited Ref: E93728P

Submitted to
Materials Technology Centre
Fleet Technology Limited
311 Legget Drive
Kanata, Ontario
K2K 1Z8

Prepared by
S.R.Bala, P.Eng.
Research Engineer
Materials Technology

JUNE 1990

HEAD OFFICE / SIEGE SOCIAL: 391 Burnhamthorpe Road East, Oakville, Ont. L6J 6C9 — Ph: (416) 845-9881 Fax: (416) 845-9886
CENTRE DU QUEBEC / QUEBEC CENTRE: 325 Ruy Mond Dupuis Boul., Mont-St-Hilaire, Que. J3H 5H6 — Ph: (514) 446-3053 Fax: (514) 446-3055

TABLE OF CONTENTS

EXECUTIVE SUMMARY

1.0 INTRODUCTION 1
1.1 The Rolfe Approach 1
1.2 The NKK Approach 2
1.3 Fracture Control for Arctic Ships 3
2.0 OBJECTIVES 5
3.0 EXPERIMENTAL PROCEDURE 5
3.1 Material 5
3.2 Wide Plate Tests 6
3.2.1 Loading End Attachments 6
3.2.2 Through Thickness Defect and Instrumentation 7
3.2.3 Cooling and Wide Plate Testing 8
3.2.4 Fractography 10
4.0 RESULTS 10
4.1 Strain Gauge Readings for the Wide Plate Tests 10
4.2 Crack Tip Opening Displacement Values 14
4.3 Fractography 15
5.0 ACKNOWLEDGEMENTS 15
6.0 REFERENCES 15

APPENDIX A

APPENDIX AA

STUDY OF WIDE PLATE TESTING OF STRUCTURAL STEELS FOR ARCTIC SHIPS

Task 4, MTC, Fleet Technology Limited Project E93728P

Welding Institute of Canada Report RC 391/1/1990

to

Fleet Technology Limited

EXECUTIVE SUMMARY

Welded structures and marine vessels operating in the Arctic regions must have high reliability to withstand the harsh service conditions because structural failure can cause a substantial risk to life and environment. To minimize the risk of failure an appropriate fracture control plan has been developed in the latest steel toughness specifications of the Canadian Coast Guard's CASPPR Schedule 3. These toughness specifications have been developed from empirical relations developed in Japan. The objective of the present program is to perform wide plate brittle fracture initiation tests to validate the structural steel toughness requirements in CASSPR Schedule 3. An analysis of these wide plate test results will be compared with the Schedule 3 toughness requirements to ensure the latter are satisfactory.

The experimental procedures for the 4 wide plate tests carried out on 25 mm thick ABS DH36 steel at 4 different temperatures and the results obtained are presented in this report. Further analysis and interpretation of the results will be carried out at Fleet Technology Limited.

STUDY OF WIDE PLATE TESTING OF STRUCTURAL STEELS FOR ARCTIC SHIPS

Task 4, MTC, Fleet Technology Limited Project E93728P

Welding Institute of Canada Report RC 391/1/1990

to

Fleet Technology Limited

1.0 INTRODUCTION

The design criteria and toughness specifications for ship structures vary from organization to organization and country to country. Increasingly, efforts are being made to rationalize and, if necessary, modify the toughness requirementsbased on fracture mechanics analysis. The two notable efforts in this regard have been presented by Rolfe et al (1) and by N.K.K. (2) to International Association of Classification Services.

1.1 The Rolfe Approach

The basic premise of the scheme presented by Rolfe et al (1) is that the ship hull can be subjected to dynamic loads of yield point magnitude when the effects of residual stresses and strain concentration are included and that there is a significant probability of large undetected through thickness flaws existing in the ship at some time during the life of the ship. Therefore, to prevent catastropic failures, they recommended a two pronged approach - design against unstable fracture initiation and design for long crack arrest.

To maintain a fail-safe philosophy, these authors also require incorporation of properly designed crack arresters fabricated from steels with a very high level of dynamic notch toughness. Since the actual measurement of dynamic toughness (2,3) above the limits of plane strain behaviour is expensive and difficult if not impossible, the steel toughness requirements have been presented in terms of absorbed energy at the minimum design temperature in 16 mm thick dynamic tear specimens.

1.2 The NKK Approach

This approach is formulated by the Japanese Classification Society NKK (Nippon Kaiji Kyokai) in 1979 and is based on wide plate test (centre-notched tension tests) results for ship steels.

The suitability of a steel based on its CVN toughness specification for any particular location or structural member of the ship structure is judged in two stages. First, its minimum fracture toughness is estimated and next it is compared to the fracture toughness requirement for that location. The steps involved in calculating the minimum fracture toughness can be summarized as follows:

i) An energy transition temperature (T_E) is estimated for CVN absorbed energy (EN_T) at the test temperature T_t.
ii) The brittle fracture initiation temperature T_i is estimated (wide plate tests) as a function of energy transition temperature (T_E), the steel thickness (t) and yield strength (σ_y).
iii) The fracture toughness K_c (blunt notch) of the steel is estimated.
iv) The fracture toughness K_{cf} (fatigue sharpened notch) is estimated based on an empirical relationship $K_{cf}/K_c = 0.68$.

The fracture toughness K requirement for the structural member is then estimated from

$$K = (\alpha + \beta)\ \sigma_y\ \sqrt{(\pi a)},$$

where, α is the design stress as a fraction of the yield strength σ_y, β is the magnitude of the residual stress as a fraction of σ_y (assumed to be 0.6) and 2a is the defect size (assumed to be 250 mm). Then K is compared to K_{cf} to see if the steel meets toughness requirements.

The approach is essentially used to specify steel grades for various structural members. Though not a part of the steel specification, the approach implicitly assumes that crack arrestors are incorporated in the structure and the steel for these would be capable of arresting long propagating cracks.

1.3 Fracture Control for Arctic Ships

The minimum design temperature for structural members in Arctic Ships that are exposed to the environment (i.e. above the waterline), is understood to be -40° C, compared to 0° C for the ships navigating in open waters.

Application of the Rolfe approach as presented above would require an NDT temperature of ≈ -58° C for a 25 mm thick structural steel plate and implicitly a similar requirement for the heat affected zone and weld metal. With conventionally processed structural steel (IACS Grades A to E steels), it is virtually impossible to obtain such low NDT temperatures. Even accelerated cooled steels, available only from a few offshore mills, could have difficulty in reliably meeting such a requirement. For example, Kawasaki's MACS EH36 steel, 50 mm thick and produced about four years ago, has an NDT temperature of only -55° C (4).

Similarly, the application of the NKK approach for a design temperature of -40° C would require a significant new supply of steels with toughnesses greater than IACS Gr. E (CVN energy specified at -40° C).

All the same this method, with one modification to make it less conservative, is the basis of the current structural steel toughness requirements in the CASPPR Schedule 3. The modification relates to the assumption of $\beta = 0.6$ in the empirical equation used. This was considered to be too conservative.

However, there is some concern that the empirical relationships which are the basis of the NKK approach were formulated more than a decade ago so these need to be confirmed for steels that are produced today using different steel making practices. Thus, there is a need for a verification exercise based on wide plate tests. Secondly, it would be desirable to base the fracture control plan on sounder fracture mechanics principles, taking into consideration service strain rates in service. Also while empiricism in terms of correlations between the results of different fracture tests cannot be completely eliminated, it can be sharply reduced in the NKK approach.

Another approach has evolved through industry-government consensus for toughness requirements. The CSA S473 Draft Standard "Code for the Design, Construction and Installation of Fixed Offshore Structures, Part III - Steel", follows a philosophy of fracture prevention based on a combination of resistance to crack initiation and resistance to crack propagation. For Arctic ship steels, a similar approach would require consideration of:

i) Prevention of initiation of unstable fractures from long fatigue cracks (with tips in base material) at intermediate strain rates mentioned earlier.

ii) Prevention of initiation of unstable fracture from cracks and other tight crack-like flaws in the weld zone.

iii) Short crack arrest capability of structural steel and its heat affected zone.

There is a significant global research effort ongoing on the subject of brittle fracture initiation resistance of weld metals and heat affected zones (5). Most of these programs are quite complex and therefore instead of pinning acceptance on toughness, this approach would focus on quality assurance to minimize the incidence of flaws and only require a certain minimum level of toughness. As a result, there would be a finite but acceptably small probability of brittle fracture initiation in the weld zone.

Once the possibility of brittle fracture initiation from small flaws in the weld zone is accepted, then flaws perpendicular to the weld axis will need to be arrested in the base material. The steel toughness requirement for arresting relatively small cracks would of course be less than that for arresting long cracks. In the literature, there are only a limited number of publications which have looked at short crack arrest capability for steels and fewer still for heat affected zone. It is therefore apparent that to verify and further develop the structural steel toughness requirements in CASPPR Schedule 3, the short crack arrest capability of structural steels and their weld heat affected zones need to be investigated by wide plate tests. Also a few wide plate tests should be run to verify their resistance to brittle fracture initiation from long cracks.

2.0 OBJECTIVES

In light of the above, the prime objective of this program was to perform wide plate tests for assessing brittle fracture initiation resistance and to validate the structural steel toughness requirements in CASPPR Schedule 3. This was done primarily by comparing the predictions based on analysis of these tests with the Schedule 3 requirements.

In this report the experimental procedure for wide plate brittle fracture initiation tests is described and the results are given.

3.0 EXPERIMENTAL PROCEDURE

3.1 Material

The steel used for the wide plate test program was 25 mm thick ABS DH36. This steel was supplied by Algoma Steel Corporation. The tensile and toughness properties of the steel, from Algoma, were reported to WIC by Fleet Technology Limited and are given in Tables 1 and 2.

Four plates, approximately 1 m x 1 m in size, were cut for the wide plate tests. The rolling direction was marked on each plate.

3.2 Wide Plate Tests

3.2.1 Loading End Attachments

To perform the wide plate test, the test plate first had to be secured to loading end attachments. This was done in a special alignment jig which consisted of a platform with horizontal and vertical I-beam supports as shown in Figure 1.

The loading end attachment consists of a 140 mm thick steel plate with two steel lugs welded symmetrically on each side of the plate. The loading surface of each lug is perpendicular to the plate surface. Each lug has a hole where the centre rod from the loading capsule of the wide plate test rig is inserted for performing the test. The lugs are positioned and machined to exactly line up with and fit the loading capsules of the wide plate test rig (Figure 9). The plates of the two end attachments, that are to be welded to the test plate, are placed vertically on the horizontal I-beam and the free ends of the attachments are pushed against the vertical I-beams and the lugs are strapped loosely against these I-beams. The ends of the plates of the attachments, to be welded to the wide plate, are reduced in thickness to 50 mm and rested on rollers. The roller heights can be adjusted using four vertical bolts attached to the rollers. The bottom lugs are supported by hydraulic jacks. The loading surfaces are adjusted to the vertical by using the jacks and the support rollers. This is checked by a spirit level and plumb line. The bottom horizontal I-beam can be moved along the length of the platform and fastened by bolts. Fine movement, horizontal or angular, of the horizontal I-beams can be made using two horizontal bolts.

In each test the loading ends were first aligned. The plate surfaces and the loading surfaces of the lugs were adjusted to the vertical using the roller support, the jacks and the horizontal movement of the I-beams. After checking the verticality with the spirit level, the alignments of the loading end plates were accomplished by keeping the distance between the holes of the lugs corresponding to the same loading capsule to be same (2500 mm). Also, the alignment of the plates was checked by measuring the diagonal distance between the holes of the top four and bottom four lugs. After alignment, the loading ends were strapped and secured tightly against the vertical I-beams to prevent movements that might be caused by welding.

The wide plate was placed vertically in between the loading ends such that the rolling direction of the test plate was horizontal i.e. parallel to the loading axis. The ends of the test plate being welded to the loading end attachments were bevelled to 45° for a K-prep. (Figure 2). The central axis of the plate was lined up symmetrically with the central axis of the 50 mm thick plates of the loading end attachments. Standard welding parameters with CLA LA T-91 wire were used for FCAW. The first wide plate was welded by two welders, one on each end of the plate, on opposite sides of the plate. Three other wide plates were welded by two welders, simultaneously welding the same joint on opposite sides of the plate (Figure 3). The welding parameters used and the bead sequencing are given in welding data sheets 1 and 2. Once a plate was welded, the effects of welding distortion were determined i.e. the plate axiality with the loading end attachments and the distance between the loading faces of the lugs belonging to the same capsule were measured. A deviation in axiality and a difference in the distance between the loading faces belonging to each capsules of < 6 mm was observed in all four tests. The deviation and the difference were less than those usually encountered in previous wide plate test programs for 50 mm thick plates. After the test plate was welded its width was symmetrically cut to 940 mm.

3.2.2 Through Thickness Defect and Instrumentation

A 250 mm long through thickness defect was saw cut in each of the test plates to obtain centre cracked panels (CCP) using a power saw from an initial centrally drilled 20 mm diameter hole. The final 4-6 mm at the defect tip were cut using a 0.15 mm thick saw blade (Figure 4).

Three 6 mm (quarter inch) strain gauges were put on each side of the defect on both sides of the plate. An information sheet on the strain gauges is attached to the Appendix. Strain gauges were also attached 350 mm away from the defect axis: one at the central loading axis and two spaced equally at 300 mm from the central loading axis. Copper-constantan thermocouples were attached to the surface of the test plate using a "Devcon plastic" bonding cement. The strain gauge and thermocouple locations are shown schematically in Figures 5 and 6. Figure 7 shows the wide plate with the sawed-in defect and instrumentation.

The strain gauges and the thermocouples were connected to the Hewlett Packard data acquisition system. Also some of the thermocouples were connected to a manual monitoring system for quick access to the temperature readings. Six clip gauges, three on each side of the plate, were used for measuring the crack mouth opening displacements (CMOD). The clip gauges were mounted through knife edges screwed into the plate. The clip gauge locations are shown in Figure 8. Five of the six clip gauges were connected to the data acquisition system to monitor the CMODs. One of the clip gauges at/or near the crack tip was connected, through the data acquisition system, to the strip chart recorder. All the clip gauges were calibrated at room temperature (Tables AA3, AA10 and AA14).

3.2.3 Cooling and Wide Plate Testing

A 500 mm wide styrofoam cooling box (chamber) was attached to the test weld location of the wide plate (Figure 9). The box contained inlet and outlet ports to channel the liquid nitrogen vapours through the box and along the plate surface in the defect location.

The test plate assembly was placed in the wide plate test rig shown in Figure 9 and the loading lugs were aligned with the loading capsules as shown in Figures 10 and 11. Pre-calibrated LVDTs were mounted on each of the loading capsules so as to measure the strokes of the loading cylinders. The strain gauge, thermocouple, clip gauge and LVDT connections were made for monitoring the data in a data acquisition system as mentioned earlier.

The features of the wide plate test rig are given in Table 3. The hydraulic system shown in Figure 12 is operated pneumatically by high pressure nitrogen gas and is connected to the loading capsules after purging the line. The pressure applied to the capsules is measured precisely using a pressure transducer connected to a voltage monitoring system and a dial gauge. Both the pressure transducer and the dial gauge were calibrated up to 10 ksi prior to each test using a dead weight calibrator after the first test and before tests # 2, 3 and 4. The dead weight pressures and the corresponding pressure transducer voltage outputs are given in Tables AA1, AA5, AA8 and AA12 in Appendix AA. The pressure transducer output and output from one of the clip gauges (CG # 3) were continuously monitored in a strip chart recorder. Once the pressure calibration was done, the cooling chamber was connected to the liquid nitrogen vapour circulation system. The liquid nitrogen was passed through a centrifugal pump circulation system which blows and circulates the cold vapours from liquid nitrogen into the cold box thus cooling the test section. Figure 11 shows the complete wide plate test assembly. The temperature of the test section was monitored continuously and controlled manually within ± 2° C of the test temperature.

When the test section reached a stable test temperature, as indicated by the thermocouples, the strain gauges, LVDTs and clip gauges were zeroed under zero pressure loading for test # 1 (tested at -75° C). For tests # 2, 3 and 4, when the test temperature stabilized, the plate was preloaded to a pressure of 1000 psi to remove slack and then unloaded to zero pressure. The strain gauges, LVDT and clip gauges were zeroed at zero pressure. The test temperatures for tests # 1 to 4 were -75°, -40°, -20° and -55° C respectively. The temperature distribution and the temperature variation recorded during the test are given in Tables A1 to A4.

After zeroing the instrumentation, each test plate was loaded manually in steps of 250, 500 or 1000 psi pressure increments (Figure 12). With dial gauge readings as a rough guide the calibrated pressure transducer voltage outputs were used for precision loading. The pressure readings based on the transducer are stated in the report and were used to preload and pressure increments during the test. At each pressure increment the pressure transducer voltage, the strain gauge, thermocouple, LVDT and clip gauge readings were recorded. The LVDT readings were used only to compare the strokes of the loading capsules during the test. Each test was continued till fracture of the plate occurred. As soon as the plate fractured, the pressure and clip gauge readings at the verge of fracture were written down from the strip chart recorder. The cold box was removed from the plate and the fracture surfaces were sprayed with WD-40 fluid to prevent rusting. The fractured plate was then removed from the test rig (Figure 13).

3.2.4 Fractography

The fracture surfaces were extracted from the wide plate by cutting the plate approximately 50 mm away from the fracture surface parallel to the defect length. The average defect length 2a was measured for each wide plate and initial tearing if any at the defect tip was recorded.

4.0 RESULTS

4.1 Strain Gauge Readings for the Wide Plate Tests

The strain gauge readings recorded at each jack pressure level during the course of the wide plate tests are given in Tables A5 to A12 (Appendix A). For each test, the strain gauge readings are plotted against the jack pressure in Figures 14 to 20. In these tables and figures the jack pressures reported were calculated by converting the pressure transducer voltage output into psi using the respective dead weight calibration Tables (Tables AA2, AA6, AA9 and AA13 in Appendix AA). Each test showed that, at any jack pressure, the strains indicated by all the 12 strain gauges were different. This can be attributed to both the distortion due to welding and slight misalignment of the plate with loading ends giving rise to uneven distribution of the loads resulting in bending. The middle gauges along the central loading axis yielded lower strain values than the corresponding side gauges. This was due to the shadow effect from the defect yielding the lower strain values in the middle gauges. The jack pressure at fracture was taken from the strip chart record. Strain gauge readings at fracture were determined by extrapolating the strain vs pressure curves to fracture pressure (recorded from strip chart recorder). For each strain gauge, the curvature of the last 3 or 4 points of the strain vs pressure plots was used in the extrapolation to obtain strain at fracture. Fracture pressures and strains are given in Tables A5 to A12 (row corresponding to the maximum pressure applied for each test).

During the commissioning of the wide plate test rig it was found that the full applied jack pressure, as indicated by the pressure transducer output, would not be realized by the wide plate specimen due to frictional losses and hence the sluggishness of the loading capsule piston movement. The effect of preloading and subsequent loadings on the theoretical and the actual strains on a 25.4 mm thick plate was determined during the commissioning of the wide plate test rig. The results of the first and subsequent loading are shown in Figure 21. The actual strains recorded were lower than the theoretical strains. Second loading shifted the actual strains to the theoretical values.

The overall objective was to come up with a reliable number for fracture stress for each test with confidence. The stress based on jack pressure would not be reliable because frictional forces which could be different for each wide plate specimen and would overestimate the stress in the plate. The strain gauges attached on the plate ought to be the most reliable. Proper zeroing was performed for tests 1 to 4 at the test temperatures and hence the final microstrain values should be accurate. However no preloading was performed for test # 1 but for tests # 2-4 the wide plates were preloaded to 1000 psi (based on pressure transducer output) and unloaded, at the test temperature, to remove the slack.

In the elastic region the theoretical slope of the microstrain vs jack pressure regression line can be calculated, assuming full realization of the jack pressure by the test plate, from the jack pressure P, the total loading area of the capsule pistons A_1 and the cross sectional area of the wide plate A_2 as follows:

$$P.A_1 / A_2 = P.\pi d^2 / wt = \sigma = E\varepsilon$$

where, d is the diameter of the capsule pistons (254 mm), w is the width of the wide plate (~946 mm), t is the thickness of the plate (25.4 mm), σ is the nominal applied stress, E is the Young's modulous and ε is the nominal strain. Therefore,

$$\varepsilon = P.\pi d^2 / wt.E = 0.281 \text{ P (for P in psi).}$$

The frictional forces would essentially delay the development of the stress/strain in the plate as jack pressure increased. This would lead to a negative intercept and a constant slope of 0.281 provided the frictional forces remained constant. If the frictional forces would change with the jack pressure, then slopes < 0.281 could be obtained.

In this study to determine the slopes, linear regression analysis was carried out for strain gauge readings vs jack pressure for each strain gauge. Data selected for the linear regression is the initial linear portion of the strain vs pressure plots between the two arrows marked in Figures 14 to 20. Most of the strain gauges showed linear variations of the strain with jack pressure between the arrows. The linear relationships obtained are shown in Tables 4 to 7. The strain values for jack pressures lower or higher than the range used in the linear regression analyses were not considered in the regression analyses because at lower pressures the specimen might be still rearranging and at higher pressures the presence of the defect causing non-linearity of the strain vs jack pressure plots.

Gauges in the shadow of the crack showed mean values of slope about 63% of the other readings. To determine the likely effect of the crack on stress distribution away from the crack an estimate was made by Graville using the linear elastic equations. It was recognised that they were not strictly applicable away from the crack in finite plate widths but were considered good enough to give an approximate indication. The stress in the shadow was about 78% of the stress at the location of the other gauges (refer to the subtitle "Strain Gauge Locations" in Appendix AA). The average stress from the three gauges in the locations used is 98.5% of the mean gross stress. This suggests that the method of taking the average of the three gauges across the width would provide the mean stress within 2% accuracy. Also if fewer gauges were to be used they could be placed in line with the tip of the crack where the local stress would be almost equal to the mean stress. Thus, from the linear relationships an average linear relationship was calculated for each test. Above the maximum jack pressure used for the regression analysis, an average strain value was obtained for each jack pressure level, till fracture, by averaging out the strain values of all the gauges. Assuming yield at 0.2 % strain, none of the gross average strain values were greater than 0.15 %. Thus, theoretical stress values corresponding to the average strain values at each applied jack pressure were calculated from elastic behaviour. The jack pressure, applied stress, average strain and the theoretical stress from the average strain are given in Tables A13 to A16 and are plotted in Figures 22 to 25. In Table 8 the fracture pressures, the average fracture strains, the fracture stress and the applied fracture stress are given.

For test # 3, the strain values deviated from linearity at final stages of jack pressure. This was probably due to a large hysteresis in the pressure load cycle. The maximum gross theoretical stress of 310.3 MPa in the plate corresponded to a defect section (ligament) stress of 422 MPa. The defect section stress, 422 MPa, might have been about the same as the yield stress at -20° C for the material. Similar observation was also made in test # 4. In these tests there might have been some crack tip blunting prior to fracture due to yield level loading.

Various observations are possible from the regression equations given in Tables 4 to 7 :

(a) The average slopes at a given location (for all six gauges) on the west and east sides are reasonably similar but the intercepts are different as shown in Table 9. This could be due to the kinks at the welds causing the bending stresses.

(b) The difference between the average intercept for the two gauges and the middle gauge, S2 - (S1 + S3)/2 or S5 - (S4 + S6)/2, was constant in each test as shown in Table 10. This could be indicative of some in-plane bending.

(c) The actual average slopes for each test varied from 0.235 to 0.315, as compared to the theoretical slope of 0.281, and always had an intercept as shown in Table 9. The slope increased and the intercept became more negative as the test temperature increased. This could be due to the fact that zeroing was done after the test temperature was reached by the specimen rather than before and hence there might have been some stress present in the plate due to thermal contraction of the plate at the start of the test. Also the temperature at the strain gauge locations were different for each test at the time of recording. Slope larger than theoretical (0.315 vs 0.281) is not possible and the strain gauge readings were clearly an anomaly since transducer pressure and CMOD keep on increasing smoothly. Assuming that strain gauge readings are in error for some unexplained reason, then one approach to estimate the strain at fracture for test # 3 is to use the average of the overall average microstrain equations for tests # 1, 4 and 2 given in Table 10. Thus for test # 3 the fracture strain was calculated using the equation $S = 0.244\ P + 12.7$ and is given in Table 8.

4.2 Crack Tip Opening Displacement Values

The clip gauge calibration tables (Tables AA3, AA10 and AA14) and the output obtained (Tables AA4, AA7, AA11 and AA15) for each wide plate test are given in Appendix AA. The crack mouth opening displacement (CMOD) obtained using six clip gauges are given in Tables A17 to A20 and are plotted in Figures 26 to 29. The CMOD values at the fracture was recorded from the strip chart recorder and by extrapolating the CMOD vs jack pressure plots to fracture pressure. Clip gauge # 3 provided a continuous trace of the CMOD versus pressure. For the remaining clip gauges, the CMOD readings were recorded at discrete pressure intervals and the clip gauge # 3 trace was used to as a guide for extrapolating CMOD vs pressure plots from the last recorded digital reading to the fracture pressure. The CMOD values at fracture thus obtained are given in Tables A17 to A20. The CTOD values at each jack pressure were obtained directly from the CMOD of clip gauges mounted at the defect tip or by calculation from the CMOD values of the two clip gauges mounted on the same half of the defect length as shown below.

$$\text{CTOD} = \text{CMOD}_1 - (\text{CMOD}_2 - \text{CMOD}_1)(\text{distance from crack tip to CMOD}_1/\text{distance between CMOD}_1 \text{ and CMOD}_2)$$

The average CTOD values calculated from the above expression are consistent with those measured at the crack tip and they are being further analyzed using the strip yield model. Both the calculated and measured CTOD values were averaged and plotted against the theoretical stress calculated from the average strain values and the nominal stress calculated from the jack pressure in Figures 30 to 33. The CTOD values are also given in Tables A21 to A24. The CTOD values at fracture are given in Table 11.

4.3 Fractography

Figures 34 and 35 show the fracture appearance and the fracture surfaces of the wide plates. The defect lengths were measured at quarter, mid and three quarter thickness. Defect lengths measured at these three locations were averaged to obtain an average defect size 2a. The average defect size and the plate width for each plate is given in Table 12. The fracture surfaces of all wide plates showed brittle chevrons. The fracture in wide plates # 3 and 4 showed blunting of the crack tip prior to brittle fracture. Localized plastic deformation was quite evident from the edges of the fracture surface near the defect tip.

5.0 ACKNOWLEDGEMENTS

This project has been a subcontract from Fleet Technology Limited and carried out at the Welding Institute of Canada. Discussions with Dr. L. Malik, Mr. B. Graville and Dr. W. Tyson on the presentation of the test results in this report are gratefully acknowledged. Thanks are also due to WIC technical staff especially Mr. M. Irvine and Mr. B. Spahn who were of great assistance in keeping up with the schedule.

6.0 REFERENCES

1. Rolfe, S.T. et al, "Fracture Control Guidelines for Welded Steel Ship Hulls", U.S. Coast Guard, Ship Structures Committee Report SSC-244, 1974.

2. Proprietory Information (correspondence from NKK, Japan, to American Bureau of Shipping, 1979) available to Reltec Advisory Services Inc.

3. Tyson, W. et al, "Dynamic Toughness - Fracture Mechanics Interpretation of the Drop Weight (NDT) Tests", International Journal of Fracture, 25, 1984, pp. 133-141.

4. "Evaluation of Toughness of Conventional Ship Steels at Intermediate Loading Rates

and Its Implications", DSS/CANMET/CCG Contract No. 23440-7-9227/01-SQ with Fleet Technology Ltd. (in progress).

5. Bala, S.R., "Research on Materials for Offshore Structures and Arctic Vessels - Steels", WIC Report RC 307/1/89, DSS Contract Serial No. 23440-6-9143/01-SQ, June, 1989.

Table 1. Chemical Composition, Tensile and Charpy Data For ABS DH36 Steel

Composition	.17 C, 1.05 Mn, .009 S, .015 P, .13 Cr, .1 Ni, .2 Cu, .043 Al, .056 V
Yield Strength	420 MPa approx.
UTS	558 MPa approx.
CVN (Long)	95 J @ -20° C
CVN (Trans)	31 J @ -20° C

TABLE 2. Longitudinal CTOD Values for ABS DH36 Steel using Saw Cut Notch

Specimen No.	Temp. ° C	CTOD mm	Specimen No.	Temp. ° C	CTOD mm
24	-90°	0.083 (δ_c)	40	-35°	0.271 (δ_u)
4	-75°	0.091 (δ_c)	1	-25°	0.383 (δ_u)
33	-75°	0.131 (δ_c)	31	-25°	0.459 (δ_u)
47	-75°	0.212 (δ_u)	53	-25°	0.492 (δ_u)
42	-75°	0.099 (δ_c)	55	-25°	0.439 (δ_u)
38	-75°	0.055 (δ_c)	46	-20°	0.542 (δ_u)
19	-55°	0.161 (δ_c)	52	-20°	0.129 (δ_u)
11	-55°	0.170 (δ_c)	49	-20°	0.295 (δ_u)
69	-55°	0.095 (δ_c)	45	-20°	0.295 (δ_u)
71	-55°	0.432 (δ_u)	54	-20°	0.396 (δ_u)
35	-45°	0.206 (δ_c)	29	-15°	0.924 (δ_u)
48	-40°	0.459 (δ_u)	22	-15°	0.722 (δ_u)
36	-40°	0.427 (δ_u)	13	10°	1.062 (δ_m)
41	-40°	0.393 (δ_u)	27	10°	1.200 (δ_m)
70	-40°	0.125 (δ_u)	6	0°	1.231 (δ_m)
43	-40°	0.205 (δ_u)			
21	-35°	0.449 (δ_u)			
10	-35°	0.501 (δ_u)			

Table 3. Features of Wide Plate Test Rig

- Loading in uniaxial tension
  4 x 1000 metric ton capsules
  75 mm stroke
  End frames designed to have sufficient stiffness to ensure even distribution of load

- Specimens: 1220 mm in width
  1220 - 1830 mm in length
  75 mm thick at maximum capacity of 4000 metric tons

- Instrumentation: Strain gauges
  Thermocouples
  Clip Gauges

- Pneumatically driven pump to provide 30,000 psi capsule pressure, controlled through the valves, load transfer through 254 mm diameter jack from each capsule.

- Plates can be locally cooled

- Data acquisition system

TABLE 4. Linear Regression Equation for The Selected Region of the Microstrain vs Jack Pressure Plots for Wide Plate Test # 1

S1W	$S = 0.243 P + 657$, $R^2 = 0.999$	S1E	$S = 0.262 P - 504$, $R^2 = 0.999$
S2W	$S = 0.148 P + 632$, $R^2 = 0.998$	S2E	$S = 0.193 P - 412$, $R^2 = 0.999$
S3W	$S = 0.279 P + 624$, $R^2 = 0.999$	S3E	$S = 0.304 P - 431$, $R^2 = 0.999$
S4W	$S = 0.205 P - 302$, $R^2 = 0.998$	S4E	$S = 0.260 P + 493$, $R^2 = 0.999$
S5W	$S = 0.150 P - 241$, $R^2 = 0.998$	S5E	$S = 0.183 P + 475$, $R^2 = 0.997$
S6W	$S = 0.277 P - 278$, $R^2 = 0.997$	S6E	$S = 0.314 P + 465$, $R^2 = 0.999$
	Average $S = 0.235 P + 98.2$		

Regression Equation: $S = AP + B$, where S is microstrain and P is jack pressure based on pressure transducer output. R^2 is correlation coefficient.

Table 5. Linear Regression Equations for the Selected Region of the Microstrain vs Jack Pressure Plots for Wide Plate Test # 2

S1W	$S = 0.298 P - 234$, $R^2 = 0.996$	S1E	$S = 0.330 P + 40.5$, $R^2 = 0.990$
S2W	$S = 0.160 P - 53.2$, $R^2 = 0.990$	S2E	$S = 0.196 P + 158$, $R^2 = 0.983$
S3W	$S = 0.279 P - 176$, $R^2 = 0.995$	S3E	$S = 0.299 P + 90.7$, $R^2 = 0.992$
S4W	$S = 0.335 P + 236$, $R^2 = 0.983$	S4E	$S = 0.309 P - 399$, $R^2 = 0.995$
S5W	$S = 0.214 P + 303$, $R^2 = 0.970$	S5E	$S = 0.148 P - 207$, $R^2 = 0.998$
S6W	$S = 0.330 P + 184$, $R^2 = 0.989$	S6E	$S = 0.250 P - 329$, $R^2 = 0.991$
	Average $S = 0.260 P - 32$		
S7W	$S = 0.090 P + 44.8$, $R^2 = 0.989$	S7E	$S = 0.138 P - 56$, $R^2 = 0.994$
	Average $S = 0.114 P - 5.6$		

Table 6. Linear Regression Equations for the Selected Region of the Microstrain vs Jack Pressure Plots for Wide Plate Test # 3

S1W	$S = 0.326 P - 185$, $R^2 = 0.990$	S1E	$S = 0.350 P - 49$, $R^2 = 0.986$
S2W	$S = 0.225 P - 95$, $R^2 = 0.989$	S2E	$S = 0.238 P + 65$, $R^2 = 0.982$
S3W	$S = 0.350 P - 196$, $R^2 = 0.990$	S3E	$S = 0.384 P - 22$, $R^2 = 0.985$
S4W	$S = 0.400 P + 94.2$, $R^2 = 0.982$	S4E	$S = 0.326 P - 340$, $R^2 = 0.992$
S5W	$S = 0.295 P + 169$, $R^2 = 0.977$	S5E	$S = 0.185 P - 220$, $R^2 = 0.995$
S6W	$S = 0.408 P + 104$, $R^2 = 0.981$	S6E	$S = 0.299 P - 354$, $R^2 = 0.991$
	Average $S = 0.315 P - 85.8$		
S7W	$S = 0.163 P - 58.5$, $R^2 = 0.995$	S7E	$S = 0.112 P + 6.9$, $R^2 = 0.992$
	Average $S = 0.138 P - 26$		

Table 7. Linear Regression Equations for the Selected Region of the Microstrain vs Jack Pressure Plots for Wide Plate Test # 4

S1W	$S = 0.242\ P - 44.2,\ R^2 = 0.999$	S1E	$S = 0.273\ P - 26.8,\ R^2 = 0.999$
S2W	$S = 0.180\ P - 24.3,\ R^2 = 0.999$	S2E	$S = 0.195\ P + 10.5,\ R^2 = 0.999$
S3W	$S = 0.255\ P - 66.1,\ R^2 = 0.999$	S3E	$S = 0.277\ P - 17.5,\ R^2 = 0.999$
S4W	$S = 0.286\ P + 11.3,\ R^2 = 0.999$	S4E	$S = 0.279\ P - 73\ 9,\ R^2 = 0.999$
S5W	$S = 0.207\ P + 38.3,\ R^2 = 0.999$	S5E	$S = 0.169\ P - 51.7,\ R^2 = 0.999$
S6W	$S = 0.259\ P + 8.58,\ R^2 = 0.999$	S6E	$S = 0.222\ P - 100,\ R^2 = 0.999$
	Average $S = 0.237\ P - 28$		
S7W	$S = 0.121\ P - 14.5,\ R^2 = 0.999$	S7E	$S = 0.096\ P - 9.19,\ R^2 = 0.999$
	Average $S = 0.109\ P - 11.8$		

Table 8. Fracture Data

Test #	Temp. ° C	Jack Pressure at Fracture psi	Microstrain at Fracture (Avg)	Fracture Stress, MPa Nominal (1)	From ASGO (2)
1	-75°	3683	973	214	204.3
2	-40°	5548	1495	322.1	314.0
3	-20°	5779	1423*	335.5	298.8
4	-55°	5958	1369	347.6	287.6

(1) from jack pressure based on pressure transducer output, (2) from average strain gauge output (ASGO)

* Average microstrain calculated using: $S = 0.244\ P + 12.7$

Table 9. Average Slope of Microstrain vs Jack Pressure

Test #	1W, 2W, 3W	4W, 5W, 6W	1E, 2E, 3E	4E, 5E, 6E
1	0.223P+638	0.211P-274	0.253P-449	0.252P+478
2	0.246P-154	0.293P+241	0.275P+96.4	0.236P-312
3	0.300P-157	0.368P+122.4	0.324P-2	0.270P-305
4	0.226P-45	0.251P+19	0.248P-11	0.233P-75

Table 10. Average Microstrain - Pressure Regressions

Test # (Temp. ° C)	Avg. Microstrain West Side	Avg. Microstrain East Side	Overall Avg. Microstrain	Constant S2-(S1+S3)/2 or S5-(S4+S6)/2
1(-75°)	S=0.217P+182	S=0.253P+14	S=0.235P+98	23.5, 22.5
4(-55°)	S=0.238P-13	S=0.236P-43	S=0.237P-28	31.8, 31.8
2(-40°)	S=0.269P+43	S=0.255P-108	S=0.260P-32	122, 125
3(-20°)	S=0.334P-18	S=0.297P-153	S=0.310P-86	98, 98.5

Table 11. CTOD Values at Fracture

Test #	Test Temp. ° C	CTOD Value at Fracture mm
1	-75°	0.8272
2	-40°	0.9446
3	-20°	1.2322
4	-55°	1.0400

Table 12. Defect and Fracture Characteristics

Test #	Plate Width mm	Defect Length, mm				Fracture
		A	B	C	Avg	
1	946.15	250	250.8	250.5	250.4	Brittle
2	947.75	250	250.5	250.5	250.3	Brittle
3	947.75	251	251	251.5	251.2	Brittle
4	942.98	250	250	250.2	250.1	Brittle

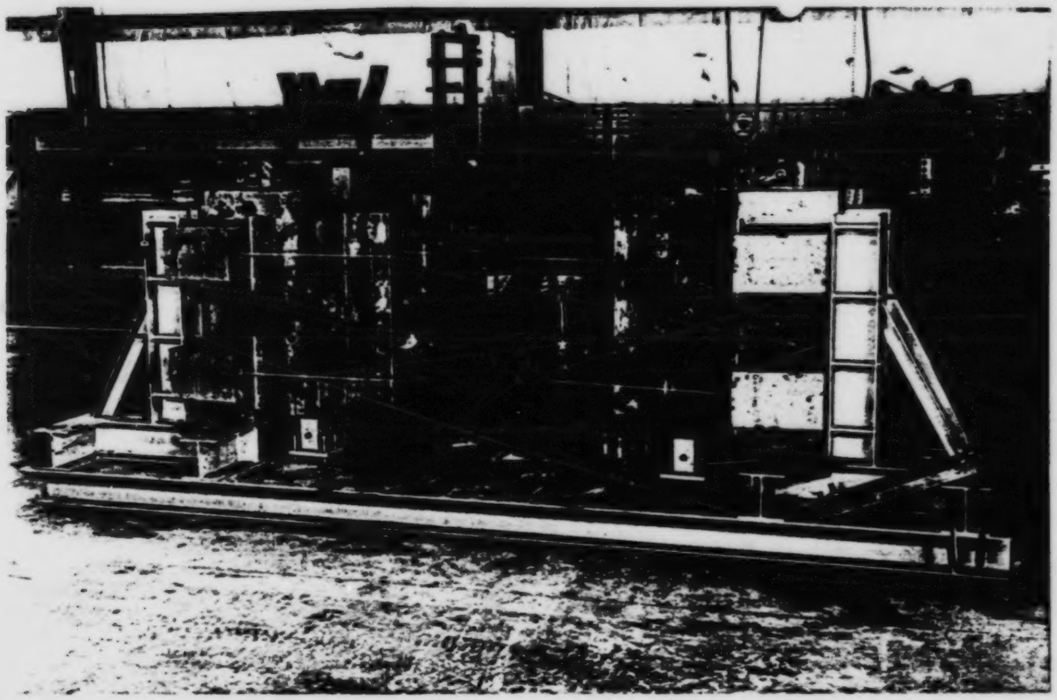

Figure 1. Alignment of loading end attachments in the alignment jig.

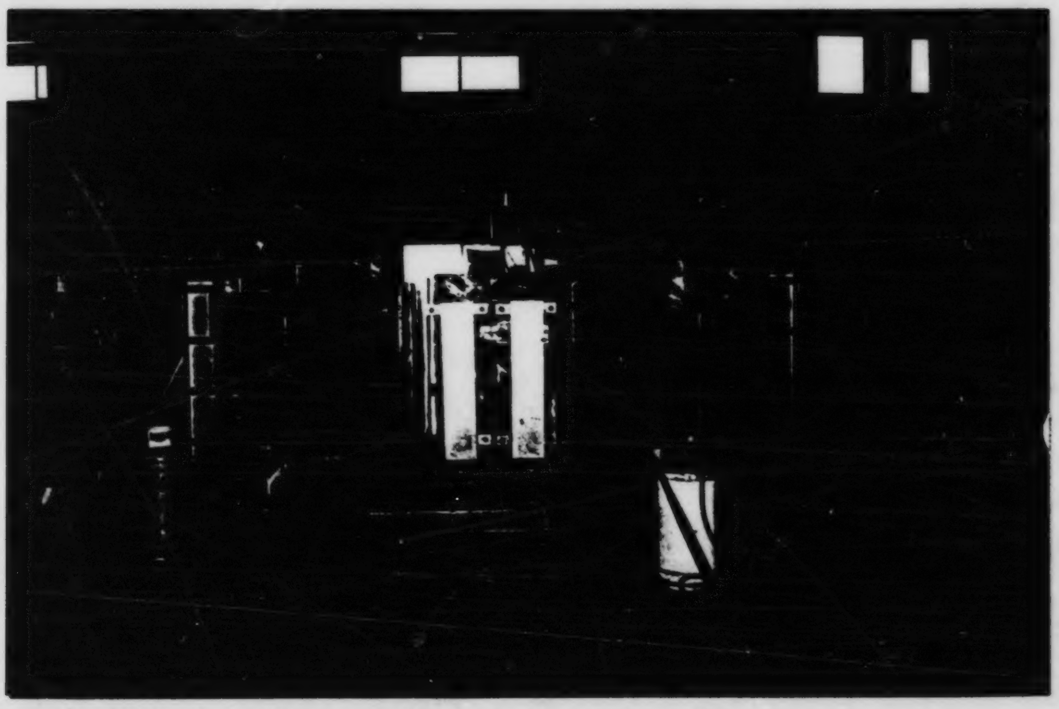

Figure 2. Wide plate alignment with the loading end attachments.

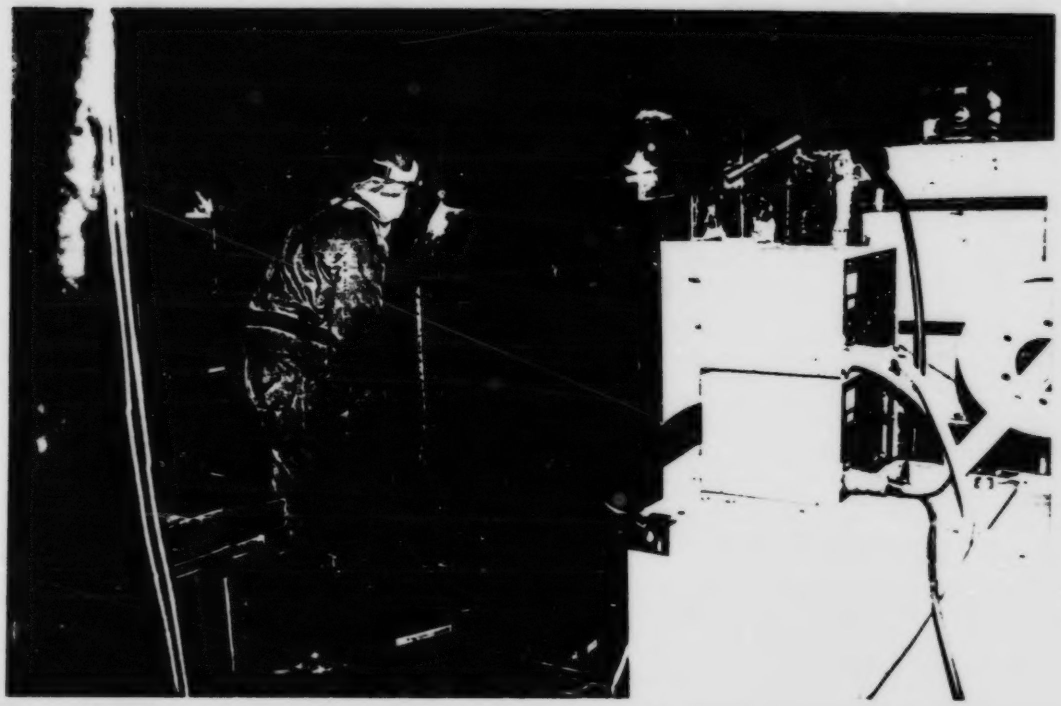

Figure 3. Welding of the wide plate to loading end attachments.

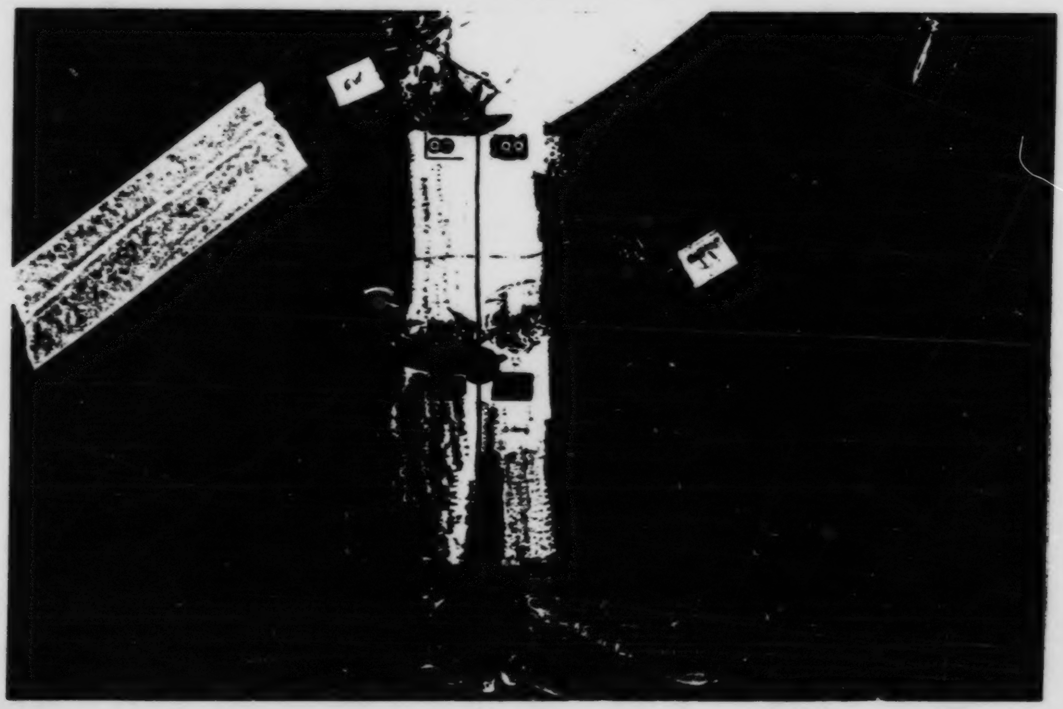

Figure 4. Through thickness defect of the wide plate.

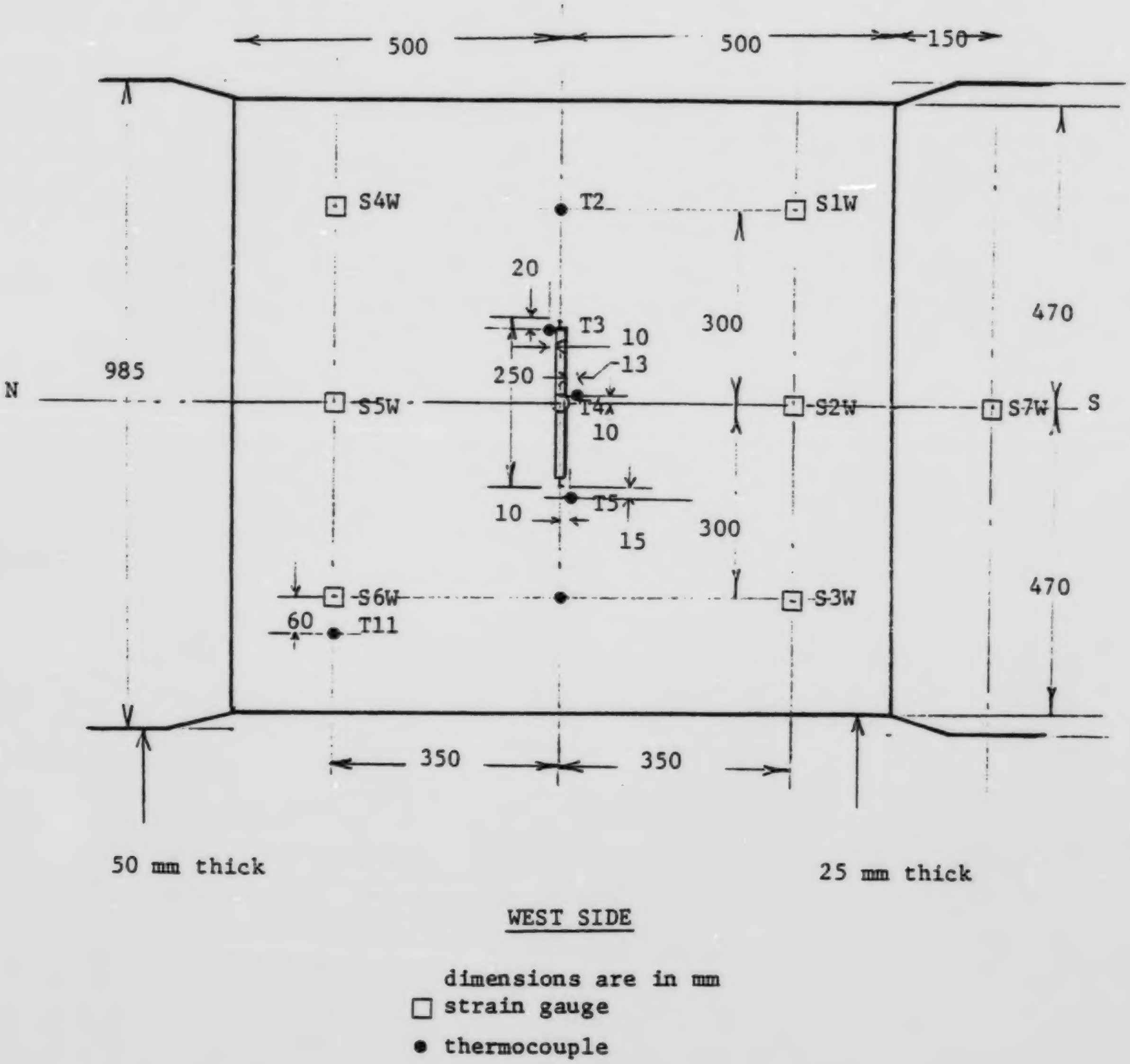
500
500
150
S4W
T2
S1W
20
T3
10
300
470
-13
250
985
N
S5W
T4
S2W
S7W
S
10
10
T5
300
15
470
S6W
S3W
60
T11
350
350
50 mm thick
25 mm thick
WEST SIDE
dimensions are in mm
☐ strain gauge
● thermocouple

Figure 5. Schematic diagram showing the strain gauge and thermocouple locations on the west side of the wide plate.

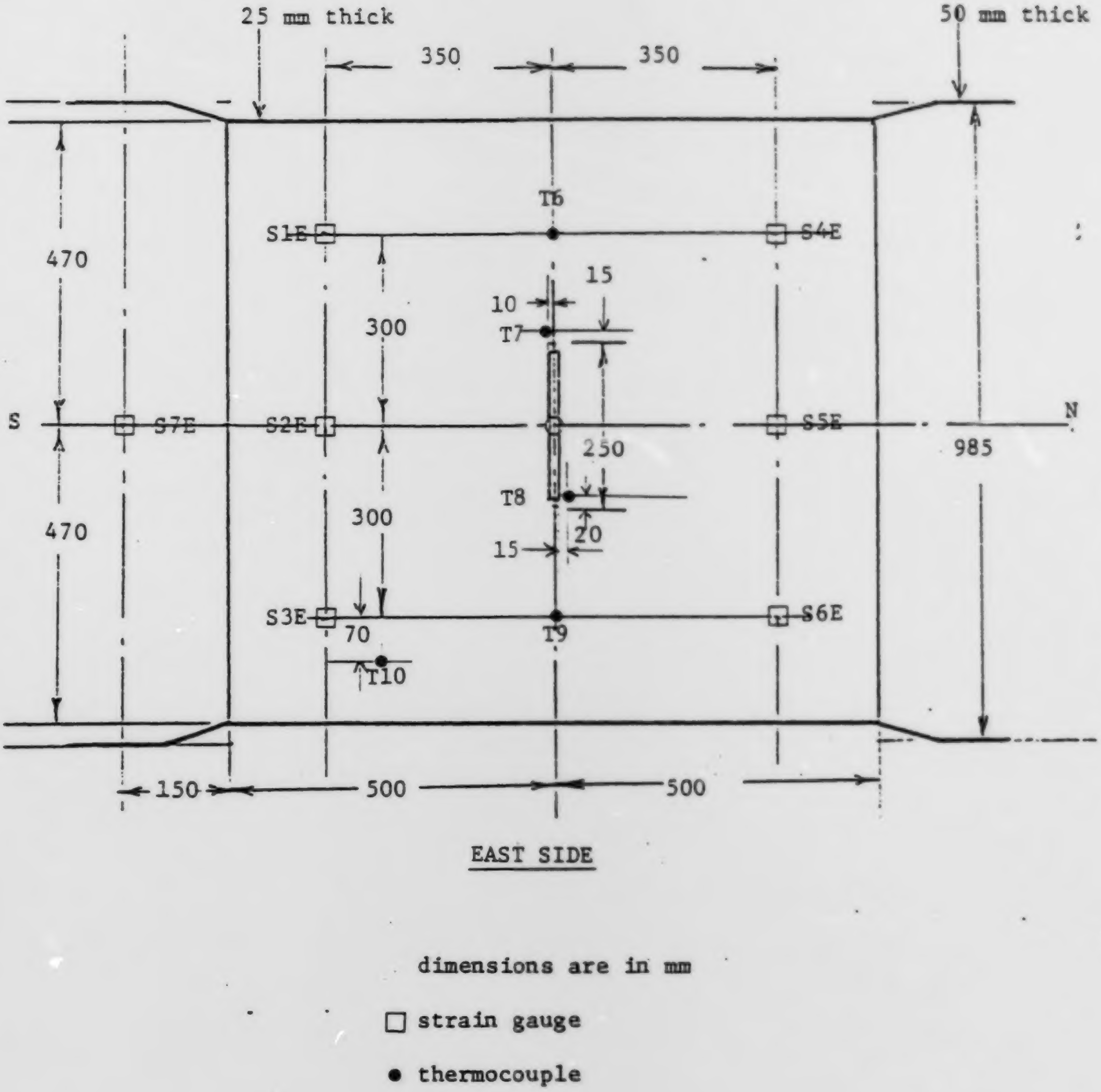
25 mm thick
50 mm thick
350
350
T6
S1E
S4E
470
300
15
10
T7
S
S7E
S2E
S5E
N
250
985
T8
470
300
20
15
S3E
S6E
70
T9
T10
150
500
500
EAST SIDE
dimensions are in mm
□ strain gauge
● thermocouple

Figure 6. Schematic diagram showing the strain gauge and thermocouple locations on the east side of the wide plate.

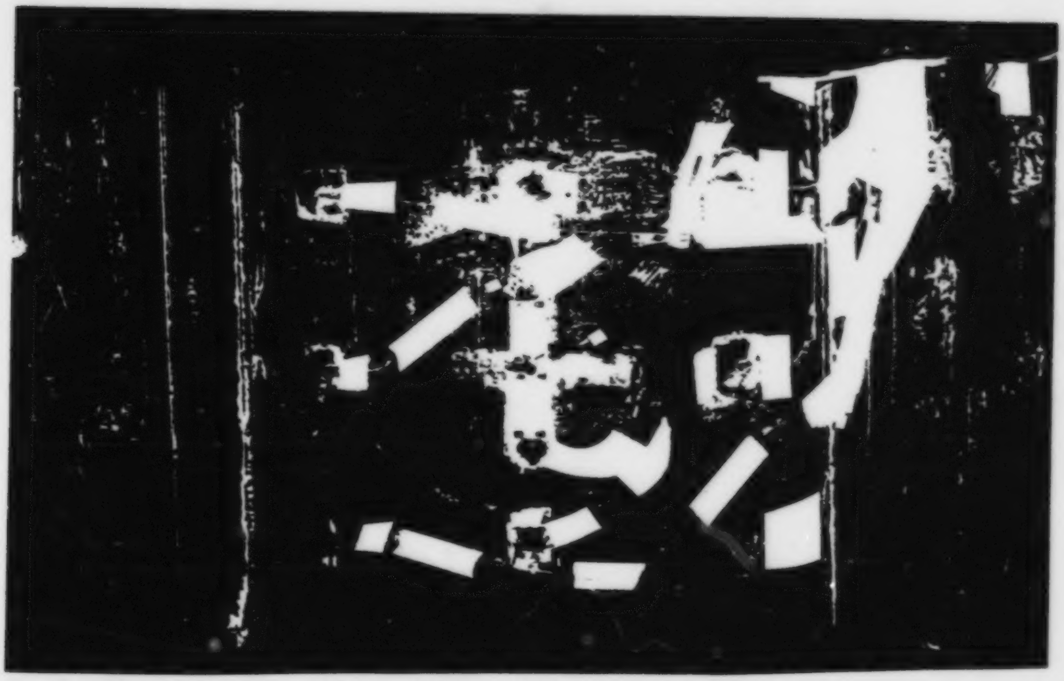

Figure 7. The wide plate with the defect and the instrumentations.

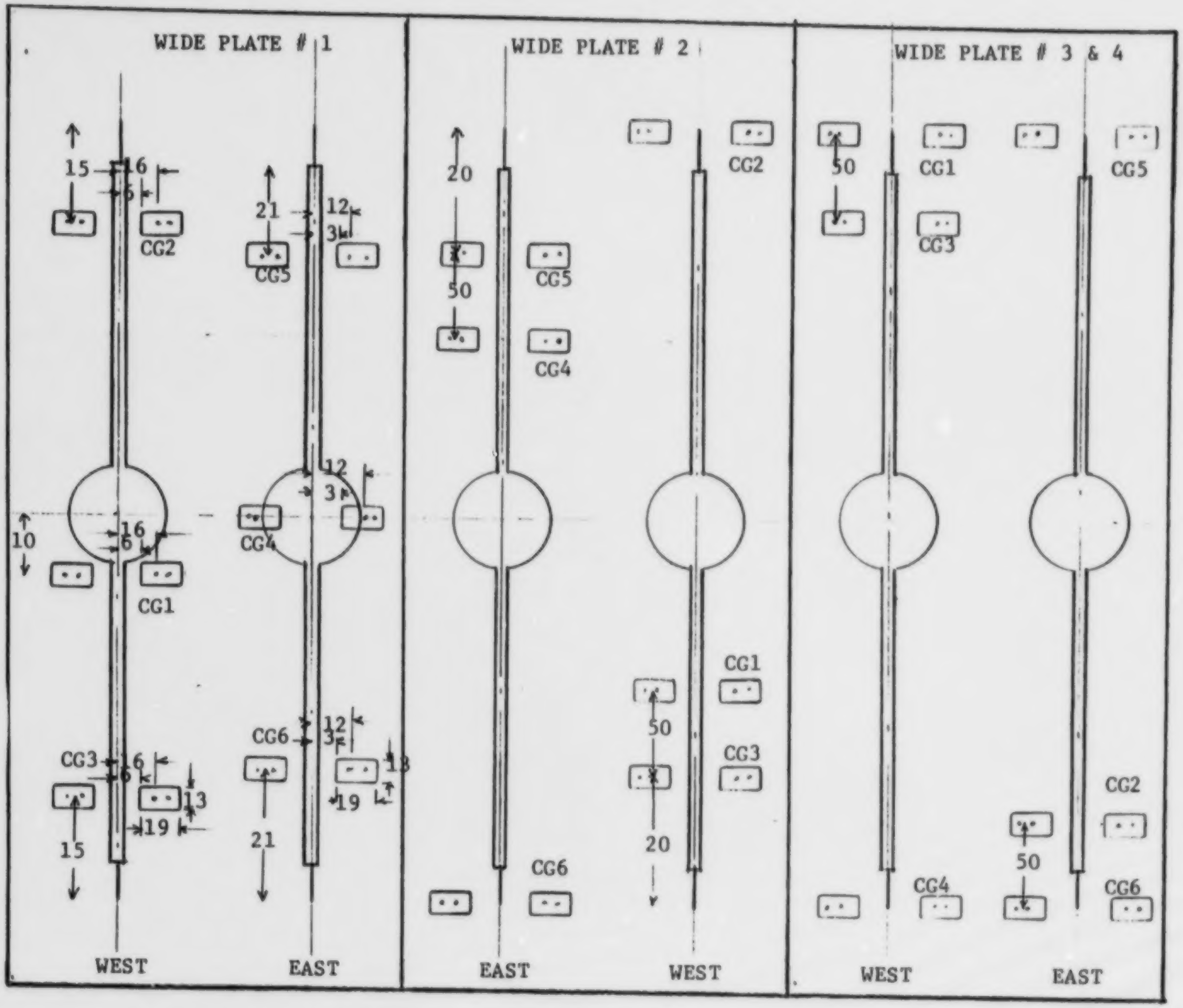
WIDE PLATE # 1
WIDE PLATE # 2
WIDE PLATE # 3 & 4
CG1
CG2
CG3
CG4
CG5
CG6
15
16
6
10
13
19
21
12
3
18
20
50
WEST
EAST
EAST
WEST
WEST
EAST

Figure 8. Clip gauge locations along the defect length for the wide plates.

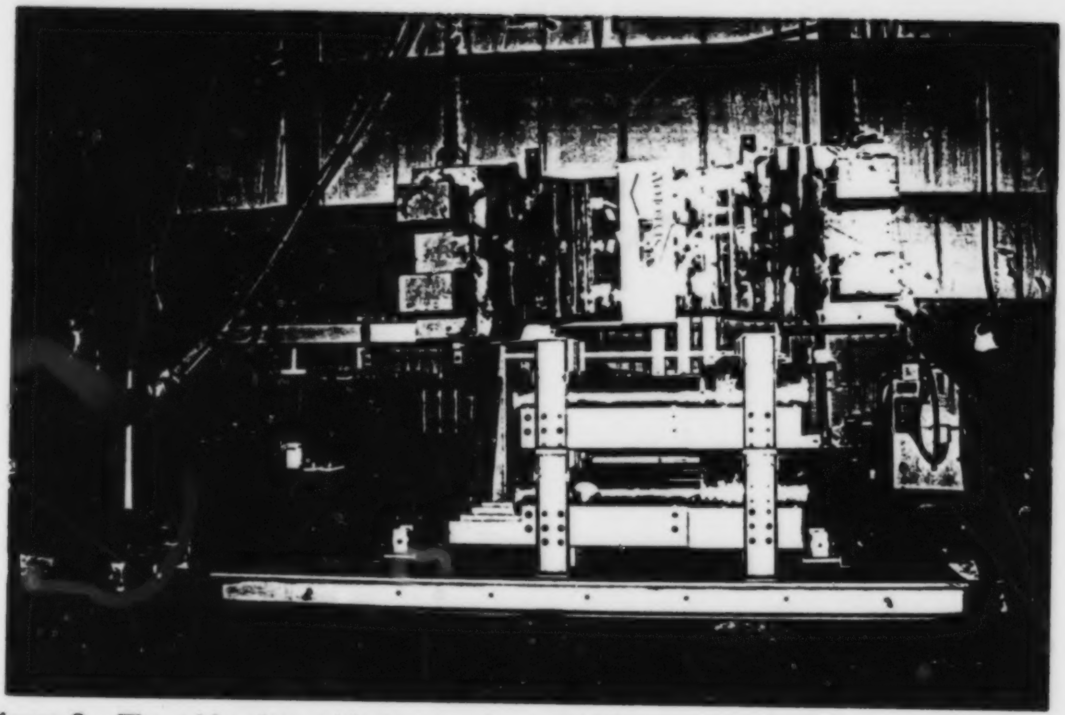

Figure 9. The wide plate with the styrofoam cold box and the test rig.

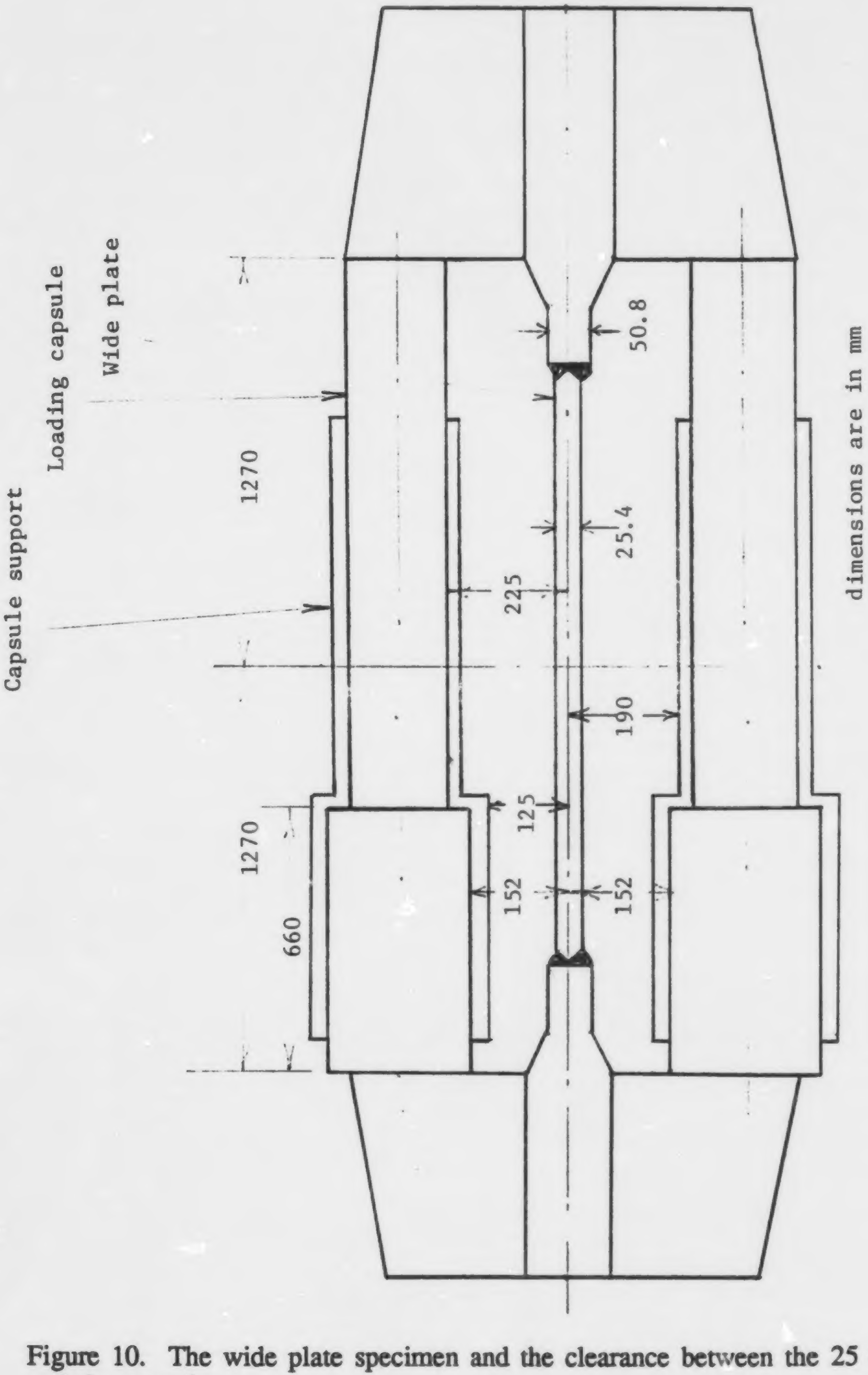
Capsule support
Loading capsule
Wide plate
1270
1270
660
225
50.8
25.4
190
125
152
152
dimensions are in mm

Figure 10. The wide plate specimen and the clearance between the 25 mm thick wide plate and the capsules.

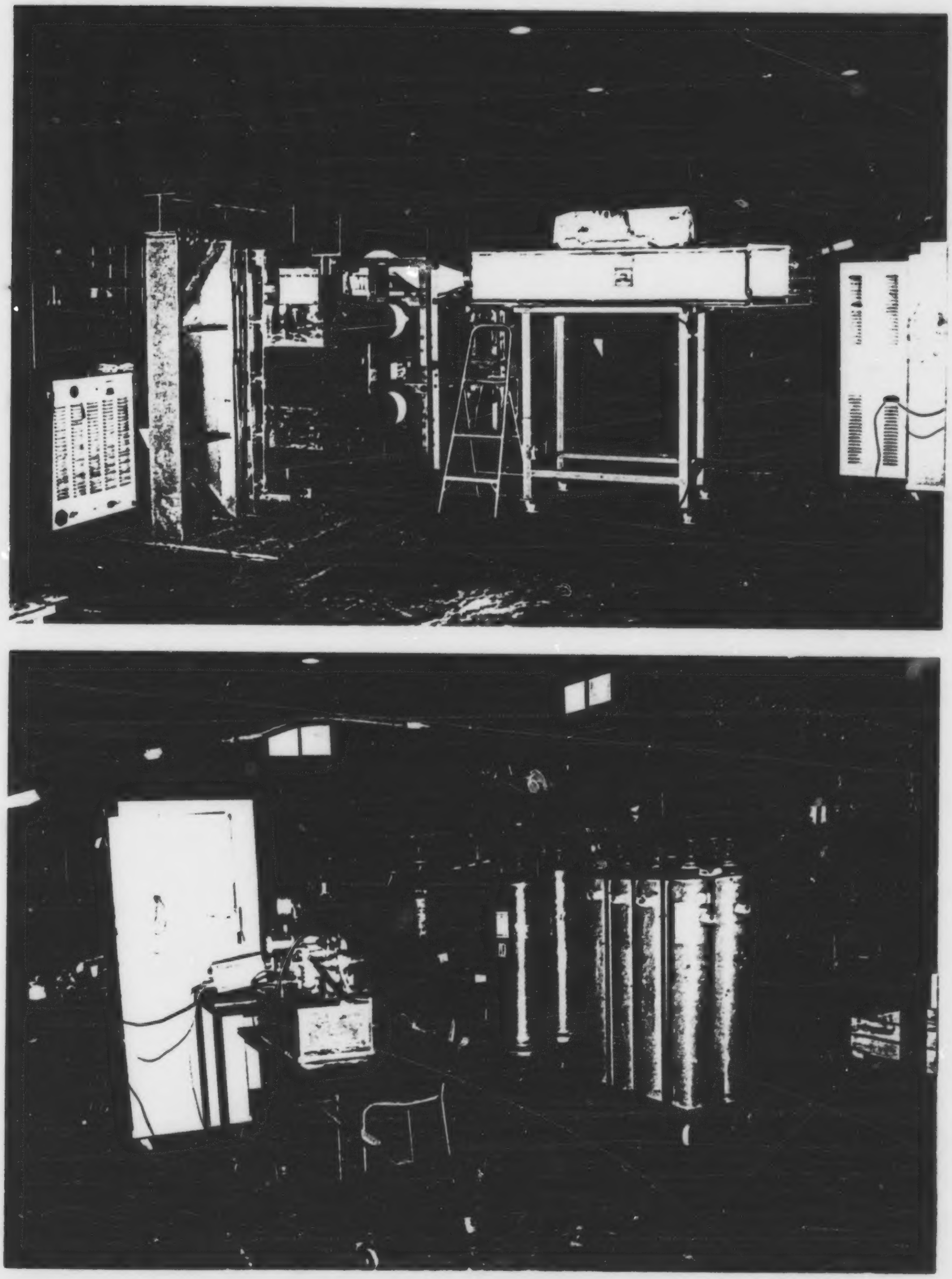

Figure 11. The wide plate test set up and the cooling system for the test section.

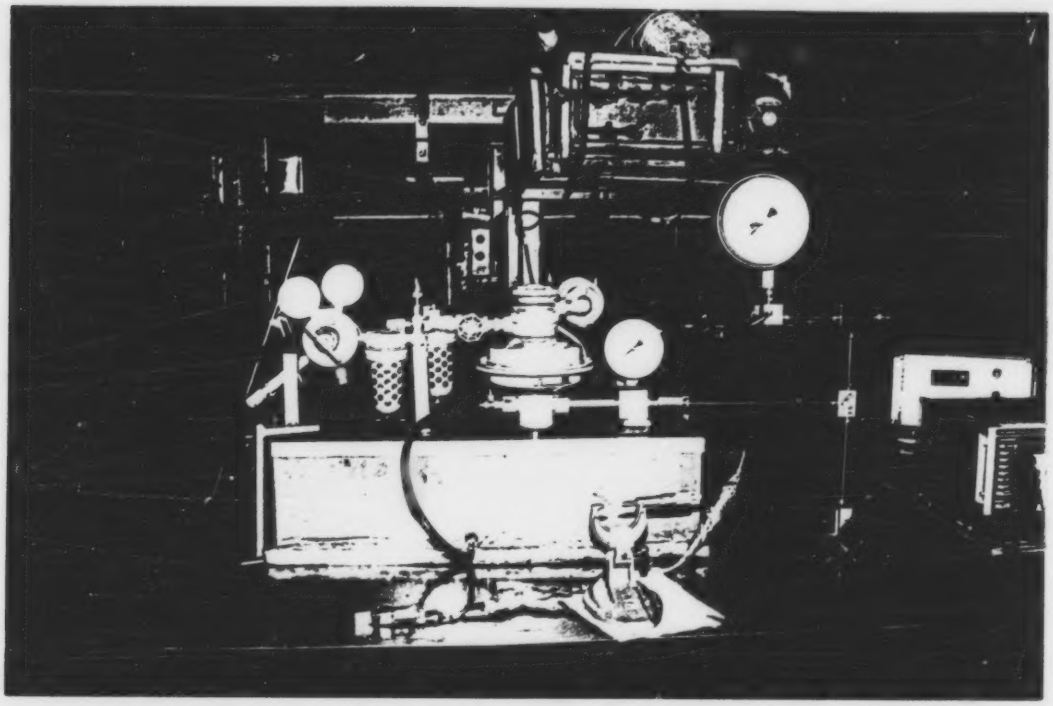

Figure 12. The hydraulic control system for loading the wide plate.

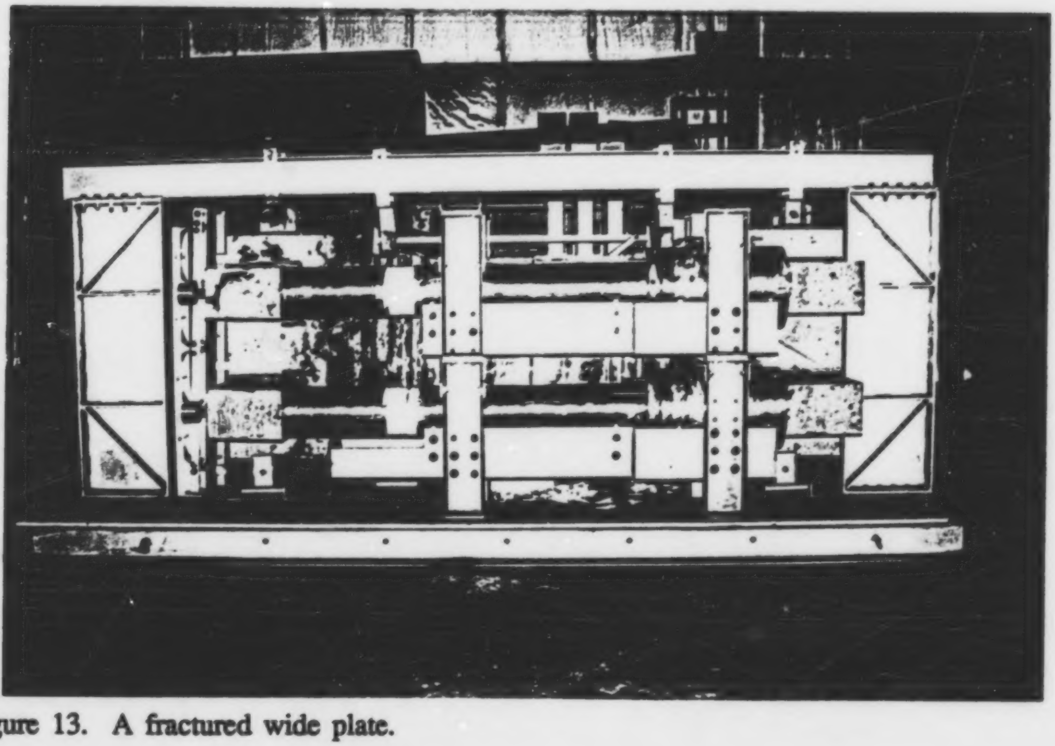

Figure 13. A fractured wide plate.

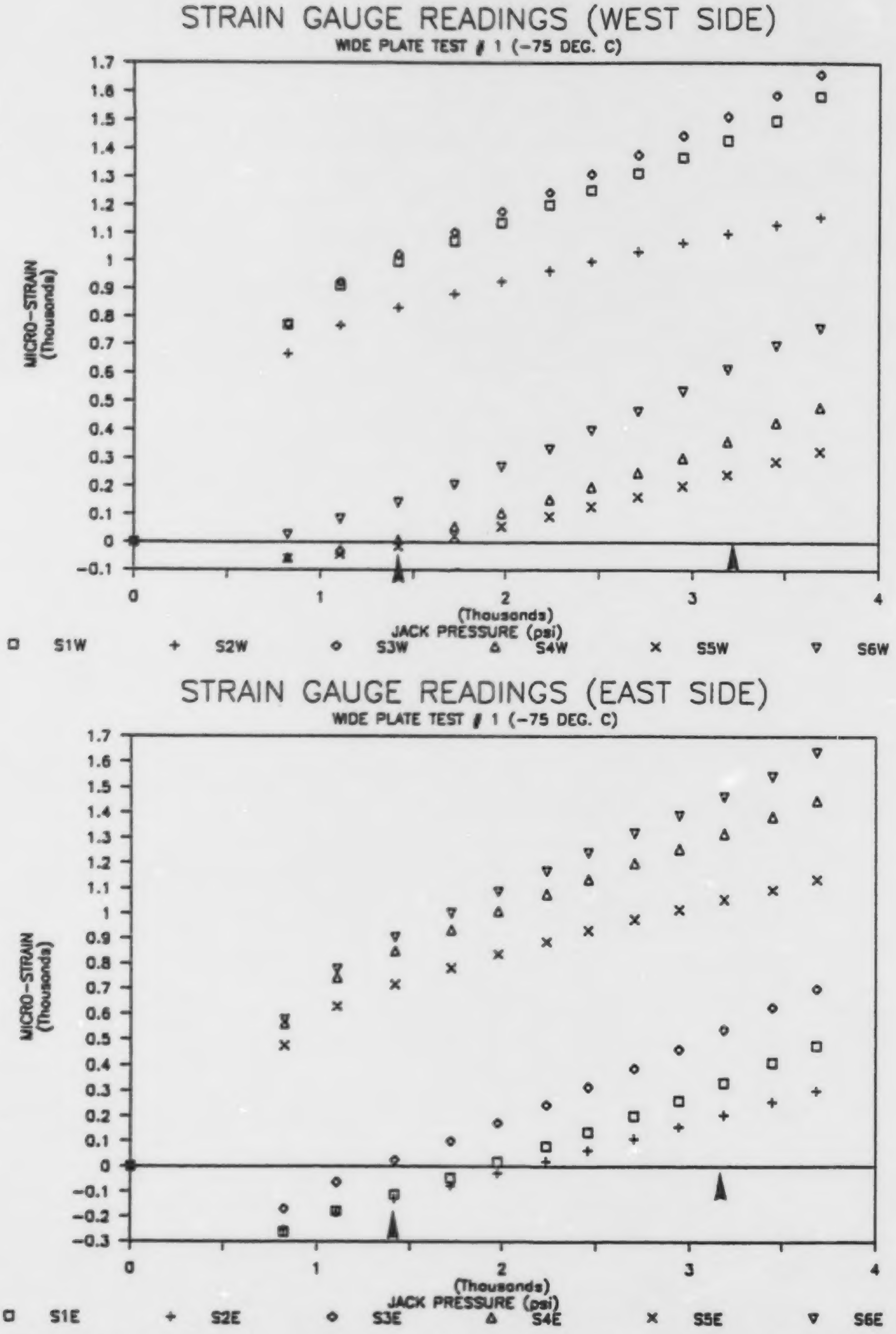

Figure 14. Strain gauge readings vs jack pressure (from transducer) for wide plate test # 1.

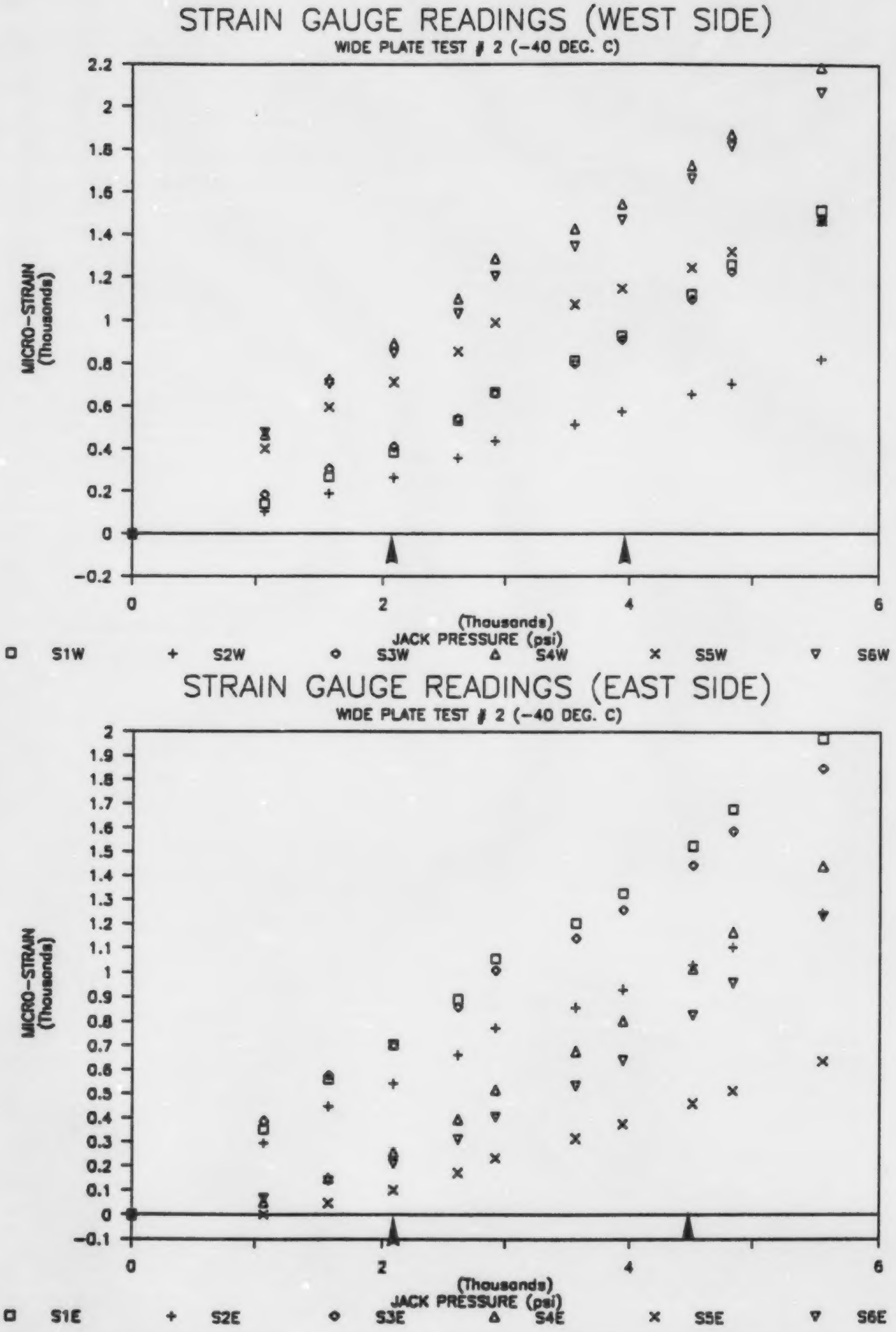

Figure 15. Strain gauge readings vs jack pressure (from transducer) for wide plate test # 2.

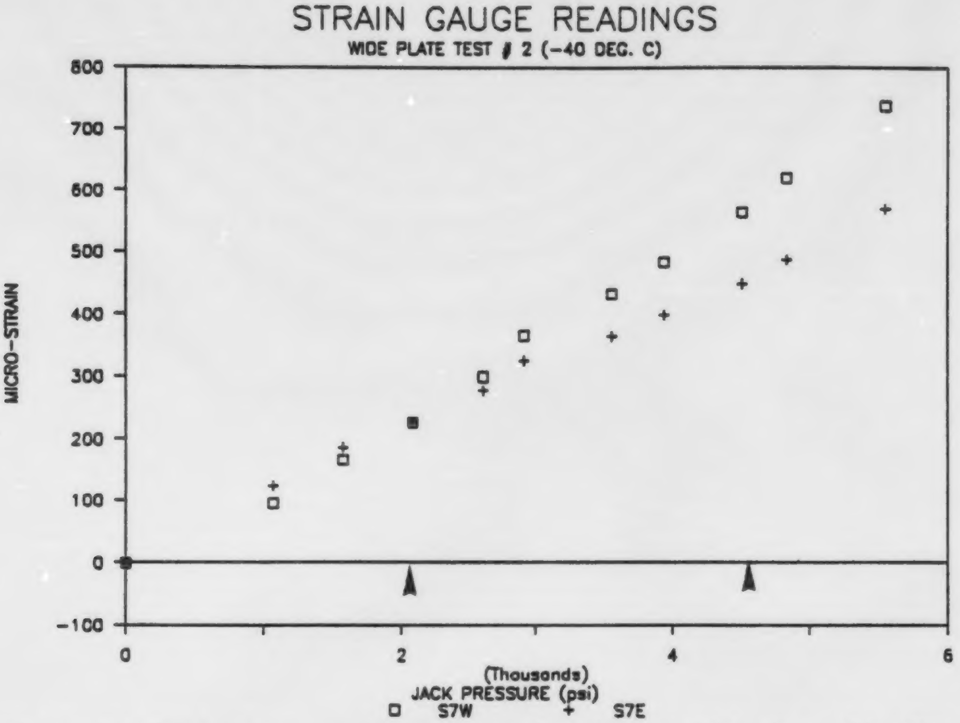

Figure 16. Strain gauge readings measured at 50 mm thick plate of loading end attachment vs jack pressure (from transducer) for wide plate test # 2.

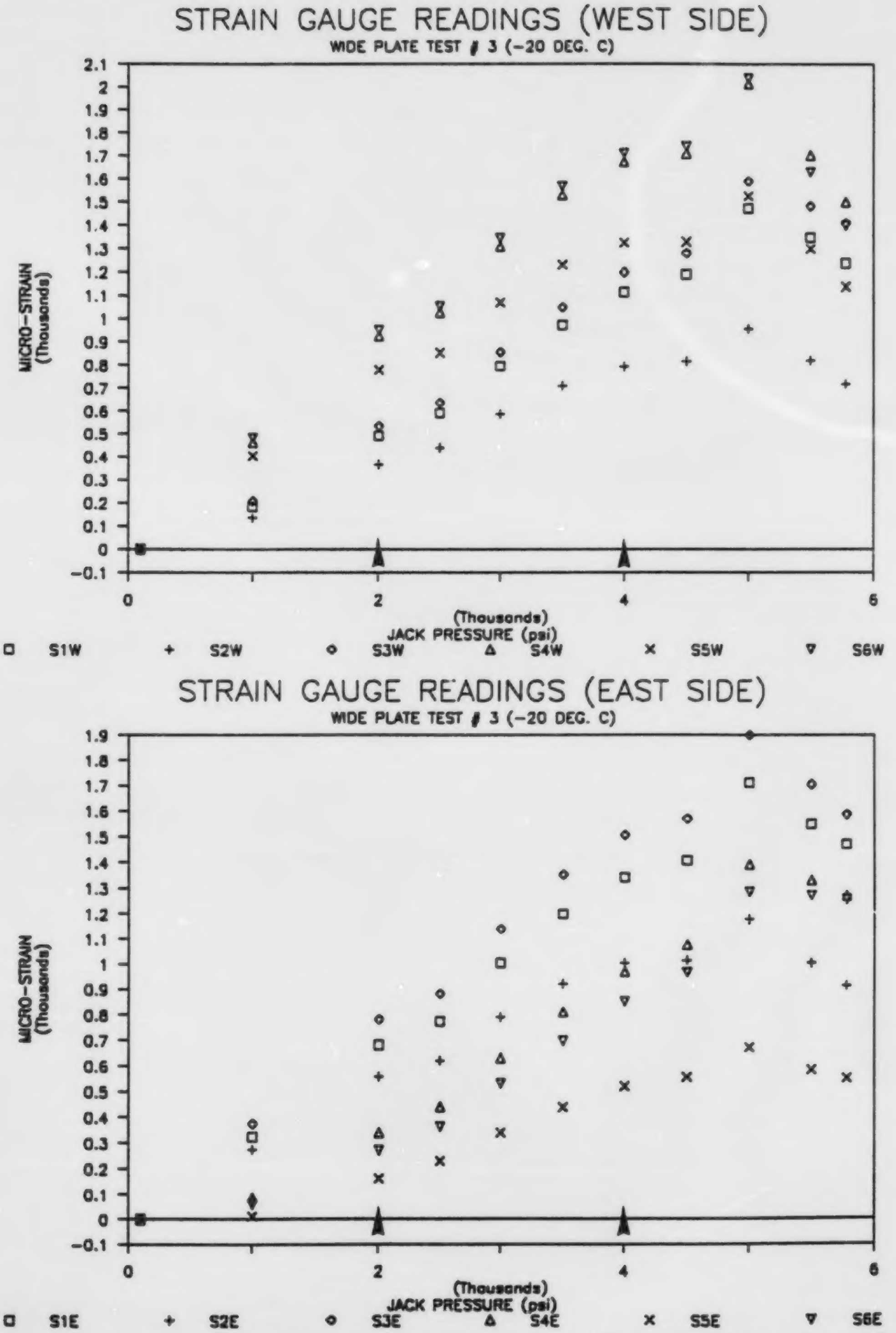

Figure 17. Strain gauge readings vs jack pressure (from transducer) for wide plate test # 3.

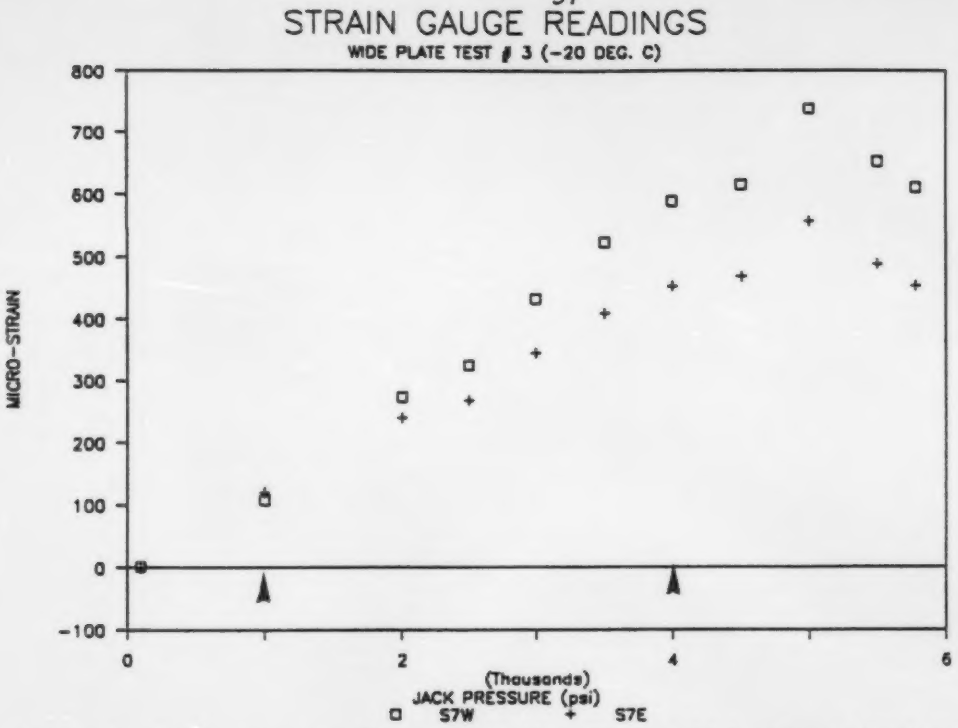

Figure 18. Strain gauge readings measured at 50 mm thick plate of loading end attachment vs jack pressure (from transducer) for wide plate test # 3.

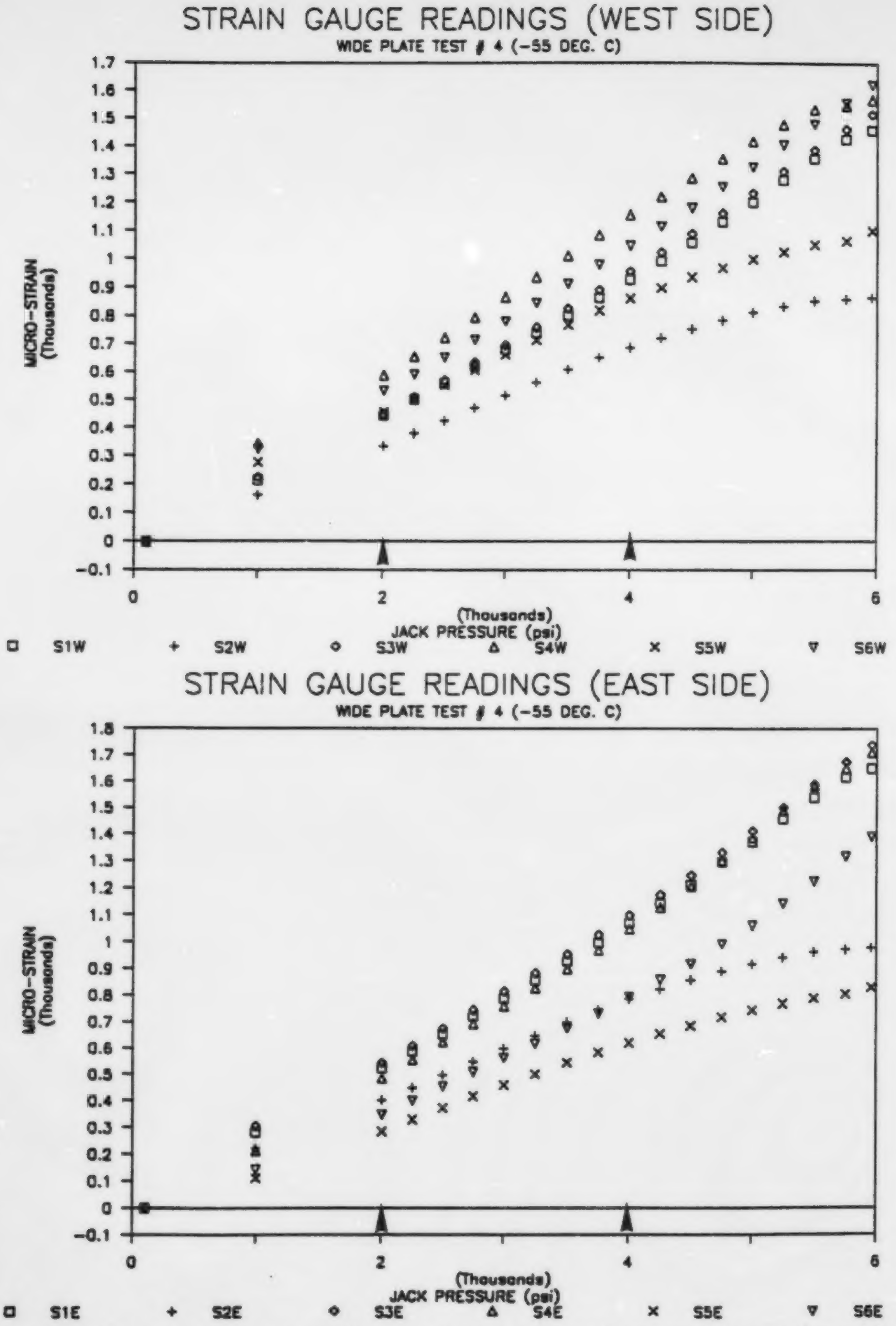

Figure 19. Strain gauge readings vs jack pressure (from transducer) for wide plate test # 4.

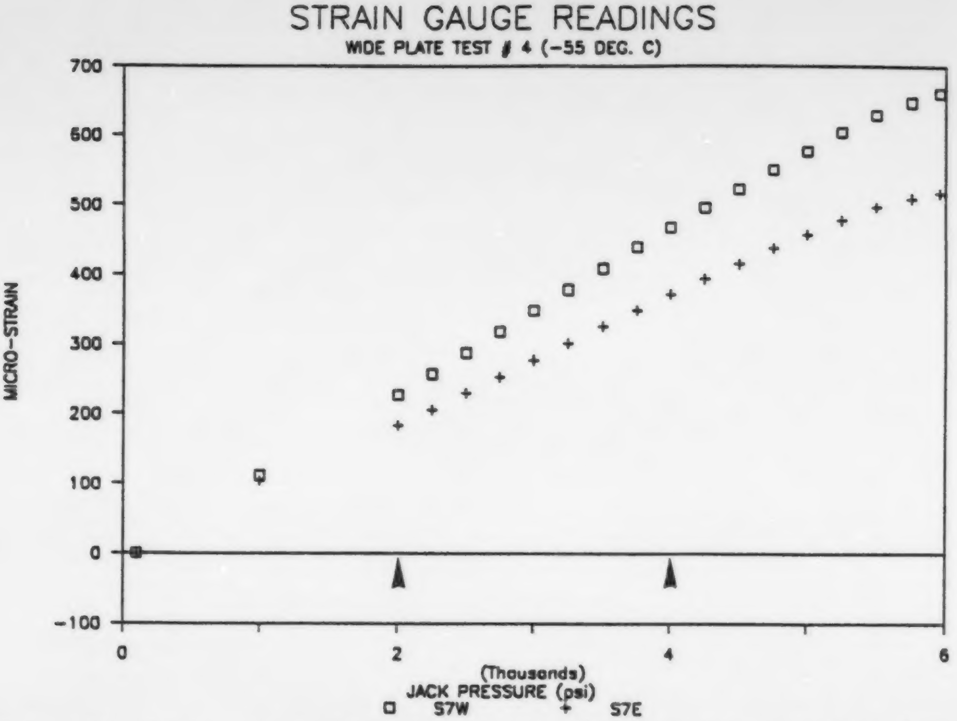

Figure 20. Strain gauge readings measured at 50 mm thick plate of loading end attachment vs jack pressure (from transducer) for wide plate test # 4.

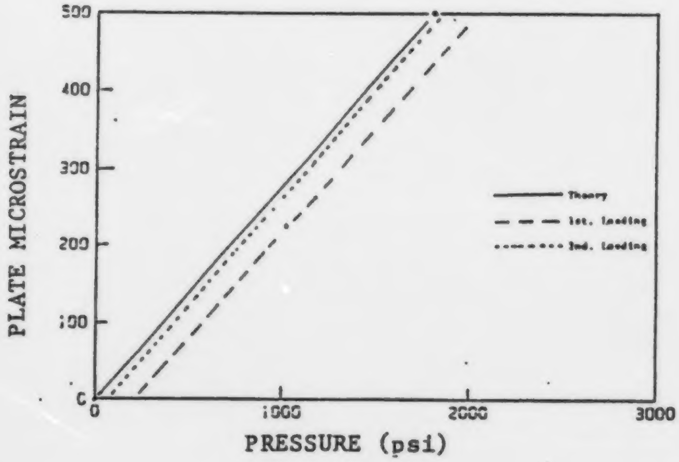

Figure 21. Jack pressure vs strain gauge readings obtained for the 25 mm thick wide plate from first and second loadings, during the commissioning of the test rig.

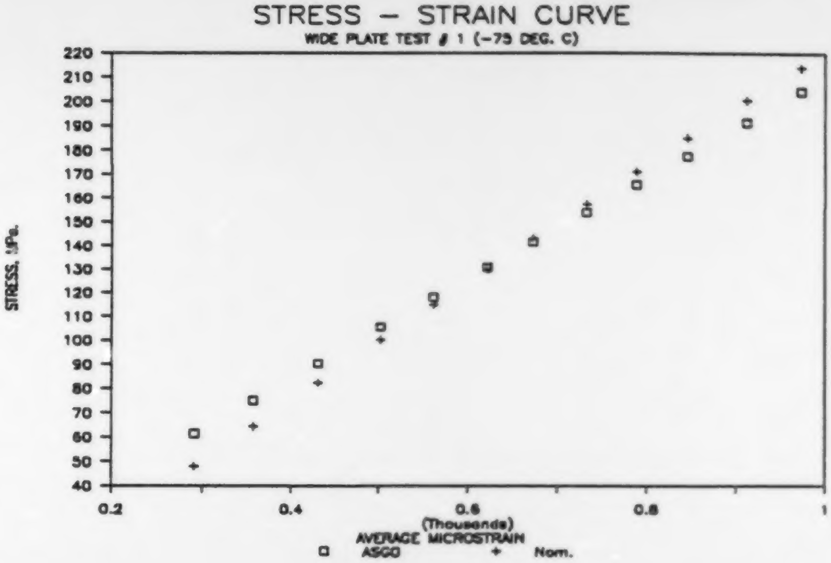

Figure 22. Average microstrain vs nominal stress and stress from average strain gauge output (ASGO) for wide plate test # 1.

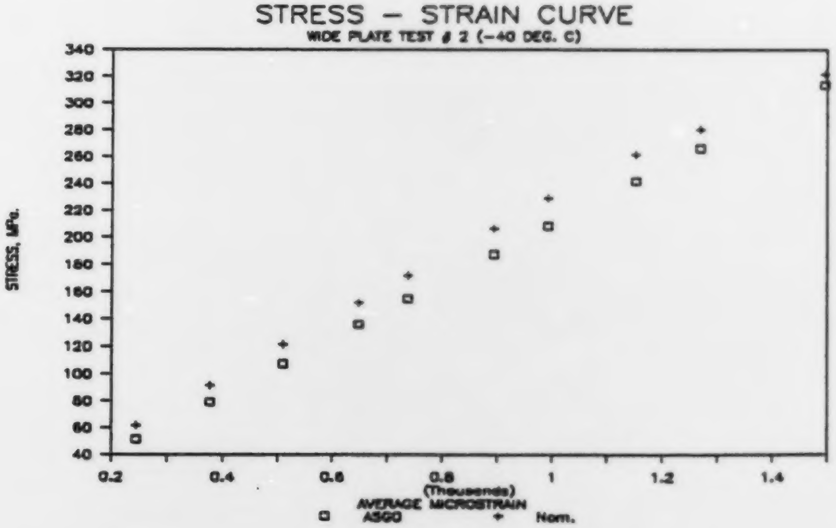

Figure 23. Average microstrain vs nominal stress and stress from average strain gauge output (ASGO) for wide plate test # 2.

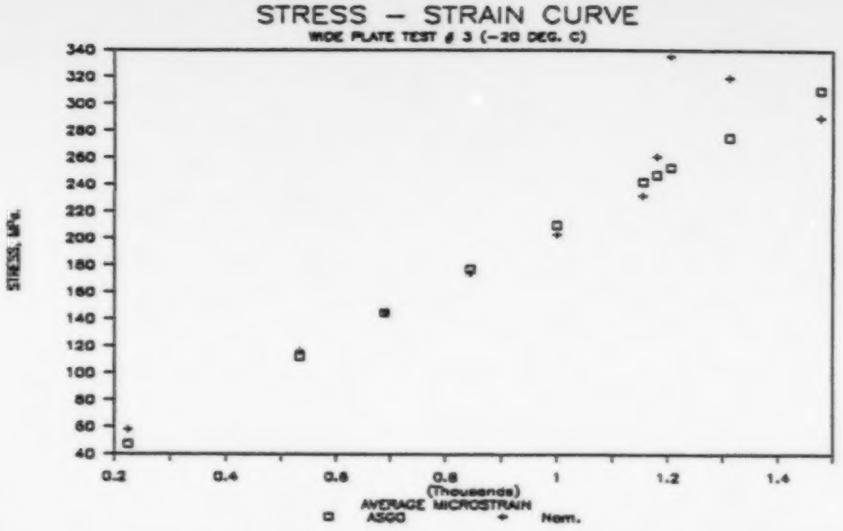

Figure 24. Average microstrain vs nominal stress and stress from average strain gauge output (ASGO) for wide plate test # 3.

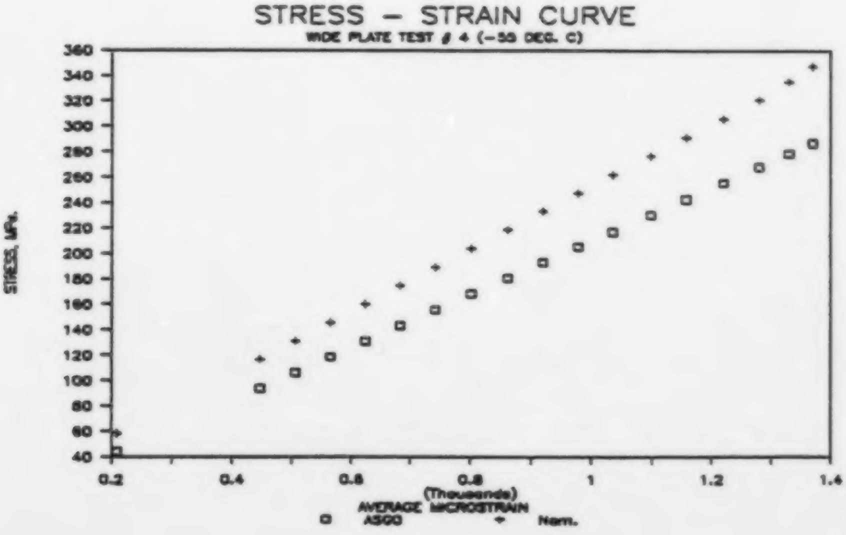

Figure 25. Average microstrain vs nominal stress and stress from average strain gauge output (ASGO) for wide plate test # 4.

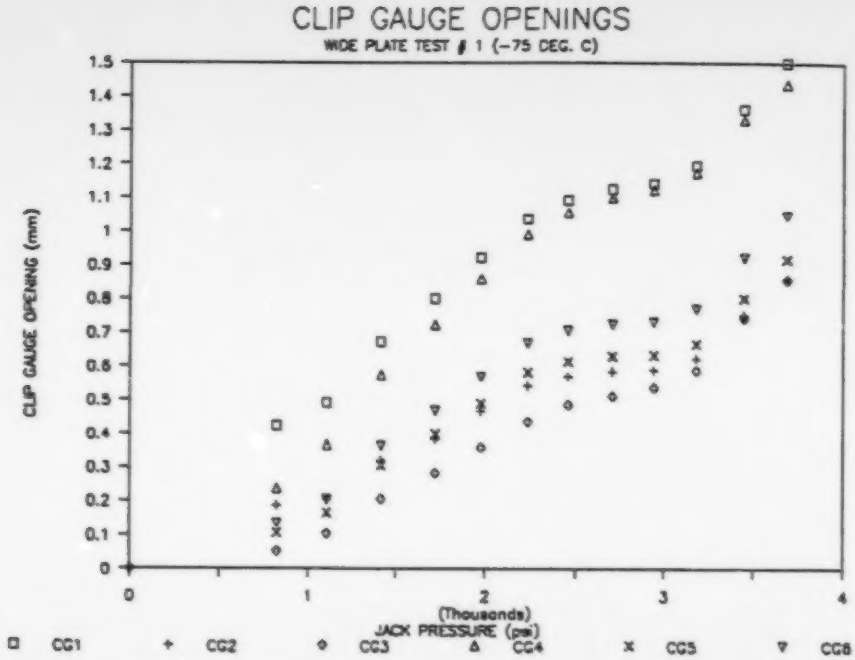

Figure 26. CMOD vs jack pressure (from transducer output) for wide plate test # 1.

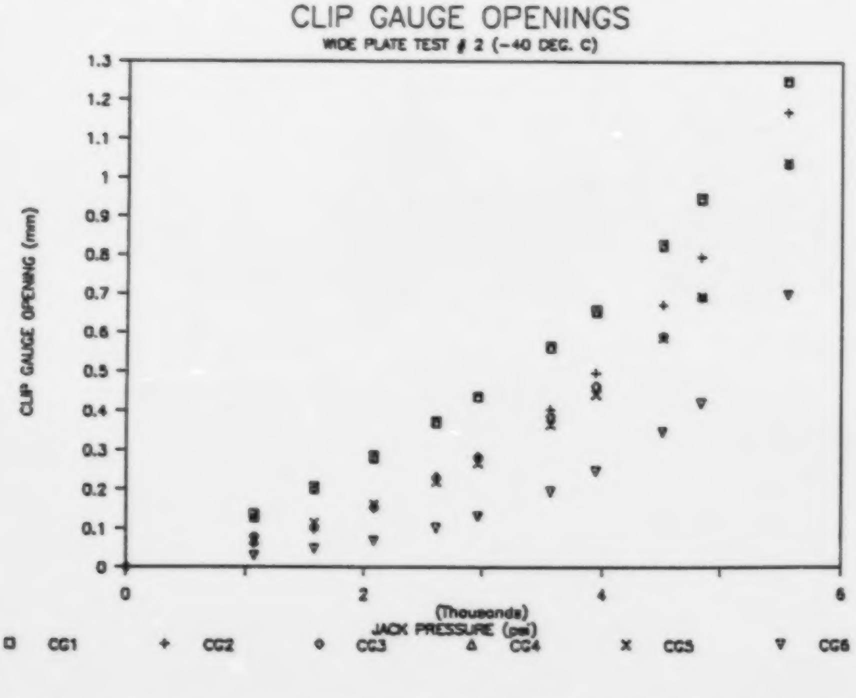

Figure 27. CMOD vs jack pressure (from transducer output) for wide plate test # 2.

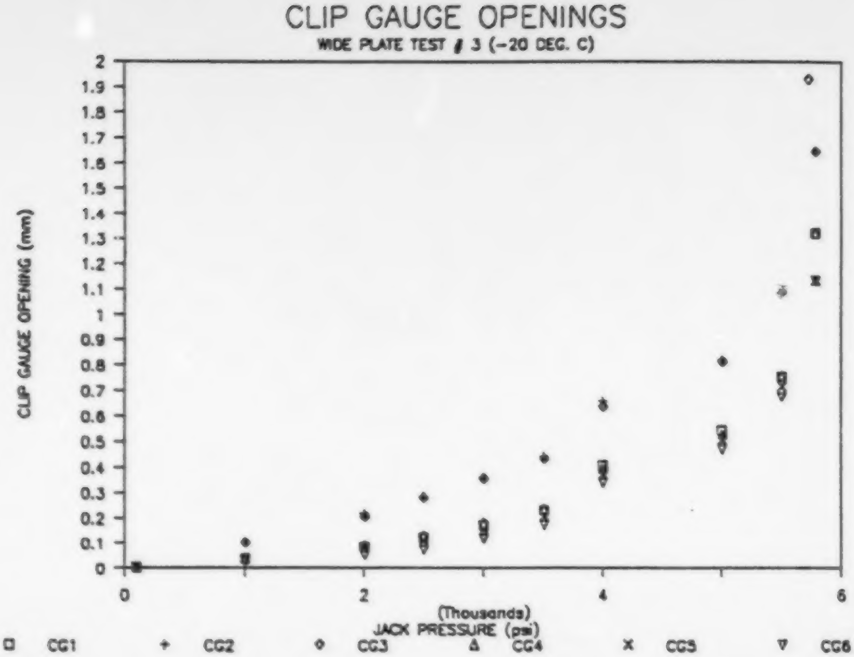

Figure 28. CMOD vs jack pressure (from transducer output) for wide plate test # 3.

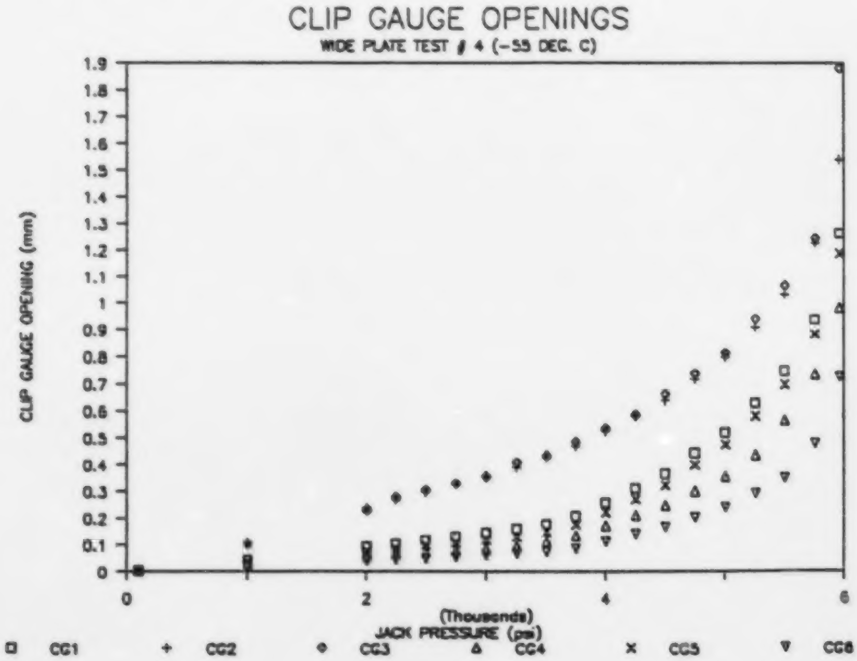

Figure 29. CMOD vs jack pressure (from transducer output) for wide plate test # 4.

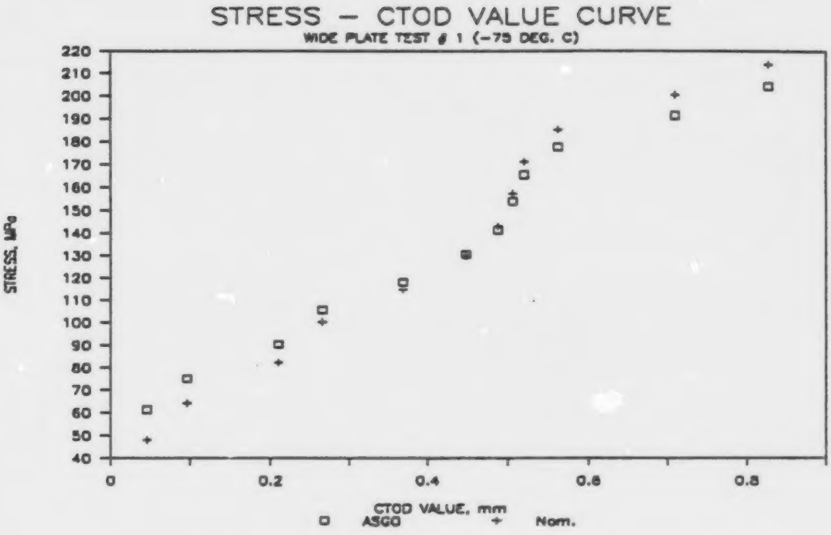

Figure 30. CTOD values vs nominal stress and stress from average strain gauge output (ASGO) for wide plate test # 1.

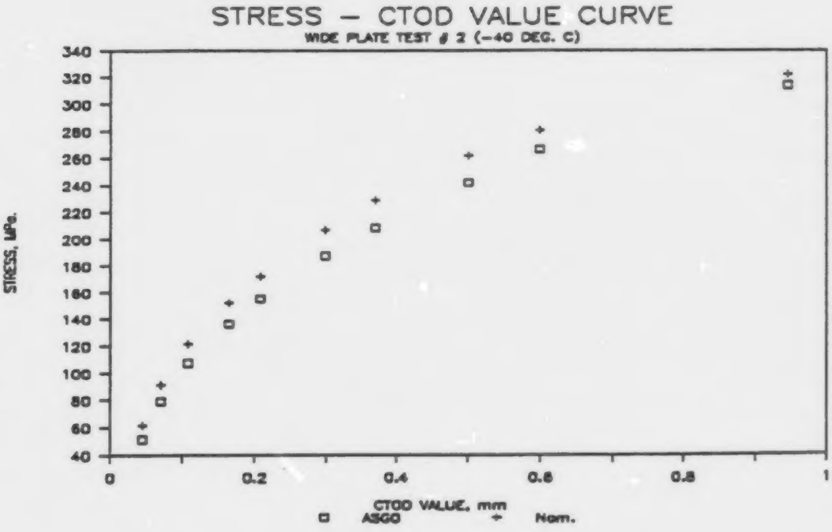

Figure 31. CTOD values vs nominal stress and stress from average strain gauge output (ASGO) for wide plate test # 2.

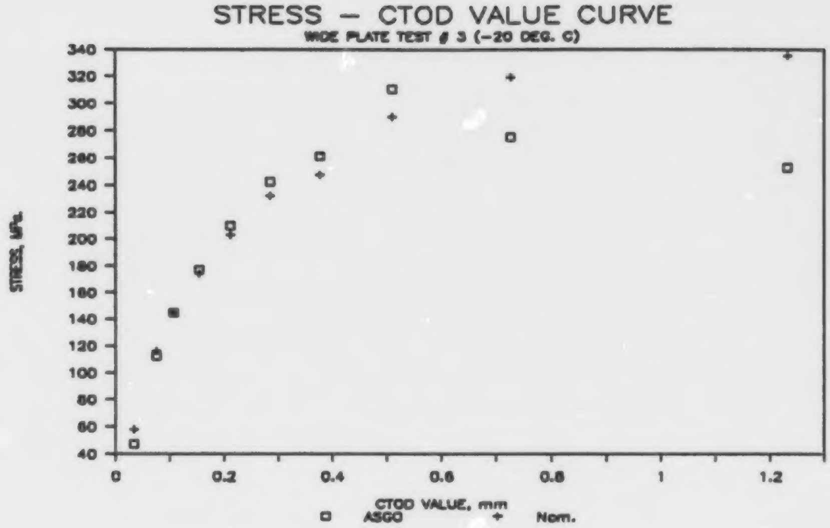

Figure 32. CTOD values vs nominal stress and stress from average strain gauge output (ASGO) for wide plate test # 3.

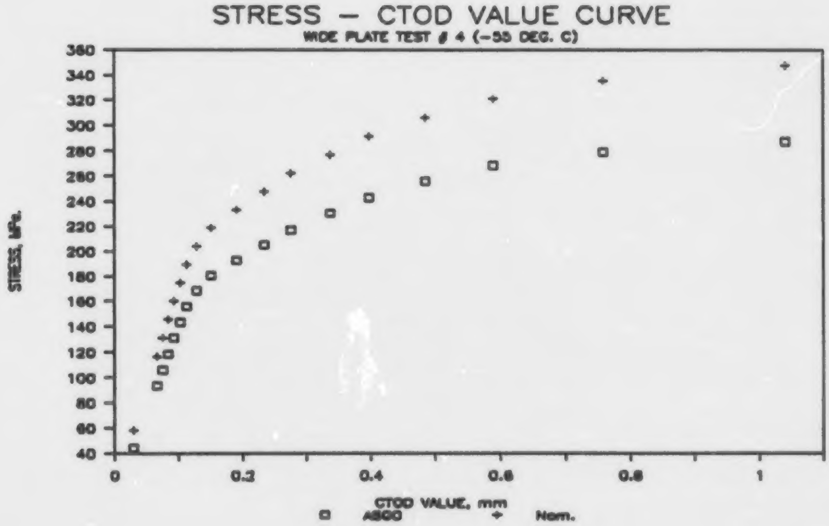

Figure 33. CTOD values vs nominal stress and stress from average strain gauge output (ASGO) for wide plate test # 4.

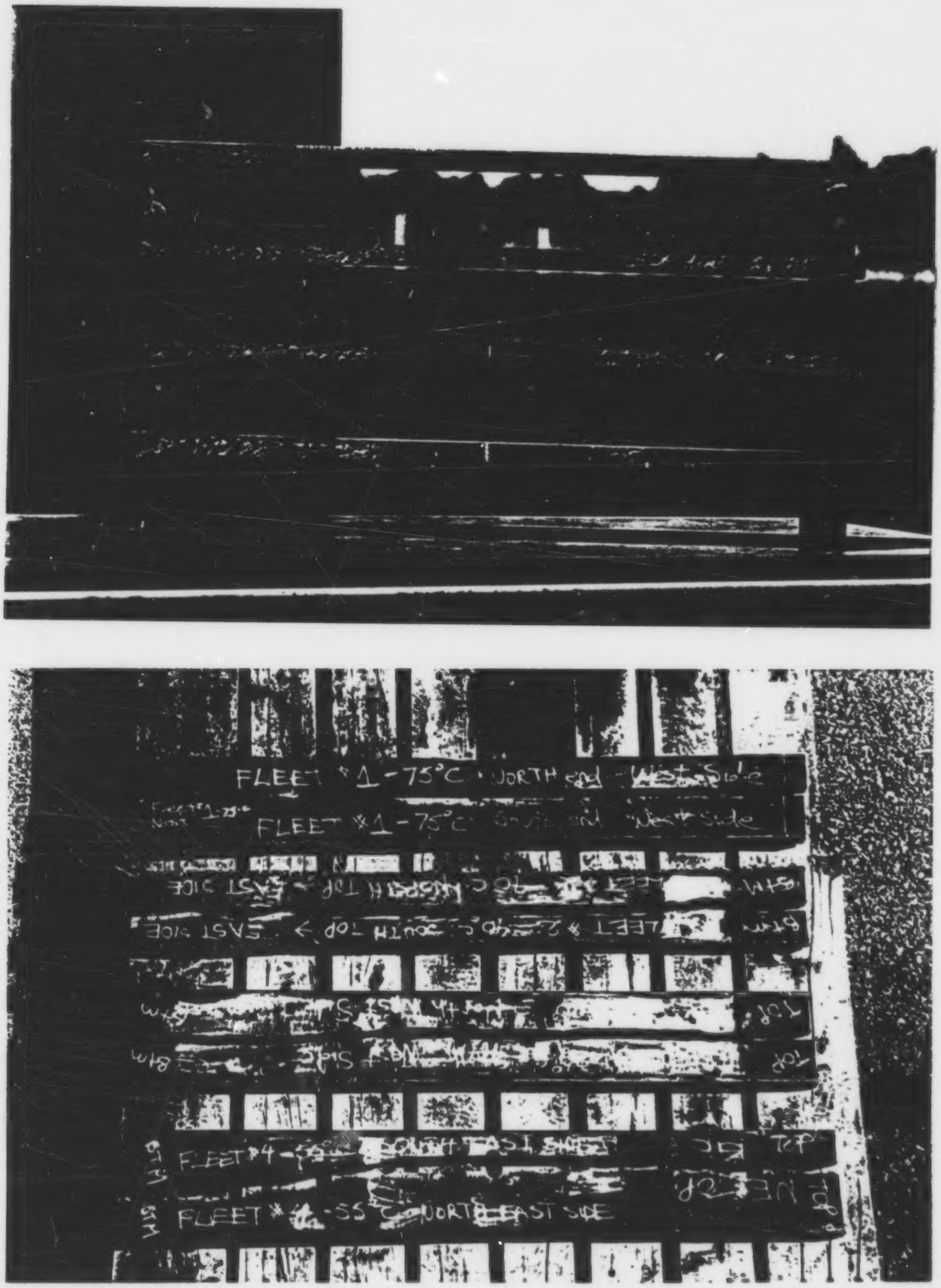
FLEET #1 -75°C NORTH end West Side
FLEET #1 -75°C South end West Side
FLEET #4 -55°C NORTH EAST SIDE
BTM
TOP

Figure 34. Fracture locations and surfaces of the wide plates.

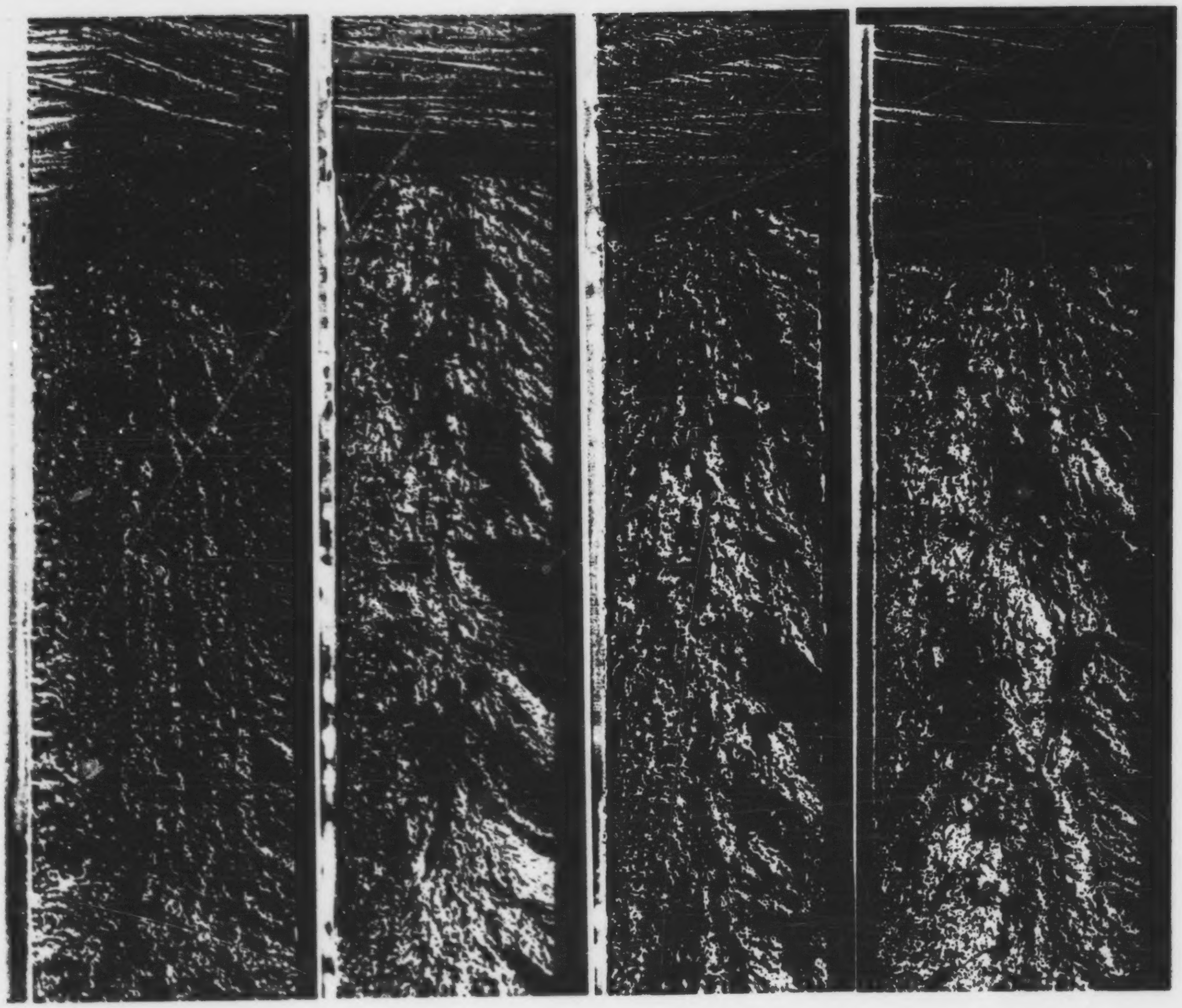

WP # 1 WP # 2 WP # 3 WP # 4

Figure 35. Fracture initiation modes of the wide plates.

APPENDIX A

WELDING DATA SHEET

WELDING INSTITUTE OF CANADA
INSTITUT DE SOUDAGE DU CANADA

CONTRACT NO. RC 391
DATA SHEET NO. 1 (wide plate # 1)

PROCESS: FCAW

MATERIALS: ABS DH 36

POSITION: Vertical up

PREHEAT:

Preheat Temp. 150 deg. C
Interpass Temp. 150 deg. C
Preheat Maintenance

FILLER METAL:

Classification E480-1T-9CH
Trade Name LA T-91 (CLA)

FLUX:

Class:
Trade Name:

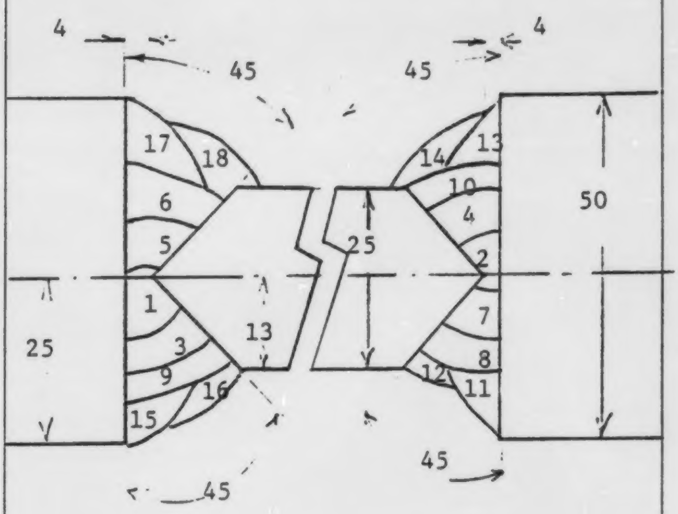

Test Plate

JOINT DETAILS

GAS COMPOSITION REQUIRED:

Shielding Gas Blue shield #8 At 40 CFH
Backing Gas At CFH
Trailing Gas At CFH

ELECTRICAL CHARACTERISTICS:

Power Source: Powcon 300 SM
Current Type: Constant current
Polarity: DCRP

SPECIAL NOTES

Tacking procedure:
150 deg. C preheat is maintained before any welding or tacking is done.

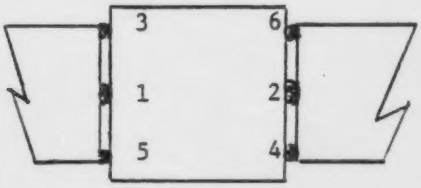

T	WELD SEQUENCE			ELECTRODE		WELDING VARIABLES					
	SIDE	LAYER	PASS	TYPE	SIZE mm	AMPS	VOLTS	E.S.O.	SPEED mmps	WFS ipm	HEAT INPUT
			1-4		1.2	204	22	13	5	200	
			5-8		"	190	23	13	4	190	
			9,10		"	195	23	13	4	190	
			11-14		"	170	22	13	4	180	
			15-18		"	170	22	13	4	180	

ISSUED BY: **DATE:** **LAB TECHNOLOGIST:**

ADDITIONAL NOTES:

T	WELD SEQUENCE			ELECTRODE		WELDING VARIABLES					
	SIDE	LAYER	PASS	TYPE	SIZE mm	AMPS	VOLTS	E.S.O.	SPEED mmps	WFS ipm	HEAT INPUT

WELDING DATA SHEET

WELDING INSTITUTE OF CANADA
INSTITUT DE SOUDAGE DU CANADA

CONTRACT NO. RC 391

DATA SHEET NO. 2 (wide plates # 2-4)

PROCESS: FCAW

MATERIALS: ABS DH 36

POSITION: Vertical up - 3G

PREHEAT:

Preheat Temp. 150 deg. C
Interpass Temp. 150 deg. C
Preheat Maintenance

FILLER METAL:

Classification E480-1T-9CH
Trade Name LA T-91 (CLA)

FLUX:

Class:
Trade Name:

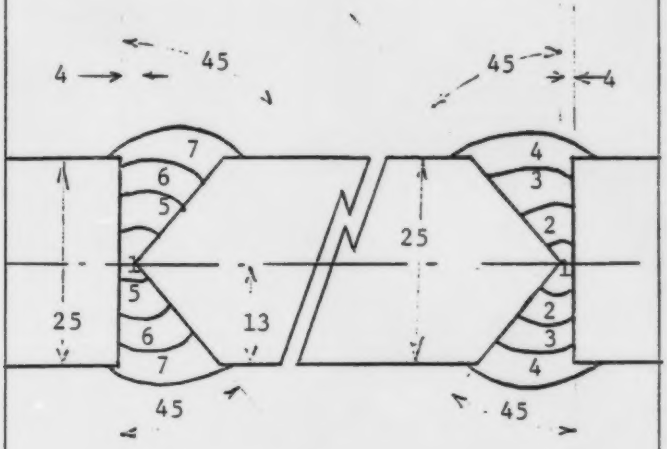

Test Plate

JOINT DETAILS

GAS COMPOSITION REQUIRED:

Shielding Gas Blue shield # 8, At 40 CFH
Backing Gas At CFH
Trailing Gas At CFH

ELECTRICAL CHARACTERISTICS:

Power Source: Powcon 300 SM and
Current Type: Hobart Mega Mig Rus 650
Polarity: Constant current, DCRP

SPECIAL NOTES

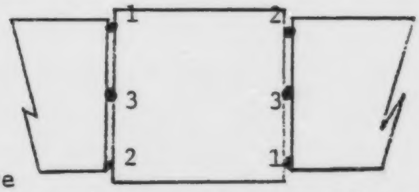

Tacking procedure:
150 deg. C preheat maintained before any welding or tacking is done.
Welding procedure:
Welds were deposited using two welders. Roots were welded first. Joint was then completed by depositing welds on opposite sides of joint.

	WELD SEQUENCE			ELECTRODE		WELDING VARIABLES					
T	SIDE	LAYER	PASS	TYPE	SIZE mm	AMPS	VOLTS	E.S.O.	SPEED mmps	WFS ipm	HEAT INPUT
Welder 1	East		1,2,5		1.2	215	22	13	5	200	
			3,4,6,7		"	170	20	"	4	180	
Welder 2	West		1,2,5		"	200	21	"	5	190	
			3,4,6,7		"	160	19	"	4	170	

ISSUED BY:

DATE:

LAB TECHNOLOGIST:

Table A1. Temperature Readings for Wide Plate Test # 1.

Pressure	Thermocouple Readings, deg. C										
psi	TC1	TC2	TC3	TC4	TC5	TC6	TC7	TC8	TC9	INLET	0UTLET
0	-74.9	-75	-74	-74	-74	-76	-74	-75	-75	-83	-91
823	-74.5	-75	-74	-74	-73	-75	-73	-74	-74	-79	-86
1103	-73.5										
1416	-74.8										
1722	-75.5										
1977	-76.3	-76	-75	-77	-75	-76	-75	-77	-75	-90	-101
2234	-77.2										
2459	-76.8										
2707	-75.6										
2943	-74.2										
3185	-73.4										
3448	-74.5	-75	-74	-75	-74	-75	-74	-76	-75	-80	-102

Table A2. Temperature Readings for Wide Plate Test # 2.

Pressure psi	Thermocouple Readings, deg. C										
	TC1	TC2	TC3	TC4	TC5	TC6	TC7	TC8	TC9	TC10	TC11
0	-39.8	-39	-41.4	-37	-36	-39	-39	-40.1	-36	1.4	0.3
1065	-40	-40	-41.5	-38	-38	-41	-40	-40.3	-38	1	0.1
1571	-40.1	-40	-41.5	-38	-38	-41	-40	-40.4	-38	0.8	-0.2
2084	-40.1	-41	-41.6	-39	-38	-41	-40	-40.4	-38	0.7	-0.4
2613	-40.2	-41	-41.6	-39	-38	-41	-41	-40.6	-38	0.6	-0.5
2961	-40.2	-41	-41.7	-39	-39	-42	-41	-40.6	-39	0.5	-0.7
3558	-40.3	-41	-41.5	-39	-39	-42	-41	-40.5	-39	0.4	-0.7
3940	-40.2	-41	-41.6	-40	-39	-42	-42	-40.6	-39	0.3	-0.8
4506	-40.4	-41	-40.6	-40	-39	-42	-42	-40.6	-39	0.1	-0.9
4833	-40.5	-40	-41.7	-39	-39	-42	-42	-40.7	-39	0	-0.9

Table A3. Temperature Readings for Wide Plate Test # 3.

Pressure psi	Thermocouple Readings, deg. C										
	TC1	TC2	TC3	TC4	TC5	TC6	TC7	TC8	TC9	TC10	TC11
0	-20.3	-22	-21.8	-21	-21	-22	-21	-20.3	-19	4.5	3.6
1000	-21.4	-23	-23	-22	-22	-23	-23	-21.5	-21	4.4	3.5
2000	-21.3	-23	-22.7	-22	-22	-23	-23	-21.7	-21	4.3	3.3
2500	-21	-23	-22.2	-21	-21	-23	-23	-21.4	-21	4.2	3.2
3000	-20.7	-23	-21.8	-21	-20	-23	-23	-21.1	-21	4.1	3.1
3500	-20.2	-22	-21.1	-20	-21	-22	-22	-20.5	-20	4.1	3.1
4000	-19.5	-21	-20.3	-20	-20	-22	-21	-19.8	-20	4	3
4500	-18.9	-20	-19.6	-19	-19	-21	-20	-19.2	-19	4	2.9
5000	-18.5	-20	-19.1	-19	-19	-21	-20	-18.8	-19	3.9	2.8
5500	-18.5	-20	-19.3	-19	-19	-21	-20	-18.9	-19	3.8	2.8

Table A4. Temperature Readings for Wide Plate Test # 4.

Pressure psi	Thermocouple Readings, deg. C										
	TC1	TC2	TC3	TC4	TC5	TC6	TC7	TC8	TC9	TC10	TC11
0	-55.4	-55	-56.7	-54	-53	-57	-58	-55.9	-54	-5.1	-6.9
1000	-55.5	-55	-56.8	-54	-53	-57	-58	-56	-55	-5.2	-7
2000	-55.5	-56	-57	-56	-54	-58	-58	-55.9	-55	-5.3	-7
2250	-55.4	-56	-56.9	-56	-54	-58	-58	-55.9	-55	-5.3	-7.1
2500	-55.3	-56	-56.9	-56	-54	-58	-58	-55.8	-55	-5.3	-7.1
2750	-55.1	-56	-56.6	-56	-54	-58	-58	-55.5	-55	-5.4	-7.1
3000	-54.9	-56	-56.4	-56	-54	-58	-58	-55.3	-55	-5.4	-7.2
3250	-54.7	-56	-56.2	-56	-54	-58	-58	-55.1	-55	-5.5	-7.3
3500	-54.8	-56	-56.3	-56	-54	-58	-58	-55.3	-55	-5.5	-7.3
3750	-55.1	-56	-56.6	-56	-54	-58	-58	-55.7	-55	-5.5	-7.3
4250	-55.4	-56	-56.8	-57	-55	-58	-58	-56.1	-56	-5.5	-7.2
5000	-55.2	-57	-56.7	-57	-55	-58	-58	-55.7	-55	-5.6	-7.3
6000	-54.9	-58	-56.5	-59	-55	-58	-58	-55.8	-56	-5.7	-7.5

Table A5. Strain Gauge readings for Wide Plate Test # 1.
(West)

Pressure psi	Micro-strain					
	S1W	S2W	S3W	S4W	S5W	S6W
0	0.204	-0.339	0.272	0.339	0.272	-0.136
823	771	666	774	-57.35	-61.42	26
1103	911	768.9	923	-28.57	-44.25	83.42
1416	998.7	831.4	1022	7.058	-15.68	144
1722	1073	882.3	1103	56.13	21.24	207.9
1977	1139	926.2	1178	105.2	57.22	270
2234	1202	964.8	1246	153	91.64	332.1
2459	1254	999.3	1311	197.3	127.1	396.8
2707	1315	1034	1378	247.4	162.3	463.8
2943	1370	1067	1444	300.5	201.3	536.2
3185	1431	1100	1513	359.3	242.3	613.1
3448	1500	1133	1589	426.5	288.3	697.6
3683	1587	1162	1662	481	325	762

Table A6. Strain Gauge Readings for Wide Plate Test # 1.

Pressure psi	Micro-strain					
	S1E	S2E	S3E	S4E	S5E	S6E
0	0.407	0.204	0.136	0.0679	0	-0.339
823	-261.5	-253.2	-170.4	558.1	473.8	574
1103	-178.5	-184.8	-63.72	741.2	626.8	776.7
1416	-112.8	-129.4	21.92	849.2	714.7	904
1722	-46.9	-77.23	99.37	933.5	780.8	1001
1977	16.97	-28.37	171.7	1008	835.6	1086
2234	79.62	18.67	243.3	1077	886.9	1167
2459	135.7	62.71	313	1135	930.9	1241
2707	200.3	110.3	385.9	1199	976	1318
2943	260.2	155.8	459.5	1256	1016	1390
3185	330.2	205	537.1	1318	1057	1464
3448	409.3	256.5	624.6	1386	1096	1544
3683	475	300	700	1450	1137	1638

Table A7. Strain Gauge Readings for Wide Plate Test # 2.
(West)

Pressure psi	Micro-strains						
	S1W	S2W	S3W	S4W	S5W	S6W	S7W
0	-2.14	-1.181	-1.403	-4.872	-5.093	-4.503	-1.329
1065	141.3	104.1	183.9	466.4	400.6	478.2	95.75
1571	269.3	190	305.3	724.1	594.7	704.8	166.5
2084	385.6	265.4	408.9	893.6	712.7	848.2	225.5
2613	534.2	358.2	541.1	1100	856.4	1033	298.9
2916	666.9	438.1	662	1287	988.6	1206	365.2
3558	813.9	515.5	797.7	1427	1073	1346	431.7
3940	929.6	574.9	910.5	1545	1146	1471	483.7
4506	1121	656.7	1096	1727	1246	1667	565.1
4833	1262	707.8	1229	1872	1324	1818	621.2
5548	1521	821	1471	2186	1471	2071	739

Table A8. Strain Gauge Readings for Wide Plate Test # 2.
(East)

Pressure psi	Micro-strains						
	S1E	S2E	S3E	S4E	S5E	S6E	S7E
0	-3.617	-2.805	-3.691	0.1476	0.4429	1.255	-2.215
1065	354.1	297	387.4	52.64	1.238	67.28	123
1571	562.5	448.5	577.9	150.1	46.49	140.3	186.1
2084	707.3	544.6	702.2	257.5	102.1	213.1	225.6
2613	891.8	664.1	860.6	395.3	173.1	312.3	277.1
2916	1059	775.8	1011	519.9	233.9	406	324.9
3558	1205	858.7	1141	679	315.8	536.3	363.8
3940	1328	930.7	1258	803.9	374.9	642.6	397.8
4506	1527	1031	1445	1017	461.1	827	449.2
4833	1680	1106	1588	1168	514.9	958.9	487.9
5548	1975	1250	1850	1444	638	1237	571

Table A9. Strain Gauge Readings for Wide Plate Test # 3.
(West)

Pressure psi	Micro-strains						
	S1W	S2W	S3W	S4W	S5W	S6W	S7W
100	0.2341	1.951	0.8583	-3.745	-3.979	-7.022	1.092
1000	184.6	136	206.8	462.6	402.4	482	107.2
2000	492.6	366.6	531.1	925.3	779	951.1	273.3
2500	590.5	439.5	635.2	1029	853.3	1055	324.6
3000	796.4	587.8	857.1	1310	1071	1346	431.9
3500	975.8	709.7	1049	1531	1232	1570	522.3
4000	1116	793.6	1199	1674	1326	1713	588.3
4500	1191	817.3	1279	1711	1329	1742	615.1
5000	1473	958.8	1589	2013	1527	2040	737.8
5500	1350	821.6	1483	1703	1301	1630	652.2
5779	1240	720	1410	1500	1140	1400	611
5715							

Table A10. Strain Gauge Reading for Wide Plate Test # 3.
(East)

Pressure psi	Micro-strains						
	S1E	S2E	S3E	S4E	S5E	S6E	S7E
100	-3.355	-2.887	-4.994	3.511	2.809	3.589	-1.639
1000	324.1	274.1	374.3	85.57	10.91	59.79	120
2000	680.7	557.6	779.8	338.7	159.8	270.8	239.8
2500	772.8	620.6	880.5	440.4	227.7	362.2	268.2
3000	1004	789.6	1138	629.2	337.9	530.4	344.1
3500	1198	920.4	1352	809.4	438.5	696	408.1
4000	1342	1002	1505	969	518	850.6	452
4500	1407	1015	1568	1075	554.4	965.8	467.7
5000	1711	1176	1898	1391	670.2	1284	556.7
5500	1549	1004	1704	1330	581.9	1273	488.8
5779	1471	914	1586	1271	550	1257	454
5715							

Table A11. Strain Gauge Readings for Wide Plate Tast # 4.

Pressure psi	Micro-strains						
	S1E	S2E	S3E	S4E	S5E	S6E	S7E
100	-3.063	-2.69	-2.615	-2.465	-1.868	-0.9712	-0.3736
1000	282.1	222.8	304	211.7	109	141.9	103.6
2000	522.8	400.1	542.4	483.7	283	346	183.2
2250	587.9	448.2	607.6	554.7	327	399.7	205.5
2500	654	497.2	674.8	623.9	371.9	454.1	229.3
2750	722.4	548.5	744.1	693.3	415.6	508.9	253
3000	789.4	597.8	813.4	760.7	458.1	562.5	277
3250	856.1	647	881.9	826.4	499.9	616.5	301.7
3500	926.6	698.3	952.4	897.2	542.9	673.9	326.3
3750	996.2	744.9	1024	968.6	582.6	730.8	350.1
4000	1070	784.7	1098	1048	618.8	792.3	372.6
4250	1142	821.5	1173	1128	652.6	856	394.9
4500	1212	856.6	1245	1205	683.7	917.3	416.6
4750	1296	889.4	1330	1300	716.4	992.4	439.2
5000	1372	917.7	1410	1387	743.5	1061	459
5250	1457	942.5	1499	1487	767.5	1144	479.2
5500	1540	963.1	1586	1582	788.5	1226	497.8
5750	1615	973	1672	1649	803.7	1317	509.8
5958	1649	979.6	1737	1709	829.4	1391	517.8

Table A12. Strain Gauge Readings for Wide Plate Tast # 4.
(East)

Pressure psi	Micro-strains						
	S1W	S2W	S3W	S4W	S5W	S6W	S7W
100	-2.615	-1.42	-1.345	-0.9712	-0.6724	-1.644	-0.2241
1000	214	162	223.7	343.4	275.9	323.2	111.8
2000	443.3	334.2	447.9	586.8	453.7	532.7	227.3
2250	501.8	379	507.5	654.2	502.7	590.9	257.4
2500	560.2	424.8	569.8	722	554.5	652.2	287.7
2750	621.5	471.6	633.2	794.4	607	715.8	318.4
3000	680.3	516.5	696.2	866	661.6	780.8	349.1
3250	740	563.1	759.8	936.5	714	846.9	379.1
3500	801.8	609.4	825.5	1011	767.6	913.2	409.3
3750	864.4	652.4	890.9	1084	818.9	980.6	439.8
4000	929.3	688.7	956.8	1155	860.5	1047	468.2
4250	994.1	722.2	1023	1220	898.2	1114	496.2
4500	1059	755	1088	1286	936.3	1181	523.1
4750	1133	785.8	1162	1355	970	1256	551.4
5000	1203	813.8	1234	1419	1001	1328	577.9
5250	1282	835	1313	1480	1027	1407	604.7
5500	1359	855.4	1390	1534	1053	1483	629.3
5750	1429	861.3	1463	1547	1067	1557	648.3
5958	1461	867	1517	1571	1101	1623	662.3

Table A13. Stress Values Calculated from Microstrain Values and jack pressure for Wide Plate Test # 1.

Pressure psi	Avge. Microstrain	Stress MPa	Nom. Stress MPa
823	291.4	61.19	47.86
1103	357.1	74.99	64.14
1416	430.54	90.41	82.34
1722	502.35	105.49	100.12
1977	562.2	118.06	114.97
2234	622.5	130.73	129.91
2459	673.33	141.39	142.99
2707	733.53	154.04	157.42
2943	788.92	165.67	171.14
3185	845.72	177.6	185.21
3448	912.3	191.58	200.5
3683	973	204.33	214

Table A14. Stress Values Calculated from Microstrain Values and Jack Pressure for Wide Plate Test # 2.

Pressure psi	Avge. Microstrain	Stress MPa	Nom. Stress MPa
1065	244.9	51.43	61.83
1571	376.46	79.06	91.2
2084	509.84	107.07	121.04
2613	647.38	135.95	151.69
2961	737.86	154.95	171.89
3558	893.08	187.55	206.55
3940	992.4	208.4	228.73
4506	1152	241.88	261.59
4833	1269	266.49	280.57
5548	1495	313.95	322.08

Table A15. Stress Values Calculated from Microstrain Values and Jack Pressure for Wide Plate Test # 3.

Pressure psi	Avge. Microstrain	Stress MPa	Nom. Stress MPa
1000	224.25	47.09	58.05
2000	534.25	112.19	116.11
2500	689.25	144.74	145.13
3000	844.25	177.29	174.16
3500	999.25	209.84	203.19
4000	1154.25	242,39	232.21
4500	1179.54	247.7	261.23
5000	1477.58	310.29	290.26
5500	1310.88	275.28	319.29
5779	1204.92	253.03	335.49

Table A16. Stress Values Calculated from Microstrain Values and Jack Pressure for Wide Plate Test # 4.

Pressure psi	Avge. Microstrain	Stress MPa	Nom. Stress MPa
1000	209	43.89	58.35
2000	446	93.66	116.69
2250	505.25	106.1	131.28
2500	564.5	118.55	145.86
2750	623.75	130.99	160.45
3000	683	143.43	175.04
3250	742.25	155.87	189.62
3500	801.5	168.32	204.21
3750	860.75	180.76	218.8
4000	920	193.2	233.39
4250	978.72	205.53	247.97
4500	1035.4	217.44	262.56
4750	1098.83	230.71	277.15
5000	1157.5	243.08	291.73
5250	1220.08	256.22	306.32
5500	1280	268.8	320.91
5750	1329.5	279.2	335.5
5958	1369.6	287.62	347.63

Table A17. Clip Gauge Readings for Wide Plate Test # 1.

Pressure psi	Clip Gauge Displacements (mm)					
	CG # 1	CG # 2	CG # 3	CG # 4	CG # 5	CG # 6
0			0			
823	0.423	0.186	0.0512	0.2357	0.1058	0.1336
1103	0.4922	0.2051	0.1024	0.3661	0.1644	0.2029
1416	0.6726	0.3201	0.2048	0.574	0.3044	0.3635
1722	0.8016	0.3835	0.2816	0.7218	0.3994	0.4691
1977	0.9226	0.4685	0.3584	0.8586	0.4904	0.5694
2234	1.0382	0.5437	0.4353	0.9914	0.5821	0.6689
2459	1.093	0.5714	0.4865	1.0569	0.6153	0.7069
2707	1.1258	0.5855	0.5121	1.0996	0.6305	0.7261
2943	1.1437	0.5903	0.5377	1.1242	0.6333	0.7328
3185	1.1958	0.6256	0.5889	1.1755	0.6672	0.773
3448	1.3637	0.7554	0.7446	1.3325	0.804	0.9248
3683	1.5	0.8625	0.8577	1.4375	0.919	1.05

Table A18. Clip Gauge Readings for Wide Plate Test # 2.

Pressure psi	Clip Gauge Displacements (mm)					
	CG # 1	CG # 2	CG # 3	CG # 4	CG # 5	CG # 6
0			0			
1065	0.1359	0.0571	0.0772	0.1289	0.0709	0.0295
1571	0.2063	0.0971	0.1026	0.2008	0.1122	0.0469
2084	0.2839	0.152	0.1534	0.2795	0.1595	0.0682
2613	0.3715	0.2248	0.2296	0.3703	0.2194	0.1006
2961	0.4342	0.2826	0.2804	0.4352	0.2664	0.1304
3558	0.5632	0.4026	0.3845	0.5619	0.3644	0.1941
3940	0.6581	0.4961	0.4607	0.6524	0.4396	0.2456
4506	0.8298	0.6718	0.5903	0.8247	0.5864	0.3444
4833	0.9495	0.7965	0.6919	0.9458	0.6936	0.4194
5548	1.25	1.17	1.0373	1.25	1.04	0.7

Table A19. Clip Gauge Readings for Wide Plate Test # 3.

Pressure psi	Clip Gauge Displacements (mm)					
	CG # 1	CG # 2	CG # 3	CG # 4	CG # 5	CG # 6
100	0.0038	0.001	0	0.0024	0.0045	0.0011
1000	0.0364	0.10295	0.1016	0.0381	0.0394	0.0241
2000	0.084	0.2174	0.2032	0.0876	0.0809	0.0521
2500	0.1198	0.2842	0.2794	0.1278	0.1091	0.0731
3000	0.1694	0.3589	0.3556	0.1798	0.1517	0.1174
3500	0.2294	0.4417	0.4318	0.2353	0.2071	0.1731
4000	0.3086	0.5398	0.5588	0.3058	0.2797	0.2483
4500	0.4058	0.656	0.635	0.393	0.3714	0.3395
5000	0.5411	0.8219	0.8128	0.5272	0.5056	0.47
5500	0.75355	1.0872	1.0922	0.7594	0.7152	0.675
5779	1.3286	1.651	1.651	1.3286	1.1357	1.1357
5715			1.9304			

Table A20. Clip Gauge Reading for Wide Plate Test # 4.

Pressure psi	Clip Gauge Displacements (mm)					
	CG # 1	CG # 2	CG # 3	CG # 4	CG # 5	CG # 6
100	0.00141	0.00143	0	0.00182	0.00073	0.0035
1000	0.0429	0.1115	0.1016	0.02731	0.0339	0.0167
2000	0.0928	0.2383	0.2286	0.05753	0.0764	0.0383
2250	0.1047	0.2688	0.2734	0.0648	0.0874	0.0432
2500	0.1174	0.2993	0.3048	0.0721	0.0979	0.0485
2750	0.1307	0.329	0.3302	0.0779	0.1077	0.0538
3000	0.1448	0.3598	0.3556	0.0852	0.119	0.0602
3250	0.1592	0.3896	0.4064	0.0954	0.1303	0.0662
3500	0.1785	0.425	0.4318	0.1121	0.146	0.0737
3750	0.2066	0.4674	0.4826	0.1336	0.1736	0.0868
4000	0.2572	0.5236	0.5334	0.1708	0.2213	0.1116
4250	0.312	0.5813	0.5842	0.2094	0.2715	0.1399
4500	0.3655	0.6383	0.6604	0.2461	0.3225	0.1661
4750	0.4438	0.7175	0.7366	0.2997	0.3979	0.2037
5000	0.5197	0.7989	0.8128	0.3554	0.4736	0.2405
5250	0.6287	0.9103	0.9398	0.4358	0.5795	0.2922
5500	0.7457	1.034	1.0668	0.5633	0.6967	0.351
5750	0.9379	1.2286	1.2446	0.7337	0.8816	0.4778
5958	1.2647	1.54	1.8796	0.982	1.1881	0.7251

Table A21. CTOD Values at Different Stress Levels
for Wide Plate Test # 1.

Pressure	Nom. Stress	Stress	CTOD, mm			(E1+E2)/2	
psi	MPa	MPa	W	E1	E2	E	(W+E)/2
823	47.86	61.19	-0.0046	0.0796	0.113	0.0963	0.0459
1103	64.14	74.99	0.0439	0.1237	0.17	0.1469	0.0954
1416	82.34	90.41	0.1346	0.25	0.321	0.2855	0.2101
1722	100.12	105.49	0.2036	0.3343	0.4181	0.3277	0.2656
1977	114.97	118.06	0.2738	0.4161	0.511	0.4636	0.3687
2234	129.91	130.73	0.3449	0.4995	0.6038	0.5517	0.4483
2459	142.99	141.39	0.3955	0.5261	0.6362	0.5811	0.4883
2707	157.42	154.04	0.4201	0.5358	0.6507	0.5933	0.5067
2943	171.14	165.67	0.4468	0.5342	0.6538	0.594	0.5204
3185	185.21	177.6	0.4979	0.5645	0.6917	0.6281	0.563
3448	200.5	191.58	0.6517	0.6973	0.8425	0.7699	0.7108
3683	214	204.33	0.7614	0.8143	0.9718	0.8931	0.8272

Table A22. CTOD Values at Different Stress Levels
for Wide Plate Test # 2.

Pressure	Nom. Stress	Stress			CTOD Values, mm				
psi	MPa	MPa	W	E	(W+E)/2	CG2	CG6	(CG2+CG6)/2	(A+B)/2
					A			B	
1065	61.83	51.43	0.0464	0.0477	0.0471	0.0571	0.0295	0.0433	0.0452
1571	91.2	79.06	0.0611	0.0768	0.0689	0.0971	0.0469	0.072	0.0705
2084	121.04	107.07	0.1012	0.1115	0.1064	0.152	0.0682	0.1101	0.1083
2613	151.69	135.95	0.1728	0.159	0.1659	0.2248	0.1006	0.1627	0.1643
2961	171.89	154.95	0.2189	0.1989	0.2089	0.2826	0.1304	0.2065	0.2077
3558	206.55	187.55	0.313	0.2854	0.2992	0.4026	0.1941	0.2984	0.2988
3940	228.73	208.4	0.3817	0.3545	0.3681	0.4961	0.2456	0.3709	0.3695
4506	261.59	241.88	0.4945	0.4911	0.4928	0.6718	0.3444	0.5081	0.5005
4833	280.57	266.49	0.5889	0.5927	0.5908	0.7965	0.4194	0.608	0.5994
5548	322.08	313.95	0.9522	0.956	0.9541	1.17	0.7	0.935	0.9446

Table A23. CTOD Values at Different Stress Levels
for Wide Plate Test # 3.

Pressure psi	Nom. Stress MPa	Stress MPa	CTOD Values, mm (CG1+CG4)/2 W	(CG5+CG6)/2 E	(W+E)/2
1000	58.05	47.09	0.0373	0.03175	0.0345
2000	116.11	112.19	0.0858	0.0665	0.07615
2500	145.13	144.74	0.1238	0.0911	0.1075
3000	174.16	177.29	0.1746	0.1346	0.1546
3500	203.19	209.84	0.2324	0.1901	0.2113
4000	232.21	242.39	0.3072	0.264	0.2856
4500	247.7	261.23	0.3994	0.3555	0.3774
5000	290.26	310.29	0.5342	0.4878	0.511
5500	319.29	275.28	0.7565	0.6951	0.7258
5779	335.49	253.03	1.3286	1.1357	1.2322

Table A24. CTOD Values at Different Stress Levels
for Wide Plate Test # 4.

			CTOD Values, mm		
Pressure psi	Nom. Stress MPa	Stress MPa	(CG1+CG4)/2 W	(CG5+CG6)/2 E	(W+E)/2
1000	58.35	43.89	0.0351	0.0253	0.0302
2000	116.69	93.66	0.0752	0.0574	0.0663
2250	131.28	106.1	0.0848	0.0653	0.0751
2500	145.86	118.55	0.0948	0.0732	0.084
2750	160.45	130.99	0.1043	0.0808	0.0925
3000	175.04	143.43	0.115	0.0896	0.1023
3250	189.62	155.87	0.1273	0.0983	0.1128
3500	204.21	168.32	0.1453	0.1099	0.1276
3750	218.8	180.76	0.1701	0.1302	0.1502
4000	233.39	193.2	0.214	0.1665	0.1902
4250	247.97	205.53	0.2607	0.2057	0.2332
4500	262.56	217.44	0.3058	0.2443	0.2751
4750	277.15	230.71	0.3718	0.3008	0.3363
5000	291.73	243.08	0.4376	0.3571	0.3973
5250	306.32	256.22	0.5323	0.4359	0.4841
5500	320.91	268.8	0.6545	0.5239	0.5892
5750	335.5	279.2	0.8358	0.6797	0.7578
5958	347.63	287.62	1.1234	0.9566	1.04

APPENDIX AA

Strain gauge locations

Gauges in the shadow of the crack showed mean values of slope about 63% of the other readings. To determine the likely effect of the crack on stress distribution away from the crack an estimate was made using the linear elastic equations. It is recognized that they are not strictly applicable away from the crack in finite plate widths but were considered good enough to give an approximate indication. Using the equation:

$$\sigma_{yy} = \sigma\,(a/2r)^{1/2}\,[1.25 \cos(\theta/2) - 0.25 \cos(2.5\,\theta)]$$

the graphs in Fig 4 were produced. The stress in the shadow is about 78 % of the stress at the location of the other gauges. The average stress from the three gauges in the locations used and based on Fig 4 is 98.5% of the mean gross stress. This suggests that the method of taking the average of the three gauges across the width will provide the mean stress within 2% accuracy. Fig 4 also suggests that if fewer gauges are used they could be placed in line with the tip of the crack where the local stress is almost equal to the mean stress.

Fig 4. Estimated stress distribution across wide plate specimen.

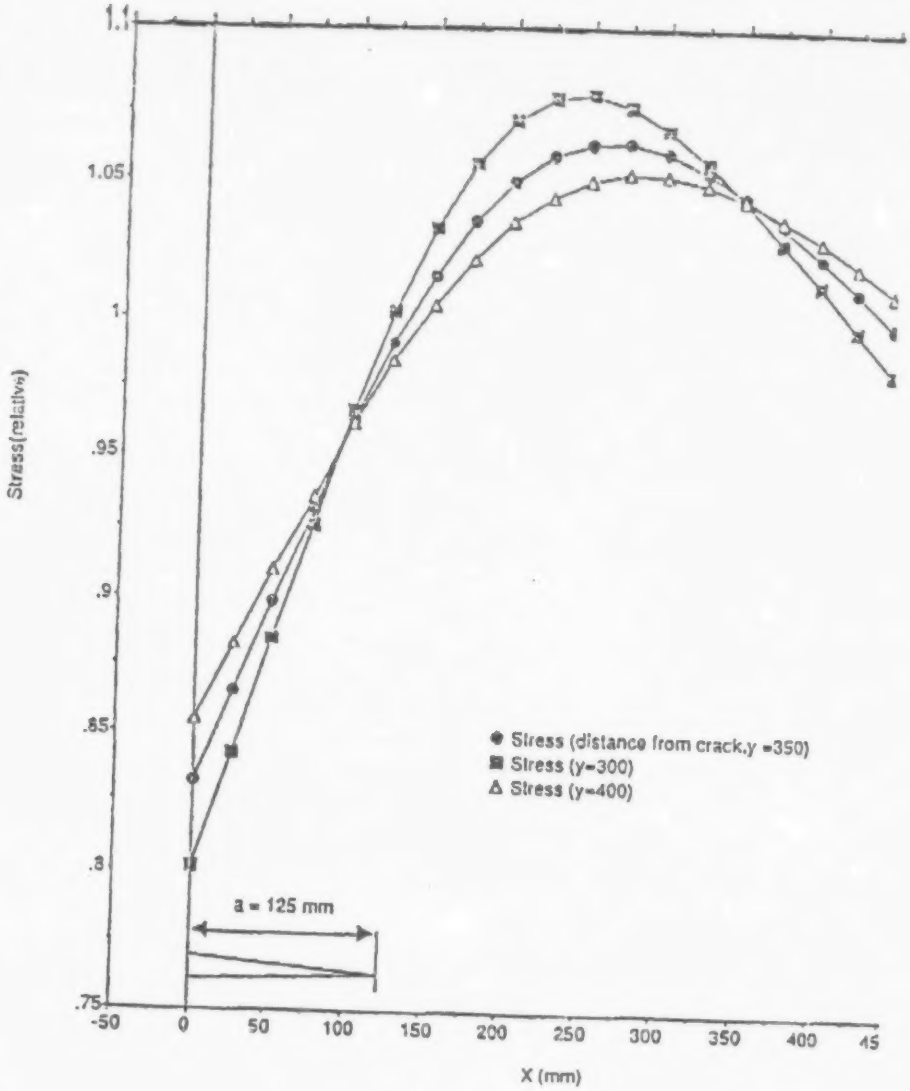

Table AA1. Pressure Transducer Calibration
for Wide Plate test # 1.

Dead Weight Load psi	Pressure Transducer Output V
0	-
500	0.078
1000	0.575
2000	1.05
3000	1.764
4000	2.001
5000	2.471
10000	4.781

Table AA2. Pressure Transducer Output
(Voltage Monitor & Chart Recorder) and Jack Pressure.

Pressure Transducer Output V	Jack Pressure psi
0.4	823
0.625	1103
0.777	1416
0.921	1722
1.039	1977
1.158	2234
1.262	2459
1.381	2707
1.495	2943
1.612	3185
1.739	3448
1.85	3683

Table AA3. Clip Gauge Calibration for Wide Plate Tests # 1 & 2.

Gauge #	mV or V	Opening , inch		Slope, mm/mV or mm/V
1	27.055	0.5		-
	23.238	0.55		0.3327
	19.494	0.6		0.3392
	15.67	0.65		0.3321
	11.309	0.7		0.3372
			Avge.	0.3353
1	25.467	0.5		-
	21.862	0.55		0.3523
	18.249	0.6		0.3515
	14.704	0.65		0.3583
	11.112	0.7		0.3536
	7.549	0.75		0.3564
			Avge.	0.3544
2	26.594	0.5		-
	22.898	0.55		0.3436
	19.392	0.6		0.3622
	15.941	0.65		0.368
	12.476	0.7		0.3665
	9.118	0.75		0.3782
			Avge.	0.3637
3	-0.1	0.475 V		-
	2.4	0.5		
	4.9	0.525		
	7.3	0.55		
	9.8	0.575		
	12.3	0.6		
	14.3	0.625		
			Avge.	0.256 mm/V
4	24.879	0.25		-
	21.094	0.3		0.3355
	17.374	0.35		0.3414
	13.758	0.4		0.3512
	10.251	0.45		0.3621
	6.834	0.5		0.3717
			Avge.	0.3524
4	23.545	0.25		-
	19.95	0.3		0.3533
	16.401	0.35		0.3579

	12.89	0.4		0.3617
	9.385	0.45		0.3623
	5.892	0.5		0.3636
			Avge.	0.3598
5	26.733	0.25		-
	22.925	0.3		0.3335
	19.247	0.35		0.3453
	15.653	0.4		0.3534
	12.03	0.45		0.3505
	8.454	0.5		0.3552
			Avge.	0.3476
5	25.324	0.25		-
	21.811	0.3		0.3615
	18.381	0.35		0.3703
	14.973	0.4		0.3724
	10.998	0.45		0.3195
	7.468	0.5		0.36
			Avge.	0.3568
5	25.358	0.25		-
	21.79	0.3		0.3559
	18.208	0.35		0.3546
	14.631	0.4		0.3551
	11.031	0.45		0.3528
	7.468	0.5		0.3518
			Avge.	0.354
6	28.029	0.25		-
	24.208	0.3		0.3324
	20.475	0.35		0.3402
	16.757	0.4		0.3416
	12.334	0.45		0.287
	9.351	0.5		0.426
			Avge.	0.3454
6	26.848	0.25		-
	23.301	0.3		0.3581
	19.773	0.35		0.36
	16.334	0.4		0.3693
	12.941	0.45		0.3743
			Avge.	0.3654

Table AA4. Clip Gauge Readings for Wide Plate Test # 1.

Transducer Output, V	Clip Gauge Readings					
	CG 1, mV	CG 2, mV	CG 3, V	CG 4, mV	CG 5, mV	CG 6, mV
0	-0.013	-0.006	3.6	-0.012	-0.005	-0.007
0.4	-1.227	-0.511	3.8	-0.662	-0.3	-0.376
0.625	-1.427	-0.564	4	-1.028	-0.466	-0.571
0.777	-1.95	-0.88	4.4	-1.612	-0.863	-1.023
0.921	-2.324	-1.082	4.7	-2.027	-1.132	-1.32
1.039	-2.675	-1.288	5	-2.411	-1.39	-1.602
1.158	-3.01	-1.495	5.3	-2.784	-1.65	-1.882
1.262	-3.169	-1.571	5.5	-2.968	-1.744	-1.989
1.381	-3.264	-1.61	5.6	-3.088	-1.787	-2.043
1.495	-3.316	-1.623	5.7	-3.157	-1.795	-2.062
1.612	-3.467	-1.72	5.9	-3.301	-1.891	-2.175
1.739	-3.954	-2.077	6.5	-3.742	-2.279	-2.602
1.85 Fracture						

Table AA5. Pressure Transducer Calibration for Wide Plate Test # 2.

Dead Weight Load psi	Pressure Transducer Output V
0	0
50	0.0086
1000	0.168
2000	0.336
3000	0.5025
4000	0.670
5000	0.838
6000	1.006
7000	1.172
8000	1.335
9000	1.502
10000	1.666

Table AA6. Pressure Transducer output (Voltage Monitor & Chart Recorder) and Jack Pressure.

Pressure Transducer Output V		Jack Pressure psi
0		0
0.179		1065
0.263		1571
0.35		2084
0.438		2613
0.496		2961
0.596		3558
0.660		3940
0.755		4506
0.810		4833
0.93	Failure	5548

Table AA7. Clip Gauge Readings for Wide Plate Teast # 2.

Transducer Output, V		Clip Gauge Readings					
		CG1, mV	CG2, mV	CG3, V	CG4, mV	CG5, mV	CG6, mV
0		0.004	0.001	2	0.001	0	0.001
0.179		-0.394	-0.157	2.3	-0.362	-0.199	-0.083
0.263		-0.598	-0.267	2.4	-0.564	-0.318	-0.132
0.35		-0.823	-0.418	2.6	-0.785	-0.452	-0.192
0.438		-1.077	-0.618	2.9	-1.04	-0.622	-0.283
0.496		-1.259	-0.777	3.1	-1.222	-0.755	-0.367
0.596		-1.633	-1.107	3.5	-1.578	-1.033	-0.546
0.66		-1.908	-1.364	3.8	-1.832	-1.246	-0.691
0.755		-2.406	-1.847	4.3	-2.316	-1.662	-0.969
0.81		-2.753	-2.19	4.7	-2.656	-1.966	-1.18
0.93	Failure			6.05			

Table AA8. Pressure Transducer Calibration for Wide Plate Test # 3.

Dead Weight Load psi	Pressure Transducer Output V
0	0
50	0.008
1000	0.179
2000	0.338
3000	0.506
4000	0.672
5000	0.840
6000	1.006
7000	1.172
8000	1.336
9000	1.501
10000	1.666

Table AA9. Pressure Transducer Output (Voltage Monitor & Chart Recorder) and Jack Pressure.

Pressure Transducer Output V		Jack Pressure psi
0.017		100
0.178		1000
0.337		2000
0.422		2500
0.506		3000
0.590		3500
0.672		4000
0.755		4500
0.840		5000
0.920		5500
0.968		5779
0.957	Fracture	5715

Table AA10. Clip Gauge Calibrations for Wide Plate Test # 3.

Gauge #	mV or V	Opening, inch		Slope, mm/mV or mm/V
1	26.71	0.5		-
	24.86	0.525		0.3432
	23.02	0.55		0.3451
	21.216	0.575		0.352
	19.4	0.6		0.3497
	17.6	0.625		0.3528
	15.745	0.65		0.3423
	13.929	0.675		0.03497
	12.112	0.7		0.3495
	10.24	0.725		0.3392
	8.415	0.75		0.348
			Avge.	0.3471
2	31.503	0.5		-
	29.65	0.525		0.3427
	27.806	0.55		0.3444
	25.975	0.575		0.3468
	24.133	0.6		0.3447
	22.315	0.625		0.3493
	20.491	0.65		0.3481
	18.664	0.675		0.3476
	16.859	0.7		0.3518
	15.041	0.725		0.3493
	13.241	0.75		0.3528
			Avge.	0.3478
3	-0.1 V	0.475		
	2.4	0.5		
	4.9	0.525		
	7.4	0.55		
	9.9	0.575		
	12.4	0.6		
	14.3	0.635		
			Avge.	0.254 mm/V
4	27.375	0.25		-
	25.606	0.275		0.359
	23.785	0.3		0.3487
	21.981	0.325		0.352
	20.181	0.35		0.3528
	18.388	0.375		0.3542
	16.614	0.4		0.358
	14.864	0.425		0.3629

	13.066	0.45		0.3532
	11.302	0.475		0.36
	9.533	0.5		359
			Avge.	0.356
5	25.8	0.25		-
	23.975	0.275		0.348
	22.125	0.3		0.3432
	20.289	0.325		0.3459
	18.482	0.35		0.3514
	16.673	0.375		0.351
	14.839	0.4		0.3462
	13.022	0.425		0.3495
	11.202	0.45		0.3489
	9.402	0.475		0.3528
	7.587	0.5		0.3499
			Avge.	0.3487
6	31.492	0.25		-
	29.886	0.275		0.3954
	28.071	0.3		0.3499
	26.26	0.325		0.3506
	24.416	0.35		0.3444
	22.619	0.375		0.3534
	20.796	0.4		0.3483
	18.969	0.425		0.3476
	17.166	0.45		0.3522
	15.341	0.475		0.348
	13.561	0.5		0.3567
			Avge.	0.3547

Table AA11. Clip Gauge Readings for Wide Plate Test # 3.

Pressure Transducer Output, V	Clip Gauge readings CG1, mV	CG2, mV	CG3, V	CG4, mV	CG5, mV	CG6, mV
0.017	-0.011	-0.003	2	-0.007	-0.013	-0.003
0.178	-0.105	-0.296	2.4	-0.107	-0.113	-0.068
0.337	-0.242	-0.625	2.8	-0.246	-0.232	-0.147
0.422	-0.345	-0.817	3.1	-0.359	-0.313	-0.206
0.506	-0.488	-1.032	3.4	-0.505	-0.435	-0.331
0.59	-0.661	-1.27	3.7	-0.661	-0.594	-0.488
0.672	-0.889	-1.552	4.2	-0.859	-0.802	-0.7
0.755	-1.169	-1.886	4.5	-1.104	-1.065	-0.957
0.84	-1.559	-2.363	5.2	-1.481	-1.45	-1.325
0.92	-2.171	-3.126	6.3	-2.133	-2.051	-1.903
0.968			8.5			
0.957			9.6			

Table AA12. Pressure Transducer Calibration for Wide Plate Test # 4.

Dead Weight Load psi	Pressure transducer Output V
0	0.001
50	0.009
1000	0.17
2000	0.337
3000	0.502
4000	0.667
5000	0.829
6000	0.997
7000	1.165
8000	1.332
9000	1.495
10000	1.657

Table AA13. Pressure Transducer Output (Voltage Monitor & Chart Recorder) for Wide Plate Test # 4.

Pressure Transducer Output, V	Jack Pressure psi
0.017	100
0.170	1000
0.337	2000
0.3783	2250
0.4195	2500
0.4608	2750
0.502	3000
0.5433	3250
0.5845	3500
0.6258	3750
0.667	4000
0.7065	4250
0.746	4500
0.7885	4750
0.829	5000
0.871	5250
0.913	5500
0.955	5750
0.99	5958

Table AA14. Clip Gauge Calibration for Wide Plate Test # 4.

Gauge #	Opening, inch	mV or V	Slope, mm/mV or mm/V
1	0.5	26.11	-
	0.525	24.26	0.3432
	0.55	22.454	0.3516
	0.575	20.675	0.3569
	0.6	18.853	0.3485
	0.625	17.059	0.354
	0.65	15.234	0.348
	0.675	13.457	0.3573
			Avge. 0.3514
2	0.5	31.24	-
	0.525	29.424	0.3497
	0.55	27.625	0.353
	0.575	25.909	0.37
	0.6	24.158	0.3627
	0.625	22.308	0.3432
	0.65	20.43	0.3381
	0.675	18.737	0.3751
	0.7	17.044	0.3751
			Avge. 0.3584
3	0.475	0	
	0.5	2.5	
	0.525	5	
	0.55	7.5	
	0.575	10	
	0.6	12.5	
	0.625	14.3	
			Avge. 0.254 mm/V
4	0.25	27.23	
	0.275	25.525	
	0.3	23.725	
	0.325	21.941	
	0.35	20.19	
	0.375	18.415	
	0.4	16.67	
	0.425	14.87	
	0.45	13.19	
	0.475	11.477	
	0.5	9.791	
			Avge. 0.3641

5	0.25	25.508		
	0.275	23.721		
	0.3	21.936		
	0.325	20.146		
	0.35	18.347		
	0.375	16.637		
	0.4	14.895		
	0.425	13.185		
	0.45	11.474		
	0.475	9.802		
	0.5	8.063		
			Avge.	0.364
6	0.275	29.602		
	0.3	27.79		
	0.325	25.93		
	0.35	24.12		
	0.375	22.304		
	0.4	20.5		
	0.425	18.751		
	0.45	17.054		
			Avge.	0.3542

Table AA15. Clip Gauge Readings for Wide Plate Test # 4.

Pressure Transducer Output, V	Clip Gauge Readings					
	CG1, mV	CG2, mV	CG3, V	CG4, mV	CG5, mV	CG6, mV
0.017	0.004	0.004	0.2	0.005	0.002	0.001
0.17	-0.122	-0.311	0.6	-0.075	-0.093	-0.047
0.337	-0.264	-0.665	1.1	-0.158	-0.21	-0.108
0.3783	-0.298	-0.75	1.3	-0.178	-0.24	-0.122
0.4195	-0.334	-0.835	1.4	-0.198	-0.269	-0.137
0.4608	-0.372	-0.918	1.5	-0.214	-0.296	-0.152
0.502	-0.412	-1.004	1.6	-0.234	-0.327	-0.17
0.5433	-0.453	-1.087	1.8	-0.262	-0.358	-0.187
0.5845	-0.508	-1.186	1.9	-0.308	-0.401	-0.208
0.6258	-0.588	-1.304	2.1	-0.367	-0.477	-0.245
0.667	-0.732	-1.461	2.3	-0.469	-0.608	-0.315
0.7065	-0.888	-1.622	2.5	-0.575	-0.746	-0.395
0.746	-1.04	-1.781	2.8	-0.676	-0.886	-0.469
0.7885	-1.263	-2.002	3.1	-0.823	-1.093	-0.575
0.829	-1.479	-2.229	3.4	-0.976	-1.301	-0.679
0.871	-1.789	-2.54	3.9	-1.197	-1.592	-0.825
0.913	-2.122	-2.885	4.4	-1.547	-1.914	-0.991
0.955	-2.669	-3.428	5.1	-2.015	-2.422	-1.349
0.99	-3.599	-4.297	7.3	-2.697	-3.264	-2.047

APPENDIX C

SHORT CRACK ARREST (SCA) TEST DEVELOPMENT AND DETAILED PROCEDURES AND RESULTS.

WELDING INSTITUTE OF CANADA
INSTITUT DE SOUDAGE DU CANADA

STUDY OF WIDE PLATE TESTING OF STRUCTURAL STEELS FOR ARCTIC SHIPS

TASKS 6, 8 AND 12

Welding Institute of Canada Report RC 391/2/1991

Final Report to Tasks 6, 8 and 12
Fleet Technology Limited Ref: E93728P

Submitted to
Materials Technology Centre
Fleet Technology Limited
311 Legget Drive
Kanata, Ontario
K2K 1Z8

Prepared by
S. R. Bala, P.Eng.
Welding Institute of Canada

B. Graville, P.Eng.
Graville Associates Inc.

JULY 1991

HEAD OFFICE / SIÈGE SOCIAL: 391 Burnhamthorpe Road East. Oakville. Ont. L6J 6C9 — (416) 257-9881 Fax: (416) 257-9886
CENTRE DU QUÉBEC / QUEBEC CENTRE: 325 boul. Raymond Dupuis, Mont-St-Hilaire, Qué. J3H 5H6 — (514) 446-3053 Fax: (514) 446-3055
WESTERN CENTRE / CENTRE DE L'OUEST: c/o Metal Dept. S.A.I.T., 1301-16 Ave. N.W., Calgary, Alta. T2M 0L4 — (403) 284-8522 Fax: (403) 284-7164

STUDY OF WIDE PLATE TESTING OF STRUCTURAL STEELS FOR ARCTIC SHIPS

TASKS 6, 8 AND 12

Welding Institute of Canada Report RC391/2/1991

EXECUTIVE SUMMARY

Tasks 6,8 and 12 of the "Study of Wide Plate Testing of Structural Steels for Arctic Ships" include development and performance of short crack arrest tests of 25.4mm thick ABS DH36 steel and its heat affected zone (HAZ). The test design is based on the original Tanaka test although considerable modifications have been made for compatibility with the limited access in the Welding Institute of Canada (WIC) wide plate test rig and the type of material being tested.

The objective of the short crack arrest test was to determine the stress/temperature transition for short crack arrest. The short crack arrest concept was developed by Tanaka where arrest of running cracks about 120mm long was considered. The objective was to introduce a running crack into the plate from a separate crack starter device, allow the crack to run to a length of about 120mm in a grooved section where plane strain conditions are assumed to hold, then determine whether the crack arrests at the end of this region or continues to propagate across the specimen. The test was therefore a go/no go type, each test providing a single point of either fracture arrest or propagation on the stress temperature graph.

Development of short crack arrest tests involved designing a crack starter and attachment weld brittle enough to drive a crack through them into the test plate using a loading system. Due to space limitations, the crack starter was a compact tension type, 25.4mm thick x 100mm wide x 280mm long, with an edge crack. Initially 1045 steel was selected for the crack starter plate with blunt notches and side grooves to ensure a high stress intensity (K) value at crack initiation. Some preliminary tests were carried out on the starter steel to determine fracture loads and confirm that adequate jack capacity was available in the loading rig.

The final dimensions of the DH36 steel test plate (parent material or HAZ) were 500mm wide and 1.2 m long, taking into account the limitations of the wide plate test rig, with length parallel to the loading direction. The crack starter was attached to the test plate with a weld 50mm long of brittle material. Initial tests on the original selection, Hobart 320, indicated it was not brittle enough, so it was changed in later tests to Hobart 400. The groove in the main plate opposite the crack starter was 120mm long and 8mm deep. Both the notch plane and the groove length were perpendicular to the loading direction. The notch and the groove were at the centre of the parent plate or in the grain coarsened HAZ (GC HAZ) plane depending on whether the test was for the base plate or the HAZ. The short crack arrest tests involved cooling the test location to the test temperature, loading the main plate to the required stress level and loading the crack starter to fracture.

As testing continued several problems were encountered with the crack starter system and this led to a series of tests to improve the design. Calculations showed that the bending moment transferred to the test plate from the fracture of the edge cracked starter could be significant. However various approaches such as the use of a centre notched crack starter or welding of a strap across the edge of the starter were not successful. The other problem was that the toughness of the crack starter was too high particularly at room temperature. This was overcome by using 20mm thick 1060 steel for the starter.

The short crack arrest tests of the DH36 steel base plate and its GC HAZ were carried out in the wide plate test rig. A straight GC HAZ was obtained using a double bevel joint (K-joint) and submerged arc welding with 5 KJ/mm heat input. For the tests the plates were loaded in the test rig to required stress levels using appropriate end connections. Two stress levels were used: 263 MPa and 350 MPa which were 0.75 and 1.0 of the nominal yield strength of the material. The test temperatures were -15° and 5° C at 263 MPa and 5° and 20° C at 350 MPa for the base plate. Same test temperatures were also used for the HAZ tests except at 263 MPa a test was carried out at -5° C also. Even though these tests did not give the exact arrest temperatures, they yielded complete fracture of the plate/no fracture temperatures. The minimum no fracture temperatures for the base plate and HAZ at 263 MPa stress were 5° and -5° C respectively. At 350 MPa stress it was 20° C for both.

A control test performed showed that the effect of tensile load on the starter and the bending resulting from the edge crack design was to increase the applied stress on the test plate which depended on the magnitude of the starter load, e.g. an increase in applied stress of 30 MPa or 42 MPa at an applied starter jack pressure of 5000 or 8000 psi.

This report contains the experimental and results portion of the project. The analysis of the results (Tasks 9 and 13) will be presented in a separate report.

TABLE OF CONTENTS

EXECUTIVE SUMMARY ii

1.0 INTRODUCTION 1

2.0 OBJECTIVES 3

3.0 EXPERIMENTAL PROCEDURE 3
- 3.1 Materials 3
  - 3.1.1 Shipbuilding Steel 3
  - 3.1.2 Crack Starter 4
- 3.2 Development of Crack Starter 4
  - 3.2.1 Preliminary Progress 5
    - 3.2.1.1 Crack Starter Specimen DSCA (i) 5
    - 3.2.1.2 Crack Starter Specimen DSCA (ii) 6
    - 3.2.1.3 Crack Starter Specimen DSCA (iii) 6
- 3.3 Loading Unit for Crack Starter Specimen 7
- 3.4 Further Progress on Crack Starter Specimens 7
  - 3.4.1 Crack Starter Specimen DSCA #0 7
  - 3.4.2 Crack Starter Specimen DSCA #1 8
  - 3.4.3 Crack Starter Specimen DSCA #2 8
  - 3.4.4 Crack Starter Specimen DSCA #3 8
  - 3.4.5 Crack Starter Specimen DSCA #4 9
  - 3.4.6 Crack Starter Specimen DSCA #5 9
  - 3.4.7 Crack Starter Specimen DSCA #6 9
  - 3.4.8 Crack Starter Specimen DSCA #7 10
  - 3.4.9 Crack Starter Specimen DSCA #8 10
  - 3.4.10 Crack Starter Specimen DSCA #9 10
  - 3.4.11 Crack Starter Specimen DSCA #10 11
  - 3.4.12 Crack Starter Specimen DSCA #11 11
  - 3.4.13 Crack Starter Specimen DSCA #12 11
  - 3.4.14 Crack Starter Specimen DSCA #13 12
  - 3.4.15 Crack Starter Specimen DSCA #14 12
  - 3.4.16 Crack Starter Specimen DSCA #15 13
  - 3.4.17 Crack Starter Specimen DSCA #16 13
- 3.5 Discussion of Crack Starter Experiments 14

TABLE OF CONTENTS
(continued)

3.6 Short Crack Arrest Tests 15
  3.6.1 Design Considerations 15
    3.6.1.1 Test Plate Dimensions 15
    3.6.1.2 End Connections 18
  3.6.2 Short Crack Arrest Test Specimen for Base Plate 18
  3.6.3 Short Crack Arrest Tests for Base Plates 21
    3.6.3.1 SCA Test #1 21
    3.6.3.2 SCA Test #2 21
    3.6.3.3 SCA Test #3 21
    3.6.3.4 SCA Test #4 22
    3.6.3.5 SCA Test #5 22
    3.6.3.6 SCA Test #6 22
    3.6.3.7 SCA Test #7 23
    3.6.3.8 SCA Test #8 23
  3.6.4 Short Crack Arrest Tests for the HAZ 23
    3.6.4.1 SCA Test #9 - HAZ Test #1 24
    3.6.4.2 SCA Test #10 - HAZ Test #2 25
    3.6.4.3 SCA Test #11 - HAZ Test #3 25
    3.6.4.4 SCA Test #12 - HAZ Test #4 25
    3.6.4.5 SCA Test #13 - HAZ Test #5 25
  3.6.5 Effect of Crack Starter Load on Main Test Specimen 25
  3.6.6 SCA Test #14 27

4.0 RESULTS 27
  4.1 Strain Data for Short Crack Arrest Tests 27
  4.2 Difficulties and Limitations of SCA Tests 28

5.0 CONCLUSIONS 29

6.0 ACKNOWLEDGEMENTS 30

7.0 REFERENCES 30

1.0 INTRODUCTION

A judicious approach that has evolved with industry-government consensus for toughness requirements in the CSA S473 Standard Code for the Design, Construction and Installation of Fixed Offshore Structures, Part III - Steel, follows a philosophy of fracture prevention based on a combination of resistance to crack initiation and resistance to crack propagation. For Arctic ships, a similar approach would require consideration of:

(i) Prevention of initiation of unstable fractures from long fatigue cracks (with tips in base material) at intermediate strain rates.

(ii) Prevention of initiation of unstable fracture from flaws in the weld zone.

(iii) Short crack arrest (SCA) capability of structural steel and its heat affected zone (HAZ).

Once the possibility of brittle fracture initiation from small flaws in the weld zone is accepted, then flaws oriented perpendicular to the weld axis will need to be arrested in the base material. The steel toughness requirement for arresting relatively small cracks would of course be less than that for arresting long cracks. However, flaws such as lack of side wall fusion or hydrogen induced cold cracking can be arrested in the HAZ weld metal or base material. Whether they will be arrested in the HAZ or not is difficult to predict since local brittle zones in the HAZ may not affect the SCA capability as much as the potential for brittle fracture initiation.

In the literature, there are only a limited number of publications that have looked at the SCA capability of steels and those on the HAZ are even fewer. It is therefore apparent that to verify and further develop the structural steel toughness requirements in Canadian Arctic Safety and Pollution Prevention Regulations, schedule 3, the SCA capability of structural steels and HAZs therein needed to be investigated. Also, a few wide plate tests would verify their resistance to brittle fracture initiation from long cracks. Some wide plate fracture initiation tests already have been carried out and the test results analyzed and reported.

The type of large scale crack arrest test to be used must be selected with due consideration to the fracture criteria adopted. For example, if arrest performance is to be based on stopping a very long crack running entirely across a plate by specifying adequate toughness in the adjacent plate that the crack runs into, then the test must reproduce the correct mechanical conditions at the tip of the crack. The design of such a test must consider reflected stress waves and total energy loss from the system and probably requires a fully dynamic analysis. If, however, the fracture criterion is based on arresting a short crack that initiates in a low toughness region of a weld, the fracture properties of the steel would not be as critical. Then design of the test would be simpler and a static analysis would probably suffice. One criterion of interest in ships is that of arresting a short running crack that may initiate in a low toughness region of a weld or be injected into the shell plate from fracture of a secondary member.

The SCA concept requires the arrest of a brittle fracture immediately after it starts to propagate. Such a crack produced should be as small as possible (Fig. 1). Recently, Tanaka et al[1,2] studied the short crack arrest concepts. Their test piece design involved a separate compact tension crack starter section, independently loaded, that injects a crack into the plate or HAZ. The compact tension specimen used for a crack starter is in a bend loading mode. To ensure the crack is fully established in the plate, a groove maintains plane strain conditions locally sustaining the brittle fracture. The test plate is loaded at a constant stress level under isothermal conditions. When the crack runs out beyond the grooved area and constraint relaxes, the crack either arrests or continues to run across the test specimen. The test is therefore of the go/no-go type, each test providing a single data point of either fracture or arrest on the stress temperature graph. A number of tests are required for bracketing. One advantage of the injector plate system for initiation is that it facilitates the placement of the crack in specific location such as the HAZ.

2.0 OBJECTIVES

The main objectives of this program are to (1) develop SCA testing capability in Canada. This involves the development and design of a crack starter attachment to the test plate to inject a crack into the plate or the HAZ and (2) to assess the SCA capability of a conventionally processed shipbuilding steel and its HAZ.

The objective of the SCA test is to determine the stress/temperature transition for SCA. The crack arrest curve is determined by bracketing the value using several isothermal specimens conducted at various nominal stresses and temperatures. Single tests using temperature gradients such as the double tension test were not considered suitable for the present application. Because of the limited number of test specimens available a rather coarse bracketing procedure was inevitable, thus reducing the precision with which the crack arrest temperature could be determined.

3.0 EXPERIMENTAL PROCEDURE

3.1 Materials

3.1.1 Shipbuilding Steel

The steel used to assess the SCA capability in this program was 25.4 mm thick ABS DH36. This steel was supplied by Algoma Steel Corporation. For the HAZ SCA tests, the butt welds were prepared in this steel using a double bevel joint (K-joint) preparation so that a straight HAZ could be obtained. These HAZ test plates were prepared by Fleet Technology and supplied to the Welding Institute of Canada. The welding parameters are given in the welding data sheet provided in the Appendix. The welds were prepared using the submerged arc process with about 5 kJ/mm heat input. The welding parameters are given in the Appendix (see Welding Data

Sheet). The tensile and the nil-ductility transition temperatures (NDTT) of the base plate and the HAZ are given in Table 1.

3.1.2 Crack Starter

For the development of the crack starter specimen, 25.4 mm thick steels such as Lloyds LT60, SAE 1045 and SAE 1060 were used. The weld metals used for the initiation, propagation and/or injection into the test plate were deposited using one of Stoody, E70-S, Hobart Smoothare 320 or 400 electrodes.

3.2 Development of Crack Starter

Because of the space limitations in the WIC wide plate rig, it was not possible to use a crack starter system following the design used by Tanaka at Nippon. The Nippon design uses a starter piece 267 mm wide and loaded with a 4 ton jack. In the present case, the maximum available space was 125 to 130 mm and the maximum practical width of starter plate was 100 mm. The crack starter system must initiate a crack under slow loading conditions that do not introduce any dynamic effects into the main test piece. The crack must also enter the test piece without slowing or arresting. The loading system for the crack starter must therefore have enough stored elastic energy to insure a rising K value at the tip of the crack during propagation across the crack starter plate. Two general design approaches were considered. The first was a high energy system in which loads were applied to the crack starter plate via end beams loaded by jacks outside the cold box. The second was a compact design using a low-height jack.

The crack tip K value relative to applied stress is shown as a function of crack size in Fig. 2. To insure an increase in K value across the specimen, a maximum w/l = 1 is required. For an edge crack under tensile loading, a crack starter plate width of 100 mm was selected as being a compromise between the space limitations in the rig and a sufficient crack run before entry into the test plate. Thus, a width of 200 mm and a minimum effective starter plate length of 200 mm was required. This consideration eliminated the original compact design but suggested the high energy system would not be required since adequate effective length could be achieved in a smaller design. The design selected is shown in Fig. 3. Tensile loading is applied to the crack starter plate via single pins (loose bolts) and no special clamps or grips are required. The design also has the advantage that the two separate sections can move apart after the crack starter plate fractures without damage to the loading rig.

SAE 1045 steel 25.4 mm thick was selected for the crack starter plate (as used in the Nippon design) and blunt saw cut notches were used to ensure a high K value at crack initiation. Some preliminary tests were carried out on the starter steel to determine fracture loads and to confirm that adequate jack capacity was available in the loading rig.

The crack starter was attached to the main plate with a weld 40 to 50 mm long of brittle material. Initial tests on the original selection (Hobart Smoothare 320) indicated it was not brittle enough, so it was changed in later tests to Hobart Smoothare 400. The groove in the main plate opposite the crack starter was 8 mm deep as illustrated in Fig. 30 in Section 3.6.2.

As testing continued, several problems were encountered with the crack starter system and this led to a series of tests in an attempt to improve the design. Some of the problems encountered were deviation of the crack as it entered the test plate, rotation of the crack starter plate and excessive load owing to high toughness of the starter material. Tests were carried out to explore these problems as they occurred and the complete series of development tests is summarized in the following sections.

3.2.1 Preliminary Progress

3.2.1.1 Crack Starter Specimen DSCA (i)

A crack starter specimen was prepared from 25.4 mm thick Lloyds LT60 steel. A butt weld joint was prepared using Stoody weld metal. The specimen was machined to size, notched and side grooved as shown in Fig. 4. The specimen was pulled in tension in the MTS tensile testing machine at room temperature. The specimen did not break when loaded up to 56,200 lbs. This load seemed to be too high for the type of loading device that can be accommodated in the space available in the wide plate test rig.

3.2.1.2 Crack Starter Specimen DSCA (ii)

A crack starter specimen of the dimensions shown in Fig. 5 was machined using SAE 1045 steel, notched and side grooved. The 25.4mm thick specimen was pulled in tension to fracture at room temperature. The specimen fractured in the notch plane at a tensile load of 39,900 lbs.

3.2.1.3 Crack Starter Specimen DSCA (iii)

A compact tension crack starter specimen machined from SAW 1045 steel, with CT notch and side grooves was welded to a 25.4mm thick x 250mm wide x 250mm long steel strip (401 MPa yield). The attachment weld was 50 mm long and deposited with E70-S electrodes (welding data in Appendix 2). The weld metal was not side grooved. The crack starter was pulled in tension in a MTS machine to fracture. The crack starter fractured in the notch plane through the ligament and deviated from the notch plane near the attachment weld. The attachment weld did not crack (Fig. 6).

At this point it was decided to use SAE 1045 steel for the crack starter because of its lower tensile properties and lower impact toughness values at the probable test temperatures. From a survey of the electrodes producing brittle weld metals, Hobart Smootharc 320 and 400 were selected. The impact toughness of SAE 1045 steel and the weld metals produced from Hobart Smootharc 320 and 400 electrodes are given in Table 2. To produce crack-free welds using Smootharc 320 or 400 electrodes preheat, interpass and post weld temperatures as high as 350°C were required. After welding, the welds needed to be cooled slowly. Handling characteristics of Smootharc 320 were much better than those of Smootharc 400.

3.3 Loading Unit for Crack Starter Specimen

The system designed for loading the crack starter or injector compact tension specimen is as shown in Figs. 3, 7 and 8. The system uses two 20-ton hydraulic jacks operated by a 10 ksi hydraulic Enerpac pump. The jacks are attached to the tension loading steel frame assembly. The tension frame members are attached to the compact tension specimen and secured at the loading points by means of two high strength bolts. The compact tension specimen is loaded in tension using the hydraulic pump and the pressure in the system is read from a dial gauge attached to the pump. The loading system is compact and can be accommodated in the space available in the wide plate test rig.

3.4 Further Progress on Crack Starter Specimens

3.4.1 Crack Starter Specimen DSCA #0

A compact tension crack starter specimen with notch and side grooves as shown in Fig. 9 was machined from 25.4mm thick SAE 1045 steel. The distance between the loading points was 250 mm. The crack starter was welded to a 25.4mm thick x 200mm wide x 200mm long DH 36 steel plate using Smoothare 320 electrodes. Smoothare 320 electrodes were selected over Smoothare 400 because they handled easier. The bottom of the crack starter was bevelled. A 60° groove was machined where the crack starter was to be welded to the plate. The crack starter was tacked to the plate to provide a T-joint with a root gap of 3 mm. The T-joint was welded maintaining a preheat, interpass and post-weld heat temperature of 315° C. A 50mm long weld was deposited with 3mm diameter electrodes, 120 to 140 A and 24 V (see welding data sheets in the Appendix). The weld was cooled slowly to room temperature in an hour. The side grooves in the crack starter were extended into the weld metal up to the plate surface. The crack starter was pulled in tension using the newly built hydraulic jack loading unit. The crack starter specimen fractured in tension at approximately 5500 psi (38 MPa) crack starter load. The crack ran in the notch plane into the weld metal and then deviated from the notch plane and ran sideways in the direction of the weld ends.

3.4.2 Crack Starter Specimen DSCA #1

The crack starter specimen is similar to DSCA #0 except for the length between the loading points which is 180 mm. The crack starter was welded to a 14mm thick x 48mm wide x 865mm long steel strip (420 MPa yield) with the length of the crack starter parallel to the length of the strip. Smoothare 320 electrodes were used for welding. The bottom of the crack starter was bevelled to give clearance between the plate and the starter. The notch ligament and the crack starter weld were cooled to -20° C. The steel strip was loaded in tension to half the yield in a MTS machine and the crack starter specimen was loaded to fracture. The crack starter fractured at 5000 to 6000 psi (35 to 42 MPa) starter load. The crack progressed in the notch plane into the weld and stopped at the plate surface. However, there was extensive bending of the steel strip and the weld metal was lifted from the surface of the steel strip (Fig. 10).

3.4.3 Crack Starter Specimen DSCA #2

The test is similar to that of DSCA #1. In this case, Smoothare 400 electrodes were used for the weld instead of Smoothare 320. The welding procedure was similar to that of Smoothare 320. This further reduced the weld metal toughness and hence the assembly was tested at room temperature instead of -20° C. The crack starter fractured at 5000 to 6000 psi (35 to 42 MPa) crack starter load. The fracture was through the notch plane and through the weld on to the surface of the strip. Also, the crack had progressed parallel to the strip surface along the length of the weld (Fig. 11).

3.4.4 Crack Starter Specimen DSCA #3

The crack starter specimen geometry was same as that of DSCA specimens 1 and 2. The crack starter was welded to a 25.4 mm thick x 200 mm x 200 mm DH36 plate using Smoothare 400 electrodes and the same welding procedures used earlier. Side grooves were extended into the weld and the crack starter specimen was loaded in tension to fracture using the loading unit. The crack starter fractured at a load of 6000 psi (42 MPa). The crack progressed in the notch plane and when it hit the weld, it deviated from the notch plane at an angle. This appeared to be due to an anchoring effect provided by the weld ends and the clearance between the plate and the crack starter specimen (Fig. 12).

3.4.5 Crack Starter Specimen DSCA #4

In this case, the crack starter specimen was welded to the steel strip following the procedure given in Section 3.4.3 (see welding data sheets in the Appendix). The wedges were spot welded on to the crack starter to close the gap between the crack starter and the steel strip. The steel strip was loaded to half yield at room temperature and the crack starter was loaded to fracture. The crack starter specimen fractured at a load of approximately 6500 psi (45 MPa). The crack progressed in the plane through the weld metal and stopped at the strip surface. The strip was bent due to the release of the fracture load (Fig. 13).

3.4.6 Crack Starter Specimen DSCA #5

Here the crack starter, as in Section 3.4.5, was welded to a 25.4mm thick, 200mm x 200 mm steel plate using Smoothare 400 electrodes. Wedges were spot welded to the crack starter to cover the clearance between the crack starter and the steel plate. The crack starter was loaded at room temperature. The crack starter fractured at a load of 8500 psi (60 MPa). The crack progressed in the notch plane and stopped at the plate surface after travelling through the weld metal (Fig. 14).

3.4.7 Crack Starter Specimen DSCA #6

In the case of compact tension specimens, the fracture of the specimens transferred the fracture energy into the plates or the strips to which they were welded (attached) by bending them. In order to retain the fracture energy in the crack starter itself, a centre cracked tensile (CCT) specimen geometry as shown in Fig. 15 was selected. The crack starter CCT specimen with the side grooves was welded to a 25.4mm thick, 250mm x 250mm DH36 steel plate using

Smootharc 400 electrodes. Side grooves were extended into the weld. The bottom of the crack starter was not bevelled, but was touching the plate surface. The crack starter was loaded to the maximum capacity, 9200 psi (~63 MPa), of the hydraulic loading unit at room temperature. The crack starter did not fracture.

3.4.8 Crack Starter Specimen DSCA #7

The crack starter specimen machined here was a compact tension type, similar to the one used in DSCA #5. However the bottom of the starter was not bevelled. Also, after welding to the 25.4mm thick plate with Smootharc 400 electrodes the clearance between the plate and the starter was ~2 mm. To the top of the crack starter a 15mm wide x 6mm thick x 200mm long steel support strip was welded at its ends. The crack starter was loaded in tension using the loading system. Crack starter fractured at 6500 psi (~46 MPa). The crack did not run into the plate surface. The steel strip welded at the top deformed plastically and bent towards the plate (Fig. 16).

3.4.9 Crack Starter Specimen DSCA #8

This crack starter is similar to that of DSCA #7. In this case the bottom of the crack starter was bevelled to get a maximum clearance of 5 mm at the crack starter ends, hoping to drive the crack into the plate surface. The crack starter was loaded to fracture at room temperature. The fracture load was 8000 psi (~56 MPa) and the crack had followed the side groove on one side of the crack starter but not on the other side. The crack plane deviated from the notch plane at an angle of 45° showing the anchoring effect of the weld ends. One half of the crack starter specimen lifted off the plate and bent the steel support strip away from the plate (Fig. 17).

3.4.10 Crack Starter Specimen DSCA #9

This crack starter is similar to that of DSCA #8. The crack starter was welded to a 14mm thick x 48mm wide x 865mm long steel strip using Smootharc 400 electrodes and side grooved. The steel strip was loaded to 150 MPa in a MTS testing machine and the crack starter was loaded to fracture. The crack starter fractured at 7500 psi (~52 MPa). The crack deviated from the notch plane. The steel strip bent away from the crack starter and the support strip bent towards the steel strip (Fig. 18).

3.4.11 Crack Starter Specimen DSCA #10

The specimen geometry was same as that of DSCA (ii). The notched and side grooved specimen was heated at 850° C for 45 minutes and water quenched. The heat treatment was given in anticipation that the toughness and hence the fracture load of SAE 1045 steel could be reduced. The notch of the heat treated specimen was fine saw-cut and loaded in tension to fracture in the MTS machine. The room temperature fracture load was 53,300 lbs. Thus, heat treatment was not beneficial in reducing the fracture load (Fig. 19).

3.4.12 Crack Starter Specimen DSCA #11

The crack starter specimen geometry was similar to DSCA #10. The specimen was cut into two halves at the notch plane. Double-V groove of 60° angle was machined at the cut ends and butt welded using Smoothare 400 electrodes. The weld reinforcements were ground flush with the plate surface. Saw-cut notch was put with difficulty using a fine saw for the final cut. The specimen was side grooved and loaded in tension at room temperature in a MTS machine. The specimen fractured in the notch plane at 27,400 lbs load level. This test was carried out in anticipation that the fracture load could be reduced to a level low enough to make crack starter of CCT configuration work (Fig. 20).

3.4.13 Crack Starter Specimen DSCA #12

The crack starter, 25.4 mm thick, was machined to have a CCT configuration as shown in Fig. 21. The notch ligament was prepared to give double-V groove with 60° angles. The notch ligament was welded with Smoothare 400 electrodes. The weld was ground flush with the crack starter specimen surface and side grooved. The bottom of the crack starter was bevelled and welded to a 14mm thick x 48mm wide x 865mm long steel strip. The crack starter contained a deeper notch (long defect) than the earlier specimens. The strip was loaded in tension to 150 MPa in a MTS machine and the crack starter was loaded to full capacity, ~ 10,000 psi (70 MPa) of the loading unit. The crack starter cracked with intermittent growth as the load level increased above 56 MPa. The steel strip was bent. The crack did not appear to grow too much. Macroscopic examination revealed crack growth in only part of the ligament it never reached the strip surface.

3.4.14 Crack Starter Specimen DSCA #13

This test was essentially similar to that of DSCA #12 except for the thickness of the crack starter and the notch length. The crack starter specimen thickness was 20 mm. This crack starter had still deeper notch than DSCA # 12. While loading, the first cracking sound in the crack starter was heard at 6300 psi (44 MPa) and the full fracture was observed at 8000 psi (56 MPa.). The crack starter fractured at the notch plane. One half of the crack starter lifted up from the strip surface at the attachment weld. The crack progressed sideways in the attachment weld (Fig. 22).

3.4.15 Crack Starter Specimen DSCA #14

The crack starter was machined to have CT geometry. The notch tip location and the notch ligament was deposited with Smoothare 400 weld. The crack starter with side grooves was attached to a 25.4mm thick x 48mm wide x 865mm long steel strip using 40mm long Smoothare 400 weld metal. The bottom of the crack starter was straight and there was no gap between the crack starter and the steel strip. The strip was loaded to 150 MPa in a MTS machine at room temperature. The crack starter was loaded to fracture. The first onset of cracking sound was heard at 6000 psi (42 MPa) load and the complete fracture occurred at 6500-7000 psi (45 to 50 MPa). The cracking progressed in the notch plane straight into the plate surface and the steel strip was bent (Fig. 23).

3.4.16 Crack Starter Specimen DSCA #15

The impact strength of SAE 1045 steel at room temperature was better than the Smootharc 400 weld metal. To perform the short crack arrest test at room temperature it was required to use a steel with still lower impact strength than the 1045 steel so that the crack starter would crack at a lower fracture load and drive the crack into the test plate. For this, 25.4mm thick SAE 1060 steel was procured. The impact strength of this steel is given in Table 2.

A crack starter specimen of CT geometry with side grooves, as shown in Fig. 24, was machined. The thickness of the specimen was 20 mm. The notch length was 60 mm with the final 5 mm of the notch was fine saw-cut. The crack starter was pulled in tension to fracture in a MTS machine. The fracture load was 16,860 lbs. It was a clean fracture in the notch plane.

3.4.17 Crack Starter Specimen DSCA #16

This was the final test performed on the development of crack starter specimen. The crack starter specimen of same geometry as DSCA #15 was machined. The bottom edges of the crack starter were tapered. The crack starter was attached to a 50mm thick 300mm x 300mm LT60 steel plate using 60mm long Smootharc 400 weld metal (welding data sheets are in the Appendix). A gap of 1.5mm was maintained between the bottom of the crack starter and the plate surface. This space was filled with 1.5mm thick Teflon sheets. The crack starter was loaded to fracture. Initial cracking was at 4200 psi (29 MPa) and the load dropped to 3900 psi (26 MPa). There was only a minor visible crack. The crack starter was again loaded to complete fracture at 5200 psi (36 MPa). At full fracture, the crack had progressed in the notch plane to the plate surface and one half of the crack starter was pulled out of the 50 mm thick plate at the attachment weld (Fig. 25).

3.5 Discussion of Crack Starter Experiments

The main problem encountered with the edge notch and tensile design of the crack starter was divergence of the crack as it reached the edge of the specimen and entered the test plate. This was believed to be due to bending of the crack starter plate about the hinge point formed at the end of the attachment weld (Fig. 26). When wedges were inserted between the test plate and the starter plate to prevent the bending or allow the bending moment to be transferred to the test plate, the divergence did not occur. However, calculations indicated that the bending moment transferred to the test plate would be significant, thus leading to uncertainty in the applied stress on the test plate. In the design used by Tanaka, the bending moment from crack starting is also transferred to the test plate, but this does not appear to have been taken into consideration. In the present work, various attempts were made to remove the bending component either by using centre notch crack starter plates (see Fig. 15) or by welding a strap across the edge of the plate. These approaches were not successful because of the high loads required and also because of the lack of a clear indication when fracture occurred. It was concluded that the edge notch design was preferred but that the load should be reduced to minimize the bending effects.

A second problem that arose was that the toughness of the starter material (SAE 1045 steel) appeared to be too high, particularly when tests were carried out at room temperature. Attempts were made to overcome this by using a design employing brittle weld metal rather than the SAE 1045 steel, but further problems were encountered with this approach. There was a tendency for the crack to run into the HAZ of the weld rather than through the weld metal. There was also a risk of weld cracks occurring in the brittle weld metal. The final design of the crack starter used SAE 1060 steel and the thickness of the plate was reduced to 20 mm. Steel wedges inserted after the crack starter plate was attached to the test plate appeared to be the best means of keeping the crack straight by removing bending without excessively increasing the crack starter load. The alternate method of using a long attachment weld (as in the Japanese design) was considered, but it was believed this would result in excessively high tensile loads in the starter plate. A deep brittle weld penetrating into the test plate was also tried but did not appear to offer any advantage (see section 3.6.4.1. and Fig. 44). Furthermore there was concern that the high residual stresses from such a weld could influence the results without the stress state being accurately known.

3.6 Short Crack Arrest Tests

3.6.1 Design Considerations

3.6.1.1 Test Plate Dimensions

The simulation of fracture processes in the laboratory has been a difficult challenge especially for crack arrest tests. There have been three main areas of concern:

1) changes in the stress intensity factor distribution as the crack length to plate width ratio becomes large,
2) stored energy in the system and
3) reflection of elastic waves.

The objective of a laboratory test is to try and simulate conditions for crack arrest behaviour similar to those that would be experienced in an infinite plate in practice, i.e., crack arrest should be a feature of the material being tested, not a feature of the test design. After a crack is injected into the plane and established over the grooved region it has an opportunity to arrest. Owing to tunnelling effects, this arrest can occur over a distance typically 1.5 times the plate thickness. If the grooved section is 120mm long, then the total crack length at arrest could be about 200 to 250mm long. To avoid edge effects, the total crack run should not exceed about 70% of the plate width, suggesting a minimum plate width of 360mm. In base metal tests with longitudinal welds, arrest can occur when the crack runs out of the residual stress field, which typically might be 120 mm wide. Crack runs in these tests are therefore likely to be less than 250 mm, suggesting that the minimum plate width of 360 mm would also suffice for base metal tests for welds. To provide a margin of conservatism, a width of 500 mm for the present program was tentatively selected.

The second area of concern is the effect of stored energy in the system and the influence of specimen length on the distribution of the stress intensity factor at the crack tip. If the fracture process requires a greater amount of energy than can be supplied by the local relaxation of elastic strain then continued extention of the crack depends on the supply of energy from the system and remote from the crack. If a test were being conducted in a stiff testing machine such as the wide plate test rig, arrest may occur in the test, although arrest may not occur in practice. In such a case, a load drop would be recorded following arrest. To insure adequate energy is available to complete the fracture process, the test specimen must be made long enough.

For a plate of finite length (l), and width (w), with a central crack of 1/2 length (α) and initial applied stress (σ), the expression for the stress intensity factor K is

$$K = \sigma[W \tan(\pi\alpha/w)]^{1/2}/[1 + (4w/\pi l) \ln.\sec(\pi\alpha/w)]$$

The term in the denominator takes account of the drop in stress as the crack proceeds because of the finite length of the specimen. In this expression, the length is the effective length assumed to exist between fixed grips. In practice l is greater than the specimen length because of the testing machine compliance. As the crack propagates and the α/w ratio increases the value of K will change depending upon the selected values of l and w. In Fig. 27 the ratio of K to K_∞ in an infinite plate is plotted as a function of α/w for various w/l ratios. To insure that there is no premature arrest of the crack, it is desirable to have a constant or slightly rising K value as K/w increases. From this graph it is seen that $w/l < 0.33$ would meet this requirement. Thus, for a width of 500 mm, a length of 1.5 m is suggested. Since there will be some contribution of elastic energy from the machine itself, the actual specimen length could be somewhat smaller than 1.5 m.

The third area of concern is the effect of elastic stress wave reflections. As the crack propagates, the material behind the crack tip is unloaded and an unloading stress wave moves out from this region. This wave can be reflected from surfaces and boundaries in the specimen and return from the crack tip where it is superimposed on the main load. If the reflected wave is an unloading wave the net stress at the tip is reduced and the crack may prematurely arrest. Reflections from the free surfaces at the edge of the specimen involve a change of sign, thus unloading stress waves become loading stress waves on reflection. Reflections from these surfaces are therefore less critical since they would lead to conservative results in the test, i.e., promote propagation.

Waves striking the ends of the specimen where it is attached to larger end plates are reflected without change of sign and remain unloading waves. To insure the complete propagation arrest event takes place without the influence of reflected waves, the specimen must be made sufficiently large. Crack velocities range from 500 to 1000 m/s or higher in some specimen configurations. The crack rapidly arrests when the speed drops below 300 to 500 m/s. If 500 m/s is taken as a conservative lower limit for average crack velocity, the duration τ of the propagation event is

$$\tau = \alpha/500 \quad \text{where } \alpha \text{ is the crack run length in meters.}$$

If the velocity of elastic waves is of the order of 5000 m/s, the minimum path distance (d) that can be travelled without causing a disturbance at the crack tip is

$$d = \tau \times 5000 = \alpha \times 5000/500 = 10 \times \alpha \text{ (in meters)}$$

Since the wave must travel to the boundary and back, the distance from the crack to the nearest fixed boundary at the end of the specimen is conservatively estimated as 5 times the crack run length. In the present case, a crack run of 250 mm is assumed, thus giving a conservative minimum length of 1.25 m.

Based on the foregoing considerations and taking into account the limitations of the wide plate test rig, the final dimensions of the test plate were selected as width, 500mm, and length between section changes, 1.2 m. A sketch of the specimen design is shown in Fig. 28. The final dimensions selected agree quite well with those used by Tanaka in the original work on short crack arrest (width 420 mm and length 1 m).

3.6.1.2 End Connections

Wide plate tests conducted at WIC in the past have been welded into the rig using electroslag welding. This can be relatively time consuming and the use of welding requires a separate aligning procedure before the completed specimen can be placed in the rig. To determine if there was any advantage in using other methods of connection two mechanical systems were examined in detail. The first was a single-pin design that would have the advantage of being self-aligning, thus offering the possibility of eliminating the time consuming step of alignment. The second was a bolted system using two rows of standard high strength steel bolts (Fig. 29). Although no alignment would be possible with the bolted design, the specimen would still have to be placed in the alignment rig in order to insert the bolts.

It was concluded from the design studies that the single pin design would not be feasible because the end distances required resulted in a total connection length that was too great to leave an adequate specimen length. The overall length was limited by the wide plate rig itself. It was also concluded that the bolted connection offered no advantage over a welded connection since the alignment step would not be eliminated. It was, however, concluded that GMAW or even SMAW might be simpler and just as efficient as ESW for making the end connection welds in the 25.4mm thick plate under consideration (welding data sheets are in the Appendix).

The method finally adopted incorporated a 25.4mm reusable, shaped-end extension piece (see Fig. 28). As each test was completed the test was removed by cutting adjacent to the weld and rewelding the next test piece, which was made slightly longer. In this way several tests were done using the same extension piece and maintaining the length of 25.4mm plate constant between the shoulders.

3.6.2 Short Crack Arrest Test Specimen for Base Plate

The test plate was 25.4 mm thick x 500 mm wide x 1.2 m long. A back groove, 120 mm long and 8 mm deep was machined on the centre, on one side of the test plate, perpendicular to the loading direction. The crack starter specimen was then welded to the plate, at the centre, on the other side of the plate as shown in Fig. 30. The notch plane and the side groove in the crack starter were lined up with the root of the slot. Initially Hobart Smootharc 320 electrodes were used to join the crack starter to the test plate (refer to welding data sheet in the Appendix). Later Smootharc 400 electrodes were used to join the crack starter to the test plate. The welding parameters are given in the welding data sheet. To prepare the specimen for testing, the loading-end attachments were attached to the test specimen. This was performed following the procedure described in the previous report. The loading-end attachments were aligned in an alignment jig. The end of the test plate was bevelled to 45° for a double bevel (K-prep), aligned symmetrically and tack welded to the loading-end attachments. The welding was performed by two welders, using GMAW process in vertically up position. Each joint was welded simultaneously on both sides of the plate by the two welders . The welding parameters used are given in the welding data sheet (Appendix).

Once the loading ends were attached (Fig. 31), the test specimen was removed from the alignment jig. The distance between the flat loading faces was measured. The distance between the faces corresponding to the same loading capsule did not differ more than 2 to 3mm. The Smootharc 320 or 400 attachment weld was ground flush with the test plate and the crack starter surface. The side grooves in the crack starter were extended into the test plate surface via attachment weld.

Four 6mm (¼ in.) strain gauges were put on both sides of the test plate, two on each side of the back groove and the crack starter. Three copper constantan thermocouples were attached to the surface of the test plate using a Devcon Plastic bonding cement. The locations of the strain gauges are shown in Fig. 32. The strain gauge identification numbers for each test are shown in Fig.33.

The crack starter loading unit was attached to the crack starter. The loading unit was further supported by two hooks suspended from the top edge of the test plate (Fig. 34). A cooling box made of styrofoam and plywood was used to cool the back grooved test location and the notch location of the crack starter (Figs. 35 and 36). The box contained inlet and outlet ports to channel the liquid nitrogen vapours through the box along the plate surface. The cooling box was attached to the plate surface to allow cooling of an area 100mm wide along the plate width.

The test plate assembly was placed in the wide plate test rig and the loading lugs were aligned with the loading capsules. The strain gauge and thermocouple connections were made for monitoring the data. The description of the wide plate rig is given elsewhere[3] (Fig. #37). The pressure applied to the capsules was measured precisely using a pressure transducer connected to a voltage monitoring system and a dial gauge. Both the pressure transducer and the dial gauge were calibrated up to 10 ksi prior to each test using a dead-weight calibrator (Fig. 38). The dead-weight pressure and the corresponding pressure transducer voltage outputs are given in Table 3. Same calibration data was observed for each test. Once the calibration was done, the liquid nitrogen vapour circulation system was connected to the cooling box to bring the test section to the desired test temperature which was monitored continuously and controlled manually within ± 2° C of the test temperature.

When the test section reached a stable test temperature, the plate was loaded to a preload of 500 psi to remove the slack and then unloaded to zero pressure. The strain gauges were zeroed at zero pressure. After zeroing the strain gauges, each test plate was loaded manually in steps of 1000 psi pressure increments. With dial gauge readings as a rough guide, the calibrated pressure transducer voltage outputs were used for precision loading. At each pressure increment the strain gauge outputs were recorded. The plate was loaded to one of the two maximum test loads (2500 psi and 3327 psi). The maximum pressure levels were selected from the previous wide plate test results so that the translated stresses in the plate corresponding to the maximum stresses would be 263 MPa (0.75 of nominal yield stress) and 350 MPa (nominal yield stress).

The NDT temperature for the DH 36 steel plate was about -10° to -15° C. The test temperatures used at the maximum test load of 2500 psi were -15°, -5° and +5°C and for 3327 psi were 5° and 20° C.

After loading, the plate was held at the maximum load level and the crack starter was loaded in increments of 1000 psi. At each increment the strain gauge reading was recorded. The crack starter was loaded to fracture. The test was terminated when the crack starter fractured fully or a cracking sound was heard.

3.6.3 Short Crack Arrest Tests for Base Plates

3.6.3.1 SCA Test #1

The crack starter type was DSCA #1. Attachment weld was deposited using Smootharc 320 electrodes. The maximum load and test temperature were 2500 psi and -15° C respectively. Complete fracture of the test plate (Fig. 39) and the fracture of crack starter occurred at 5000 psi (35 MPa) crack starter load.

3.6.3.2 SCA Test #2

The crack starter and attachment weld were the same as in SCA Test #1. The maximum load and test temperature were 2500 psi and 5° C respectively. Crack starter fractured at approximately 4000 psi (28 MPa), crack path deviated away from the notch plane. No fracture of the test plate was seen (Fig. 40).

3.6.3.3 SCA Test #3

The crack starter and attachment weld were the same as in SCA Test #1. The maximum load and temperature were 3327 psi and 5° C. Complete fracture of the crack starter occurred at approximately 5000 psi (35 MPa). Fracture was in the notch plane of the crack starter (Fig. 41). Test plate did not fail. Crack starter was removed from the plate and the attachment weld was ground flush with the plate surface. The test plate was reused in SCA Test #4.

3.6.3.4 SCA Test #4

The SCA Test #3 was repeated after making the following changes. The crack starter used was the type DSCA #2. Attachment weld was deposited using Smootharc 400 electrodes. Wedges were welded to the bottom of the crack starter as in DSCA #4. The crack starter was loaded to the full capacity of about 9200 psi (65 MPa) of the loading unit. Crack starter did not fracture. The crack starter was unloaded and reloaded to the maximum capacity loading unit. The crack starter as well as the test plate fractured fully (Fig. 42). Crack path was in the notch plane. The fracture in the second loading might have occurred because of the slippage of one of the wedges from the bottom of the crack starter.

3.6.3.5 SCA Test #5

The crack starter and the attachment weld were the same as in DSCA #14. The maximum load and temperature for the test were 2500 psi and 5°C respectively. As the crack starter was loaded to the full capacity of the loading unit, the first cracking was heard at 8000 psi (56 MPa) and the full fracture of the crack starter occurred at 9200 psi (65 MPa). The fracture had progressed into the test plate. The test was terminated. The fracture surface was heat tinted and opened. The fracture path deviated from the side groove and the notch plane at an angle. The crack had progressed into the test plate and arrested as a pop-in at mid-thickness of the plate (Fig. 42).

3.6.3.6 SCA Test #6

The test specimen was the same as in SCA Test #5. The maximum load and test temperature were 3327 psi and 22° C respectively. The crack starter was loaded to the maximum capacity of the loading unit. Cracking of the crack starter was heard at approximately 7000 psi (49 MPa) and approximately 8000 psi (56 MPa). Only a small extension of the crack (6 mm) was observed in the crack starter. The crack starter was removed from the test plate and the test plate was reused in SCA Test #7.

3.6.3.7 SCA Test #7

The crack starter was the type DSCA #16. The attachment weld was deposited using Smootharc electrodes. The bottom of the crack starter was gapped with the plate surface to accommodate 1.5mm thick teflon sheet. The teflon sheet prevented the crack starter from digging into the plate. The bottom edges of the crack starter were tapered. The maximum load and test temperature were 2500 psi and 5°C respectively. The crack starter was loaded to fracture. First cracking was heard at 2800 psi (20 MPa) and this load dropped to 2600 psi (18 MPa).

After termination of the test the crack surface was examined. The crack surface had deviated from the notch plane. The crack starter was heat tinted and removed from the test plate. The crack was opened and the boundary where the crack had stopped was marked. The metallography was carried out to see where the crack had stopped with respect to the attachment weld. The microstructural analysis showed that the crack had stopped at the boundary between the HAZ of the attachment weld and the SAE 1060 crack starter (Fig. 43). The test plate was reused for SCA Test # 8.

3.6.3.8 SCA Test #8

The crack starter was of the type DSCA #16. The bottom of the crack starter was gapped, 1.5 mm, with the plate surface. The tapered bottom edges of the crack starter were wedged and tack welded. No teflon sheet was used in the gap. The maximum load and the test temperature were 3327 psi and 20° C respectively. The crack starter was loaded to fracture. First cracking sound was heard at 4200 psi (30 MPa). On cracking the load dropped to 4000 psi (28 MPa). The test plate did not fracture. The test plate was cut and the crack starter was heat tinted and opened to see the extent of cracking. The cracking was in the notch plane and the crack had stopped on the plate surface.

3.6.4 Short Crack Arrest Tests for the HAZ

The welds for the HAZ SCA tests were supplied by Fleet Technology Ltd. (welding data sheet is given in the Appendix). These welds were prepared in double bevel joints (K-grooves) to obtain fairly straight HAZ. The ends of the welds on the thickness side were ground, polished and etched to reveal the coarse grain HAZ (CG HAZ). A line parallel to the width of the test plate was marked at the CG HAZ on each side of the plate. The 120mm long x 8mm deep back groove was machined at the centre of first side (side 1) of the weld with the root of the back groove lining with the CG HAZ. The crack starter was attached on the other side of the plate or the weld (side 2), lining up the notch plane with the CG HAZ. Only for SCA Test #9 a deep, brittle weld puddle was deposited on the plate where the crack starter was going to be attached. The SCA tests were carried out using the crack starter specimens essentially of the type DSCA #16. No teflon sheet was used for the test. The crack starter tapered edges at the bottom were wedged and welded to the crack starter. Tests were carried out similar to the base plate tests.

3.6.4.1 SCA Test #9 - HAZ Test #1

This was the first HAZ test. Here, to drive the crack into the back groove of the test plate, a brittle, deep weld metal puddle was deposited. This was done by arc-air gouging and grinding a pit 40mm x 30mm x 15mm deep at the location where the crack starter was attached (welding parameters are in the Appendix). The pit was preheated and filled with weld metal deposited with Smootharc 400 electrodes using the standard procedure. The crack starter was attached to the test plate at the deep, brittle weld location, lining the notch plane with the CG HAZ and the root of the back groove (Fig. 44).

The maximum load and the test temperature were 3327 psi and 20°C respectively. The crack starter fractured at 5500 psi and load dropped to 4000 psi. The cracking was very loud. The crack starter along with the test plate was heated to heat tint the crack surface and the crack was opened. The fracture progressed into the weld puddle and stopped. The weld puddle had fractured fully in the notch plane of the crack starter. There appeared to be no crack in the HAZ of the weld puddle and the test plate (Fig. 45).

3.6.4.2 SCA Test #10 - HAZ Test #2

The maximum load and the test temperature were 3327 psi and 5°C respectively. The crack starter fractured at 6000 psi (42 MPa) fully fracturing the CG HAZ of the test plate. There was no deviation of the crack from the crack plane (Fig. 46).

3.6.4.3 SCA Test #11 - HAZ Test #3

The maximum load and the test temperature were 2500 psi and -5°C respectively. Crack starter fractured at 5200 psi and load dropped to 5000 psi. The crack progressed at an angle to the notch plane (CG HAZ plane) into the weld metal of the double bevel (K-groove) and arrested in the test plate weld metal. No metallography was carried out to examine the extent of cracking in the weld metal of the test plate (Fig. 47).

3.6.4.4 SCA Test #12 - HAZ Test #4

The maximum load and the test temperature were 2500 psi and -15°C respectively. The crack starter fractured at 5000 psi and load dropped to zero. The CG HAZ of the test plate also fractured fully (Fig. 48).

3.6.4.5 SCA Test #13 - HAZ Test #5

The maximum load and the test temperature were 2500 psi and 5°C respectively. The crack starter fractured at 5700 psi and load dropped to 4800 psi. The crack deviated from the notch plane (CG HAZ). There was no cracking of the CG HAZ. The crack starter was removed and the test plate was used for the control test, SCA Test #14.

3.6.5 Effect of Crack Starter Load on Main Test Specimen

Because of the space limitations in the WIC wide plate rig, a crack starter system employing loads significantly higher than those used in the Japanese design were necessary. If these loads contributed to the load in the main test plate there would be some uncertainty in the applied stress. In a stiff crack system there would be some unloading as the crack propagated, thus the load applied to the test plate could be less than the load at which the crack starter plate initiated fracture. A conservative estimate of the maximum contribution of the starter load of the test plate is therefore obtained by exploring the effects of the starter load at initiation.

The two main effects are: the direct effect of tensile crack starter load on effective tensile stress in the test plate and the effects of bending resulting from the edge crack design. The bending components would cause an increase in the effective tensile stress on one side of the plate and a decrease on the other side with no change in the average. The effect would be greatest where the crack starter plate is attached but would diminish along the grooved section away from the crack starter plate. No detailed analysis of the effect at the end of the grooved section was carried out, but the final design of the crack starter system attempted to reduce bending effects by minimizing load.

The effect of the tensile load on the stress intensity at the tip of a crack extending to the end of the grooved region was estimated both by rough theoretical calculations and experimentally. The objective was to estimate the equivalent increase in applied stress on the main test piece that would then provide the same increase in stress intensity as the load from the crack starter. This would then provide upper level of uncertainty in the stress applied to the main plate. The theoretical calculation was done by using the equations for the compact tension specimen modified them to represent a centre notch crack loaded at the mid point of the crack. This rough calculation suggested that the crack starter loads could contribute 62 MPa to the effective applied stress.

3.6.6 SCA Test #14

The effect of crack starter load was determined experimentally in this test by cutting a slot in the test plate to represent a crack along the grooved section and placing strain gauges near the tip of this slot as shown in Fig. 49. The strain gauge output was then recorded as a function of the main applied load in the test rig and also as a function of crack starter loads. The strains measured near the tip of slot (~10 mm) were intended to provide an indication of the stress intensity, and thus enable the effects of starter loads on crack tip stress intensity to be determined in terms of equivalent main load. The crack starter was in two sections, representing the condition after fracture. The results of these tests are shown in Table 4 and are summarized as follows:

Starter jack pressure: 5000 psi	increase in applied stress:	30 MPa
Starter jack pressure: 8000 psi	increase in applied stress:	41.9 MPa

These values are somewhat less than the theoretical estimates but show that there is significant uncertainty in the applied stress. These values have been used to provide upper limits of applied stress in the analysis of short crack arrest tests which are reported in a separate report.

4.0 RESULTS

4.1 Strain Data for Short Crack Arrest Tests

The jack pressures and corresponding strain data for the SCA tests are given the Appendix. The strain data for SCA Tests 2, 3 and 4 are given in Figs. 50a, 51a and 52a (data for SCA Test #1 was unreliable). The graphs show an intercept very close to the origin unlike the initial wide plate tests and this is probably because of the smaller specimen width and lower friction effects. The graphs also show relatively small bending effects caused by specimen misalignment. The plots of microstrain against starter pressure show negligible effect of the starter pressure on the strain in the main plate prior to fracture as shown in Figs. 50b, 51b and 52b.

The slopes and intercepts of all strain versus jack pressure lines were determined for each test to establish an average value and the applied stress at the holding pressure. The results are given in Table 5.

It is seen that the actual stress values are somewhat less than the intended nominal values. In particular the higher stress value is in the range 311 to 326 MPa, which is substantially less than the intended value of 350 MPa (nominal yield) and considerably less than the actual yield of 401 MPa. The test results are summarized in Table 6.

4.2 Difficulties and Limitations of SCA Tests

A number of difficulties were experienced with the SCA test that limit its usefulness. The concept is to arrest a crack after it has run about 120 mm. This is done by providing a grooved section in the test plate. The results have shown that either the crack arrested on entering the test plate or arrested at the end of the grooved section. This suggests that the temperature range over which partial fracture of the grooved region occurs, if it exists at all, is very narrow. This does not, therefore, appear to be the best method of establishing a running crack in the test plate. Brittle metal in the form of a large brittle weld metal deposit might be a solution, but the presence of complex residual stresses would provide uncertainty in the stress condition at the arrest point. One test was conducted with such a configuration, but the crack did not extend beyond the brittle deposit.

Two problems arise from the use of a side plate for injecting the crack. The first is that the eccentric load causes a bending moment to be applied to the test plate which leads to some uncertainty in the stresses. If a long attachment weld is used, a wide starter plate is needed to reduce the applied load. This raises the bending moment but keeps the direct tensile effect of the starter load to a minimum. This is the Japanese design. In the present test, a wide starter plate was not possible because of space limitations, so a short attachment weld was used to reduce the load required.

The second problem arises from transferring an edge crack in the starter plate to a through crack in the test plate. When the crack has traversed the starter plate, it becomes a surface crack. Much of the contribution to the crack tip stress intensity from the starter plate is lost at this point because of the change in geometry and because a short attachment weld "shields" the test plate from the starter plate. Thus, the test plate experiences a far shorter effective crack size than existed in the starter plate, making it more difficult to get the crack to enter the test plate. Arrest at this point, with an effective crack size of 10 to 15mm, becomes the controlling event in the test.

From the experience of these SCA tests it should be possible to redesign the tests to minimize some of the difficulties. A direct test of SCA is needed because the rate of rise of toughness above NDT is likely to be material dependent. Although the rate of rise in the present tests was also consistent with the compact crack arrest (CCA) test results this latter test measures properties under plane strain conditions. But these are not the conditions under which arrest occurs in practice. In practice the toughness should increase more rapidly with increasing temperature due to the loss of constraint. In the present tests no fractures were obtained above 5°C so no information was obtained on whether the toughness was higher than suggested by the CCA results. Overall CCA results tended to be higher than determined by other tests and it is difficult to obtain valid results.

5.0 CONCLUSIONS

(1) Development works showed that an edge cracked crack starter design using 20 mm thick 1060 steel coupled with a 40 mm long Hobart Smootharc 400 attachment weld was satisfactory in injecting a crack into the plate for the short crack arrest tests up to room temperatures.

(2) Control test showed that the effect of tensile crack starter load and the bending resulting from edge design was to increase the applied stress on the plate depending on the fracture

load of the starter: ~42 MPa at 8,000 psi starter jack pressure. This effect may be reduced by using an alternate starter design such as centre cracked tensile panel.

(3) Short crack arrest tests were carried out on 25.4 mm thick x 500 mm wide x 1.2 m long DH36 steel plates and their GC HAZ at two main plate stress levels: 263 MPa (0.75 of nominal yield of plate) and 350 MPa (nominal yield of plate) using the WIC wide plate test rig. The test temperatures selected were in the range of -15° to 20° C.

(4) Even though the short crack arrest temperatures could not be established, fracture/no fracture temperatures for the plate and the HAZ were obtained which had established the arrest temperatures within a narrow range of 10-15° C.

(5) The lowest no fracture temperature for the plate and the GC HAZ at 350 MPa was 20° C. The lowest no fracture temperatures for the plate and the GC HAZ at 263 MPa were 5° and -5° C respectively

6.0 ACKNOWLEDGEMENTS

This project has been a subcontract from Fleet Technology Limited and was carried out at the Welding Institute of Canada. Thanks are expressed to WIC technical staff, especially Mr. M. Irvine, Mr. B. Spahn, Mr. C. Giles, Mr. M. Lorenz and Mr. I. Montgomery for assistance in developing the test procedures and keeping up with the schedule.

7.0 REFERENCES

1. Tanaka, K., Sato, M., and Ishikawa, T., "Short Crack Arrest Concepts", International Symposium on Fracture-Safe Designs for Large Storage Tanks", The Welding Institute, 1986, pp 125-135.

2. Tanaka, K., Sato, M., and Ishikawa, T., "Fatigue COD and Short Crack Arrest Tests", Proc. Intl. Conference "Fracture Toughness Testing - Method, Interpretation and Application", The Welding Institute, UK, 1982, paper 18.

3. Bala, S. R., "Study of Wide Plate Testing of Structural Steels for Arctic Ships - Task 4", Welding Institute of Canada Report RC 391/1/1990, June 1990.

TABLE 1. MECHANICAL PROPERTIES OF ABS DH36 STEEL

Yield strength: approx. 401 MPa
Ultimate tensile strength: approx. 558 MPa
CVN (L): 95 J @ -20° C
CVN (T): 31 J @ -20° C
Composition: 0.17 C, 1.05 Mn, 0.009 S, 0.015 P, 0.13 Cr, 0.1 Ni
0.2 Cu, 0.043 Al and 0.056 V
NDT temp. for base plate: 10° to -15° C

TABLE 2. CHARPY IMPACT DATA

Material	Test Temp. °C	Absorbed Energy, J
SAE 1045	23	24
SAE 1045	23	22
320 WM	20	33
320 WM	20	38
320 WM	5	21
320 WM	5	22
320 WM	-20	13
400 WM	20	9
400 WM	20	9
400 WM	5	9
400 WM	5	6
400 WM	-20	4
SAE 1060	20	8 (T), 9 (L)
SAE 1060	20	8 (T), 9 (L)
SAE 1060	20	8.5 (T)
SAE 1060	10	6 (T), 8 (L)
SAE 1060	10	7 (T), 7.8 (L)
SAE 1060	10	6 (T)
SAE 1060	30	12 (T)
SAE 1060	30	11 (T)
SAE 1060	30	12 (T)

TABLE 3. CALIBRATION DATA FOR PRESSURE TRANSDUCER AND DIAL GAUGE OF WIDE PLATE TEST RIG

Dead-Weight Pressure (psi)	Pressure Transducer Output (V)	Dial Gauge Pressure (psi)
0	0	0
50	0.008	~ 50
1000	0.169	1000
2000	0.336	2000
3000	0.503	3000
4000	0.667	4000
5000	0.831	5000

TABLE 4. EFFECT OF CRACK STARTER LOADS
Analysis of SCA Test #14

1. Main load effect on gauges S3E, S4E, S3W and S4W close to crack tip. Neglect loads > 1250 psi because of yielding effects.

Average slope α of remaining lines:
S3E = 0.182
S4E = 0.209
S3W = 0.138
S4W = 0.130
Average α_1 0.165

2. Crack starter loads

α
S3E = 0.027
S4E = 0.043
S3W = -0.078
S4W = -0.035
Average α_2 -0.0108

3. Equivalent change in main load pressure resulting from starter pressure:

$$\Delta\alpha_1 P_m = \Delta\alpha_2 P_s = 0.0655 \times P_s$$

4. Average slope of main loading (for field stress, zero intercept assumed):

S1E = 0.45
S2E = 0.48
S1W = 0.442
S2W = 0.41
Average slope 0.446

$\mu\epsilon = 0.446\ P_m$
$\Delta P = 0.00614\ P_s$

At $P_m = 2500$ psi $\mu\epsilon = 1115$ $\sigma = 234$ MPa.
At $P_m = 3327$ psi $\mu\epsilon = 1484$ $\sigma = 312$ MPa.

Error due to crack starter

	ΔP_m (psi)	$\Delta\epsilon$ ($\mu\epsilon$)	$\Delta\sigma$ (MPa)
5000 psi	327.5	146	30.7
8000 psi	524.0	234	49.1

TABLE 5. ANALYSIS OF STRAIN DATA OF SHORT CRACK ARREST TESTS

SCA TEST 1

Unreliable data, microstrain at 2500 psi:	S2W	1249
	S3W	1249

Plate elastic stress = $1249 \times 21 \times 10^4 / 10^6$ = 262 MPa

SCA TEST 2

$\mu\epsilon = \alpha P + \beta$, where P is main load pressure in psi

Strain gauge	Slope α	Intercept β
S5W (N)	0.506	-1.5
S6W (S)	0.501	1.6
S1E (S)	0.486	-25.0
S2E (N)	0.476	-23.8
Average	0.492	-12.2

Strain at 2500 psi = 1218 $\mu\epsilon$
Stress at 2500 psi = 256 MPa

SCA TEST 3

Strain gauge	Slope α	Intercept β
S5W (N)	0.389	-41.4
S6W (S)	0.469	-18.7
S1E (S)	0.429	-1.8
S2E (N)	0.511	16.6
Average	0.4495	-11.3

Strain at 3327 psi = 1484 $\mu\epsilon$
Stress at 3327 psi = 312 MPa

SCA TEST 4

Strain gauge	Slope α	Intercept β
S2W (N)	0.456	-14.7
S3W (S)	0.394	-27.9
S2E (S)	0.440	-11.6
S3E (N)	0.506	3.6
Average	0.449	-12.7

Strain at 3327 psi = 1481 $\mu\epsilon$
Stress at 3327 psi = 311 MPa

SCA TEST 5

Strain gauge	Slope α	Intercept β
S1E (S)	0.51	33.7
S2E (N)	0.39	-35.7
S1W (S)	0.469	45
S2W (N)	0.42	9.36
Average	0.447	13.1

Strain at 2500 psi = 1131 $\mu\epsilon$
Stress at 2500 psi = 237 MPa

SCA TEST 6

Strain gauge	Slope α	Intercept β
S1E (S)	0.453	-3.7
S2E (N)	0.518	33.1
S1W (S)	0.449	7.7
S2W (N)	0.382	-25.7
Average	0.4505	2.85

Strain at 3327 psi = 1502 $\mu\epsilon$
Stress at 3327 psi = 315 MPa

SCA TEST 7

Strain gauge	Slope α	Intercept β
S1E (S)	0.46	-12.0
S2E (N)	0.524	-13.6
S1W (S)	0.459	-7.7
S2W (N)	0.402	-6.7
Average	0.461	-10.0

Strain at 2500 psi = 1143 $\mu\epsilon$
Stress at 2500 psi = 240 MPa

SCA TEST 8

Strain gauge	Slope α	Intercept β
S1E (S)	0.467	-2.6
S2E (N)	O.525	15.5
S1W (S)	0.466	1.1
S2W (N)	0.405	-18.8
Average	0.466	-1.2

Strain at 3327 psi = 1550 $\mu\epsilon$
Stress at 3327 psi = 326 MPa

SCA TEST 9

Strain gauge	Slope α	Intercept β
S1E (S)	0.472	-14.9
S2E (N)	0.475	10.4
S1W (S)	0.421	36.6
S2W (N)	0.407	9.0
Average	0.444	10.3

Strain at 3327 psi = 1487 $\mu\epsilon$
Stress at 3327 psi = 312 MPa

SCA TEST 10

Strain gauge	Slope α	Intercept β
S1E (S)	0.467	0.9
S2E (N)	0.519	-1.1
S1W (S)	0.446	-4.5
S2W (N)	0.416	-18.8
Average	0.462	-5.9

Strain at 3327 psi = 1531 $\mu\epsilon$
Stress at 3327 psi = 322 MPa

SCA TEST 11

Strain gauge	Slope α	Intercept β
S1E (S)	0.51	-5.3
S2E (N)	0.514	2.8
S1W (S)	0.427	-17.3
S2W (N)	0.417	-26.4

Strain at 2500 psi = 1156 $\mu\epsilon$
Stress at 2500 psi = 243 MPa

SCA TEST 12

Strain gauge	Slope α	Intercept β
S1E (S)	0.472	-79.7
S2E (N)	0.516	3.7
S1W (S)	0.454	102.0
S2W (N)	0.408	22.2
Average	0.463	12.1

Strain at 2500 psi = 1170 $\mu\epsilon$
Stress at 2500 psi = 246 MPa

SCA TEST 13

Strain gauge	Slope α	Intercept β
S1E (S)	0.497	16.2
S2E (N)	0.442	24.8
S1W (S)	0.418	99.8
S2W (N)	0.443	2.6
Average	0.45	35.9

Strain at 2500 psi = 1161 $\mu\epsilon$
Stress at 2500 psi = 244 MPa

TABLE 6. SUMMARY OF SHORT CRACK ARREST TESTS

SCA Test #	Temp. (° C)	Stress (MPa)	Max. Upper Stress Limit (MPa)	Description of Results
Base Plate				
1	-15	262	293	Fracture. Crack not completely straight.
2	+ 5	256		No fracture. Fracture of crack starter. Arrest in weld metal.
3	+ 5	312		No fracture. Crack starter arrested in WM.
4	+ 5	311	360	Complete fracture. On second go of starter loading.
5	+ 5	237		No main fracture, welding crack, pop-in arrest. Crack starter failed.
6	+20	315		No main fracture.
7	+ 5	240		No main fracture. Crack diverged to weld metal.
8	+20	326		No main fracture. Starter crack arrested in plate.
HAZ				
9	+20	312		No plate fracture. Crack starter fracture, pop-in arrested in brittle puddle.
10	+ 5	322	353	Complete fracture.
11	- 5	243		No fracture.
12	-15	246	277	Complete fracture of crack starter and main plate.
13	+ 5	244		No fracture. Crack starter fracture.

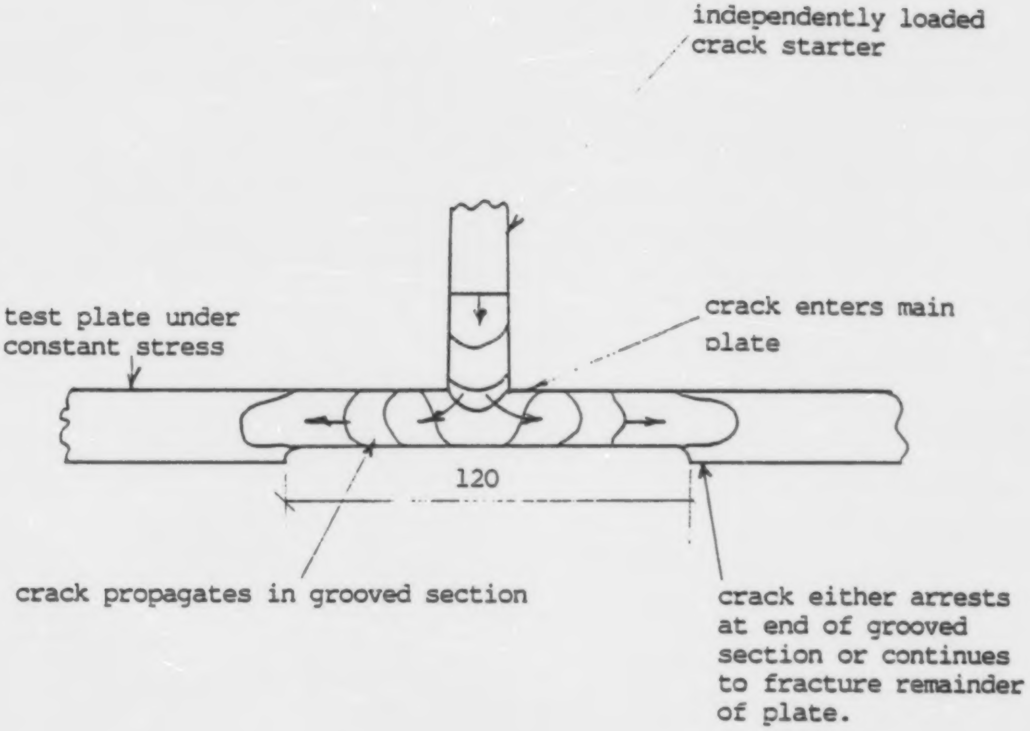
independently loaded
crack starter
test plate under
constant stress
crack enters main
plate
120
crack propagates in grooved section
crack either arrests
at end of grooved
section or continues
to fracture remainder
of plate.

Fig. 1 General principles of short crack arrest test.

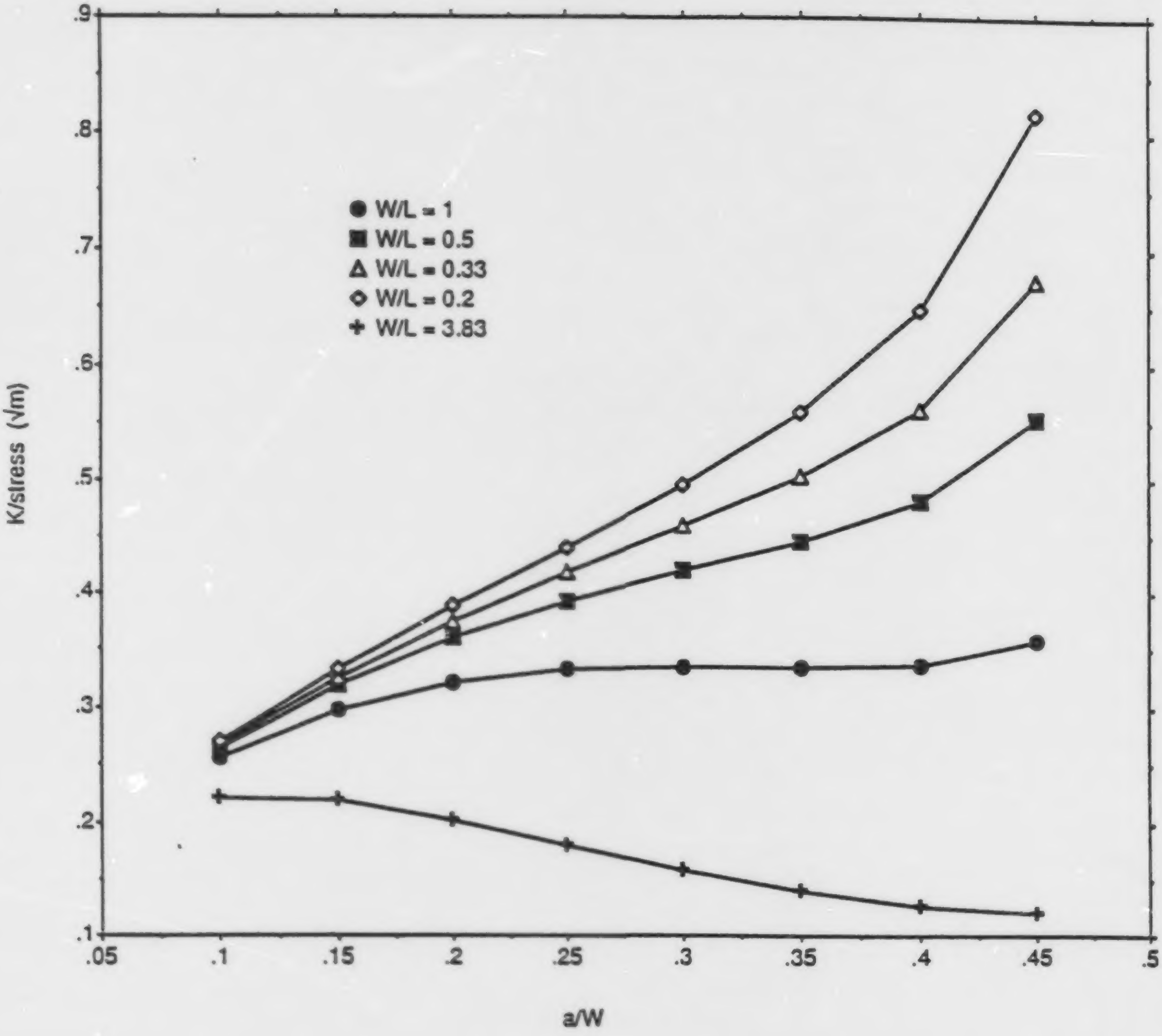

Fig. 2 Change of K value as crack propagates across crack starter plate.

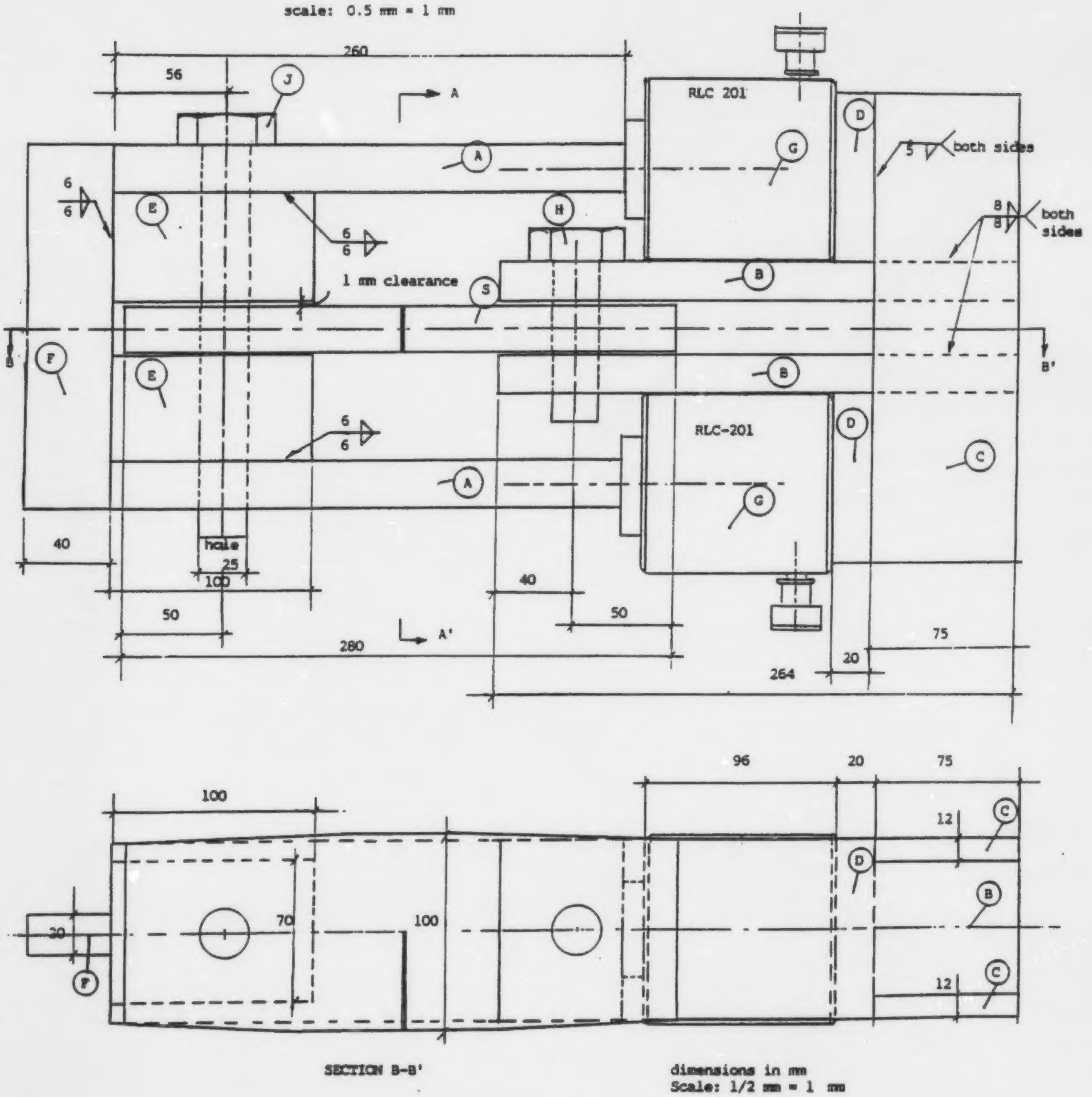
scale: 0.5 mm = 1 mm
260
56
J
A
RLC 201
G
D
5
both sides
6
6
E
H
6
6
8
8
both sides
1 mm clearance
S
B
B
F
B'
E
B
D
RLC-201
6
6
C
A
G
40
hole
25
100
40
50
50
280
A'
75
20
264
96
20
75
100
12
C
D
B
70
100
20
F
C
12
SECTION B-B'
dimensions in mm
Scale: 1/2 mm = 1 mm

Fig. 3 Hydraulic loading unit and the crack starter assembly.

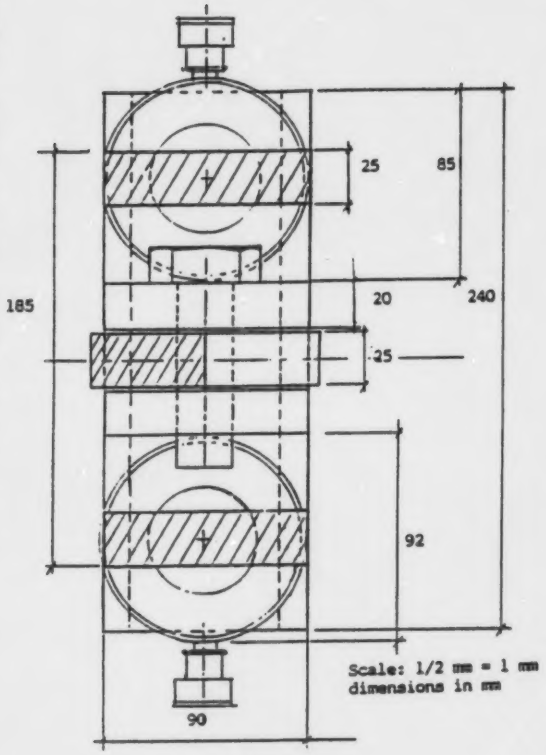
25
85
185
20
240
25
92
Scale: 1/2 mm = 1 mm
dimensions in mm
90

SECTION A-A'

ID	No. of	Size mm	Material
A	2	260x90x25	300-MS
B	2	264x90x20	350 WT
C	2	240x75x12	MS
D	2	85x90x20	MS
E	2	100x70x54	MS
F	1	185x40x20	MS
S	1	280x100x25	1045 starter plate
G	2	RLC-201	20T Hydraulic cylinder enerpac
H	1	100	A490 M24 Bolt Threads excluded
J	1	220	A490 M24 Bolt Threads excluded

Fig. 3 (Cont'd)

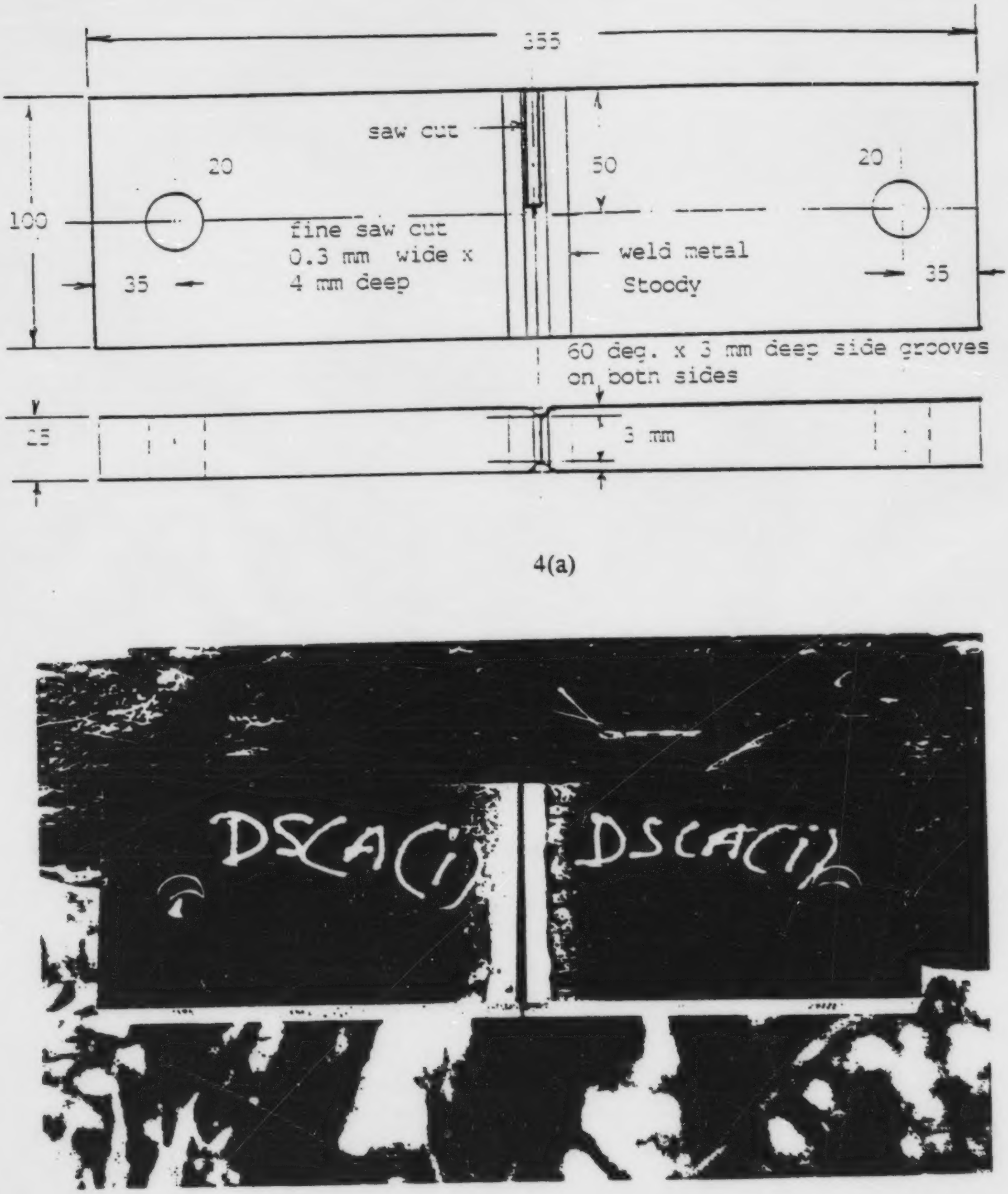
355
saw cut
20
50
20
100
fine saw cut
0.3 mm wide x
4 mm deep
weld metal
Stoody
35
35
60 deg. x 3 mm deep side grooves
on both sides
25
3 mm
DSCA(i)
DSCA(i)

4(a)

4(b)

Fig. 4 DSCA (i), (a) specimen dimensions and (b) actual specimen.

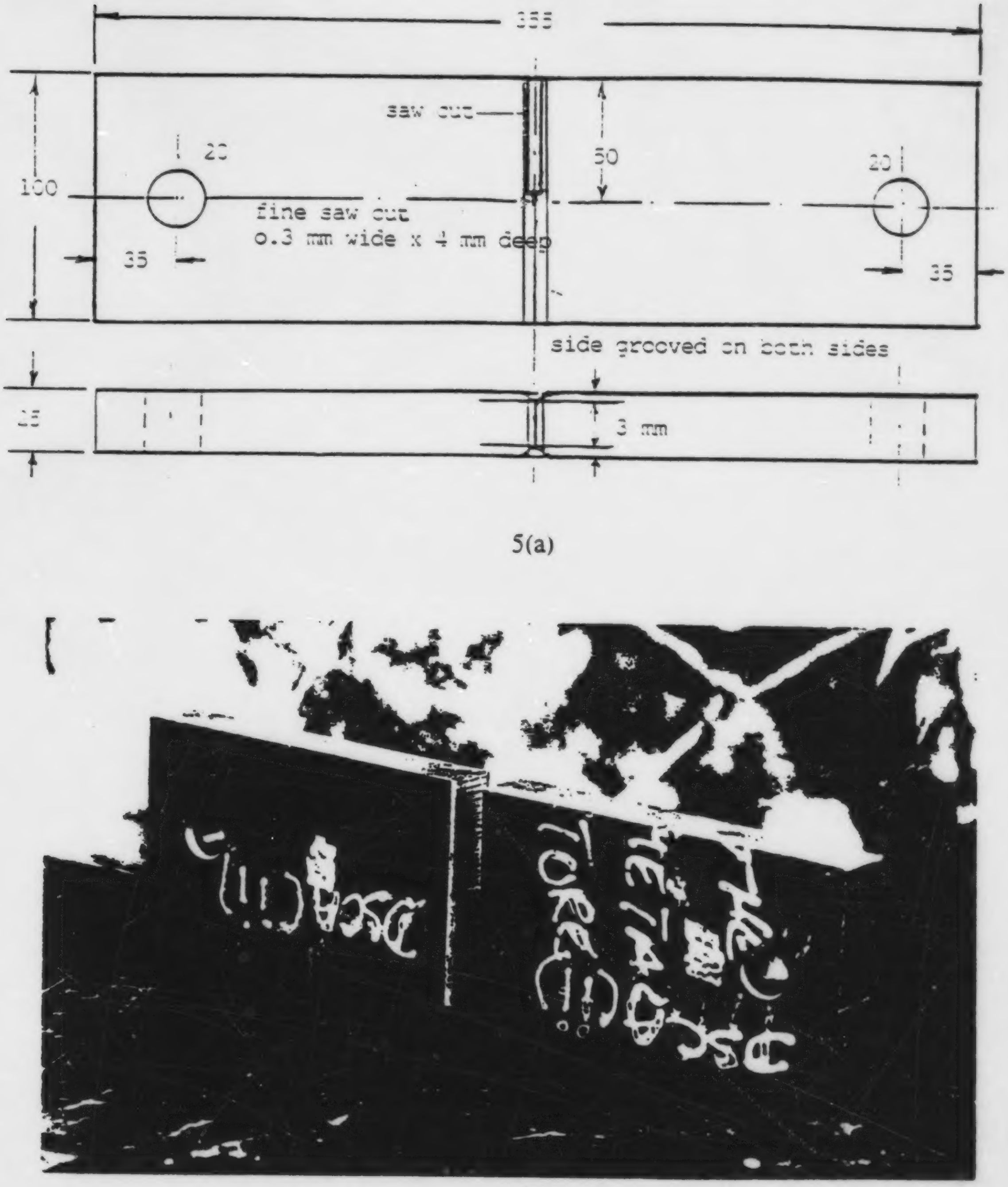
355
saw cut
20
50
100
fine saw cut
0.3 mm wide x 4 mm deep
35
20
35
side grooved on both sides
25
3 mm
DSCA(ii)

5(a)

5(b)

Fig. 5 DSCA (ii), (a) specimen dimensions and (b) actual specimen.

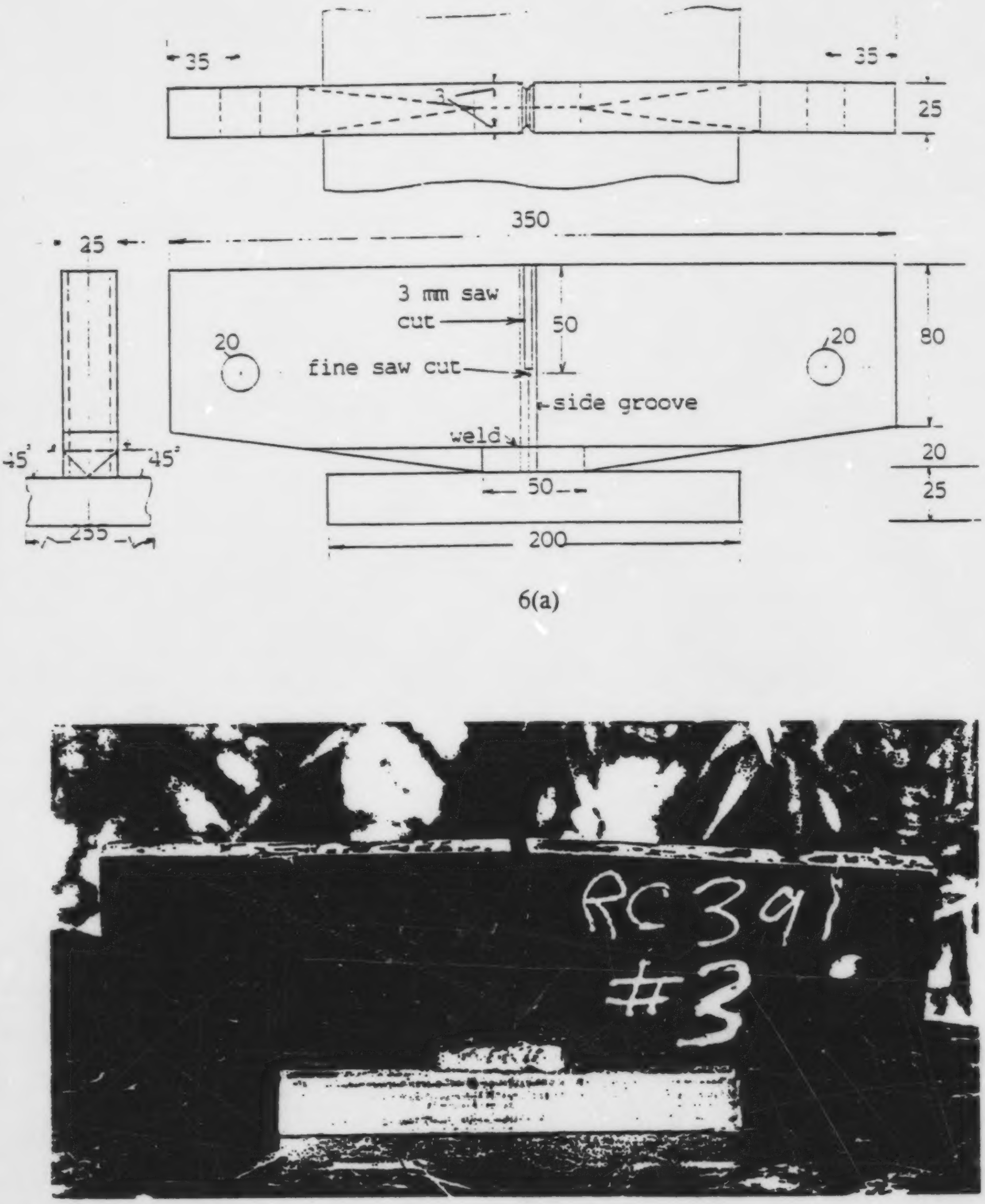
35
35
3
25
350
25
3 mm saw cut
fine saw cut
50
20
20
80
side groove
weld
45°
45°
20
25
255
50
200
RC 391
#3

6(a)

6(b)

Fig. 6 DSCA (iii), (a) specimen dimensions and (b) actual specimen.

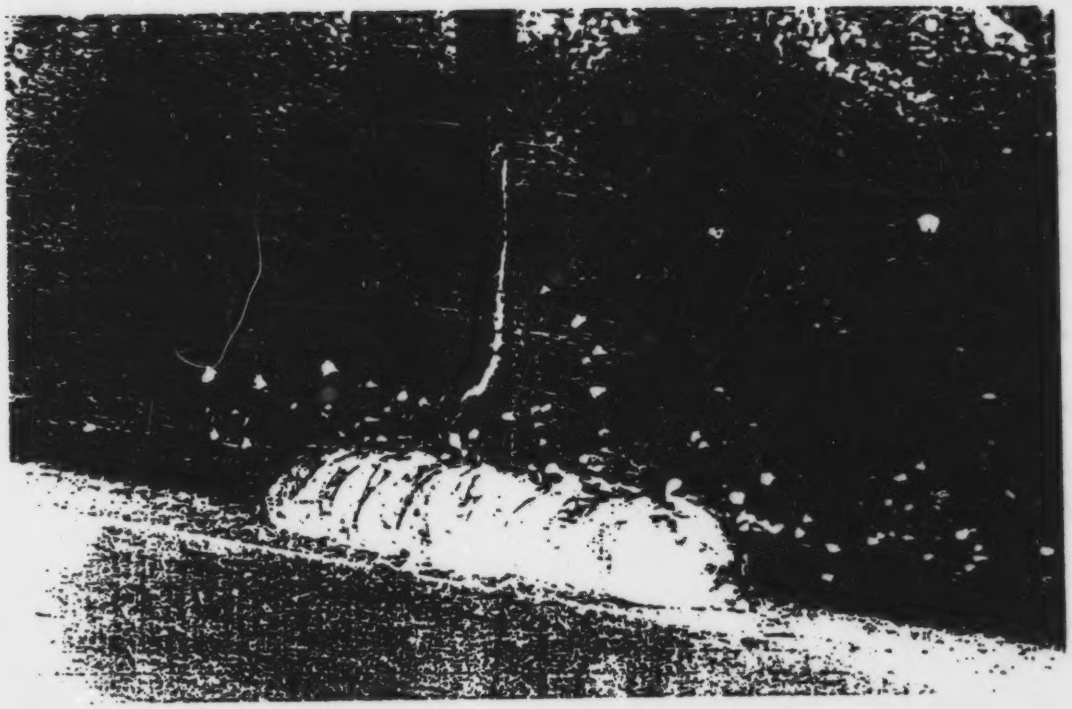

Fig. 6(c) Crack divergence away from the notch plane

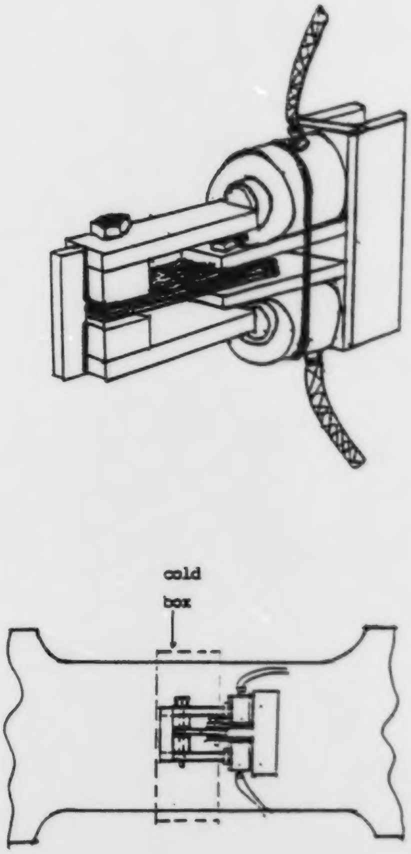

Fig. 7 Crack starter hydraulic loading unit (schematic).

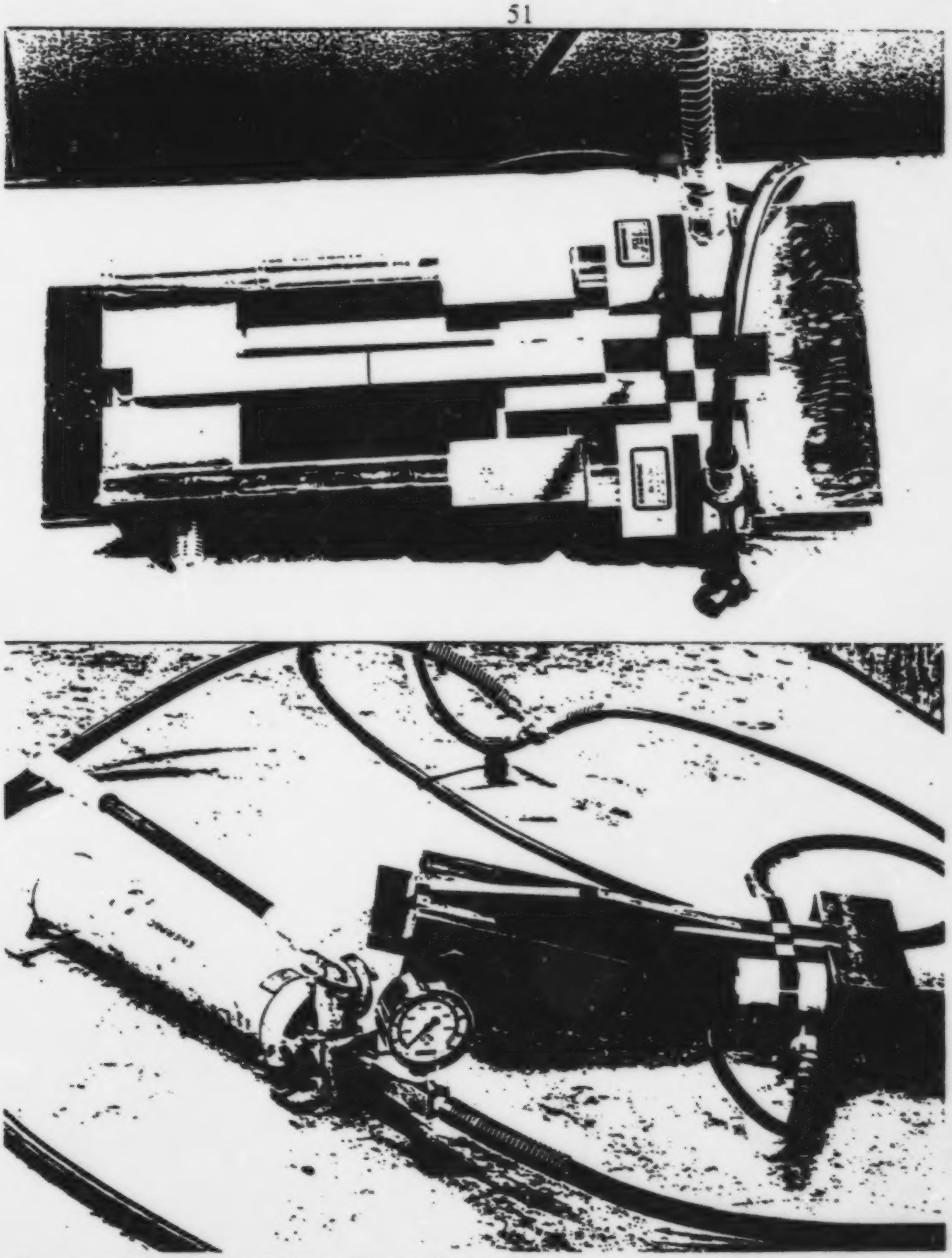

Fig. 8 Actual crack starter hydraulic loading unit.

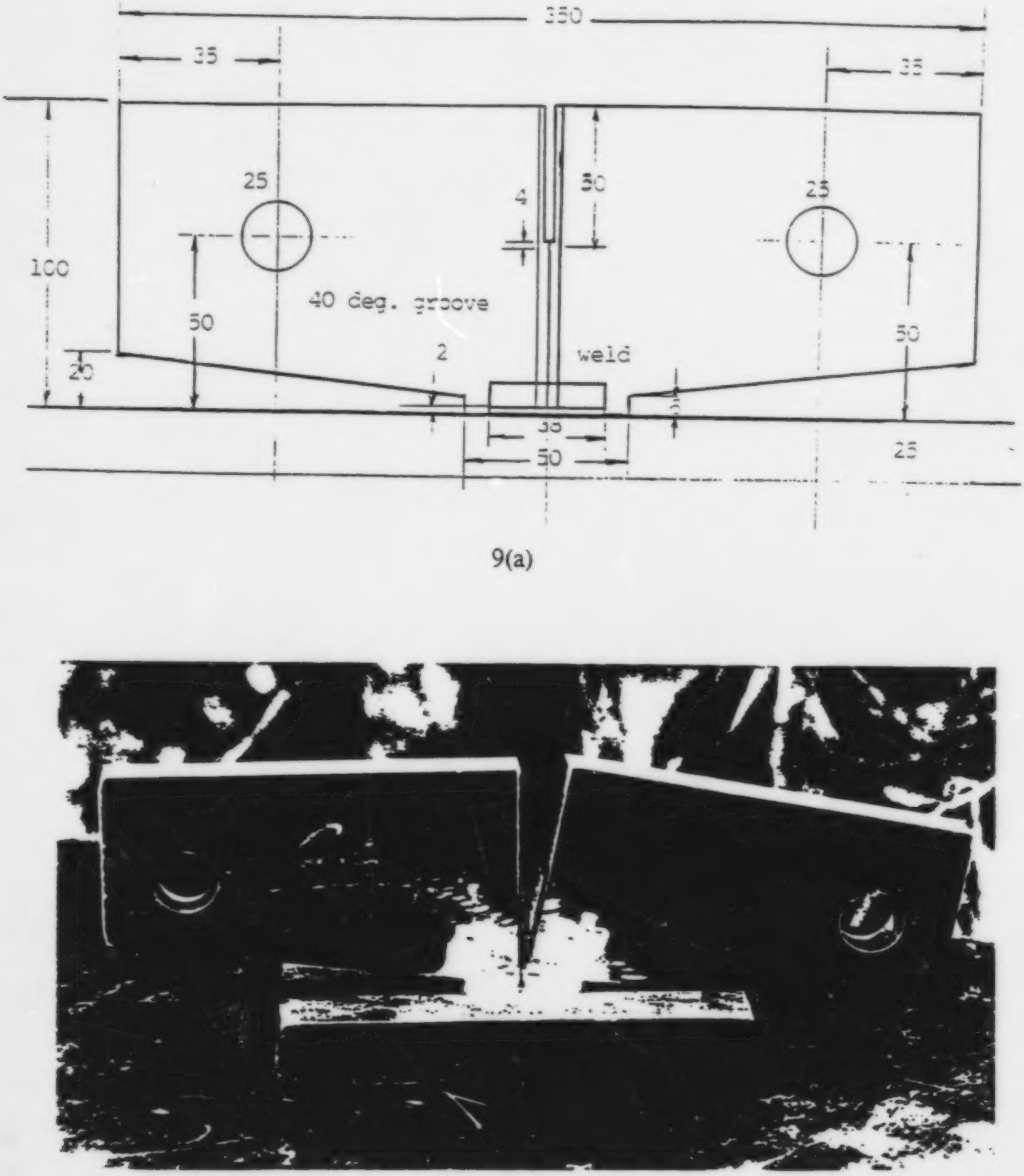
350
35
35
100
25
25
4
30
50
40 deg. groove
50
20
2
weld
50
35
50
25

9(a)

9(b)

Fig. 9 DSCA 0. (a) specimen dimensions and (b) fractured specimen

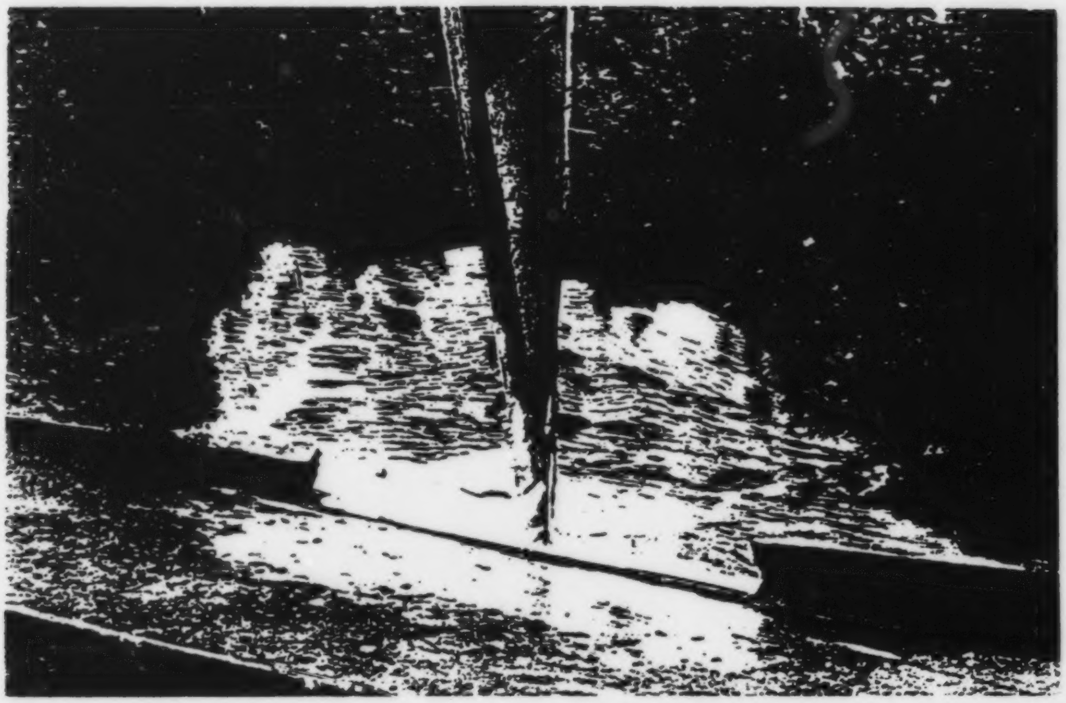

Fig. 9(c) Diversion of the crack away from the notch plane.

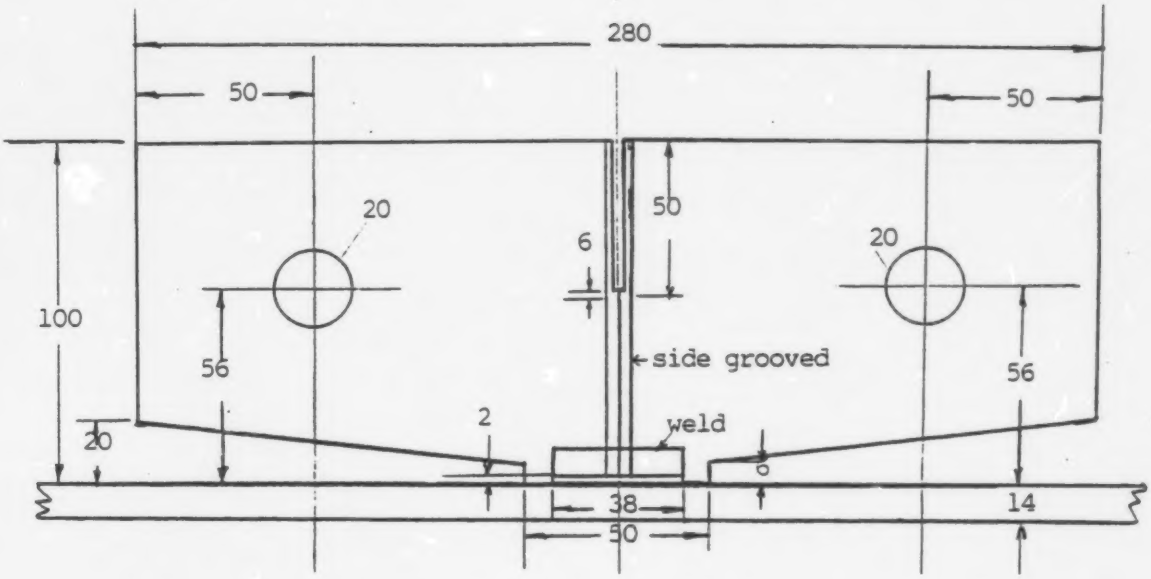
280
50
50
100
20
56
20
50
6
20
56
2
side grooved
weld
6
38
50
14

Fig. 10 DSCA 1(a) Specimen dimensions

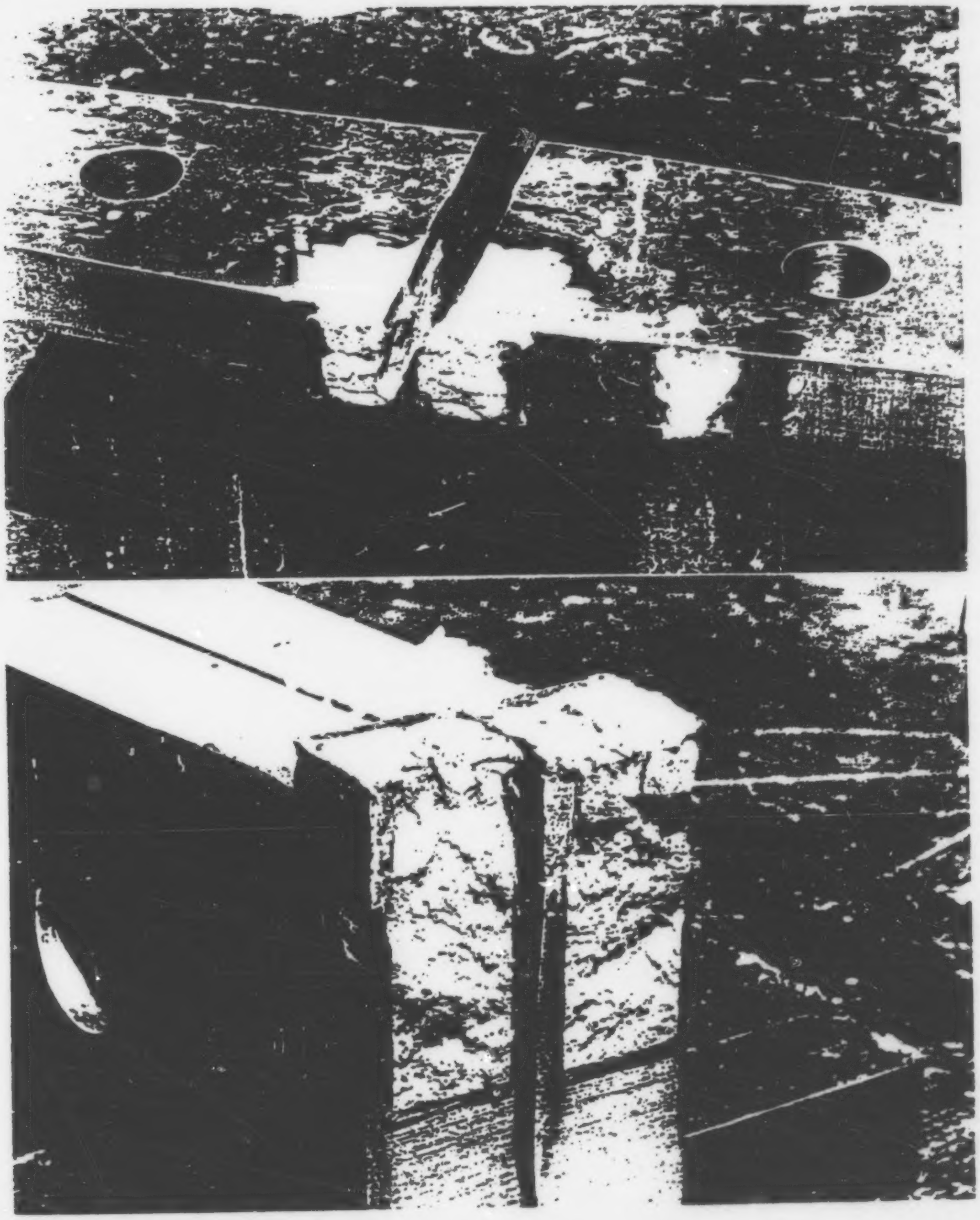

Fig. 10(b) Fractured specimen showing the crack progression in the notch plane.

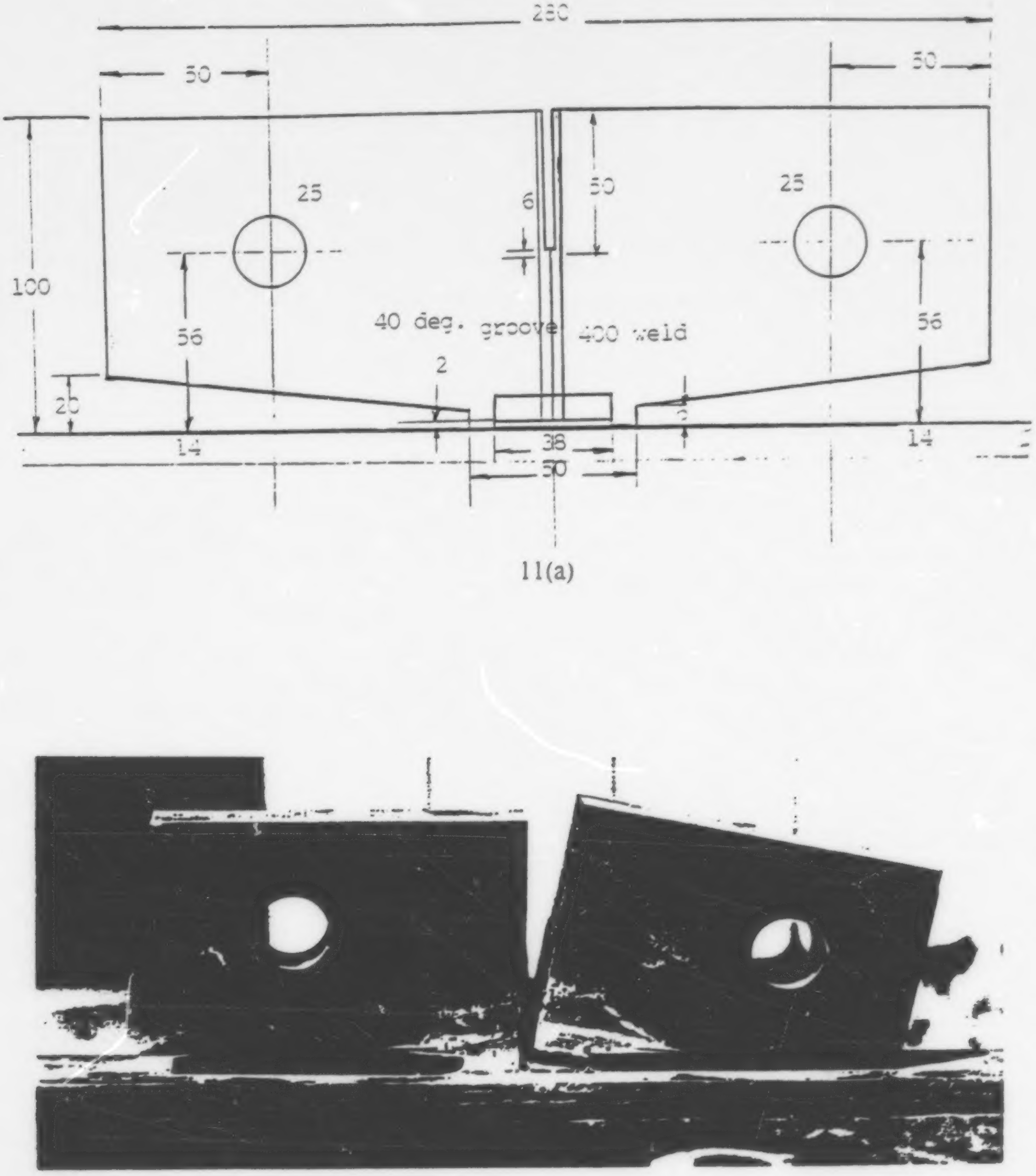
280
50
50
100
25
6
50
25
56
40 deg. groove
400 weld
56
2
20
2
14
38
50
14

11(a)

11(b)

Fig. 11 DSCA 2, (a) Dimensions of the specimen.
(b) Fractured specimen showing the crack path

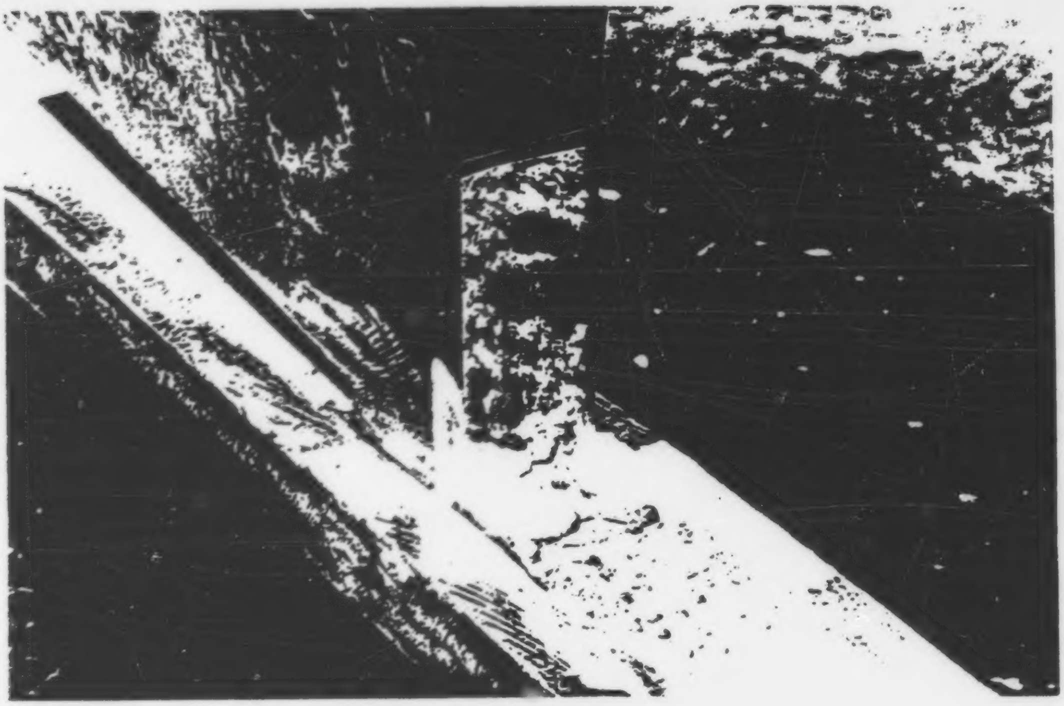

11(c)

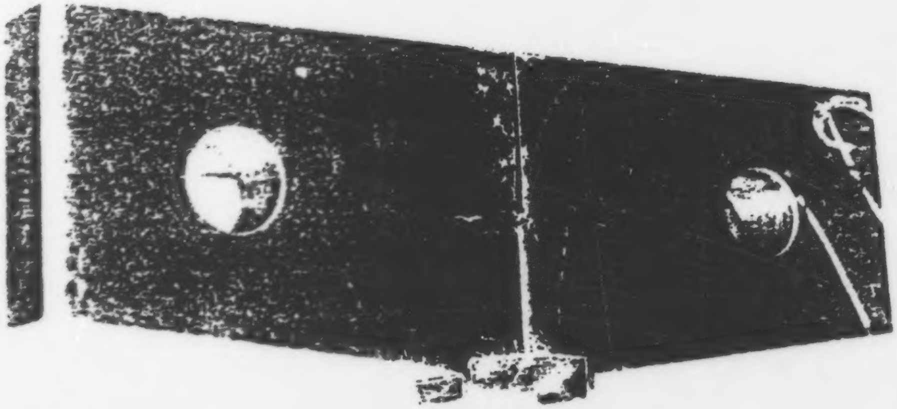

11(d)

Fig. 11 (c) sideways crack in the brittle attachment weld
(d) one of the crack starter specimens showing the bottom groove geometry for depositing the attachment weld.

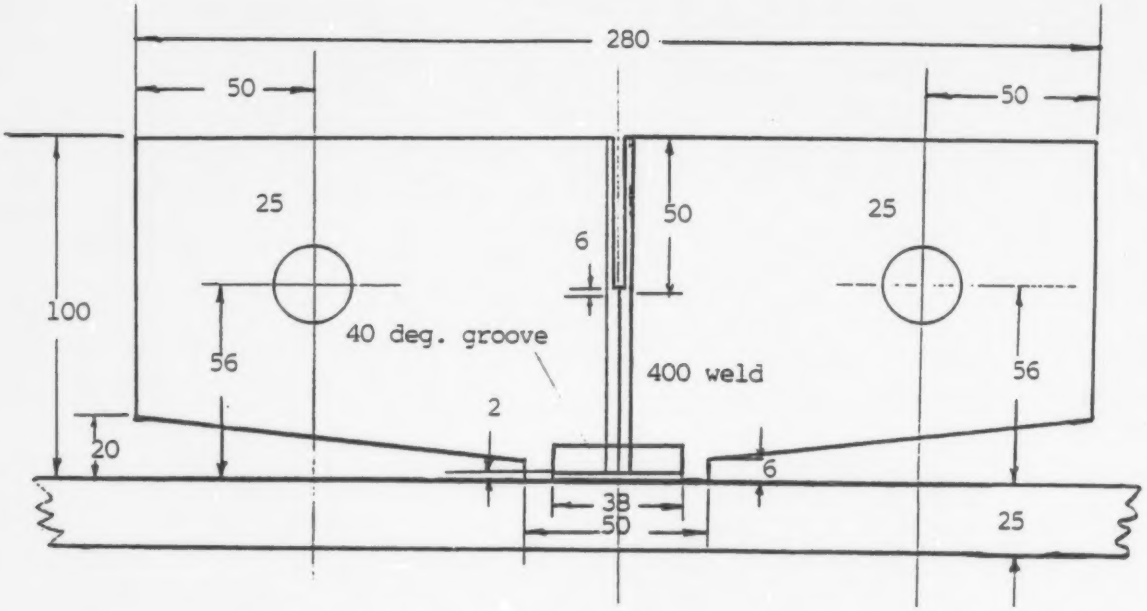
280
50
50
25
25
50
6
100
56
56
40 deg. groove
400 weld
2
20
6
38
50
25

Fig. 12 DSCA 3, (a) specimen dimensions.

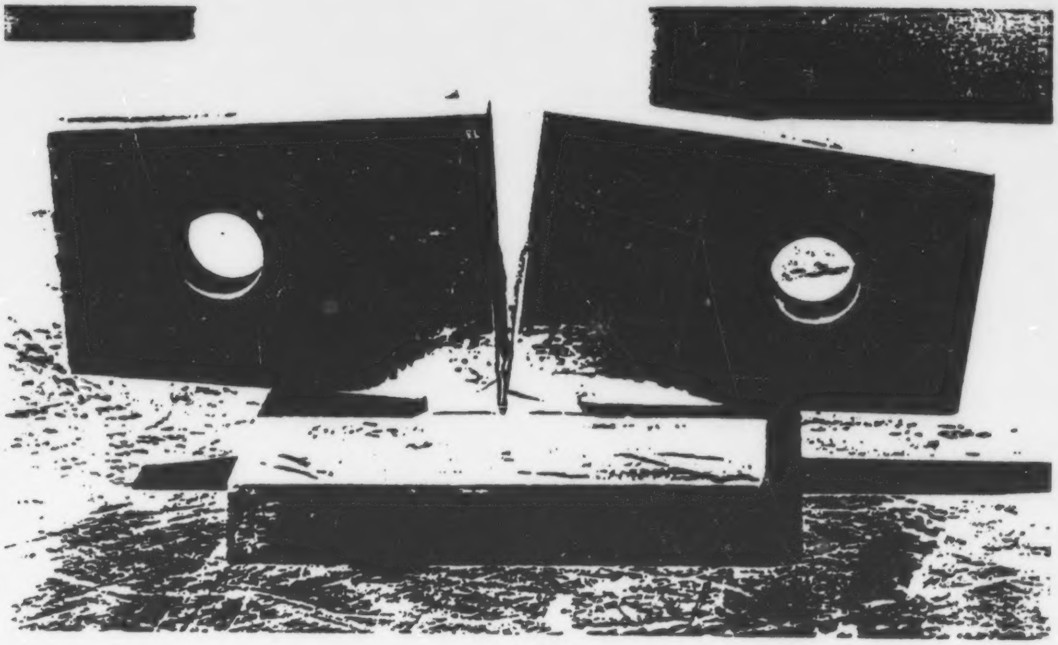

12(b)

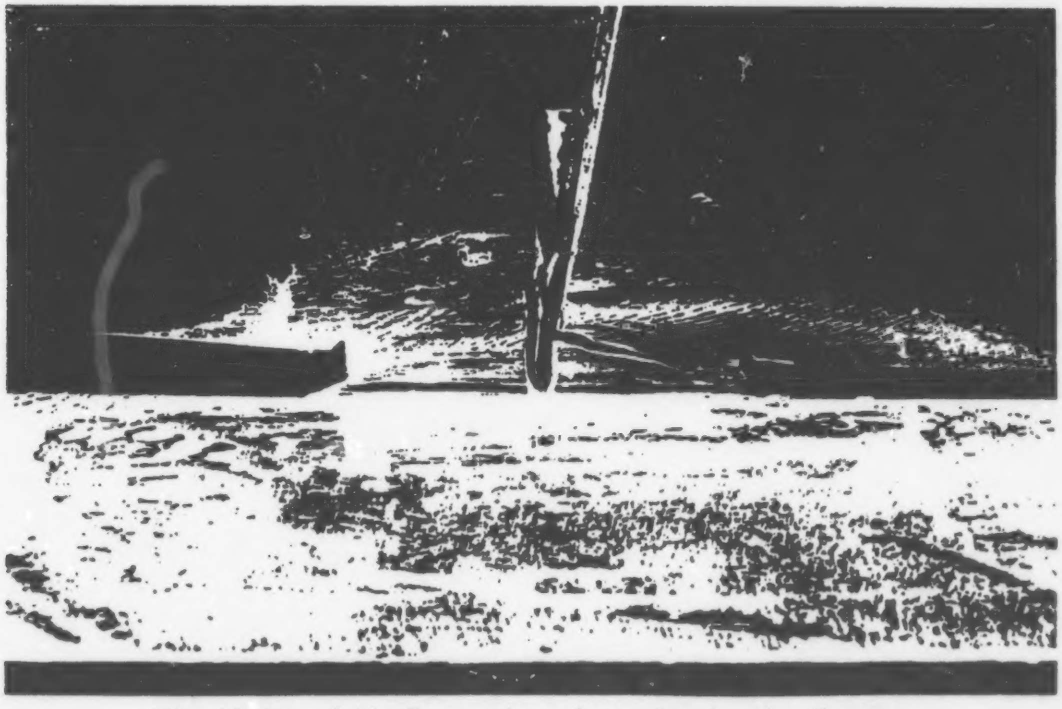

Fig. 12 (b) and (c) Fractured specimen showing the divergence of the crack from the notch plane.

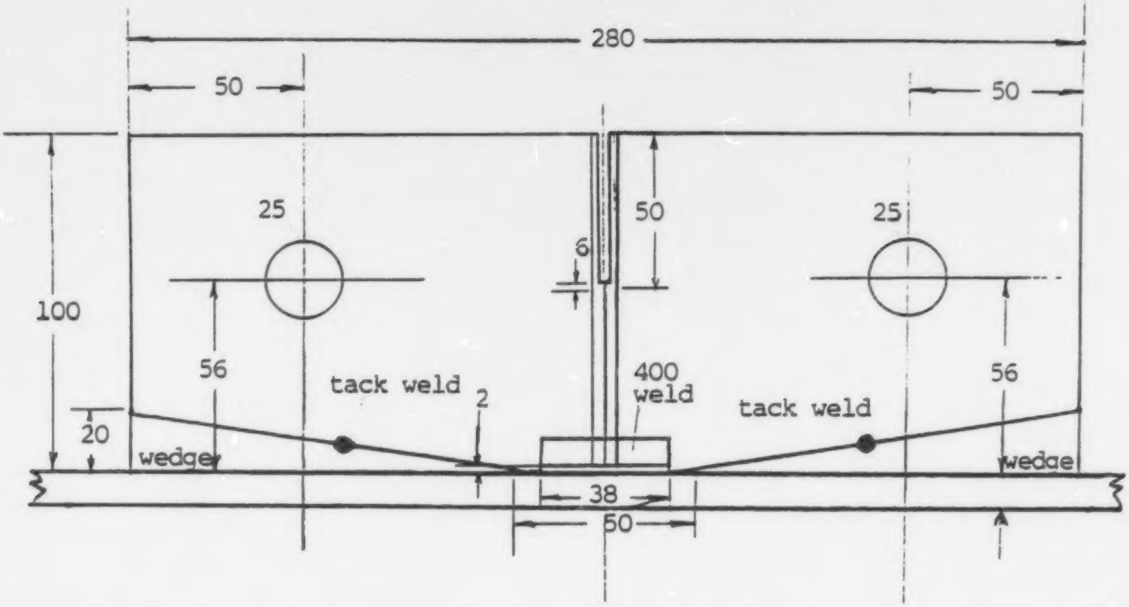
280
50
50
100
25
50
25
6
56
tack weld
2
400
weld
tack weld
56
20
wedge
wedge
38
50

Fig. 13 DSCA 4, (a) Specimen dimensions

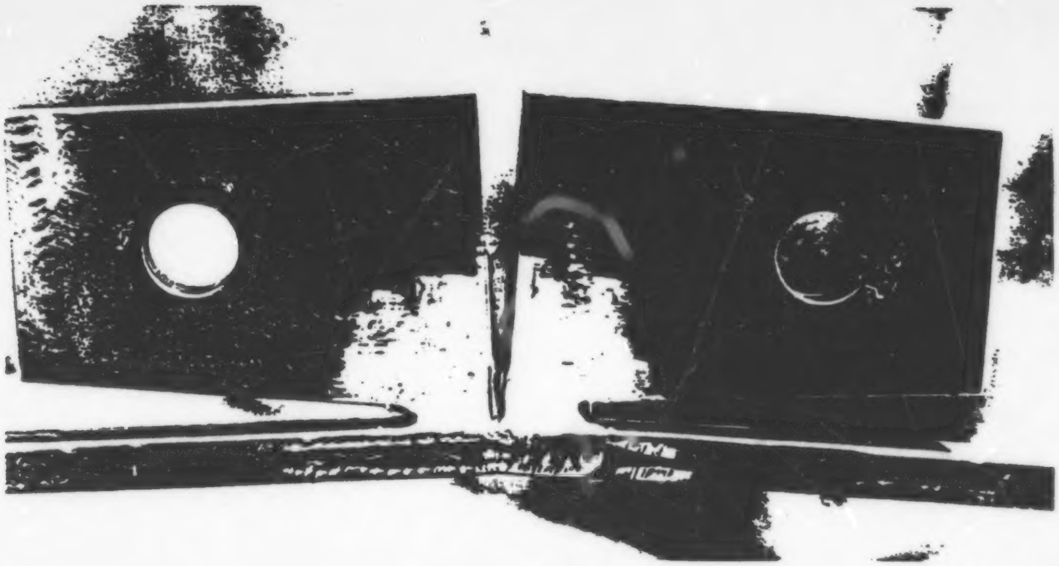

13(b)

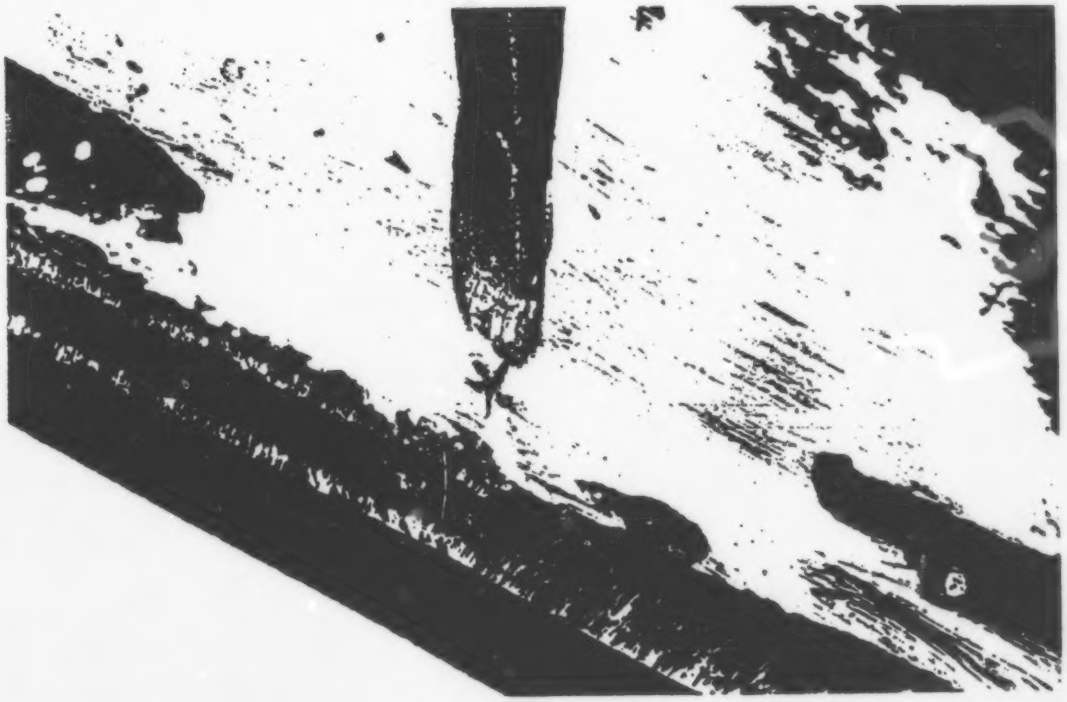

13(c)

Fig. 13(b) and (c) Fractured specimen showing the crack progression in the notch plane into the plate surface via attachment weld.

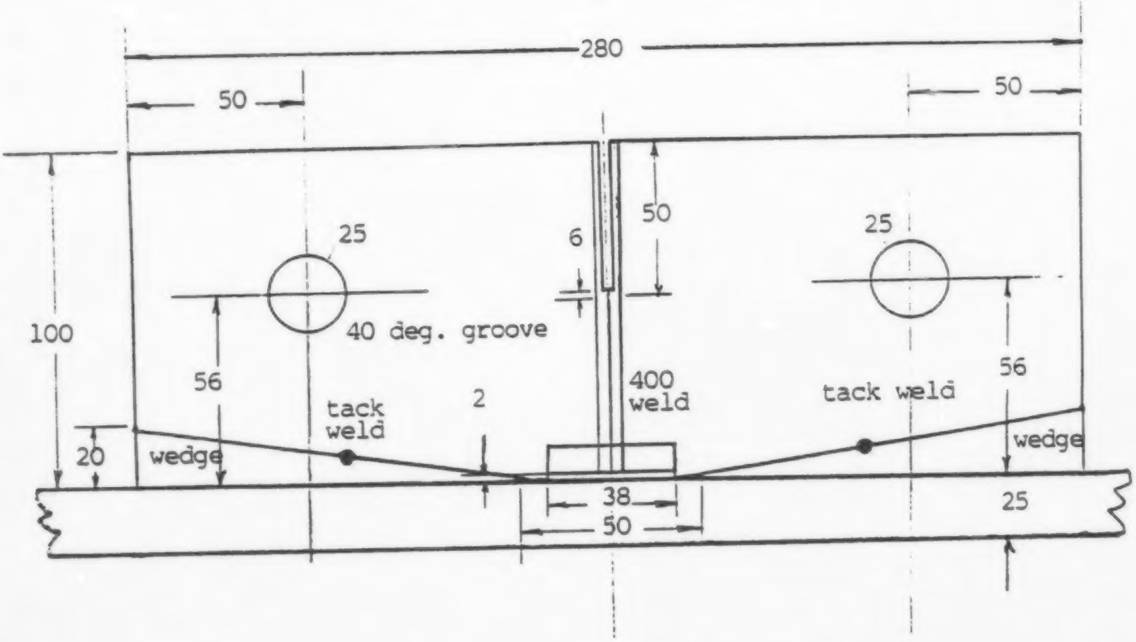
280
50
50
100
25
6
50
25
40 deg. groove
56
400
weld
56
tack
weld
2
tack weld
20
wedge
wedge
38
50
25

Fig. 14 DSCA 5 (a) specimen dimensions

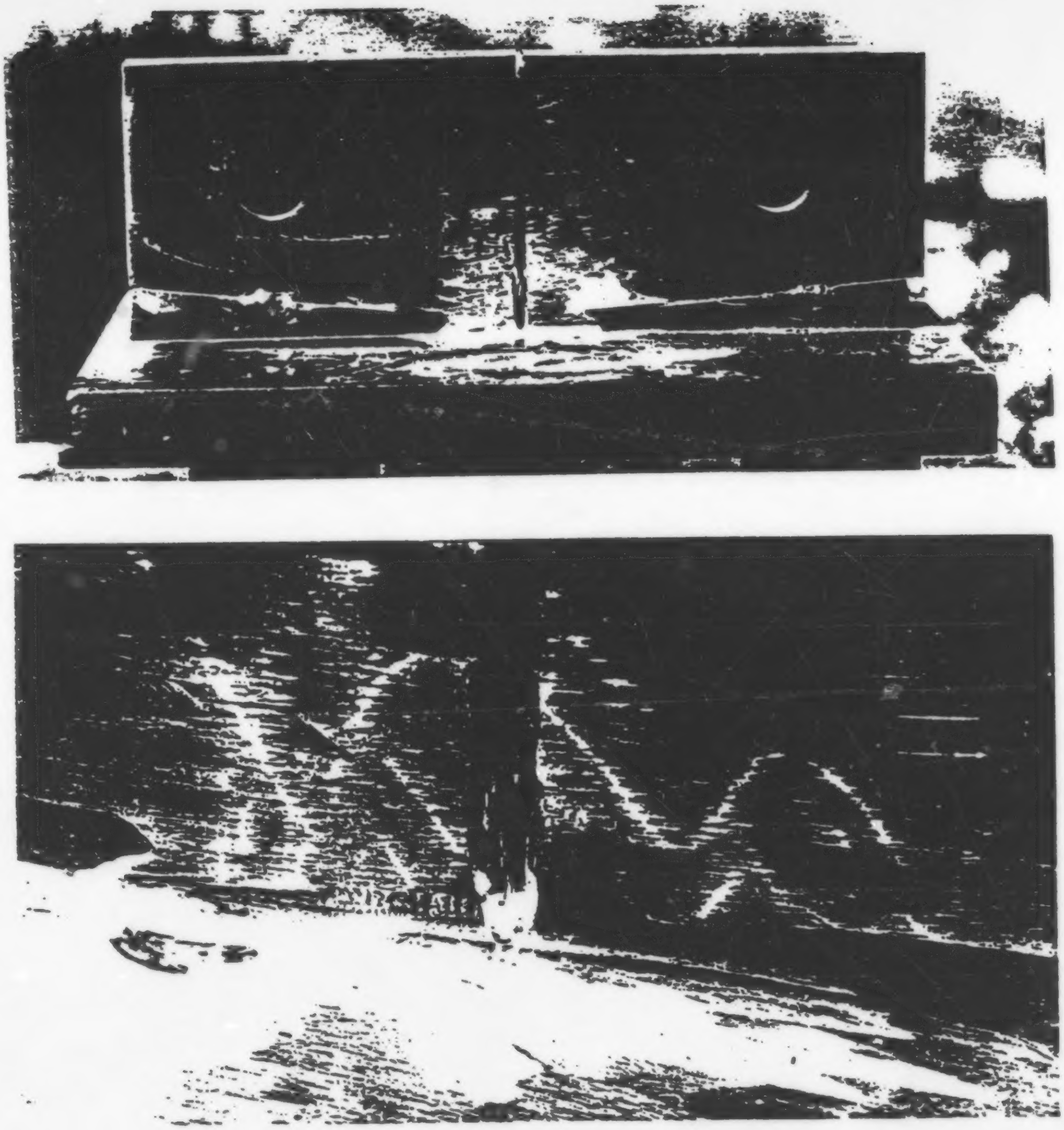

Fig. 14(b) Fractured specimen showing the crack propagation in the notch plane into the plate surface via brittle attachment weld.

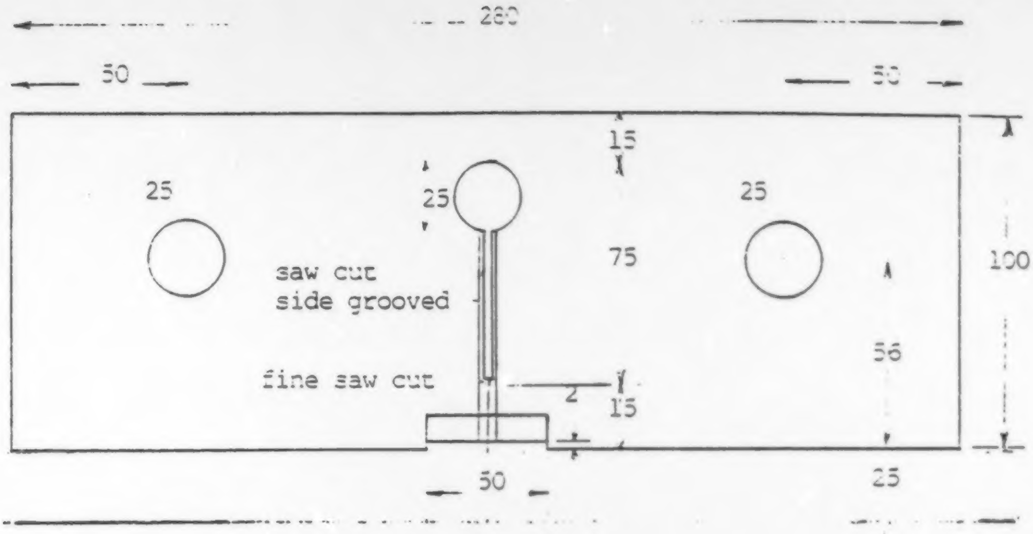
280
50
50
15
25
25
25
75
100
saw cut
side grooved
fine saw cut
2
15
56
50
25

15(a)

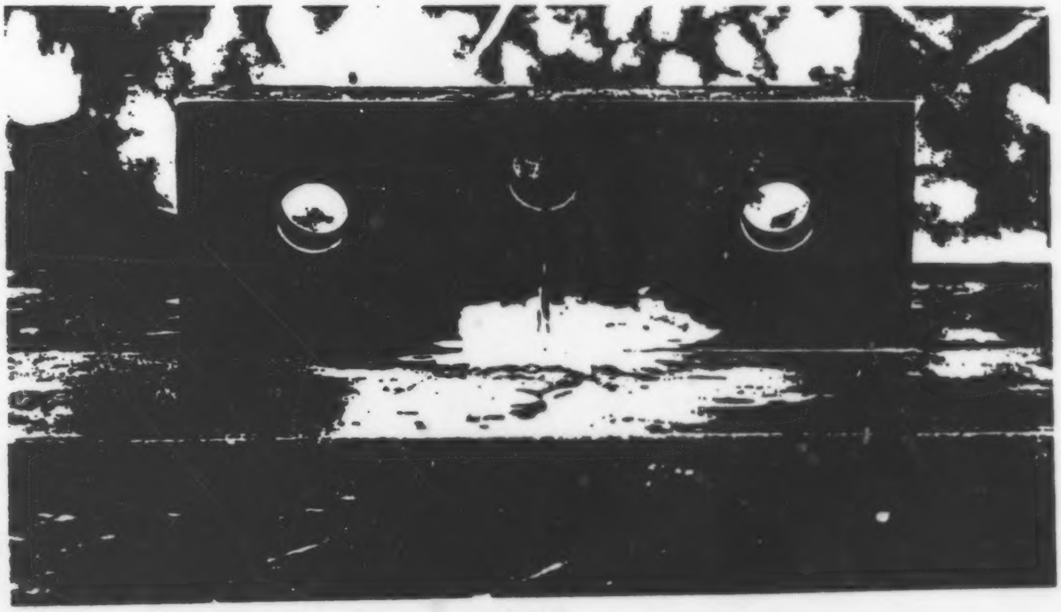

15(b)

Fig. 15 DSCA 6 Centre notch design of crack starter
(a) specimen dimensions and
(b) showing no significant crack progression after testing.

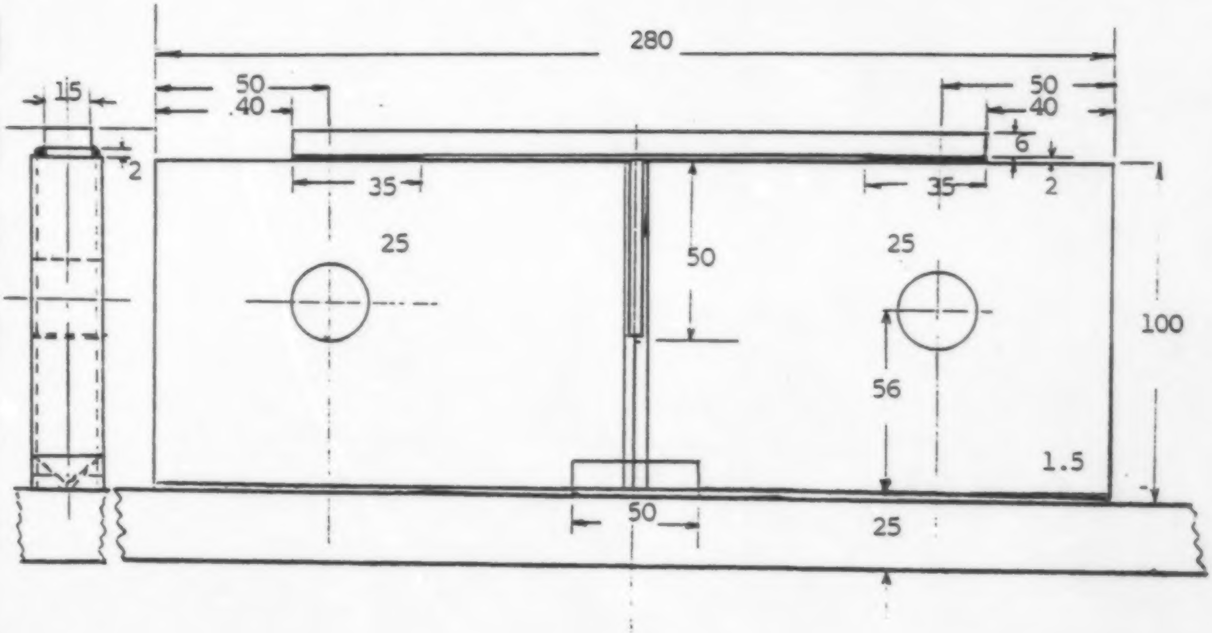
280
50
40
50
40
15
2
6
2
35
35
25
25
50
100
56
1.5
50
25

Fig. 16 DSCA 7, (a) specimen dimensions

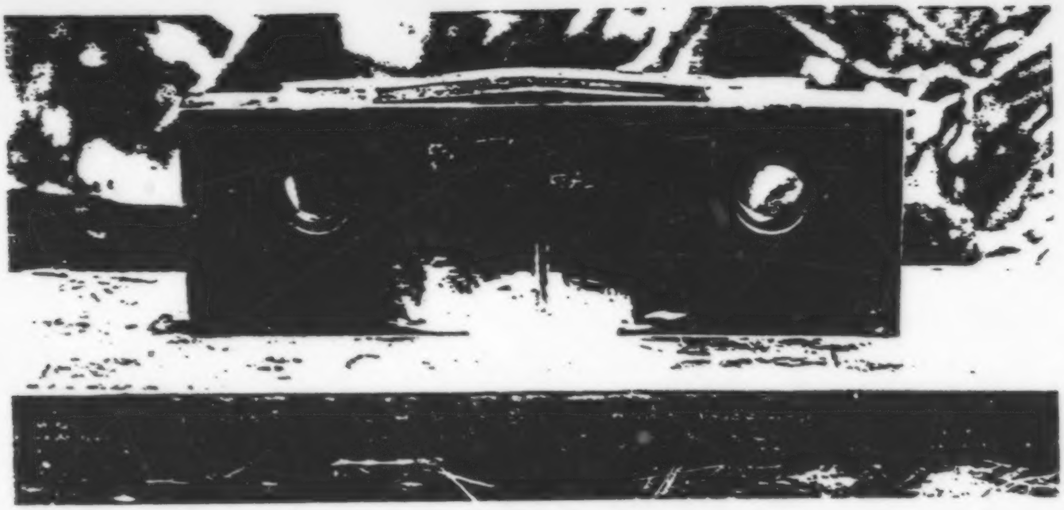

16(b)

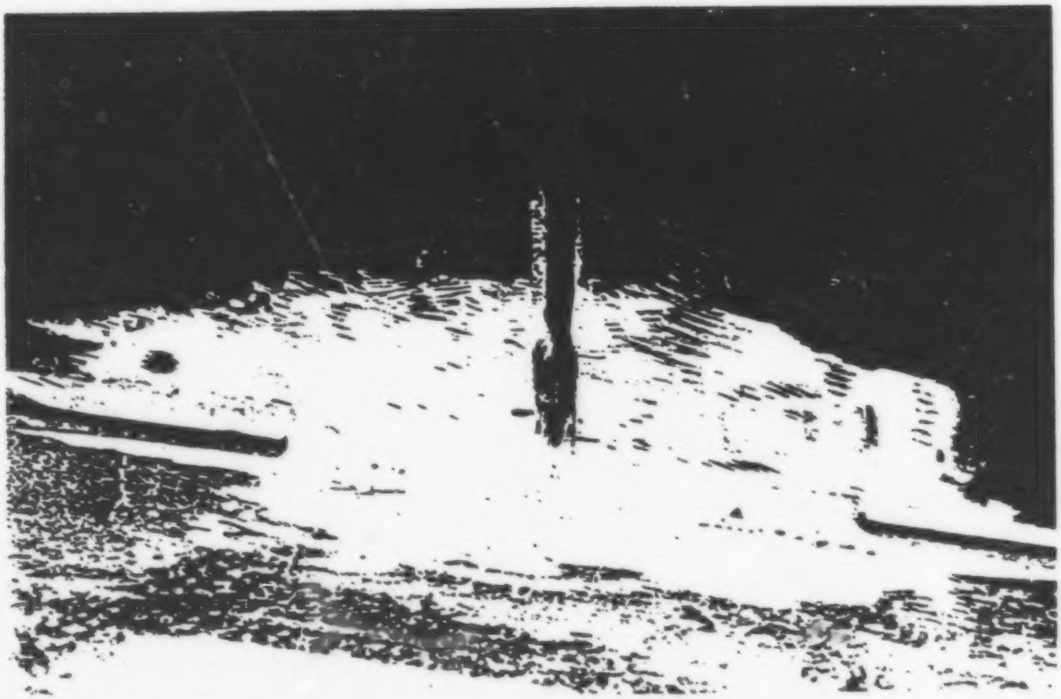

16(c)

Fig. 16(b) and (c) Specimen showing no significant crack progression after testing.

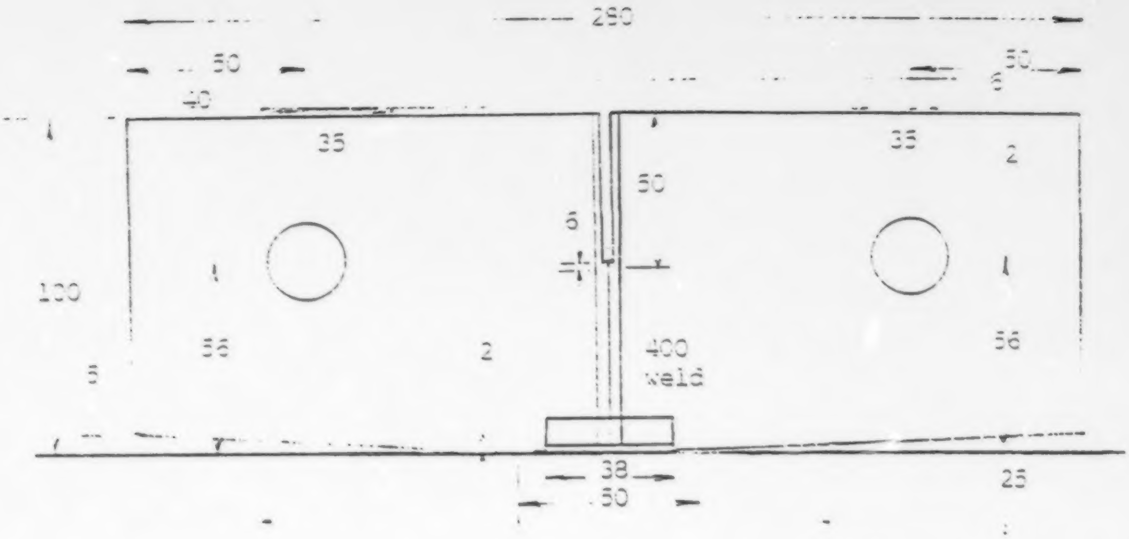
290
50
50
6
40
35
35
2
50
6
100
56
2
400
weld
56
5
38
50
25

17(a)

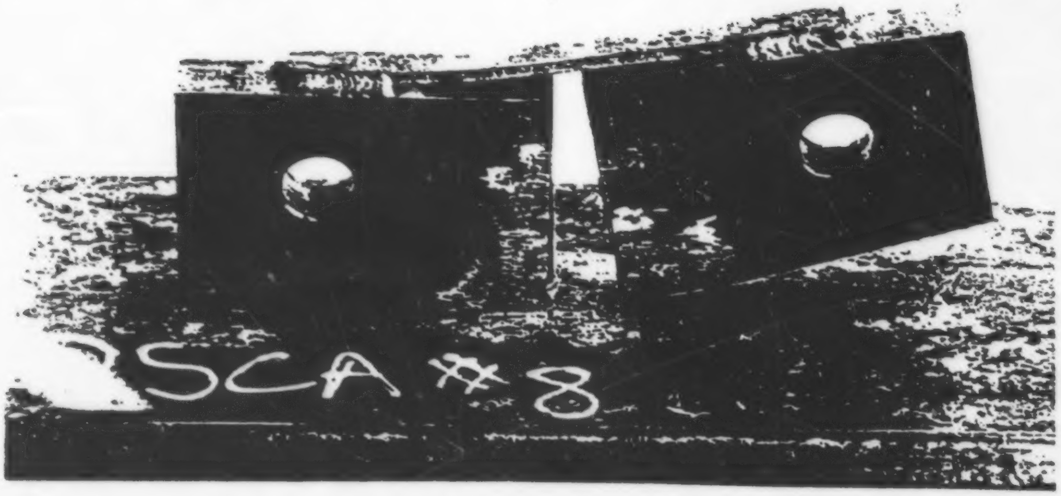

17(b)

Fig. 17 DSCA 8. (a) specimen dimensions and
(b) specimen showing crack progression in the notch plane

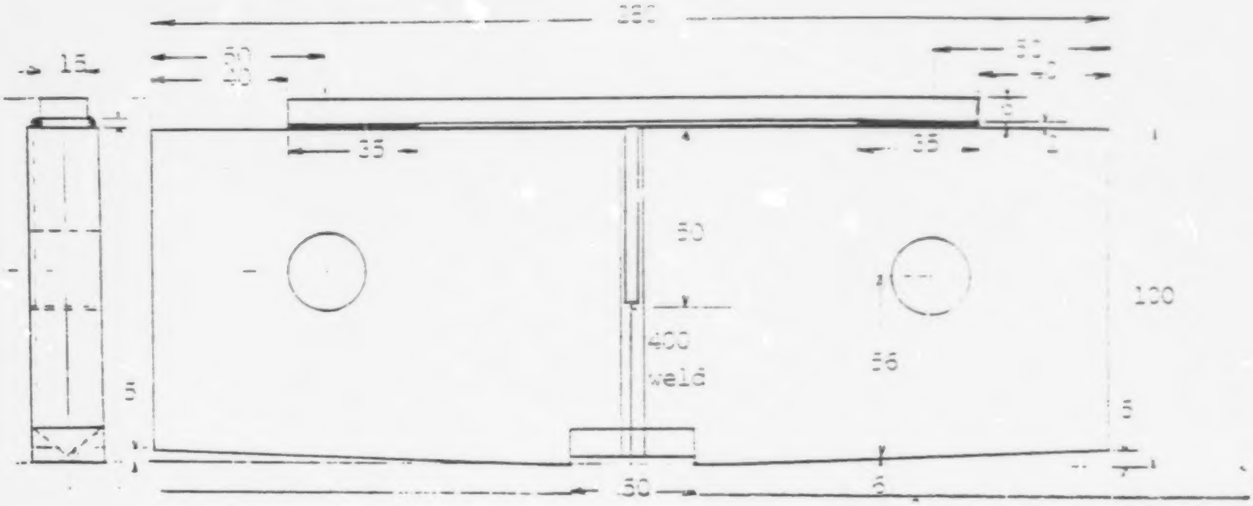
280
15
50
40
50
40
35
35
6
2
50
100
400
weld
56
5
5
60
6

18(a)

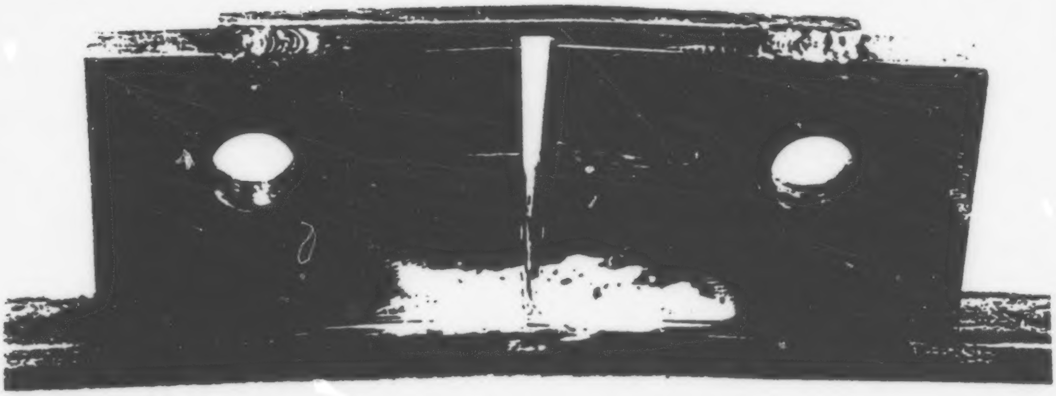

18(b)

Fig. 18DSCA 9, (a) specimen dimensions, and
(b) specimen showing divergence of the crack path from the notch plane near the attachment weld.

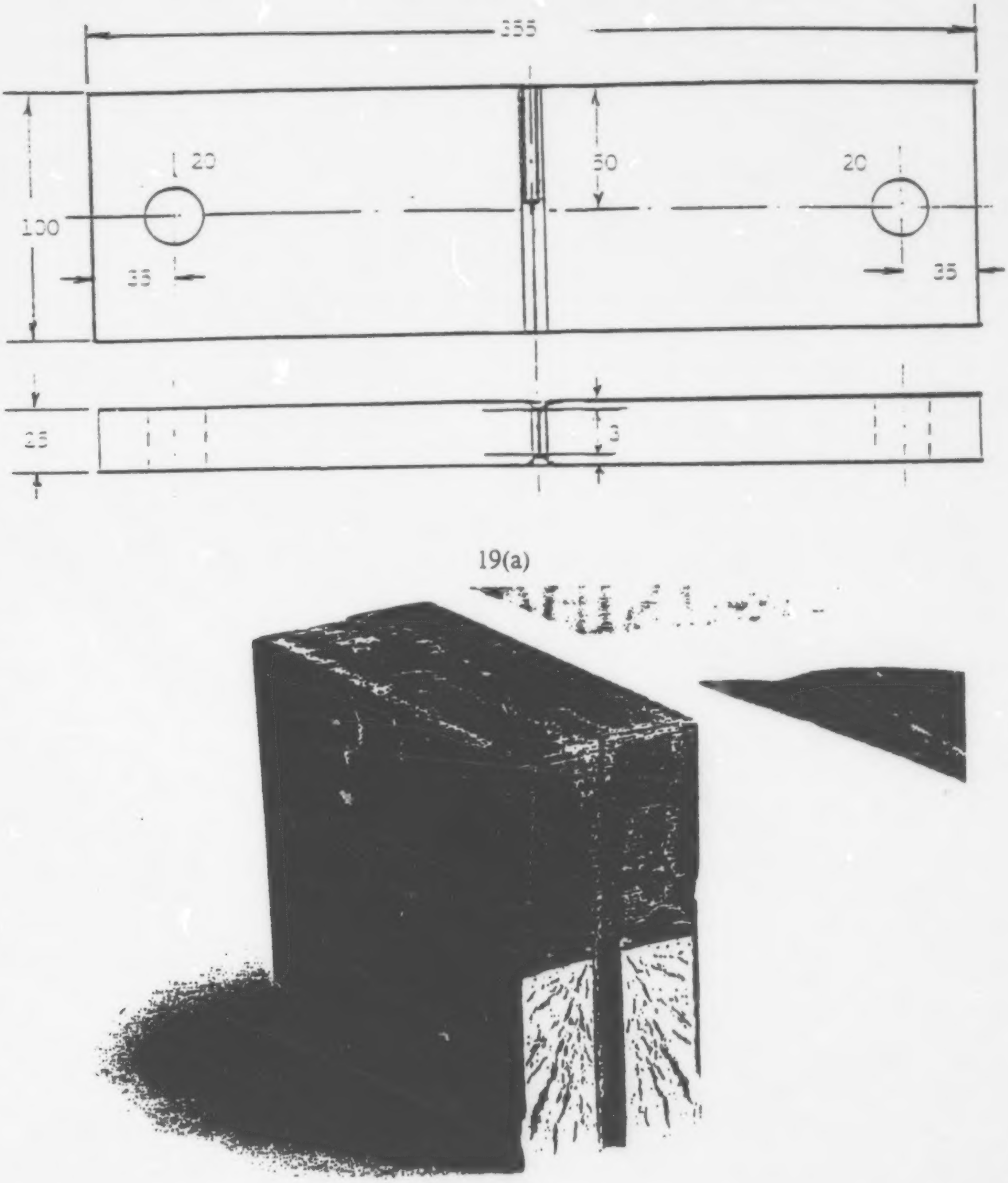
355
20
50
20
100
35
35
25
3

19(a)

19(b)

Fig. 19 DSCA 10, (a) Specimen dimensions and (b) Fractured specimen.

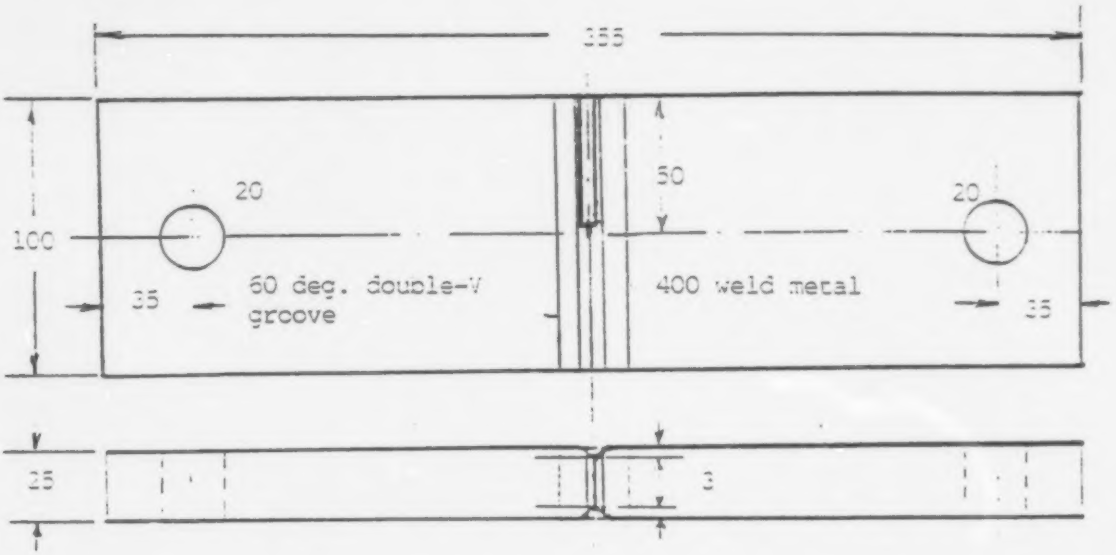
355
100
20
50
20
35
60 deg. double-V groove
400 weld metal
35
25
3

20(a)

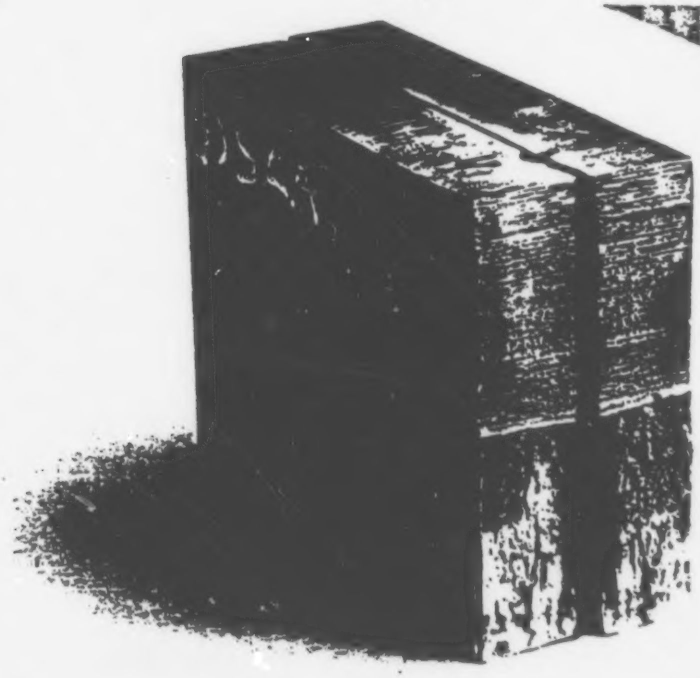

20(b)

Fig. 20 DSCA 11, (a) specimen dimensions and (b) fractured specimen.

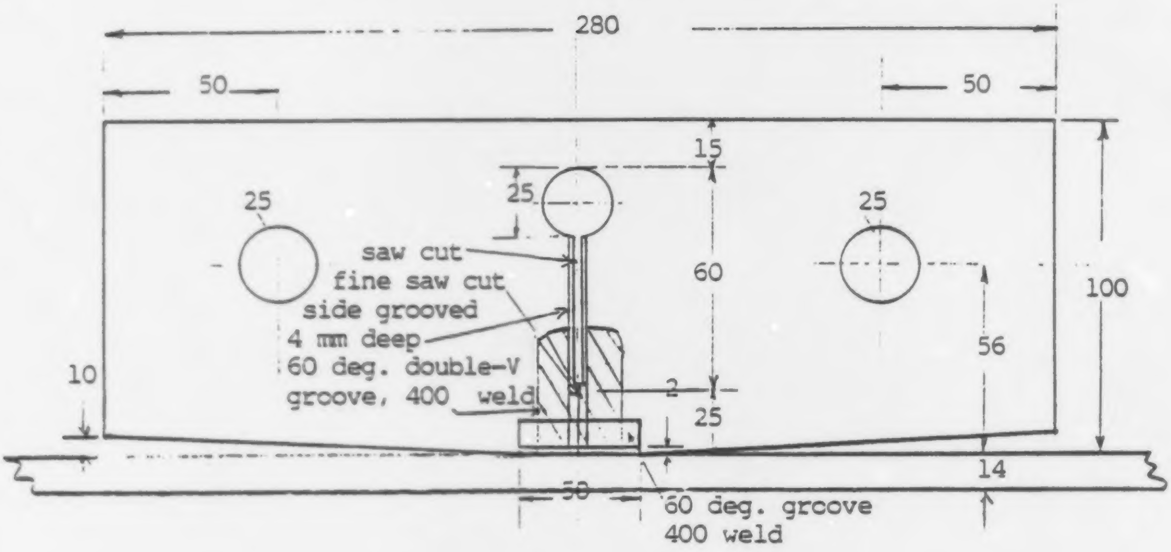
280
50
50
15
25
25
25
saw cut
fine saw cut
side grooved
4 mm deep
60 deg. double-V
groove, 400 weld
60
100
56
10
2
25
14
50
60 deg. groove
400 weld

Fig. 21 DSCA 12, (a) Specimen dimensions

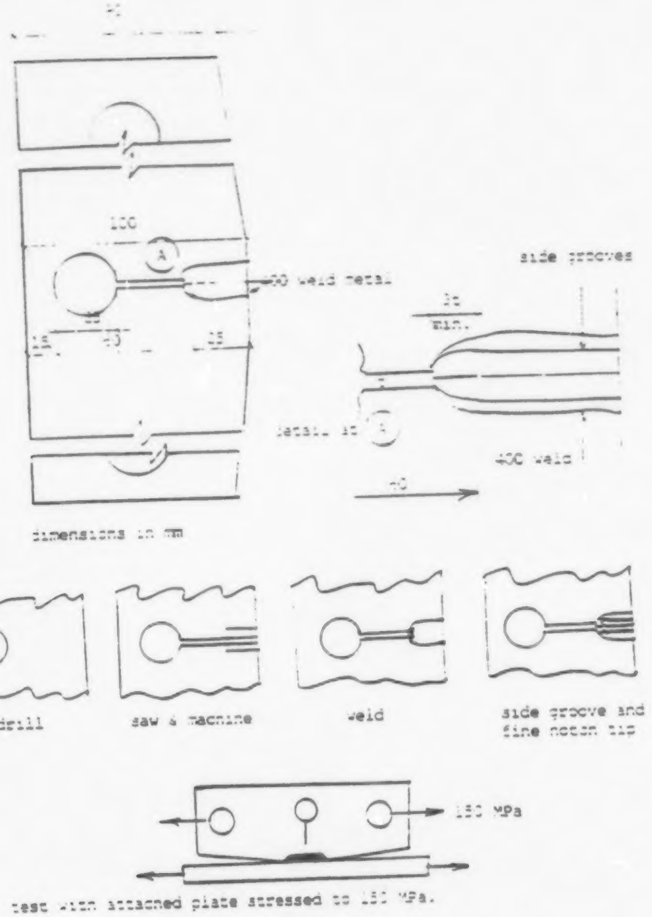
100
A
400 weld metal
30
15
40
25
side grooves
30
min.
detail at A
400 weld
40
dimensions in mm
drill
saw & machine
weld
side groove and
fine notch tip
150 MPa
test with attached plate stressed to 150 MPa.

21(b)

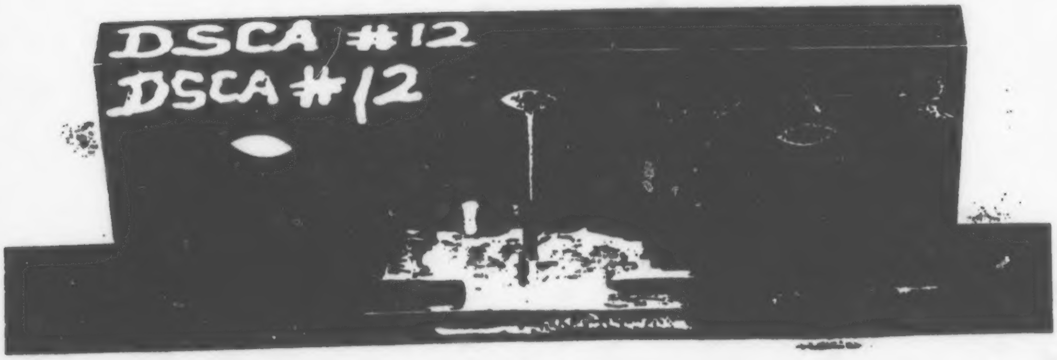
DSCA #12
DSCA #12

21(c)

Fig. 21 (b) Notch ligament & attachment weld, and
(c) specimen showing a small crack growth after testing.

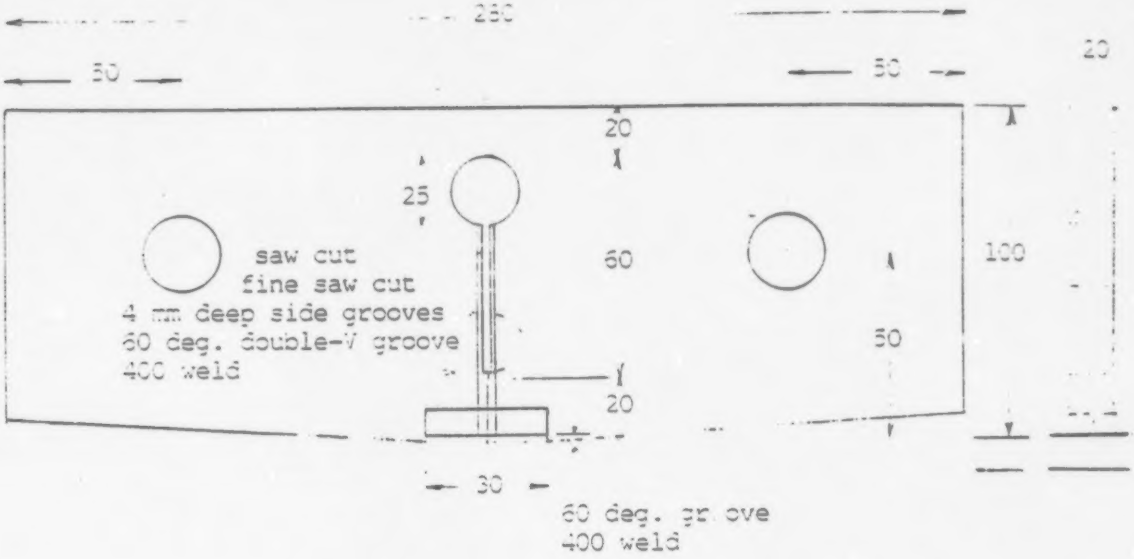
280
50
50
20
20
25
saw cut
fine saw cut
4 mm deep side grooves
60 deg. double-V groove
400 weld
60
100
50
20
30
60 deg. groove
400 weld

22(a)

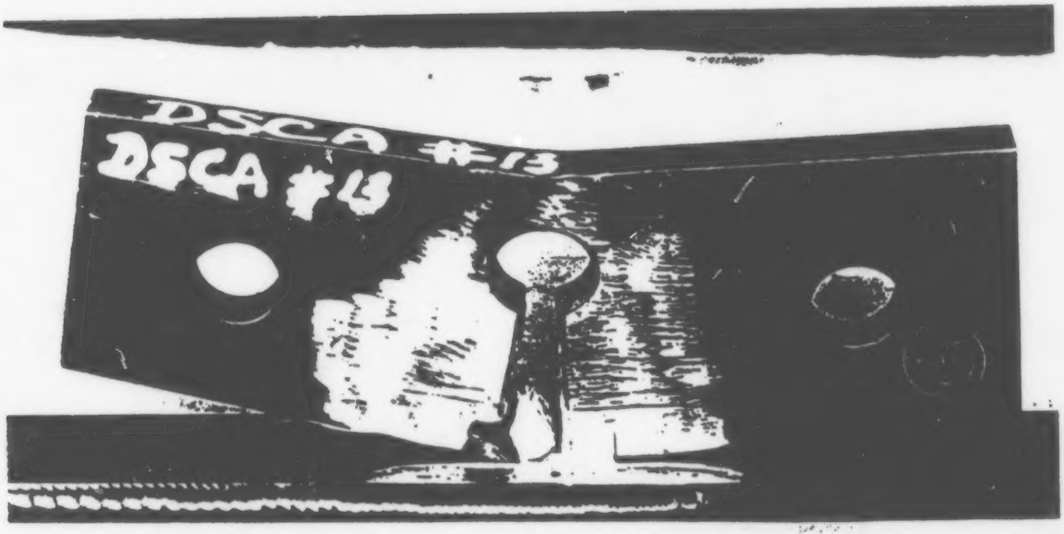
DSCA #13
DSCA #13

22(b)

Fig. 22 DSCA # 13 (a) specimen dimensions, and
(b) fractured specimen showing the crack progression in the notch plane in the starter and divergence in the attachment weld.

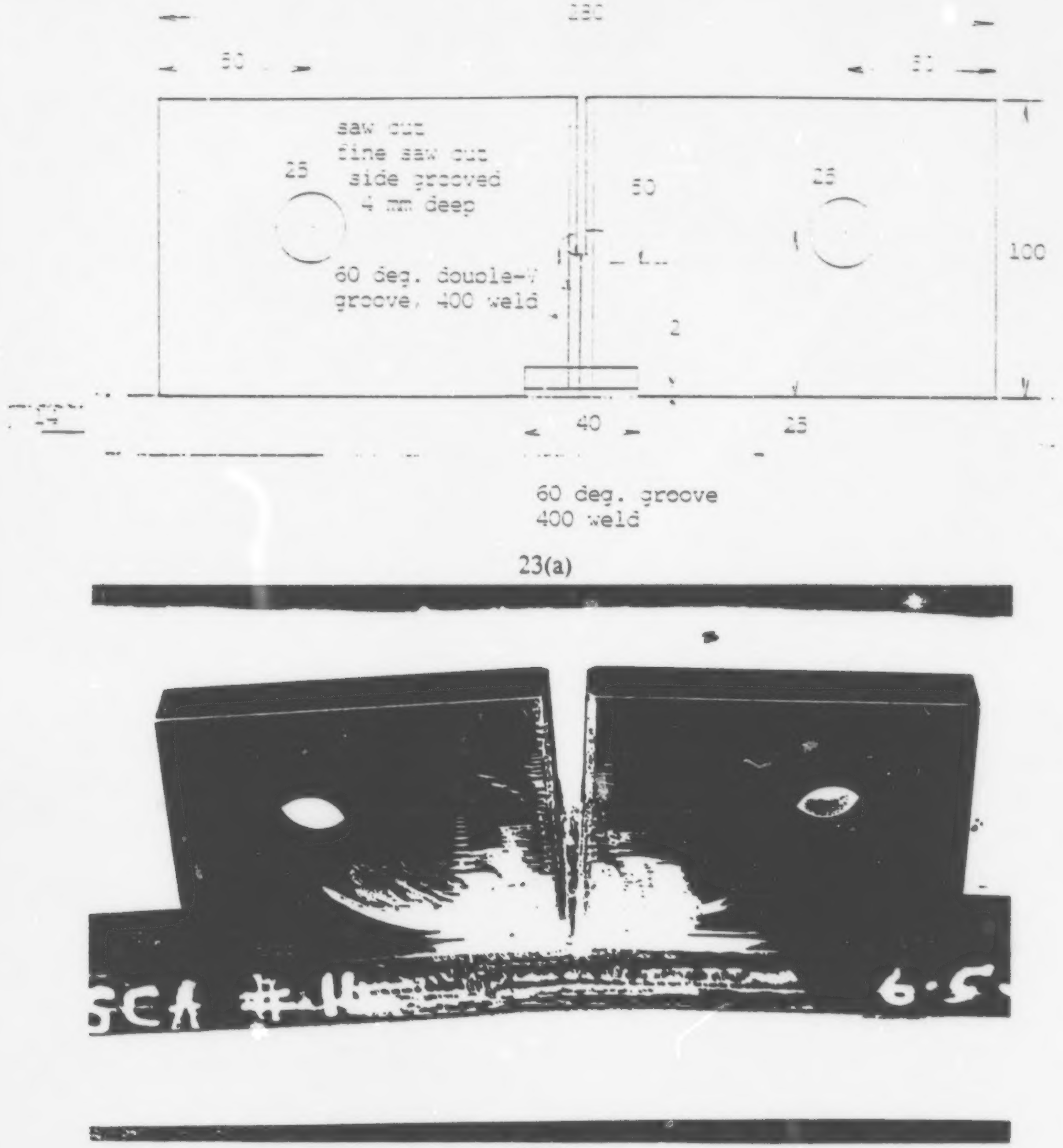
230
50
50
saw cut
fine saw cut
side grooved
4 mm deep
25
50
25
100
60 deg. double-V
groove, 400 weld
2
40
25
60 deg. groove
400 weld
SCA #14
6.5

23(a)

23(b)

Fig. 23 DSCA 14 (a) specimen dimensions, and
(b) fractured specimen showing the crack progression in the notch plane into the plate surface via attachment weld.

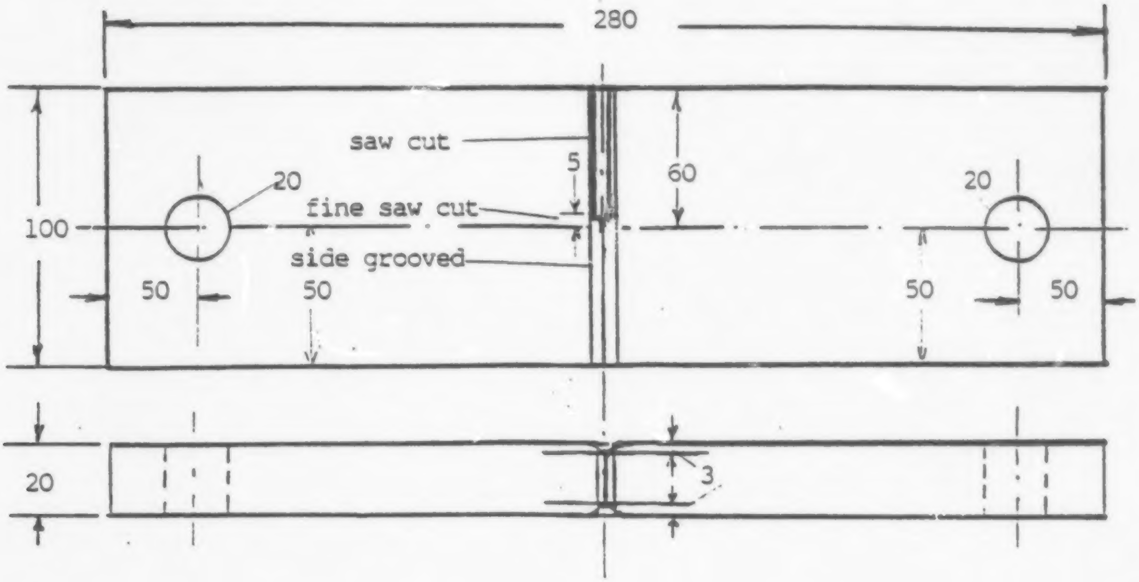
280
saw cut
5
60
20
20
fine saw cut
100
side grooved
50
50
50
50
20
3

Fig. 24 Specimen dimensions for DSCA 15.

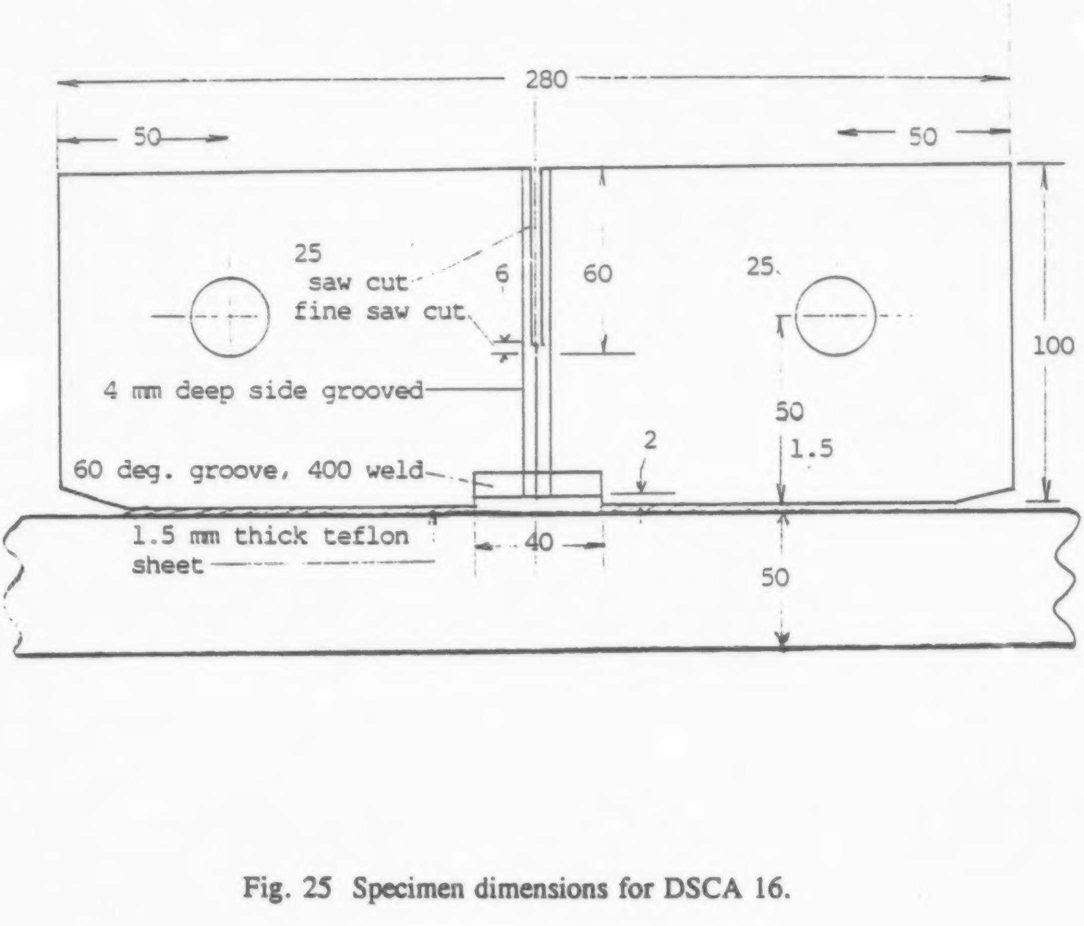
280
50
50
25
saw cut
fine saw cut
6
60
25
100
4 mm deep side grooved
50
2
1.5
60 deg. groove, 400 weld
1.5 mm thick teflon
sheet
40
50

Fig. 25 Specimen dimensions for DSCA 16.

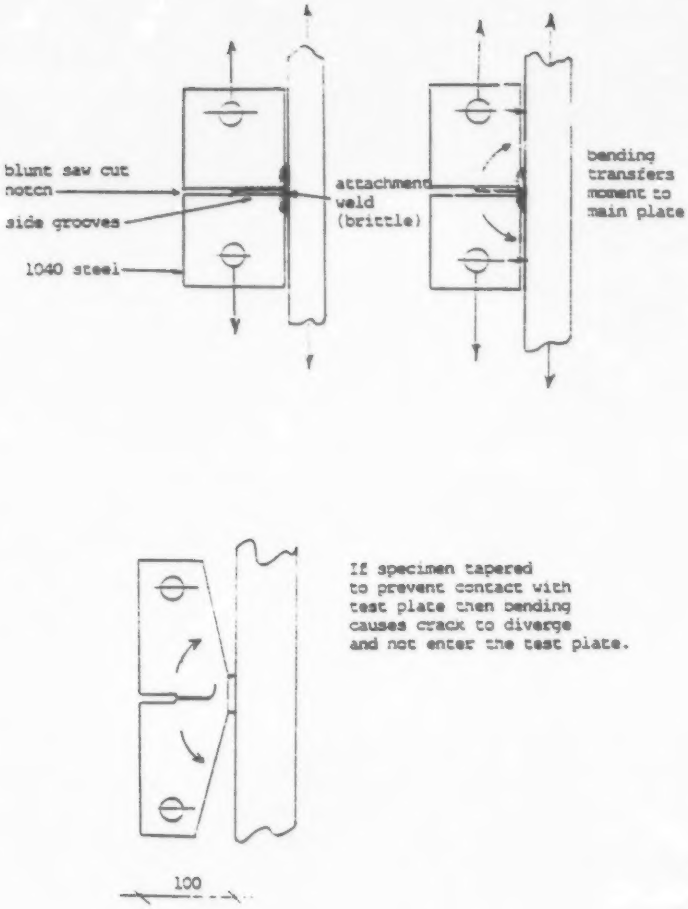
blunt saw cut notch
side grooves
1040 steel
attachment weld (brittle)
bending transfers moment to main plate
100

If specimen tapered to prevent contact with test plate then bending causes crack to diverge and not enter the test plate.

Fig. 26 Divergence of crack due to plate rotation.

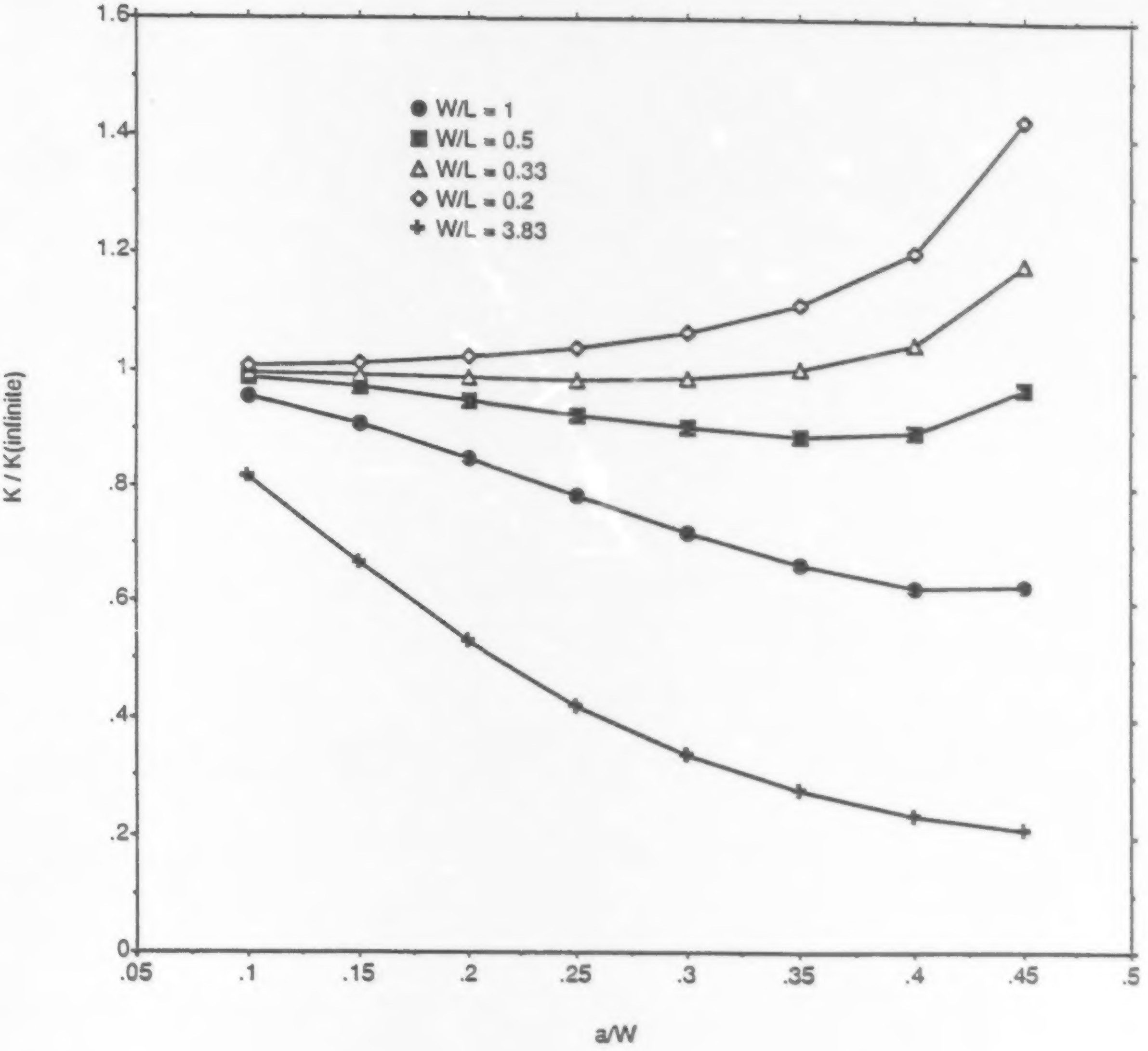

Fig. 27 Crack tip stress intensity factor K relative to that in an infinite plate as a function of plate size.

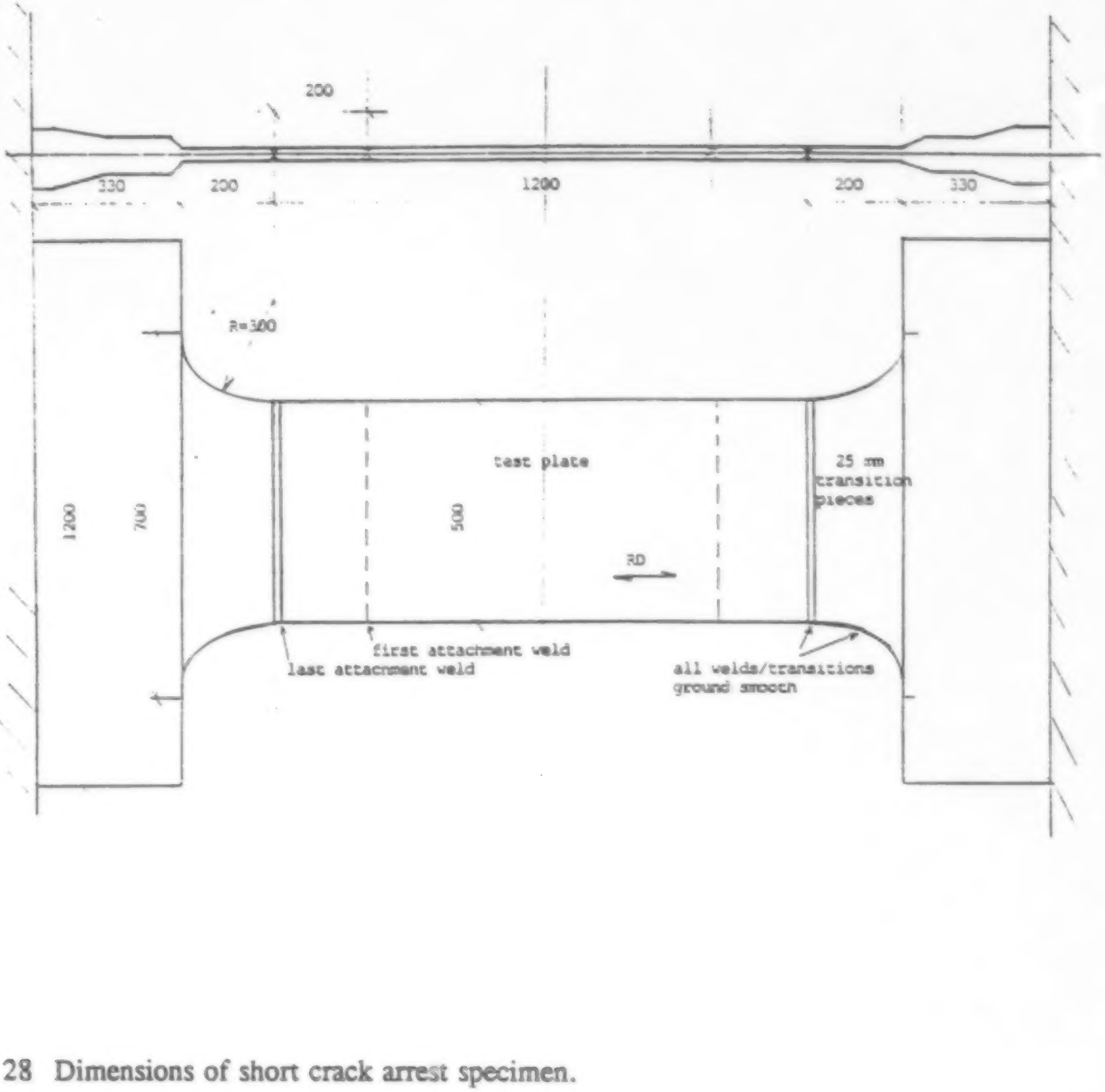
200
330
200
1200
200
330
R=300
test plate
25 mm
transition
pieces
1200
700
500
RD
first attachment weld
last attachment weld
all welds/transitions
ground smooth

Fig. 28 Dimensions of short crack arrest specimen.

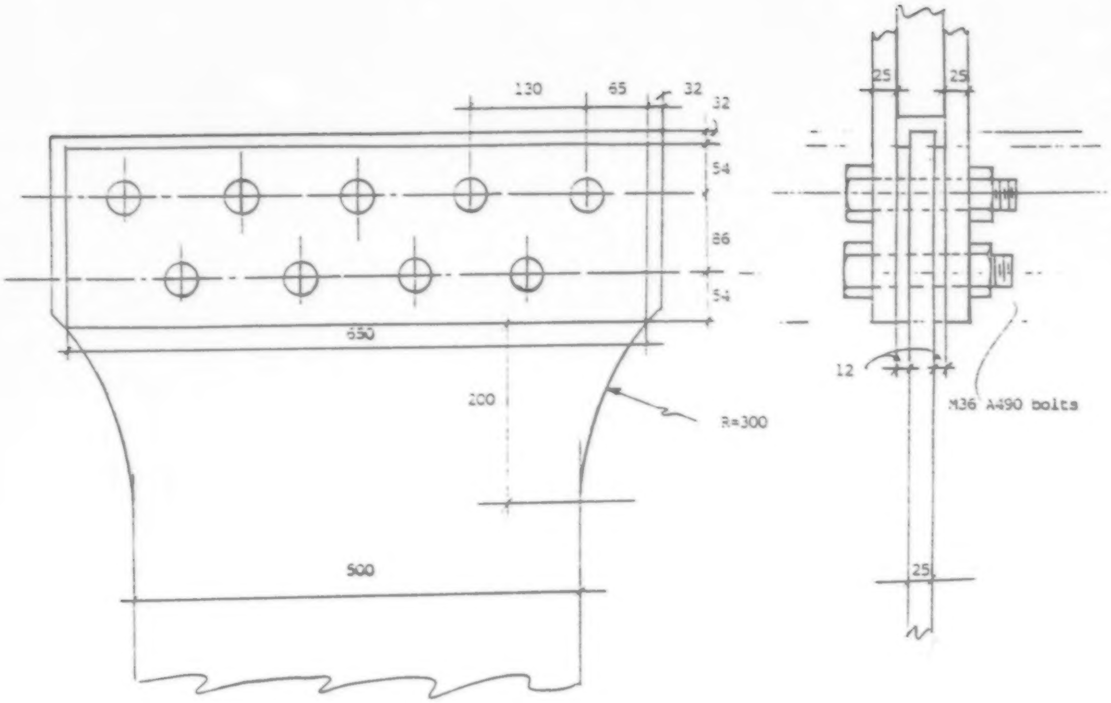
130
65
32
32
54
86
54
650
200
R=300
500
25
25
12
M36 A490 bolts
25

Fig. 29 Bolted end connection design.

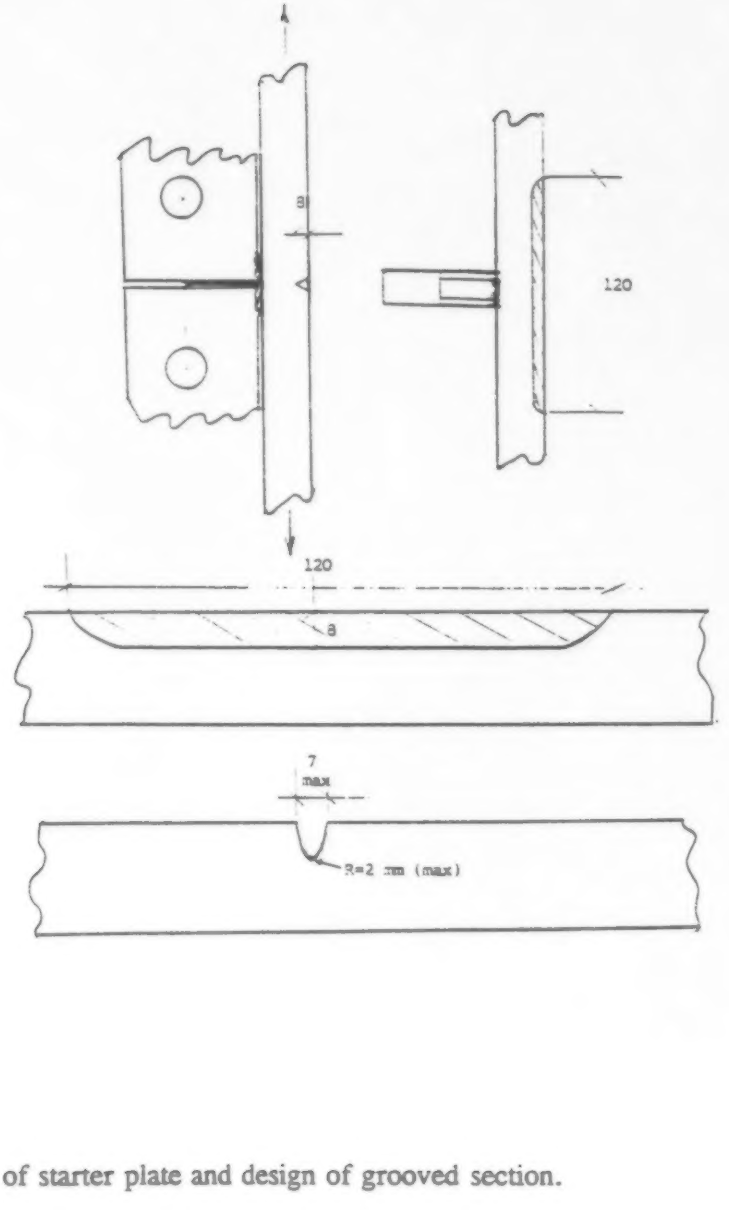
8
120
120
8
7
max
R=2 mm (max)

Fig. 30 Attachment of starter plate and design of grooved section.

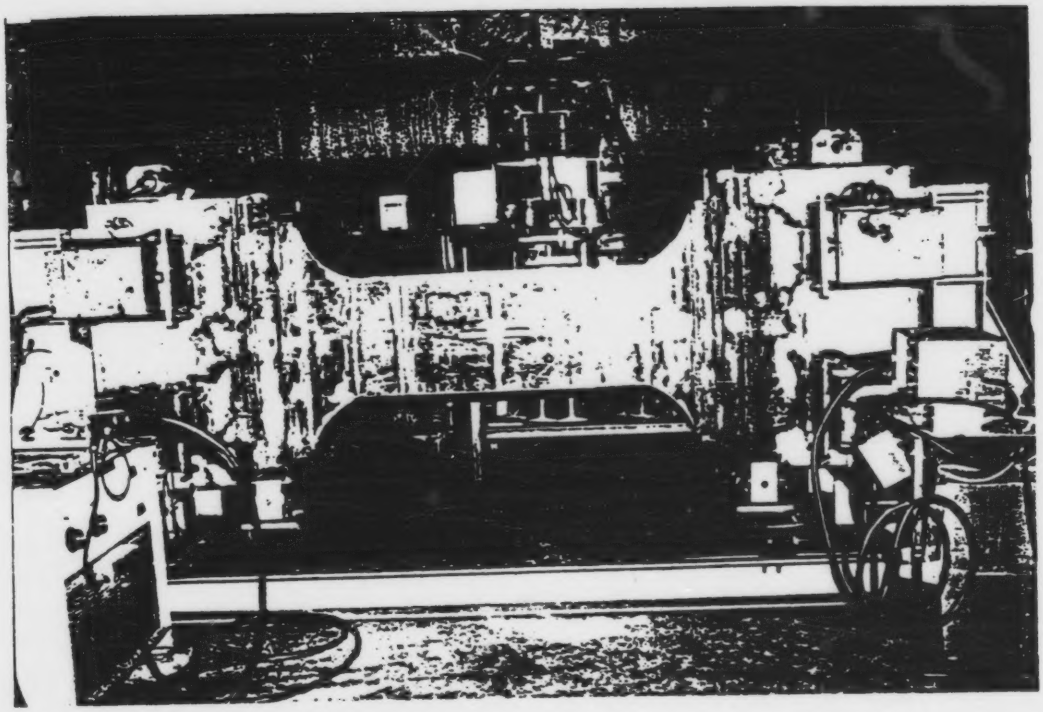

Fig. 31 The short crack arrest test plate attached to the loading end attachments.

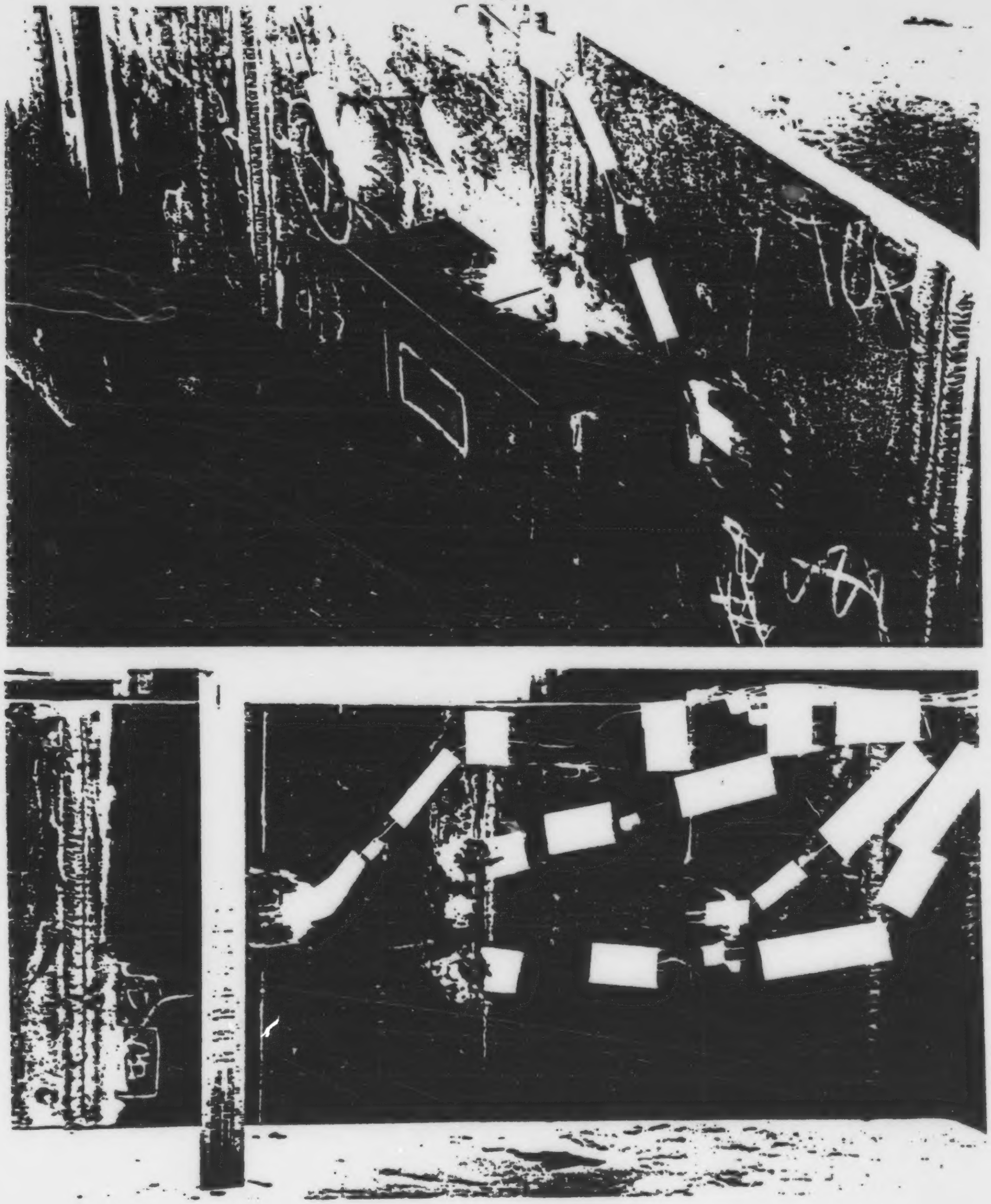

Fig. 32 Short crack arrest test specimen showing strain gauge and thermocouple locations as well as the crack starter and back groove locations.

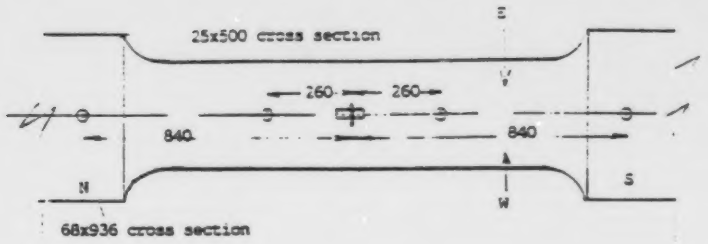
E
25x500 cross section
260
260
840
840
N
S
W
68x936 cross section

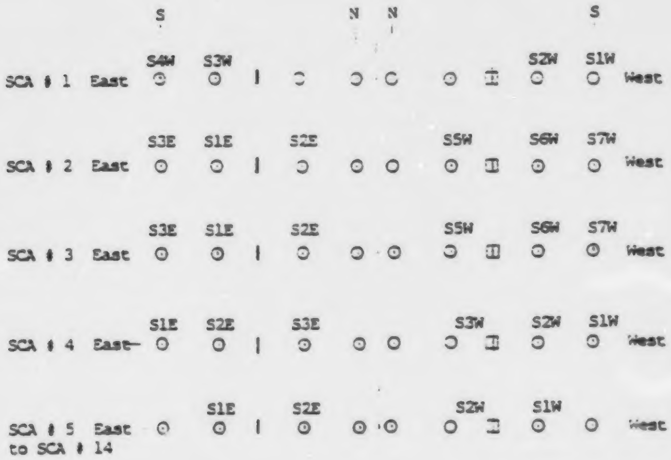
S
N
N
S
S4W
S3W
S2W
S1W
SCA # 1 East
West
S3E
S1E
S2E
S5W
S6W
S7W
SCA # 2 East
West
S3E
S1E
S2E
S5W
S6W
S7W
SCA # 3 East
West
S1E
S2E
S3E
S3W
S2W
S1W
SCA # 4 East
West
S1E
S2E
S2W
S1W
SCA # 5 East
to SCA # 14
West

Following are the additional gauges for SCA #s 5 to 14.

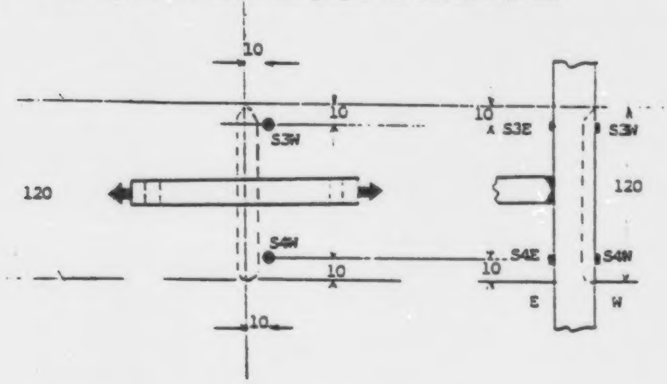
10
10
S3W
120
S4W
10
10
10
S3E
S3W
120
10
S4E
S4W
E
W

Fig. 33 Strain gauge locations and identification numbers.

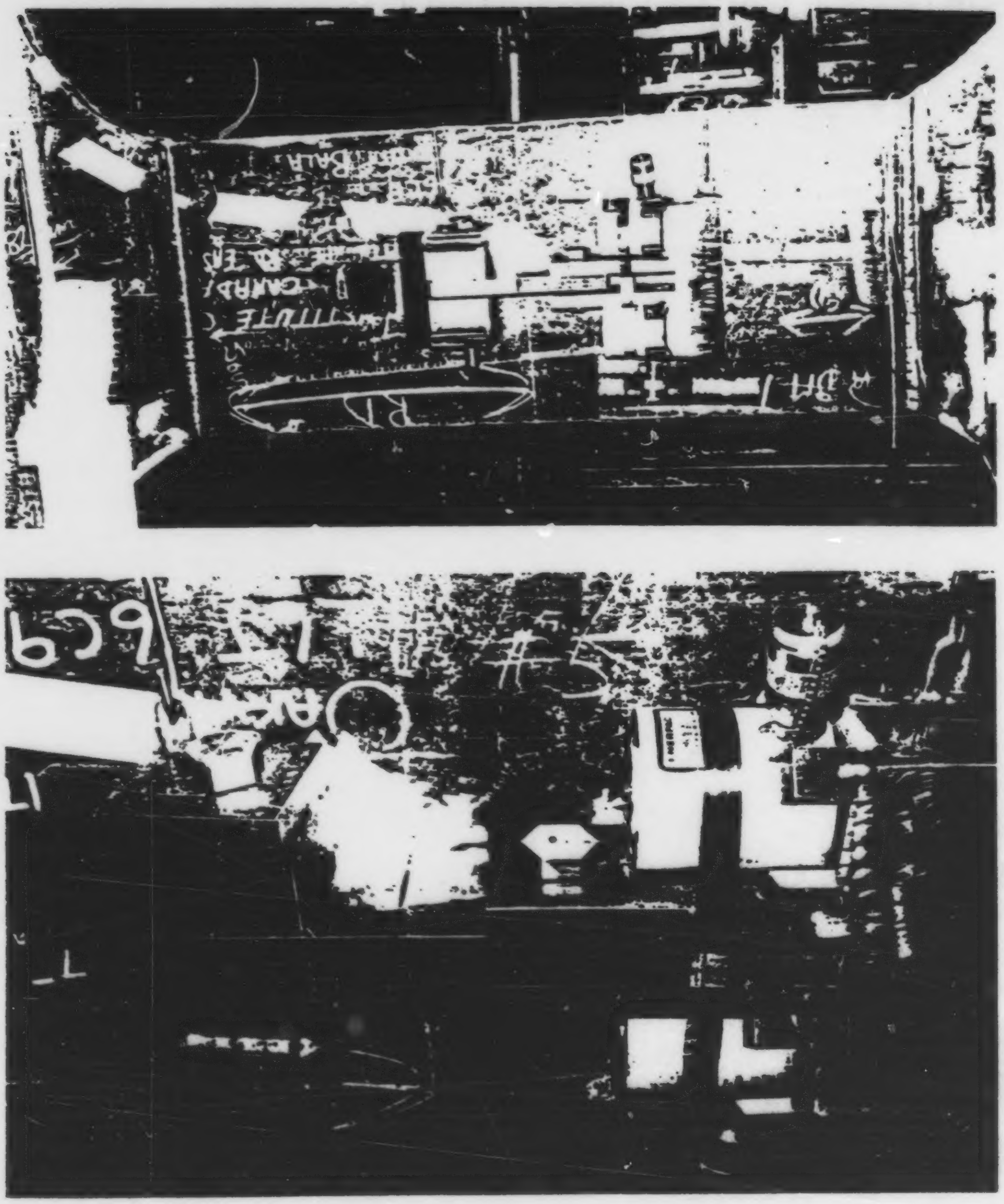

Fig. 34 Mounting of hydraulic loading unit on the crack starter.

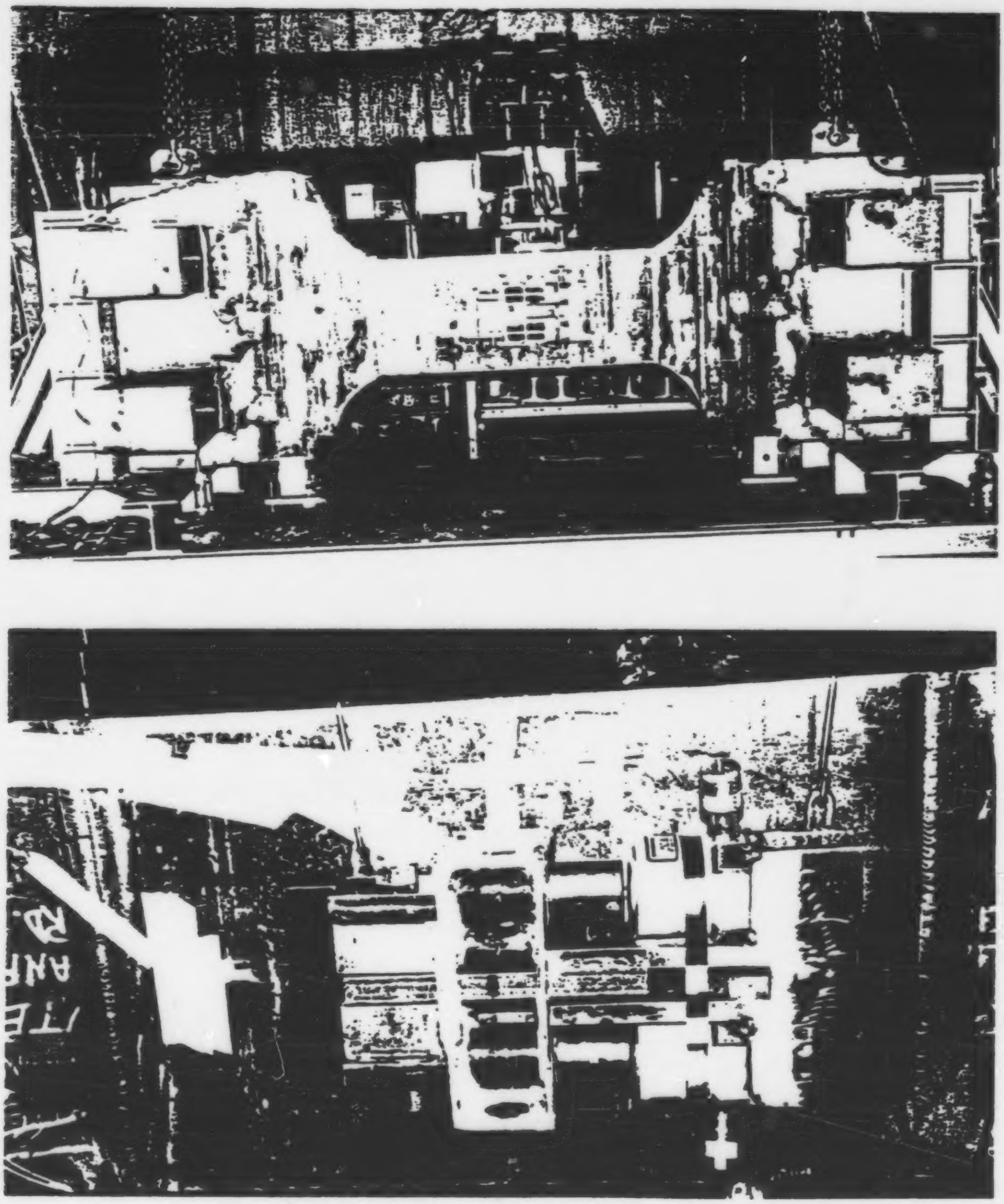

Fig. 35 Plywood cooling box supporting the columns of crack starter loading unit.

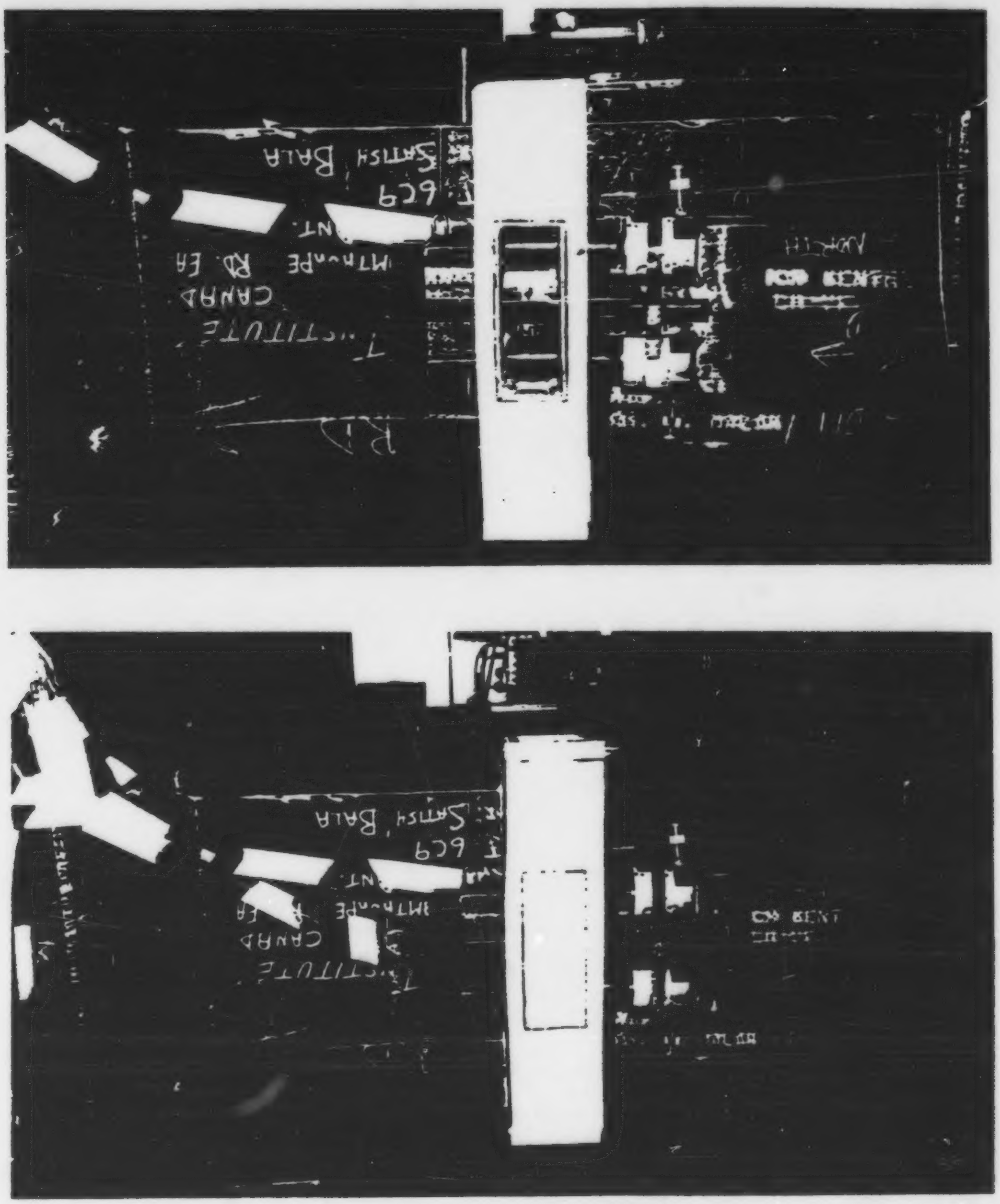

Fig. 36 Cooling box assembly made of plywood and styrofoam sheet.

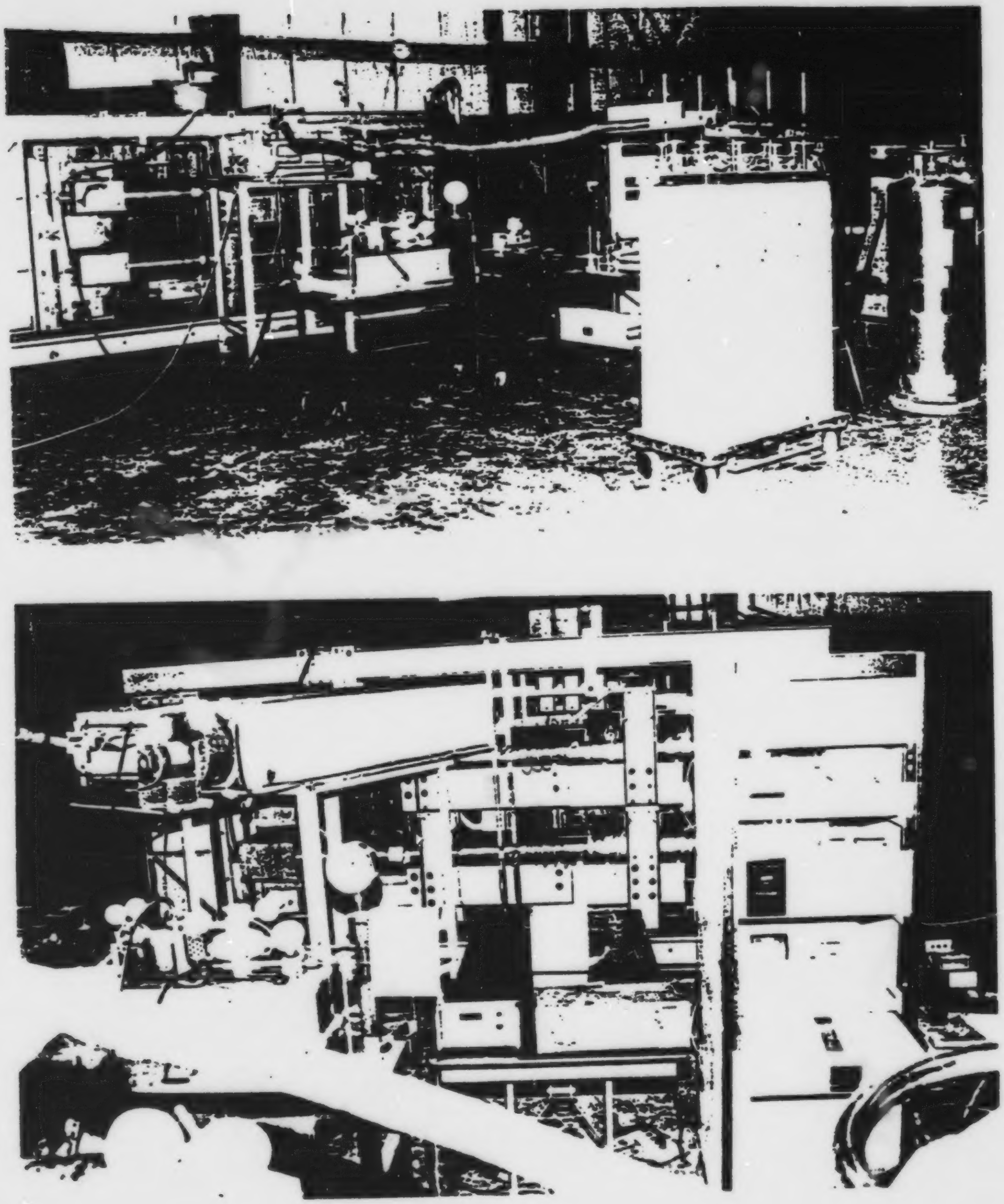

Fig. 37 Short crack arrest set up for testing in the wide plate test rig.

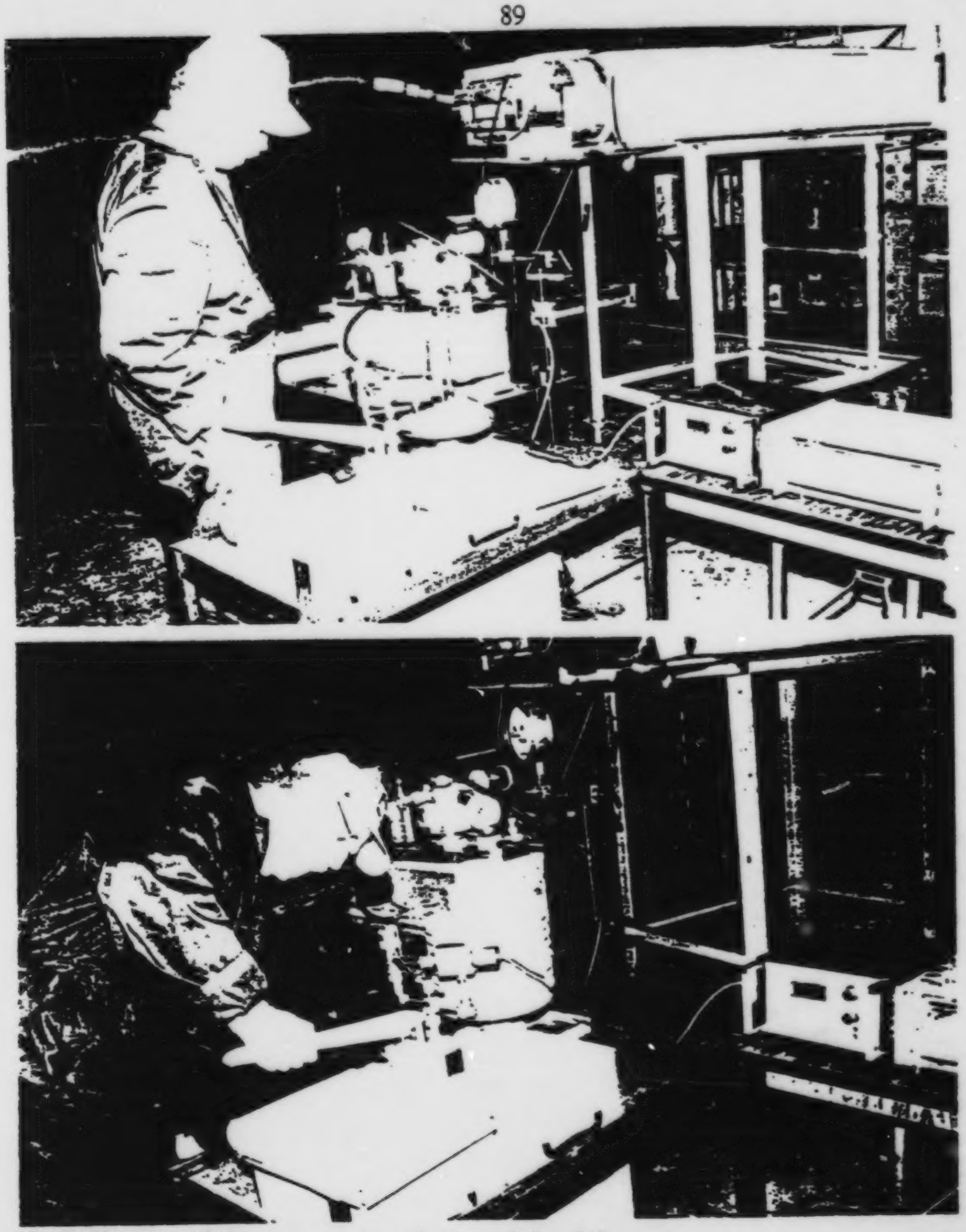

Fig. 38 Calibration of the pressure transducer and the dial gauge.

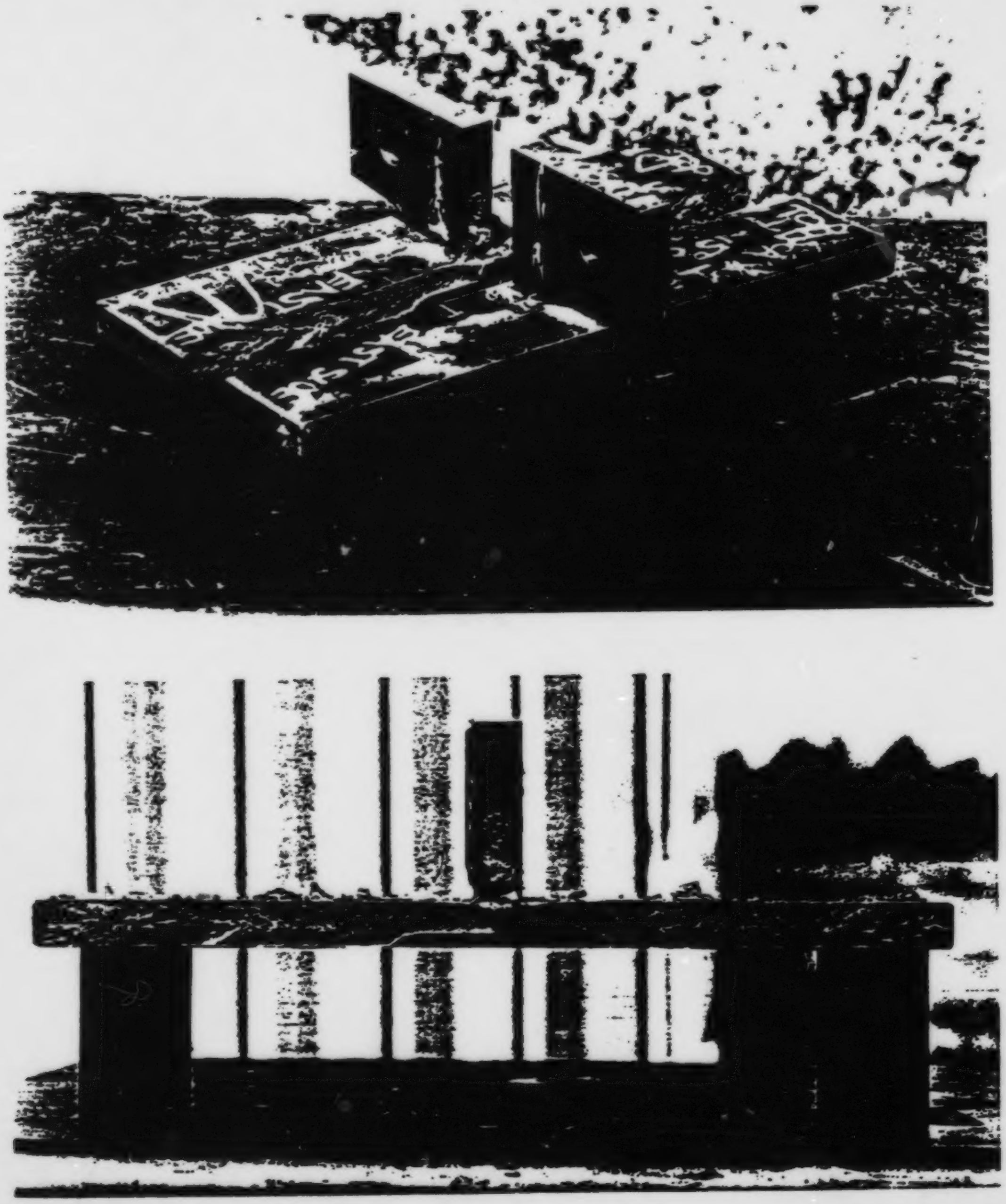

Fig. 39 Fracture surfaces of SCA Test 1.

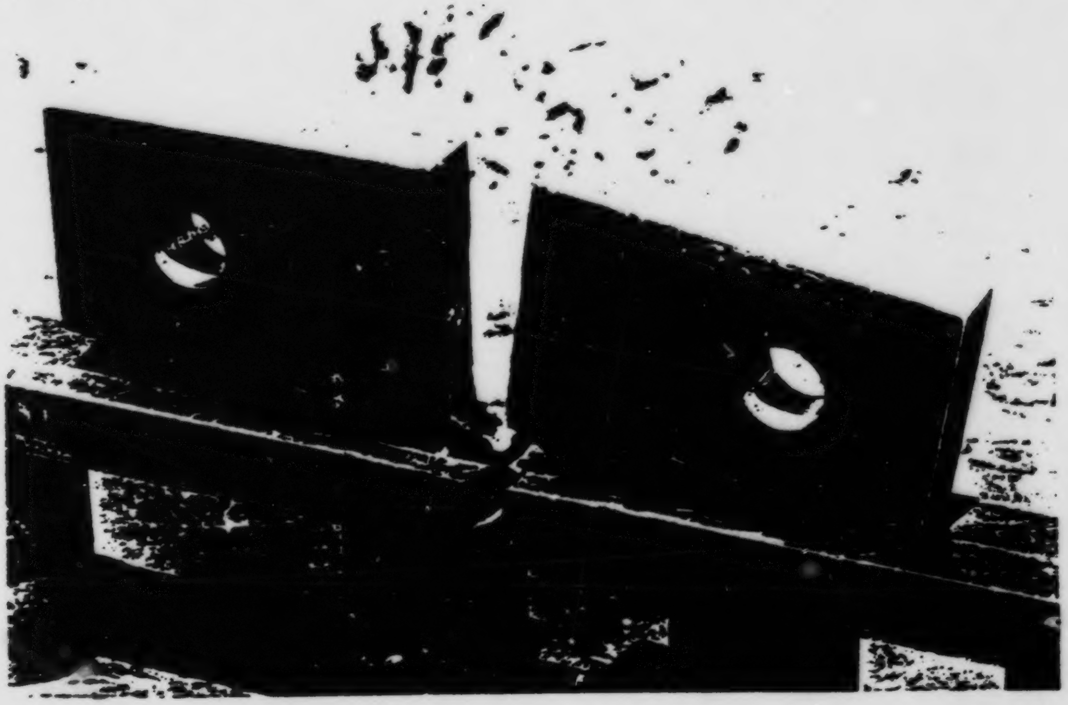

Fig. 40 Heat tinted fracture surfaces of SCA Test 2, showing the divergence and termination of the crack in the starter.

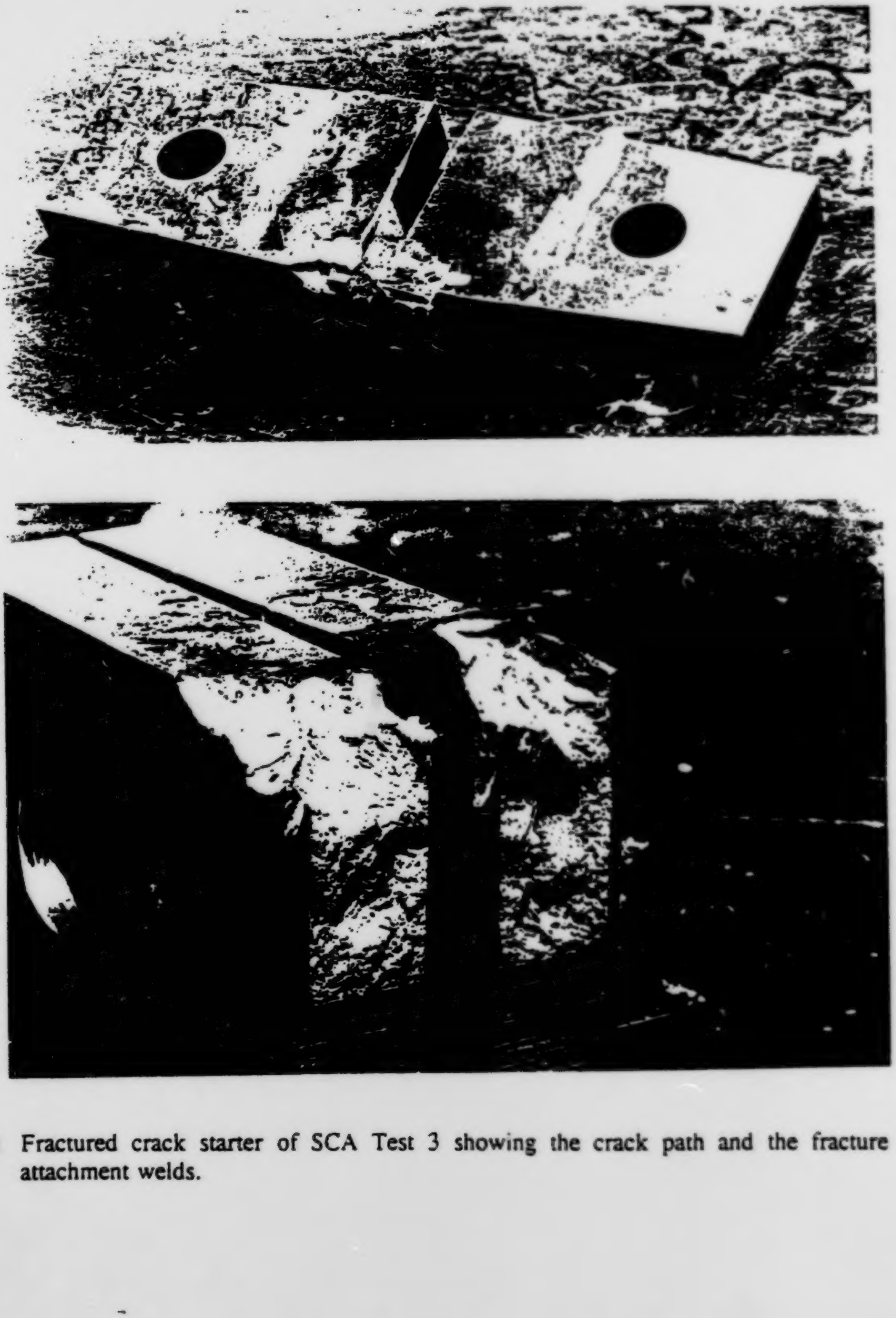

Fig. 41 Fractured crack starter of SCA Test 3 showing the crack path and the fracture of the attachment welds.

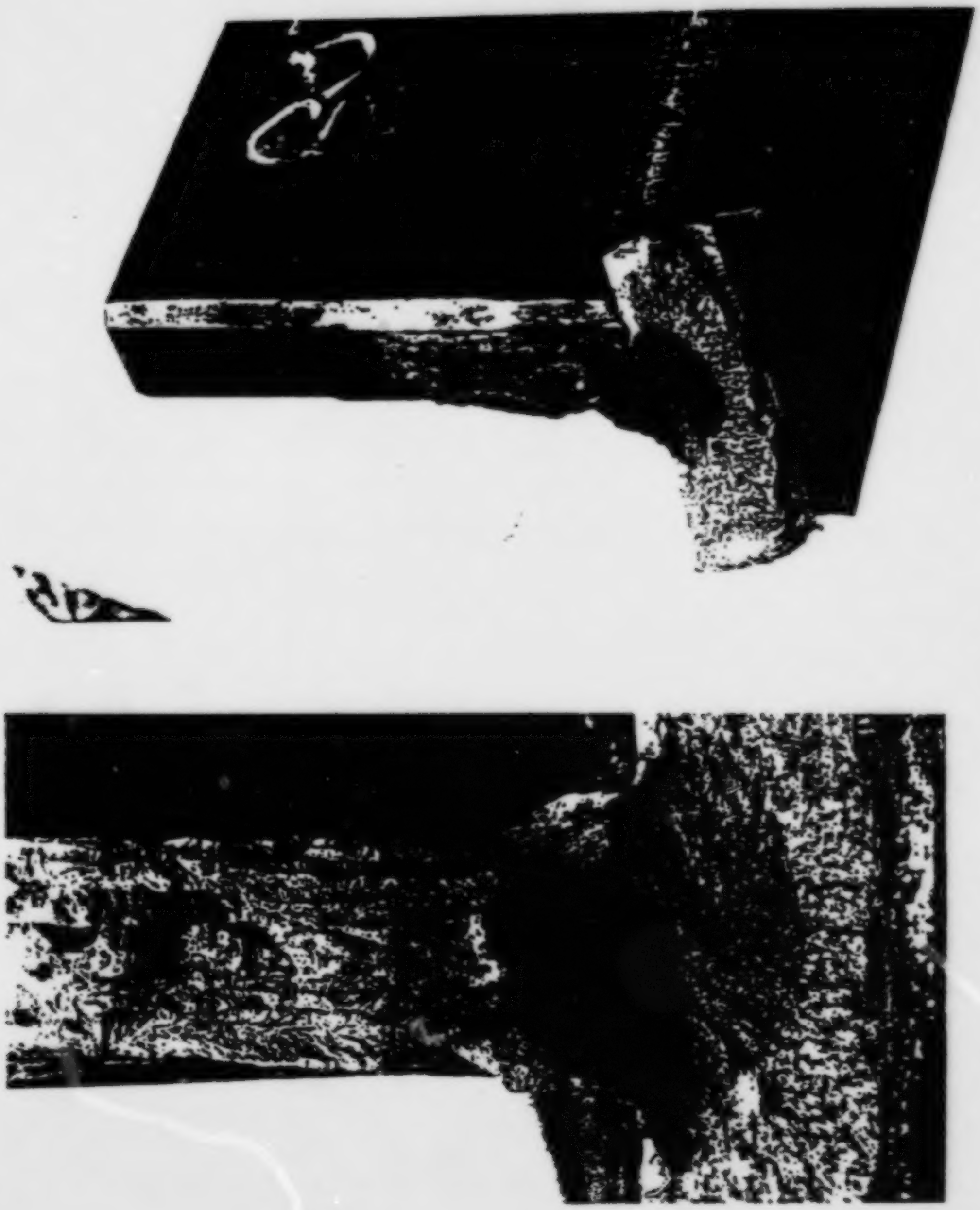

Fig. 42 Heat tinted fracture surfaces of the crack starter and the plate for SCA Test # 5, showing the divergence of the crack progression. Crack had progressed into the test plate thickness and arrested at a plane away from the back groove and the notch plane.

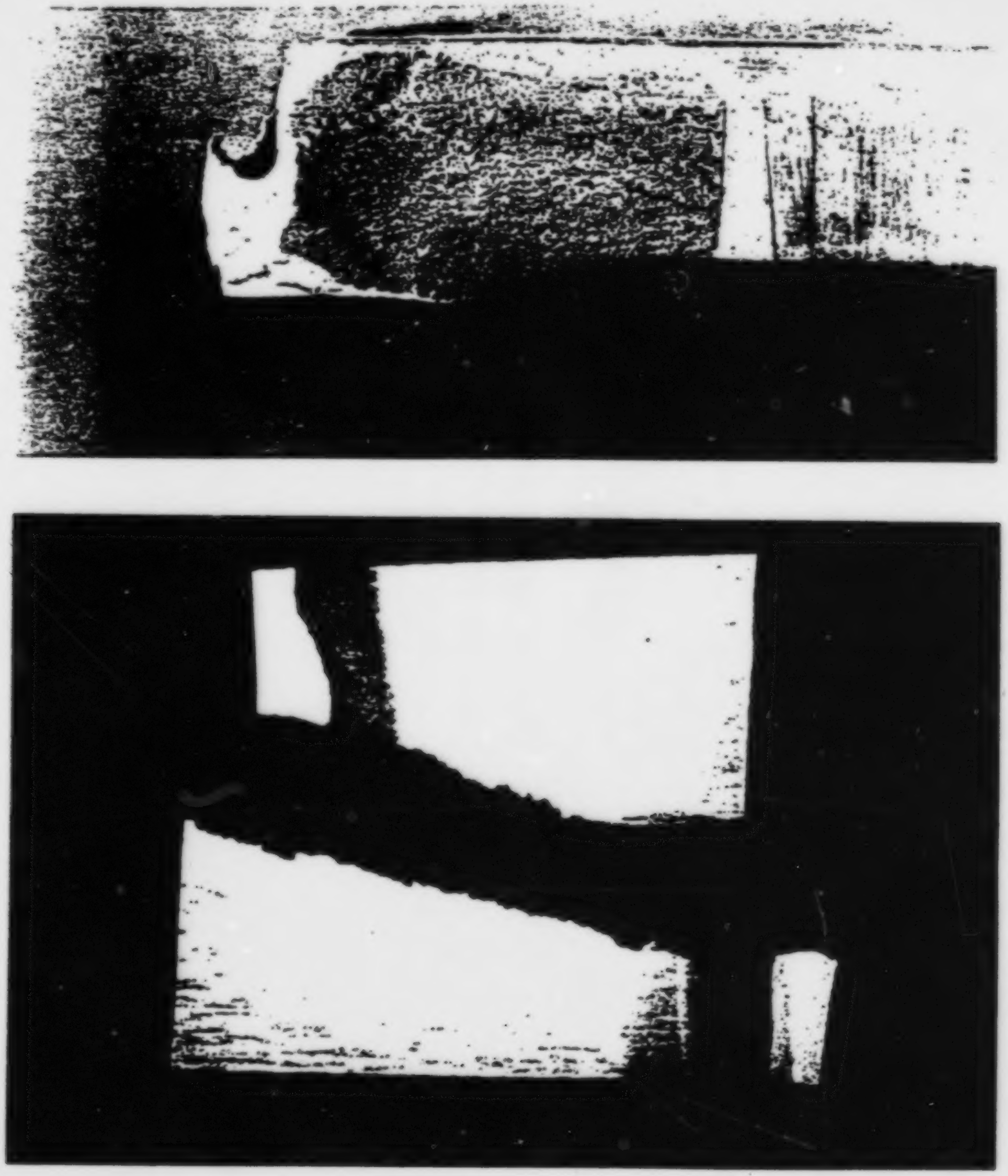

Fig. 43 Arrest of crack at the boundary between the HAZ of the attachment weld and the 1060 crack starter plate.

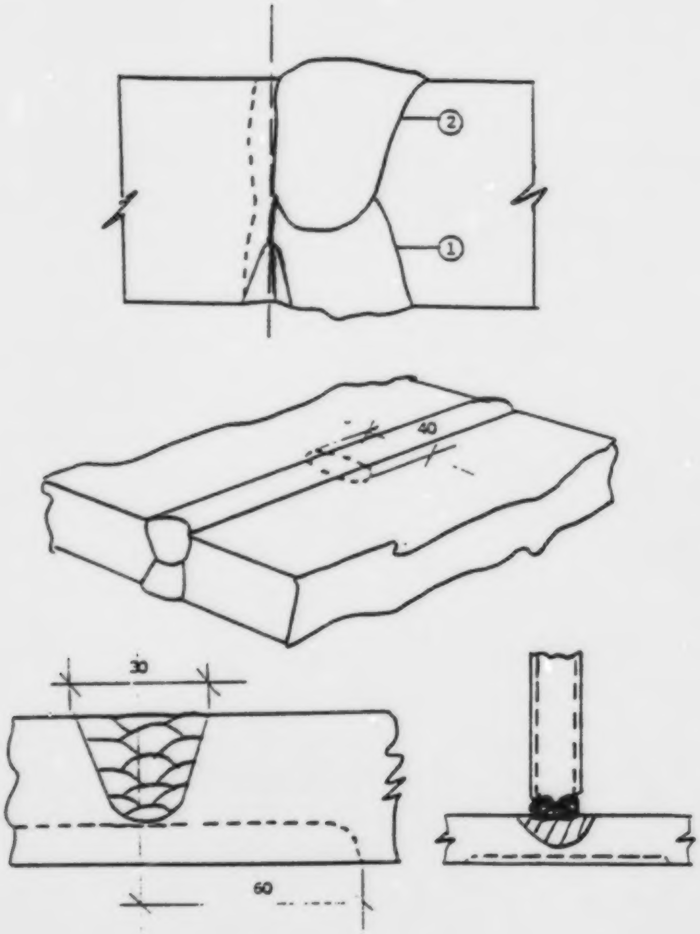

Fig. 44 Deep brittle weld for SCA Test 9 - HAZ 1.

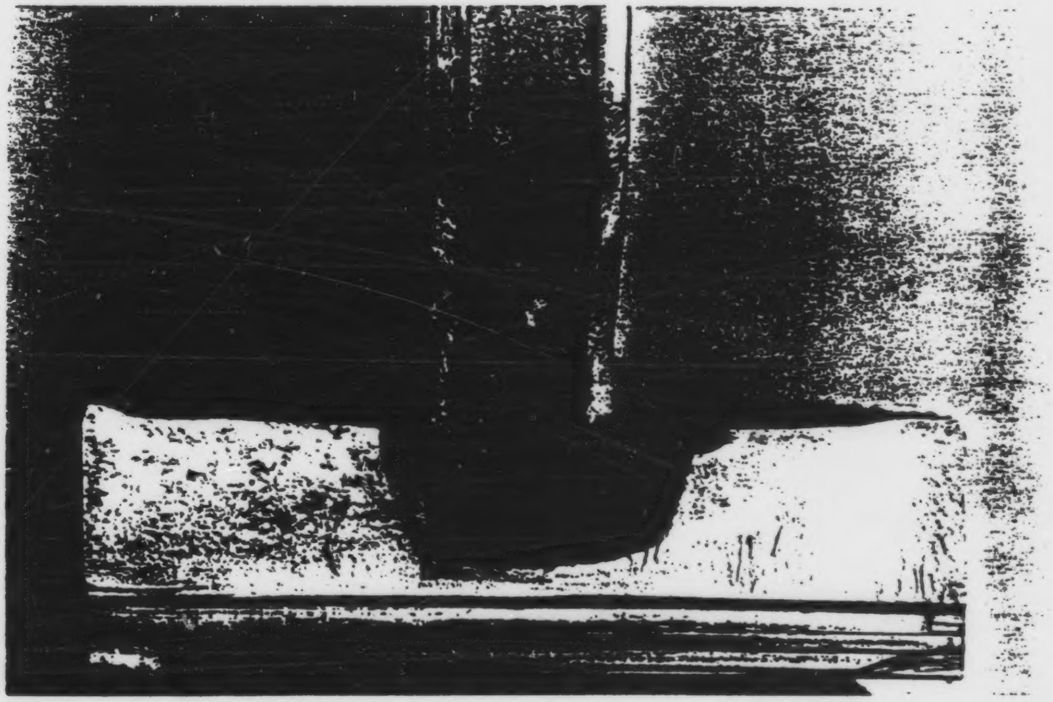

Fig. 45 Heat tinted fracture surfaces of the crack starter and the plate for SCA Test # 9 (HAZ 1) showing the crack progression in the notch plane into the brittle weld and the arrest in the deep puddle weld.

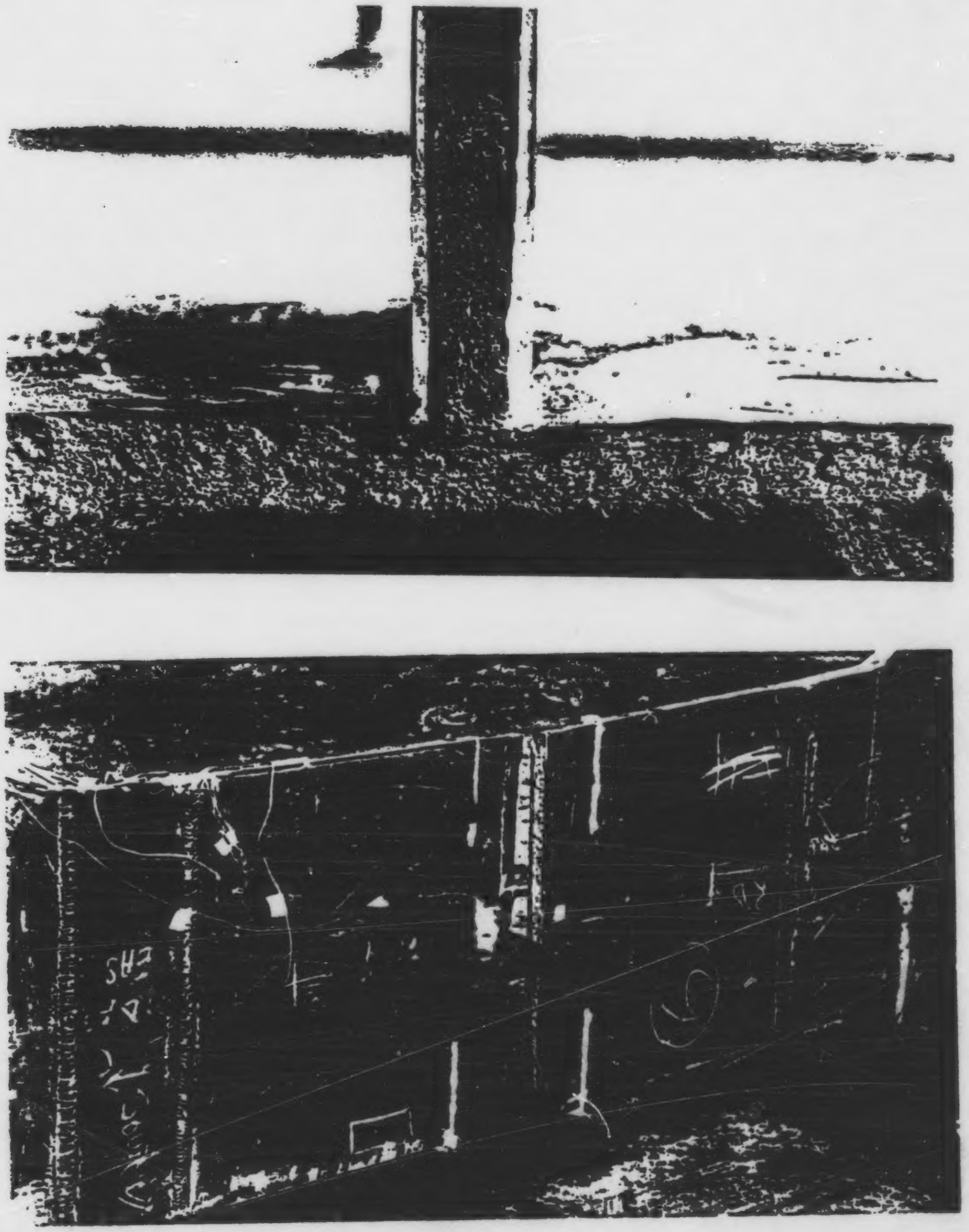

Fig. 46 Fracture surfaces of the SCA Test 10 showing the full fracture of the test plate (HAZ) in the notch and the back groove plane.

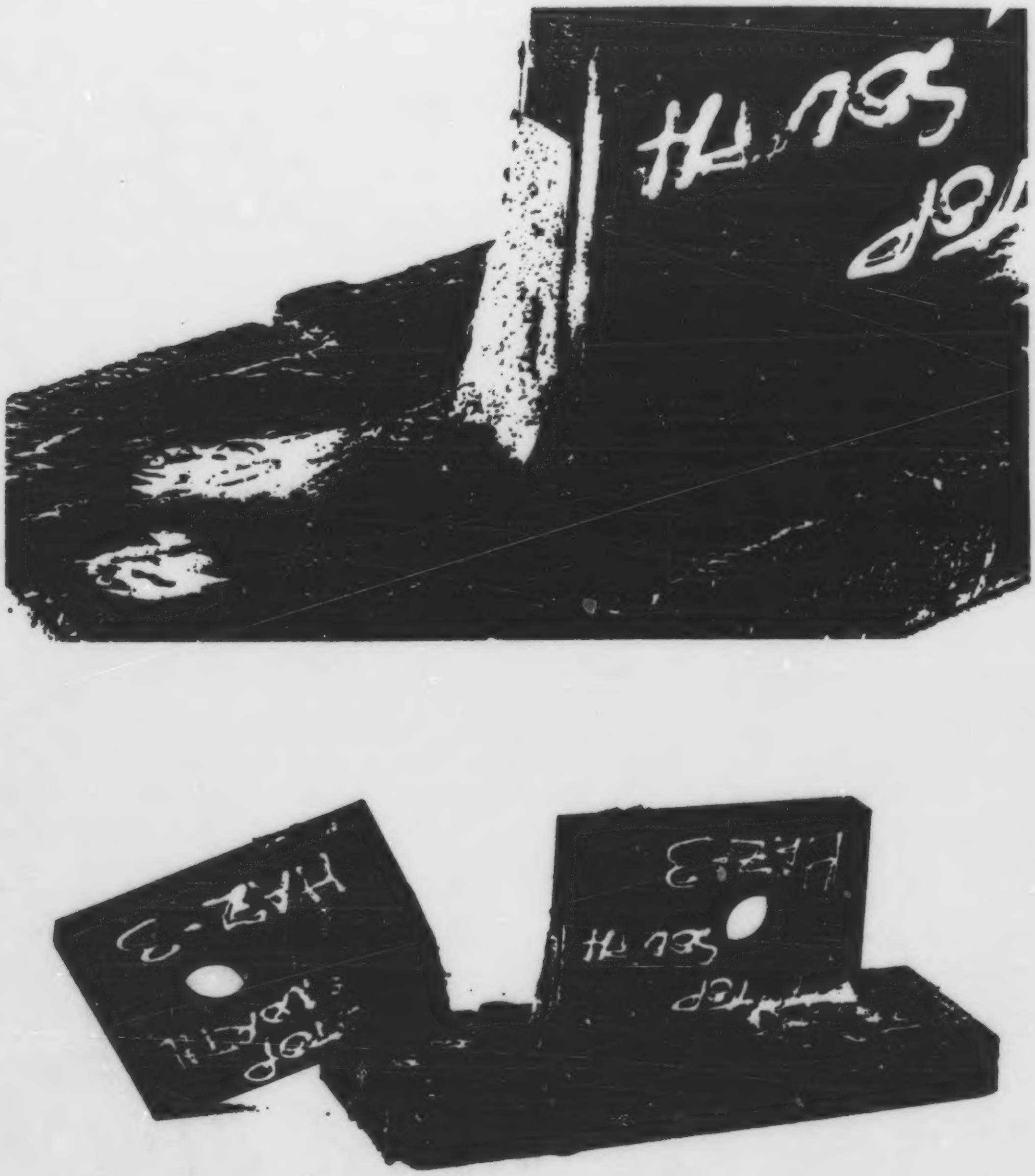

Fig. 47 Fracture surfaces of the crack starter of SCA 11 showing the divergence of the crack progression away from the notch plane into the double bevel (K-groove) weld metal of the test plate. Crack arrested in the weld metal.

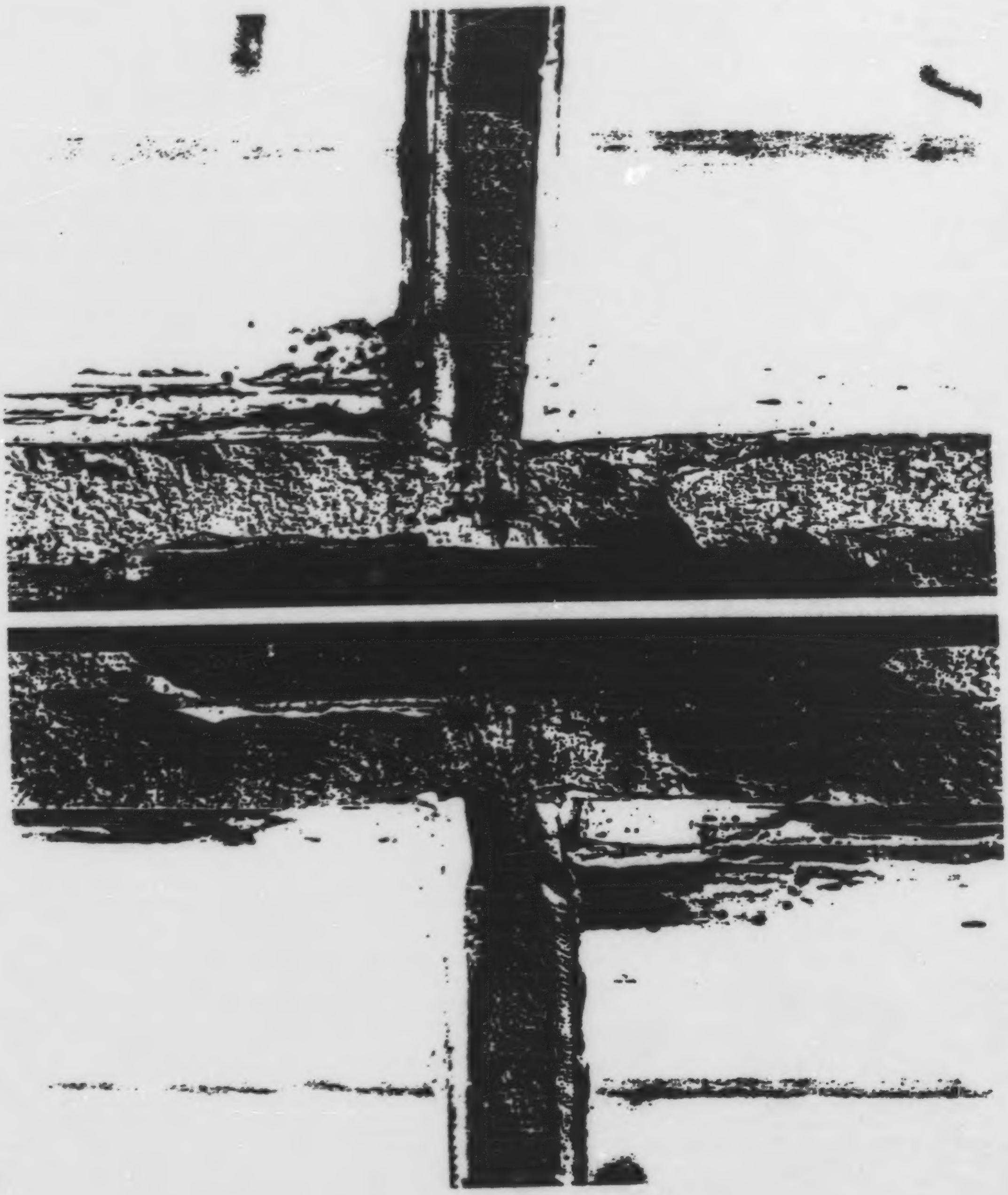

Fig. 48 Fractured SCA Test 12 specimen

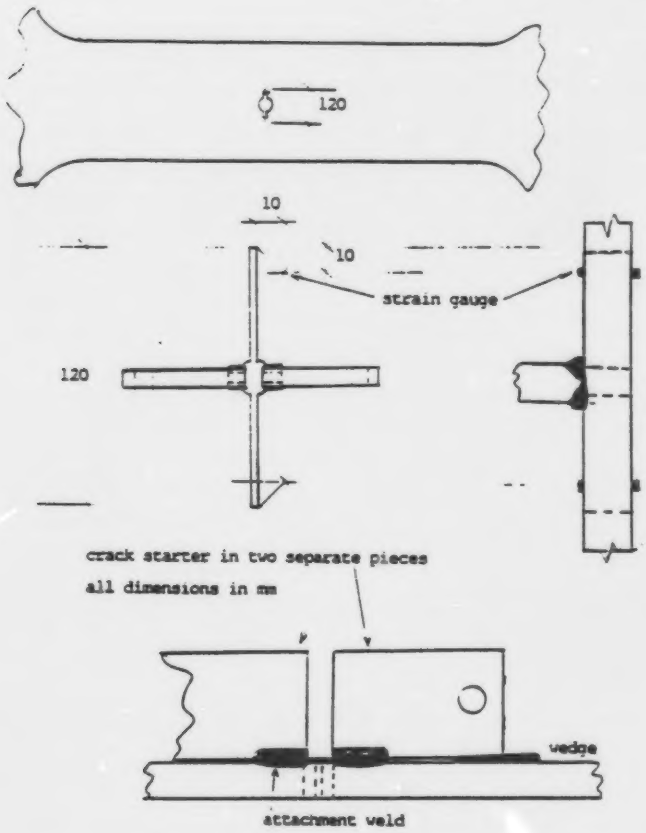
120
10
10
strain gauge
120
crack starter in two separate pieces
wedge
attachment weld

all dimensions in mm

Fig. 49 Experiment to determine effect of starter loads on stress in main test plate.

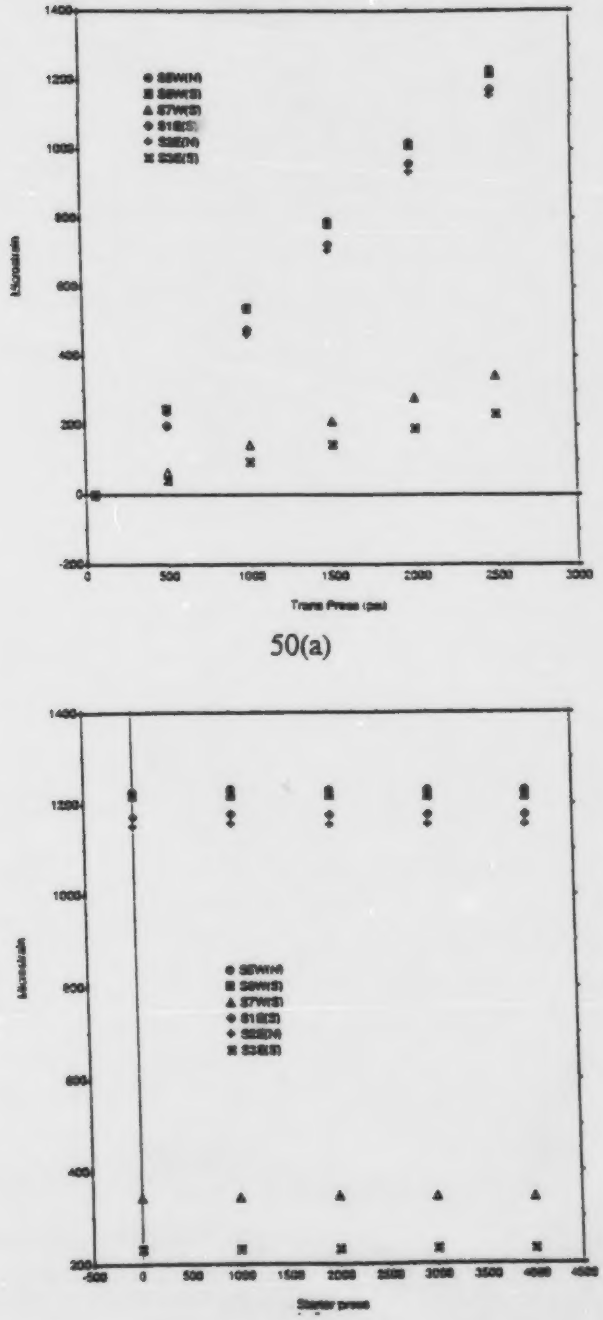

50(a)

50(b)

Fig. 50 Microstrain on main plate vs (a) jack pressure, and (b) crack starter pressure plots for SCA Test 2.

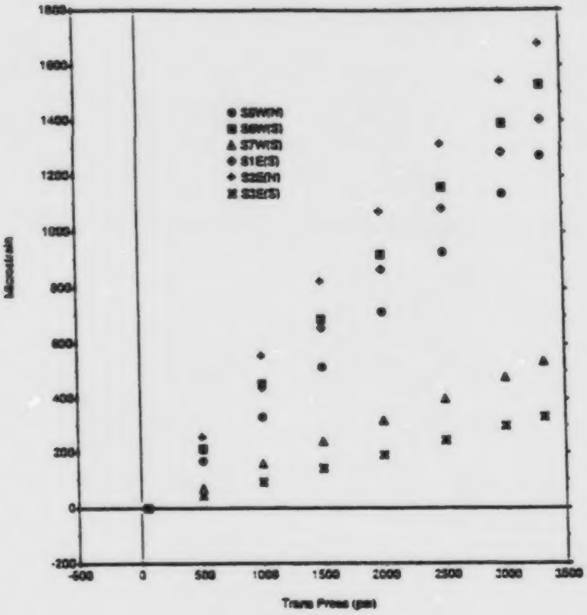

51(a)

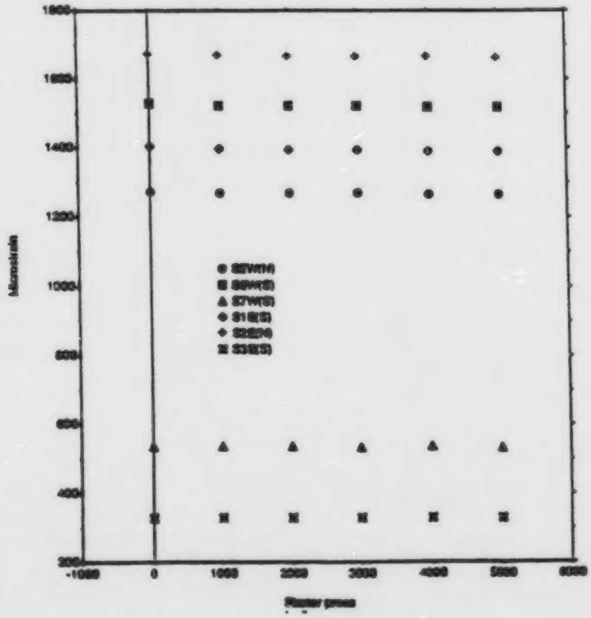

51(b)

Fig. 51 Microstrain on main plate vs (a) jack pressure, and (b) crack starter pressure plots for SCA Test 3.

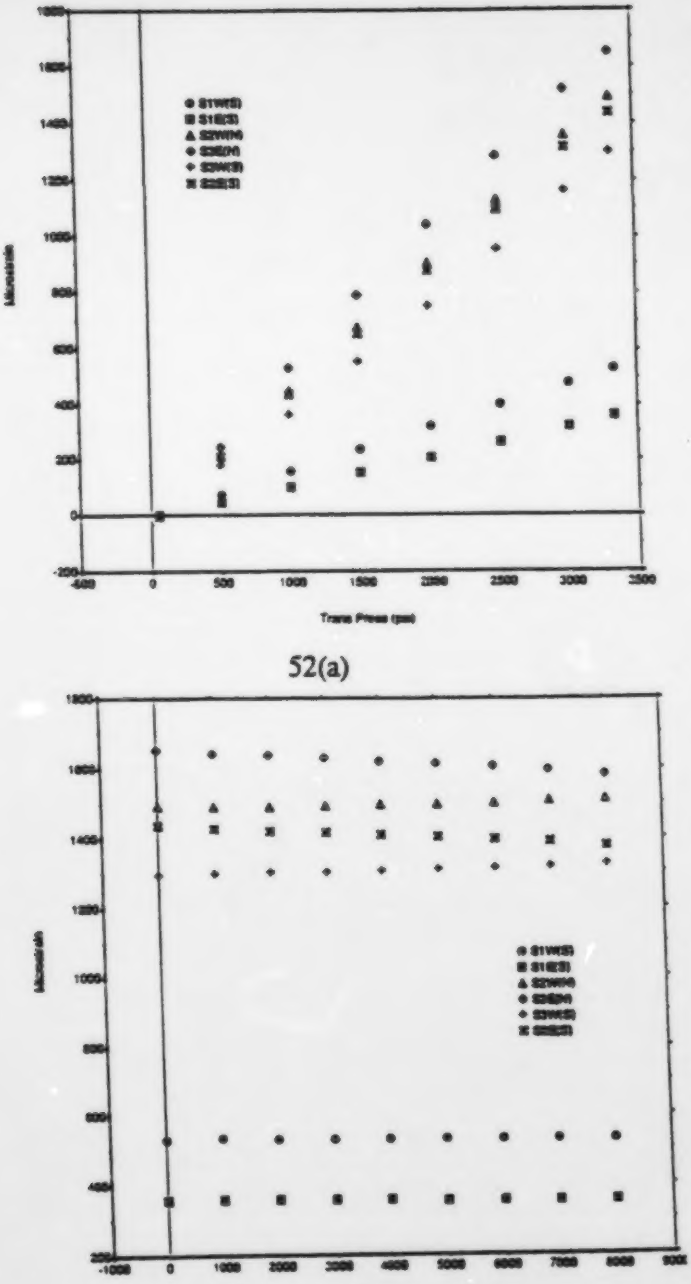

52(a)

52(b)

Fig. 52 Microstrain on main plate vs (a) jack pressure, and (b) crack starter pressure plots for SCA Test 4.

APPENDIX

WELDING DATA SHEET

WELDING INSTITUTE OF CANADA
INSTITUT DE SOUDAGE DU CANADA

CONTRACT NO. RC 391

DATA SHEET NO. DSCA # (iii)

PROCESS: SMAW & GMAW

MATERIALS: 1045 & LT60 Steel

POSITION: FLAT

PREHEAT:

Preheat Temp. 150 deg. C
Interpass Temp. 150 deg. C
Preheat Maintenance

FILLER METAL:

Classification
Trade Name Hobart ultra arc 350 and L-Tec ER 70-S2 (0.035" dia.)

FLUX:

Class:
Trade Name:

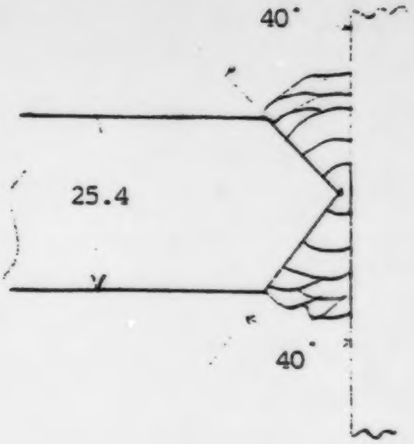

JOINT DETAILS

GAS COMPOSITION REQUIRED:

Shielding Gas	CO_2	At	40	CFH
Backing Gas		At		CFH
Trailing Gas		At		CFH

ELECTRICAL CHARACTERISTICS:

Power Source: Hobart Mega MIG RUS 650
Current Type: Powcon 300 SM, DC
Polarity: +ve

SPECIAL NOTES

T	WELD SEQUENCE			ELECTRODE		WELDING VARIABLES					
	SIDE	LAYER	PASS	TYPE	SIZE mm	AMPS	VOLTS	E.S.O.	SPEED mmps	WFS ipm	HEAT INPUT
	1&2	all	all			120	20				

ISSUED BY:	**DATE:**	**LAB TECHNOLOGIST:**

WELDING DATA SHEET

WELDING INSTITUTE OF CANADA
INSTITUT DE SOUDAGE DU CANADA

CONTRACT NO. RC 391

DATA SHEET NO. DSCA # 0 & 1

PROCESS: SMAW

MATERIALS: 1045 & LT60 Steel

POSITION: FLAT

PREHEAT:

Preheat Temp. 150 deg. C
Interpass Temp. 150 deg. C
Preheat Maintenance 150 deg. C

FILLER METAL:

Classification
Trade Name Hobart Smootharc 320 (3.2 mm)

FLUX:

Class:
Trade Name:

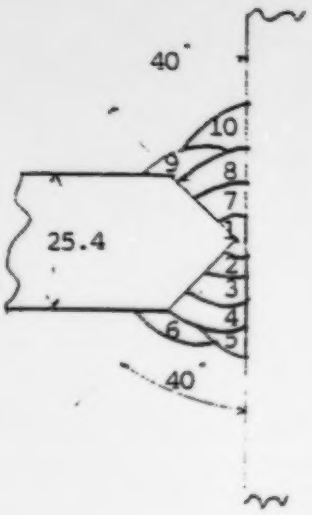

JOINT DETAILS

GAS COMPOSITION REQUIRED:

Shielding Gas	At	CFH
Backing Gas	At	CFH
Trailing Gas	At	CFH

ELECTRICAL CHARACTERISTICS:

Power Source: Miller 600 SS Gold Star
Current Type: DC
Polarity: +ve

SPECIAL NOTES

T	WELD SEQUENCE			ELECTRODE		WELDING VARIABLES					
	SIDE	LAYER	PASS	TYPE	SIZE mm	AMPS	VOLTS	E.S.O.	SPEED mmps	WFS ipm	HEAT INPUT
	1&2	all	all	320	3.2	120–140	24				

ISSUED BY:

DATE:

LAB TECHNOLOGIST:

WELDING DATA SHEET

WELDING INSTITUTE OF CANADA
INSTITUT DE SOUDAGE DU CANADA

CONTRACT NO. RC 391

DATA SHEET NO. DSCA 2 to 14

PROCESS: SMAW

MATERIALS: 1045, LT60, DH 36 & AAR 335-B

POSITION: FLAT

PREHEAT:

Preheat Temp. 320 deg. C
Interpass Temp. 320 deg. C
Preheat Maintenance 320 deg. C

FILLER METAL:

Classification
Trade Name Hobart Smootharc 400 (3.2 mm)

FLUX:

Class:
Trade Name:

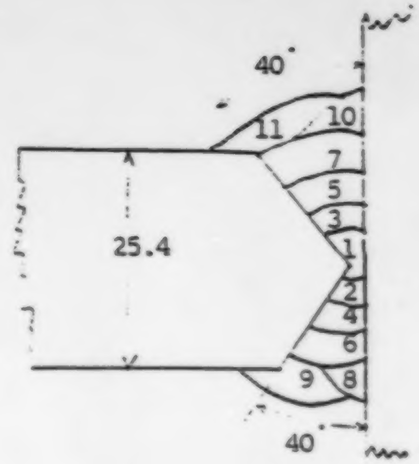

JOINT DETAILS

GAS COMPOSITION REQUIRED:

Shielding Gas	At	CFH
Backing Gas	At	CFH
Trailing Gas	At	CFH

ELECTRICAL CHARACTERISTICS:

Power Source: Miller 600 SS Gold Star
Current Type: DC
Polarity: +ve

SPECIAL NOTES

T	WELD SEQUENCE			ELECTRODE		WELDING VARIABLES					
	SIDE	LAYER	PASS	TYPE	SIZE mm	AMPS	VOLTS	E.S.O.	SPEED mmps	WFS ipm	HEAT INPUT
	1 & 2	all	all	400	3.2	110	24-28				

ISSUED BY:	**DATE:**	**LAB TECHNOLOGIST:**

WELDING DATA SHEET

WELDING INSTITUTE OF CANADA
INSTITUT DE SOUDAGE DU CANADA

CONTRACT NO. RC 391

DATA SHEET NO. DSCA # 16

PROCESS: SMAW

MATERIALS: 1060 and LT60

POSITION: FLAT

PREHEAT:

Preheat Temp. 320 deg. C
Interpass Temp. 320 deg. C
Preheat Maintenance 320 deg. C

FILLER METAL:

Classification
Trade Name Hobart Smootharc 400 (3.2 mm)

FLUX:

Class:
Trade Name:

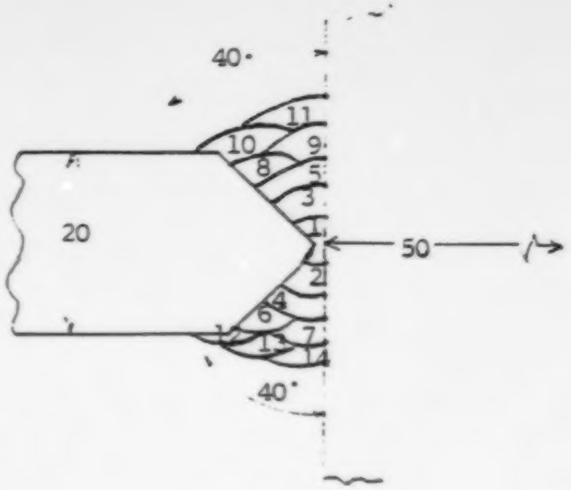

JOINT DETAILS

GAS COMPOSITION REQUIRED:

Shielding Gas At CFH
Backing Gas At CFH
Trailing Gas At CFH

ELECTRICAL CHARACTERISTICS:

Power Source: Miller 600 Gold Star
Current Type: DC
Polarity: +ve

SPECIAL NOTES

T	WELD SEQUENCE			ELECTRODE		WELDING VARIABLES					
	SIDE	LAYER	PASS	TYPE	SIZE mm	AMPS	VOLTS	E.S.O.	SPEED mmps	WFS ipm	HEAT INPUT
	1 & 2	all	all	400	3.2	110	28-30				

ISSUED BY: **DATE:** **LAB TECHNOLOGIST:**

WELDING DATA SHEET

WELDING INSTITUTE OF CANADA
INSTITUT DE SOUDAGE DU CANADA

CONTRACT NO. RC 391

DATA SHEET NO. SCA # 1

PROCESS: FCAW

MATERIALS: DH 36 to DH 36 (both 25.4 mm thick)

POSITION: Vertical up

PREHEAT:

Preheat Temp. 150 deg. C
Interpass Temp. 150 deg. C
Preheat Maintenance 150 deg. C

FILLER METAL:

Classification E480 1T-9CH (0.045" dia.)
Trade Name LA T-91

FLUX:

Class:
Trade Name:

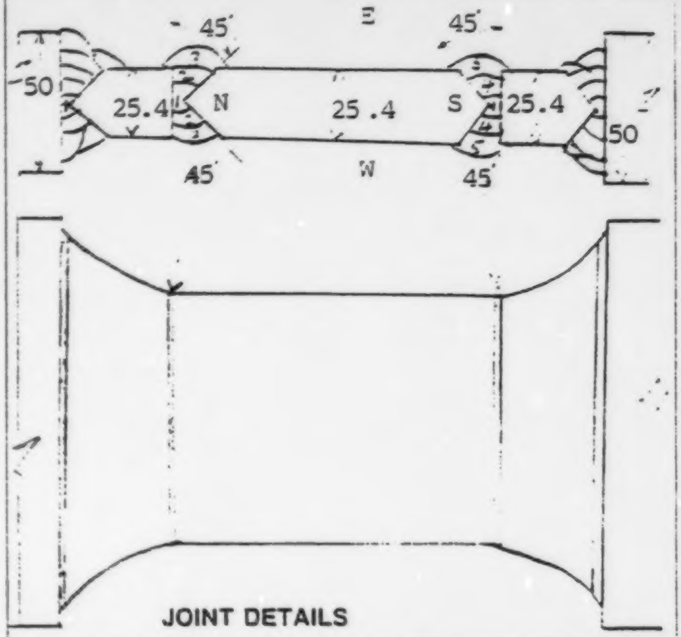

JOINT DETAILS

GAS COMPOSITION REQUIRED:

Shielding Gas Blue Shield At 40 CFH
Backing Gas #8 At CFH
Trailing Gas At CFH

ELECTRICAL CHARACTERISTICS:

Power Source: Hobart Mega MIG RUS 650
Current Type: Powcon 300 SM , DC
Polarity: +ve

SPECIAL NOTES

	WELD SEQUENCE			ELECTRODE		WELDING VARIABLES					
T	SIDE	LAYER	PASS	TYPE	SIZE mm	AMPS	VOLTS	E.S.O.	SPEED mmps	WFS ipm	HEAT INPUT
	East		1,2,4		1.2	200	22	13	5	190	
			3,5		1.2	170	20	13	4.3	180	
	West		1,2,4		1.2	190	21	13	5	180	
			3,5		1.2	170	20	13	4.3	170	

ISSUED BY:	DATE:	LAB TECHNOLOGIST:

WELDING DATA SHEET

WELDING INSTITUTE OF CANADA
INSTITUT DE SOUDAGE DU CANADA

CONTRACT NO. RC 391

DATA SHEET NO. SCA # 1

PROCESS: FCAW

MATERIALS: DH 36, 25.4 mm thick to 50 mm
LT60 Steel

POSITION: Vertical up

PREHEAT:

Preheat Temp. 150 deg. C
Interpass Temp. 150 deg. C
Preheat Maintenance 150 deg. C

FILLER METAL:

Classification E480 1T-9CH (0.045" dia.)
Trade Name LA T-91

FLUX:

Class:
Trade Name:

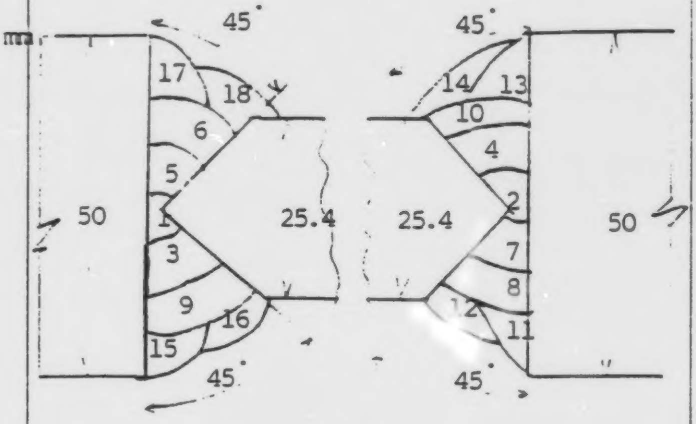

JOINT DETAILS

GAS COMPOSITION REQUIRED:

Shielding Gas Blue Shield At 40 CFH
Backing Gas At CFH
Trailing Gas At CFH

ELECTRICAL CHARACTERISTICS:

Power Source: Hobart Mega MIG RUS 650
Current Type: Powcon 300 SM, DC
Polarity: +ve

SPECIAL NOTES

To prevent distortion strong backs were used.

T	WELD SEQUENCE			ELECTRODE		WELDING VARIABLES					
	SIDE	LAYER	PASS	TYPE	SIZE mm	AMPS	VOLTS	E.S.O.	SPEED mmps	WFS ipm	HEAT INPUT
			1-4		1.2	204	22	13	5	200	
			5-8		1.2	190	23	13	4.3	190	
			9,10		1.2	195	23	13	4.3	190	
			11-14		1.2	170	22	13	4.3	180	
			15-18		1.2	170	22	13	4.3	180	

ISSUED BY:

DATE: Mar. 20, 1990

LAB TECHNOLOGIST: Brian Spahn

WELDING DATA SHEET

WELDING INSTITUTE OF CANADA
INSTITUT DE SOUDAGE DU CANADA

CONTRACT NO. RC 391

DATA SHEET NO. SCA # 2

PROCESS: GMAW

MATERIALS: DH 36 , Loading end attachment

POSITION: Vertical Up

PREHEAT:

Preheat Temp. 150 deg. C
Interpass Temp. 150 deg. C
Preheat Maintenance 150 deg. C

FILLER METAL:

Classification E480 1T-9CH (0.045" dia)
Trade Name LA T-91

FLUX:

Class:
Trade Name:

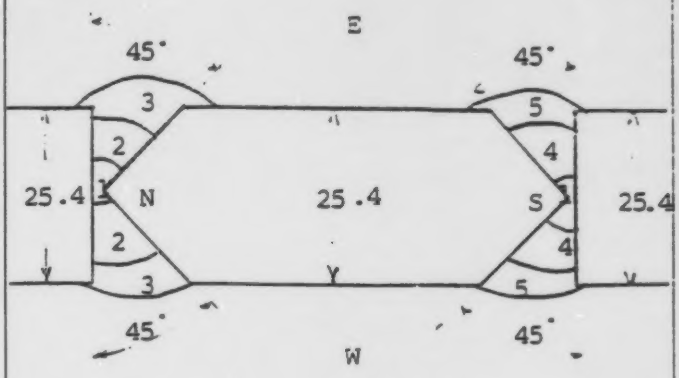

JOINT DETAILS

GAS COMPOSITION REQUIRED:

Shielding Gas Blue Shield # 8 At 40 CFH
Backing Gas At CFH
Trailing Gas At CFH

ELECTRICAL CHARACTERISTICS:

Power Source: Hobart Mega MIG RUS 650
Current Type: Powcon 300 SM, DC
Polarity: +ve

SPECIAL NOTES

T	WELD SEQUENCE			ELECTRODE		WELDING VARIABLES					
	SIDE	LAYER	PASS	TYPE	SIZE mm	AMPS	VOLTS	E.S.O.	SPEED mmps	WFS ipm	HEAT INPUT
	East		1,2,4		1.2	200	22	13	5	190	
			3,5		1.2	170	20	13	4.3	180	
	West		1,2,4		1.2	190	21	13	5	180	
			3,5		1.2	170	20	13	4.3	170	

ISSUED BY:

DATE:

LAB TECHNOLOGIST: Brian Spahn

WELDING DATA SHEET

WELDING INSTITUTE OF CANADA
INSTITUT DE SOUDAGE DU CANADA

CONTRACT NO. 3C 391

DATA SHEET NO. SCA # 2

PROCESS: SMAW

MATERIALS: 1045 & DH 36 Steels
Crack starter attachment

POSITION: FLAT

PREHEAT:

Preheat Temp. 150 deg. C
Interpass Temp. 150 deg. C
Preheat Maintenance 150 deg. C

FILLER METAL:

Classification
Trade Name Hobart Smootharc 320 (3.2 mm)

FLUX:

Class:
Trade Name:

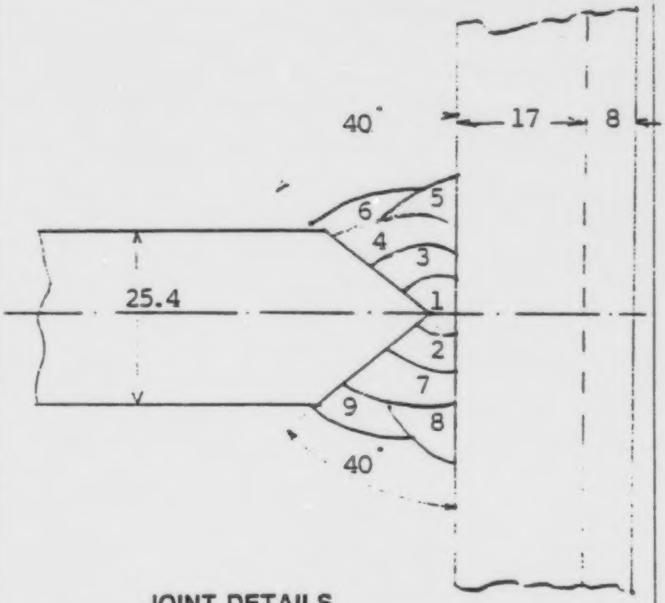

JOINT DETAILS

GAS COMPOSITION REQUIRED:

Shielding Gas At CFH
Backing Gas At CFH
Trailing Gas At CFH

ELECTRICAL CHARACTERISTICS:

Power Source: Miller Gold Star 600 SS
Current Type: DC
Polarity: +ve

SPECIAL NOTES

T	WELD SEQUENCE			ELECTRODE		WELDING VARIABLES					
	SIDE	LAYER	PASS	TYPE	SIZE mm	AMPS	VOLTS	E.S.O.	SPEED mmps	WFS ipm	HEAT INPUT
	Both		all	320	3.2	160	22				

ISSUED BY:	**DATE:**	**LAB TECHNOLOGIST:** Brian Spahn

WELDING DATA SHEET

WELDING INSTITUTE OF CANADA
INSTITUT DE SOUDAGE DU CANADA

CONTRACT NO. RC 391

DATA SHEET NO. SCA #s 9 to 14

PROCESS: GMAW

MATERIALS: DH 36 to DH 36 (25.4 mm thick)

POSITION: Vertical Up

PREHEAT:

Preheat Temp. 150 deg. C
Interpass Temp. 150 deg. C
Preheat Maintenance

FILLER METAL:

Classification E480 1T-9CH (0.045" dia.)
Trade Name LA T91

FLUX:

Class:
Trade Name:

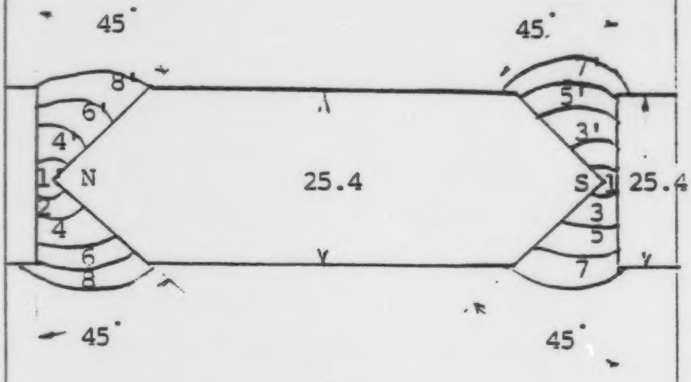

JOINT DETAILS

GAS COMPOSITION REQUIRED:

Shielding Gas	C-25	At	40	CFH
Backing Gas		At		CFH
Trailing Gas		At		CFH

ELECTRICAL CHARACTERISTICS:

Power Source: Hobart Mega MIG RUS 650
Current Type: Powcon , DC
Polarity: +ve

SPECIAL NOTES

T	WELD SEQUENCE			ELECTRODE		WELDING VARIABLES					
	SIDE	LAYER	PASS	TYPE	SIZE mm	AMPS	VOLTS	E.S.O.	SPEED mmps	WFS ipm	HEAT INPUT
	1	1	1,2		1.2	120	22				
	1	2	3,4		1.2	150	23.5				
	1	3,4	5-8		1.2	180	25				
	2	1	1,2		1.2	200	25				
	2	2	3,4		1.2	190	25				
	2	3,4	5-8		1.2	180	24				

ISSUED BY:	**DATE:**	**LAB TECHNOLOGIST:** Brian Spahn

WELDING DATA SHEET

WELDING INSTITUTE OF CANADA
INSTITUT DE SOUDAGE DU CANADA

CONTRACT NO. RC 391

DATA SHEET NO. SCA #s 4 to 14 (Base plate & HAZ)

PROCESS: SMAW

MATERIALS: 1045 or 1060 to DH 36 steel

POSITION: FLAT

PREHEAT:

Preheat Temp. 315 deg. C
Interpass Temp. 315 deg. C
Preheat Maintenance 315 deg. C

FILLER METAL:

Classification
Trade Name Hobart Smootharc 400 (3.2 mm)

FLUX:

Class:
Trade Name:

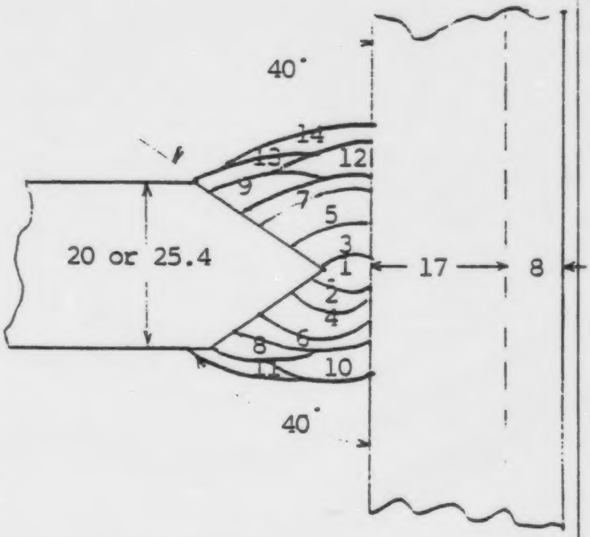

JOINT DETAILS

GAS COMPOSITION REQUIRED:

Shielding Gas At CFH
Backing Gas At CFH
Trailing Gas At CFH

ELECTRICAL CHARACTERISTICS:

Power Source: Miller Gold Star 600 SS
Current Type: DC
Polarity: +ve

SPECIAL NOTES

T	WELD SEQUENCE			ELECTRODE		WELDING VARIABLES					
	SIDE	LAYER	PASS	TYPE	SIZE mm	AMPS	VOLTS	E.S.O.	SPEED mmps	WFS ipm	HEAT INPUT
	Both		all	400	3.2	90-120	22-24				

ISSUED BY:

DATE:

LAB TECHNOLOGIST:

WELDING DATA SHEET

WELDING INSTITUTE OF CANADA
INSTITUT DE SOUDAGE DU CANADA

CONTRACT NO. RC 391

DATA SHEET NO. K-Welds, CG HAZ

PROCESS: SAW

MATERIALS: DH 36 Steel, 25.4 mm thick

POSITION: 1G, Flat

PREHEAT: None

Preheat Temp.
Interpass Temp.
Preheat Maintenance

FILLER METAL:

Classification
Trade Name LA 75 wire

FLUX:

Class:
Trade Name: Lincoln 880 M

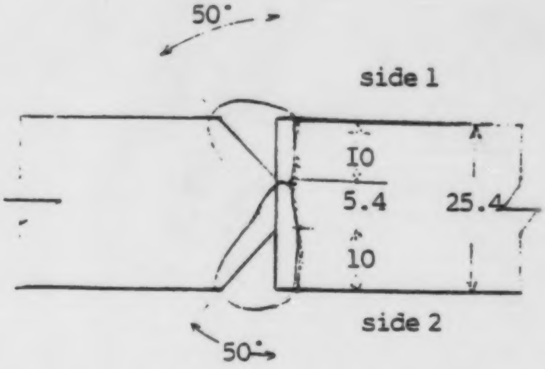

JOINT DETAILS

GAS COMPOSITION REQUIRED:

Shielding Gas	At	CFH
Backing Gas	At	CFH
Trailing Gas	At	CFH

ELECTRICAL CHARACTERISTICS:

Power Source:
Current Type:
Polarity:

SPECIAL NOTES

T	WELD SEQUENCE			ELECTRODE		WELDING VARIABLES					
	SIDE	LAYER	PASS	TYPE	SIZE mm	AMPS	VOLTS	E.S.O. mm	SPEED mmps	WFS ipm	HEAT INPUT
	1	1	1			790-810	36	32	5	49	5 kJ/mm
	2	1	1			1000-1025	38	32	6.3	67	5 kJ/mm

ISSUED BY:

DATE:

LAB TECHNOLOGIST: r.. Thompson

WELDING DATA SHEET

WELDING INSTITUTE OF CANADA
INSTITUT DE SOUDAGE DU CANADA

CONTRACT NO. RC 391

DATA SHEET NO. SCA # 9

PROCESS: SMAW

MATERIALS: DH 36

POSITION: Flat

PREHEAT:

Preheat Temp. 320 deg. C
Interpass Temp. 320 deg. C
Preheat Maintenance 320 deg. C

FILLER METAL:

Classification
Trade Name Hobart Smootharc 400 (3.2 mm)

FLUX:

Class:
Trade Name:

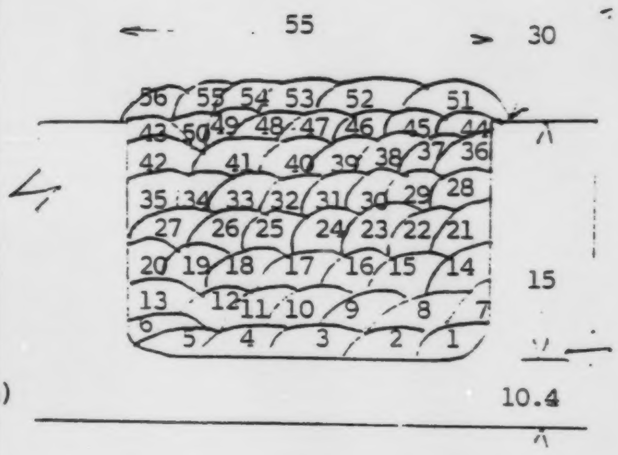
55
30
56
55
54
53
52
51
43
50
49
48
47
46
45
44
42
41
40
39
38
37
36
35
34
33
32
31
30
29
28
27
26
25
24
23
22
21
20
19
18
17
16
15
14
13
12
11
10
9
8
7
6
5
4
3
2
1
15
10.4

JOINT DETAILS

GAS COMPOSITION REQUIRED:

Shielding Gas At CFH
Backing Gas At CFH
Trailing Gas At CFH

ELECTRICAL CHARACTERISTICS:

Power Source: Miller
Current Type: DC
Polarity: +ve

SPECIAL NOTES

T	WELD SEQUENCE			ELECTRODE		WELDING VARIABLES					
	SIDE	LAYER	PASS	TYPE	SIZE mm	AMPS	VOLTS	E.S.O.	SPEED mmps	WFS ipm	HEAT INPUT
			1-56	400	3.2	88	22				

ISSUED BY:

DATE:

LAB TECHNOLOGIST: B. Spahn

Table B1. Strain Gauge Readings for SCA Test # 1
263 MPa, -15 Deg. C.

Pressure psi	Microstrains S1W	S2W	S3E	S4E
Load main plate.				
50	0	0	0	0
500	0	249.5	0	0
1000	0	249.5	249.5	0
1500	249.5	249.5	249.5	0
2000	249.5	-996.7	-996.7	249.5
2500	249.5	1249	1249	249.5
Crack Starter Loading				
1000	249.5	1249	1249	249.5
2000	249.5	1249	1249	249.5
3000	249.5	1249	1249	249.5
4000	249.5	1249	1249	249.5
5000	249.5	1249	1249	249.5

Table B2. Strain gauge Readings for SCA Test # 2
263 MPa, 5 Deg. C.

Pressure psi	Microstrain					
	S1E	S2E	S3E	S5W	S6W	S7W
Load main plate.						
50	-0.5964	-2.054	0.6627	-1.392	-2.187	-1.723
500	197.1	201.6	39.83	238	245.9	65.88
1000	475.3	461.5	94.45	539.2	534.1	142.6
1500	721.5	702.3	142.6	790.2	783.3	212
2000	955.9	933.6	188.5	1018	1012	278.9
2500	1173	1152	231.1	1227	1217	344.6
Crack Starter Loading						
1000	1177	1156	231.1	1230	1218	345.9
2000	1176	1154	231.9	1229	1217	346.2
3000	1175	1154	230.9	1228	1215	345.4
4000	1176	1153	231.8	1228	1214	345.5

Table B3. Strain Gauge Readings for SCA Test # 3
350 MPa, 5 Deg. C.

Pressure	Microstrain					
psi	S1E	S2E	S3E	S5W	S6W	S7W
Load main plate.						
60	0.1991	-1.062	-0.7965	-0.3982	-0.4646	0.1327
500	209.7	255.5	45.53	169	213.5	74.01
1000	437.5	555.5	92.73	332.3	452	160.4
1500	655.6	823.3	141.9	515.8	688.4	241.7
2000	868.9	1071	193.9	713.8	921.7	319.5
2500	1084	1313	246.3	927.5	1161	398.4
3000	1287	1540	298.2	1141	1391	479.4
3327	1402	1673	330	1272	1528	534.9
Crack Starter Loading						
1000	1396	1669	329.4	1269	1523	534.5
2000	1394	1665	328.6	1268	1521	534.2
3000	1393	1664	328.5	1267	1520	533.5
4000	1391	1664	328.6	1266	1518	534.1
5000	1390	1661	328.1	1264	1517	533.9

Table B4. Strain Gauge Readings for SCA Test # 4
350 MPa, 5 Deg. C.

Pressure			Microstrain			
psi	S1W	S2W	S3W	S1E	S2E	S3E
Load main plate.						
50	-1.457	-0.2648	0.8607	0.1324	-1.258	-0.3973
500	73.76	213.6	178.9	46.74	207.4	244.4
1000	157.5	445.1	357.3	97.27	434.1	528.3
1500	236.8	675	551.2	149.8	654.6	787.5
2000	316.6	903	749	214	875.6	1039
2500	395.8	1128	952.2	259.5	1092	1281
3000	476.7	1355	1160	317.7	1310	1518
3327	531.5	1494	1293	357.3	1437	1651
Crack Starter Loading						
1000	532.9	1491	1296	357.3	1427	1643
2000	531.5	1492	1299	356.8	1421	1639
3000	531.8	1494	1302	356.5	1416	1631
4000	530.8	1496	1305	356.7	1410	1622
5000	530.9	1499	1307	356	1404	1613
6000	530.7	1502	1312	355.3	1396	1605
7000	530.6	1507	1315	355.4	1387	1595
8000	530.8	1512	1322	354.4	1376	1583

Table B5. Strain Gauge Readings for SCA Test # 5
263 MPa, 5 Deg. C.

Pressure	Microstrain							
psi	S1E	S2E	S3E	S4E	S1W	S2W	S3W	S4W
Load main plate.								
0	0.066	-0.33	-0.46	-0.13	0.26	0.6	0.066	-0.4
500	299	142	135	155	296	221	131	133
1000	571	332	299	323	549	438	253	253
1500	817	529	461	489	773	642	370	364
2000	1062	747	633	686	990	852	497	482
2500	1278	963	787	841	1182	1050	631	600
Crack Starter Loading								
1000	1274	964	820	895	1183	1056	628	590
2000	1271	959	849	944	1187	1060	620	574
3000	1270	958	884	996	1194	1066	611	560
4000	1268	954	918	1048	1199	1071	601	549
5000	1265	951	956	1103	1205	1076	590	527
6000	1264	948	994	1154	1211	1082	579	511
7000	1262	945	1038	1212	1218	1088	565	493
8000	1259	941	1098	1286	1227	1095	545	470
9000	1256	936	1203	1406	1249	1110	509	429
9200	1254	933	1258	1462	1261	1117	490	410

At 8000 psi a small click noise was heard
and the crack starter fractured after full loading to 9200 psi and waiting.

Table B6. Strain Gauge Readings for SCA test # 6
350 MPa, 20 Deg. C

Pressure					Microstrain			
psi	S1E	S2E	S3E	S4E	S1W	S2W	S3W	S4W
Load main plate.								
0	-5	-3	-3	-2	-2.6	-1.4	-1.6	-0.2
500	219	278	133	153	225	170	123	102
1000	456	584	314	334	467	341	248	201
1500	678	847	490	507	692	525	361	292
2000	901	1094	660	667	915	722	483	387
2500	1126	1329	837	828	1132	929	624	500
3000	1355	1543	1115	1076	1336	1149	718	581
3327	1510	3231	1264	1223	1395	2156	697	561
Crack Starter Loading								
1000	1484	3833	1331	1290	1387	2789	654	528
2000	1477	3869	1392	1345	1389	2868	624	503
3000	1469	3889	1456	1407	1390	2928	593	475
4000	1463	3904	1522	1471	1391	2974	559	446
5000	1458	3915	1585	1528	1393	3016	526	415
6000	1451	3921	1646	1590	1395	3047	493	383
7000	1446	3926	1709	1651	1396	3077	458	353
8000	1438	3940	1786	1721	1397	3125	419	314
9000	1434	3943	1846	1785	1399	315	388	281
9200	1431	3947	1863	1805	1398	316	379	268

First soundof cracking at 7000 psi and second cracking at 8000 psi. Max. load on crack starter was 9200 psi. Complete fracture of the crack starter did not occur.

Unload the crack starter and unload main plate to 750 psi. Zero strain gauges.

Zero read	-0.7	-1.1	-1.3	-1.2	-1.3	-0.3	0.2	-0.4
Load crack starter to								
7000	-32	-49	432	428	35	51	-178	-153
8000	-36	-55	499	492	38	57	-206	-175
9200	-43	-63	617	613	46	65	-254	-217
Unload crack starter and load main plate.								
750	4.6	-1.6	21	19	5.9	10.8	8	4.9
1000	87	85	68	58	86	86	56	44
1500	303	307	206	211	302	300	183	149
2000	545	571	376	378	542	528	319	258
2500	784	833	544	542	777	754	451	363
3000	1013	1089	704	697	1007	978	576	463

Final load on the main plate to match crack starter loading strain.
No cracking of main plate. Only a small crack extension in the starter.

Table B7. Strain Gauge Readings for SCA Test # 7
263 MPa, 5 Deg. C

Pressure psi	Microstrain S1E	S2E	S3E	S4E	S1W	S2W	S3W	S4W
Load main plate.								
50	-3	-5	-3	-5	-2	-1	0	-1
500	212	234	156	161	220	198	99	120
1000	445	515	336	342	449	387	199	240
1500	680	783	513	520	683	590	301	362
2000	908	1038	688	691	910	795	394	480
2500	1138	1290	855	853	1140	1005	493	602
Load the crack starter.								
1000	1139	1292	891	901	1145	1010	487	592
2000	1137	1289	944	957	1145	1013	474	573
2800	1127	1281	1456	1469	1168	1033	278	363

Cracking noise heard. Unload crack starter to zero load.
Unload main plate load to 750 psi, zero instrument.
Load crack starter to 2800 psi and load the main plate
to give the strain equivalent at 2500 psi of main plate.

Pressure psi	S1E	S2E	S3E	S4E	S1W	S2W	S3W	S4W
750	0	-1	1	-1	-1	2	-1	-1
Crack starter								
2800	-20	-20	614	630	23	26	-237	-262
Main plate								
2910	955	1017	621	629	951	908	462	545

Table B8. Strain Gauge Readings for SCA Test # 8
350 MPa, 20 Deg. C.

Pressure	Microstrain							
psi	S1E	S2E	S3E	S4E	S1W	S2W	S3W	S4W
Load main plate.								
50	0	-6	0	0	0	0	-2	0
500	220	261	166	170	224	185	113	120
1000	463	557	370	370	468	373	234	249
1500	714	841	574	570	717	584	360	381
2000	935	1083	755	746	940	781	474	496
2500	1169	1336	934	917	1169	992	589	619
3000	1395	1582	1089	1073	1396	1201	714	750
3327	1545	1738	1169	1155	1543	1342	761	832
Load the crack starter.								
1000	1540	1728	1209	1223	1546	1348	746	801
2000	1540	1720	1277	1312	1550	1354	724	779
3000	1538	1711	1366	1421	1555	1360	691	740
4000	1550	-52	1526	1581	1576	1391	659	704
4200	1512	-44	1310	1387	1590	1404	324	409

Crack starter fractured.

Table B9. Strain Gauge Readings for SCA Test # 9
HAZ # 1, 350 MPa, 20 Deg. C.

Pressure	Microstrain			
psi	S1E	S2E	S1W	S2W
Load main plate.				
0	2	-2	-1	-2
500	209	240	232	197
1000	461	499	474	428
1500	687	730	694	633
2000	918	966	916	837
2500	1153	1204	1126	1038
3000	1412	1452	1309	1238
3327	1564	1561	1365	1334
Load crack starter.				
1000	1567	1554	1356	1332
2000	1565	1550	1353	1330
3000	1562	1546	1351	1329
4000	1554	1535	1356	1332
5000	1540	1521	1361	1338
5500	1300	1279	1390	1362

Crack starter broke and load dropped to 4000 psi.

Table B10. Strain Gauge Reading for SCA Test # 10
HAZ # 2, 350 MPa, 5 Deg. C.

Pressure psi	Microstrain S1E	S2E	S1W	S2W
Load main plate.				
0	-2	-4	-2	0
500	220	233	202	186
1000	471	524	441	387
1500	715	799	675	596
2000	943	1054	896	801
2500	1170	1307	1121	1018
3000	1403	1559	1340	1240
3327	1538	1701	1460	1371
Load crack starter.				
1000	1531	1693	1453	1371
2000	1526	1687	1452	1371
3000	1520	1680	1454	1374
4000	1513	1673	1455	1377
5000	1504	1663	1459	1382

Table B11. Strain Gauge Reading for SCA Test # 11
HAZ # 3, 263 MPa, -5 Deg. C.

Pressure psi	Microstrain S1E	S2E	S1W	S2W
Load main plate.				
0	-4	-1	0	-1
500	235	242	179	167
1000	514	532	403	372
1500	769	793	624	593
2000	1016	1033	842	809
2500	1260	1270	1054	1029
Load crack starter.				
1000	1264	1270	1058	1031
2000	1264	1268	1056	1031
3000	1260	1269	1056	1028
4000	1256	1258	1065	1043
5000	1249	1252	1074	1048
5200	1240	1245	1043	1018

Table B12. Strain Gauge Reading for SCA Test # 12
HAZ # 4, 263 MPa, -15 Deg. C.

Pressure	Microstrain			
psi	S1E	S2E	S1W	S2W
Load main plate.				
50	-4	0	-6	-7
100	-63	21	120	45
500	152	253	326	224
1000	377	502	540	408
1500	629	788	775	620
2000	866	1037	1012	840
2500	1108	1295	1246	1056
Load the crack starter.				
1000	1111	1111	1295	1063
2000	1104	1291	1254	1063
3000	1099	1287	1257	1067
4000	1095	1287	1267	1077
5000 fractured the crack starter.				

Table B13. Strain Gauge Reading for SCA Test # 13
HAZ # 5, 263 MPa, 5 Deg. C.

Pressure psi	Microstrain S1E	S2E	S1W	S2W
Load main plate				
0	3	39	109	-3
500	253	229	295	215
1000	541	464	522	462
1500	784	696	732	680
2000	1016	913	940	891
2500	1234	1126	1141	1094
Load crack starter.				
1000	1241	1080	1140	1101
2000	1236	1090	1140	1106
3000	1236	1100	1142	1114
4000	1232	1091	1149	1123
5000	1221	1106	1152	1131
5700	1078	1005	1205	1172

Load dropped to 4800 psi when starter cracked.

Table 14. Strain Gauge Readings for SCA Test # 14
Control Test at 18 Deg. C.

pressure				Microstrain				
psi	S1E	S2E	S3E	S4E	S1W	S2W	S3W	S4W
Load main plate.								
0	-0.9	-0.8	0	-0.3	-1.3	0	0.6	0.3
250	95	100	52	59	101	99	19	25
500	218	238	116	129	220	205	41	54
750	336	372	159	180	334	303	79	92
1000	450	498	195	223	445	402	124	128
1250	563	616	224	257	556	508	170	158
1500	675	728	247	275	664	614	207	174
1750	785	839	258	278	773	720	227	173
2000	885	938	263	273	873	820	230	169
Reduce main load to 500 psi								
500	196	260	-119	-138	226	150	-31	-81
Load crack starter.								
1000	181	243	-87	-97	235	160	-83	-116
2000	153	214	-33	-28	250	177	-170	-172
3000	124	182	19	38	265	195	-257	-215
4000	96	153	-0.87	66	282	212	-324	-230
4500	84	141	-8	36	291	223	-348	-231
5000	69	124	15	61	302	235	-386	-248
Unload and end test.								
0	-21	26	-287	-338	6	-56	6	-22

APPENDIX D

WIDE PLATE TESTS - ANALYSIS OF RESULTS.

STUDY OF WIDE PLATE TESTING OF STRUCTURAL STEELS FOR ARCTIC SHIPS

FINAL REPORT

TO

FLEET TECHNOLOGY LIMITED

Ottawa

BY

Mark J. Tomin
RELTEC Advisory Services Inc.

May 1991

FTL PROJECT REF. 3728C
RELTEC REPORT NO. REL-0191-1

TABLE OF CONTENTS

Page

1. INTRODUCTION 1

2. BACKGROUND 2

3. USE OF WIDE PLATE TESTS IN FRACTURE CONTROL PLANS 4

4. NK WIDE PLATE TESTS 6

5. EXPERIMENTAL PROGRAM 10

5.1 Selection and Characterization of Material 10
5.2 CVN Toughness Results 10
5.3 Nil Ductility Transition Temperature (NDTT) 10
5.4 Fracture Toughness (CTOD) 13
5.5 Wide Plate Test Results 14

6. DISCUSSION OF THE RESULTS 17

6.1 NK Wide Plate Test Criterion 17
6.2 Fracture Stress 21
6.3 Comparison with Sumpter 125 MPa√m Toughness Criterion 21
6.4 Other Fracture Criteria 23
6.5 Probability of Fracture 27

7. SIGNIFICANCE OF THE RESULTS WITH RESPECT TO CASPPR 31

8. REFERENCES 34

1. INTRODUCTION

In this report, the wide plate test results reported by the Welding Institute of Canada (WIC, 1990) together with the supporting material test results obtained by the Materials Technology Centre (MTC) of Fleet Technology Ltd. (Malik, 1990), are analyzed and their interpretation in view of the CASPPR (Canadian Arctic Shipping Pollution Prevention Regulations) is presented.

This work was subcontracted to RELTEC Advisory Services Inc. by Fleet Technology Limited as a part of the project "Study of Wide Plate Testing of Structural Steels for Arctic Ships", funded jointly by Canadian Coast Guard, Canada Centre for Mineral and Energy Technology (CANMET) and PERD grant.

For the experimental work, a 1" thick DH36 ship steel was selected. This steel was tested for chemical composition, standard mechanical tests (tensile properties, elongation, area reduction) as well as toughness, NDTT, CTOD (quasi-static and intermediate strain rate) and finally, four wide plate tests (WPT) were conducted at the temperatures -75°, -55°, -40° and -20° C.

The effect of intermediate strain rates on this and other ship steels in view of CASPPR materials requirements was studied by FLEET and RELTEC in a separate project (Malik and Tomin, 1991).

2. BACKGROUND

The current wide plate test program was a part of a broad effort, initiated by the Coast Guard Northern, to provide an experimental basis for material selection for arctic shipping.

The air temperatures, encountered by ships navigating in the Canadian Arctic as well as for offshore structures located in the Beaufort Sea, can be below -40° C. The minimum design temperature for arctic shipping accepted by CASPPR (Canadian Arctic Shipping Pollution Prevention Regulations) is -40° C.

The current ship steels, which have provided satisfactory resistance against brittle fracture for world-wide ship operation at 0°C (3%-tile of the service temperature distribution), would be exposed in many cases, when applied for arctic use, to operating temperatures which correspond to the lower part of their toughness transition curve. The fracture plans developed for higher operating temperatures should be carefully re-assessed with respect to the new environmental applications of structural steels.

To preserve satisfactory reliability against brittle fracture for ships and offshore structures operating in the Canadian Arctic, the conditions leading to brittle fracture at these lower temperatures need to be thoroughly examined.

Extensive research was undertaken by Canadian industry, universities and Federal Government laboratories (Canada Centre for Mineral and Energy Technology - CANMET) to develop a basis for safe application of steels in arctic environment. A number of projects, initiated during this program, aimed at the following:

- development of temperature database for arctic regions;
- study of propensity of structural steels to brittle fracture at arctic temperatures;
- fatigue and corrosion fatigue in structural steels;
- development of new steels and welding procedures.

The study of propensity of structural steels to brittle fracture in the arctic environment entailed a re-assessment of all factors contributing to brittle fracture. In particular, the following aspects of brittle fracture were the subject of the past and present studies:

- effect of temperature on fracture toughness;
- effect of strain rate on fracture toughness;
- correlation between small scale fracture toughness tests and large scale fracture tests (wide plate tests);
- crack arrest properties;

- availability of steels for arctic structures;
- application of structural reliability methods to the assessment of brittle fracture;
- significance of local brittle zones in HAZ of structural steels.

These research programs aim at providing the necessary basis for the steel selection requirements proposed in CASPPR and those stipulated in the CSA Standard S473 Code for the Design, Construction, and Installation of Fixed Offshore Structures.

The main goal of the present research program "Study of Wide Plate Testing of Structural Steels for Arctic Ships" was to provide experimental data on brittle fracture initiation from long (250 mm) cracks in the parent material representative of a typical ship steel.

The collateral goal of this program was to substantiate the fracture control plan for ships developed by the Japanese Classification Society NK (Nippon Kaiji Kyokai) and based on wide plate test results for ship steels. The NK approach was used to verify the material selection criteria used in CASPPR (Tomin, 1989).

3. USE OF WIDE PLATE TESTS IN FRACTURE CONTROL PLANS

The correlation of wide plate test results with fracture toughness (CTOD) obtained from small fracture specimens became the basis for the CTOD fracture criterion.

This correlation relates the crack size, 'a', stress and CTOD (δ) as follows:

$$\delta = \frac{\sigma \pi a}{E}\left(\frac{\sigma}{\sigma_y} - 0.25\right) \qquad (1)$$

This relation assumes that $\sigma = E\varepsilon$ up to the yield point. The above relationship is assumed to be valid for $\varepsilon/\varepsilon_y > 0.5$.

The CTOD - WPT correlation recognizes a statistical scatter in the crack size predicted based on CTOD values measured on small CTOD specimen and the actual critical crack size obtained from WPT, Figure 1 (Dawes and Kamath, 1977). There is approximately a safety factor of 2.5 on the crack size obtained from Equation (1) and corresponding to 50%-tile of the distribution.

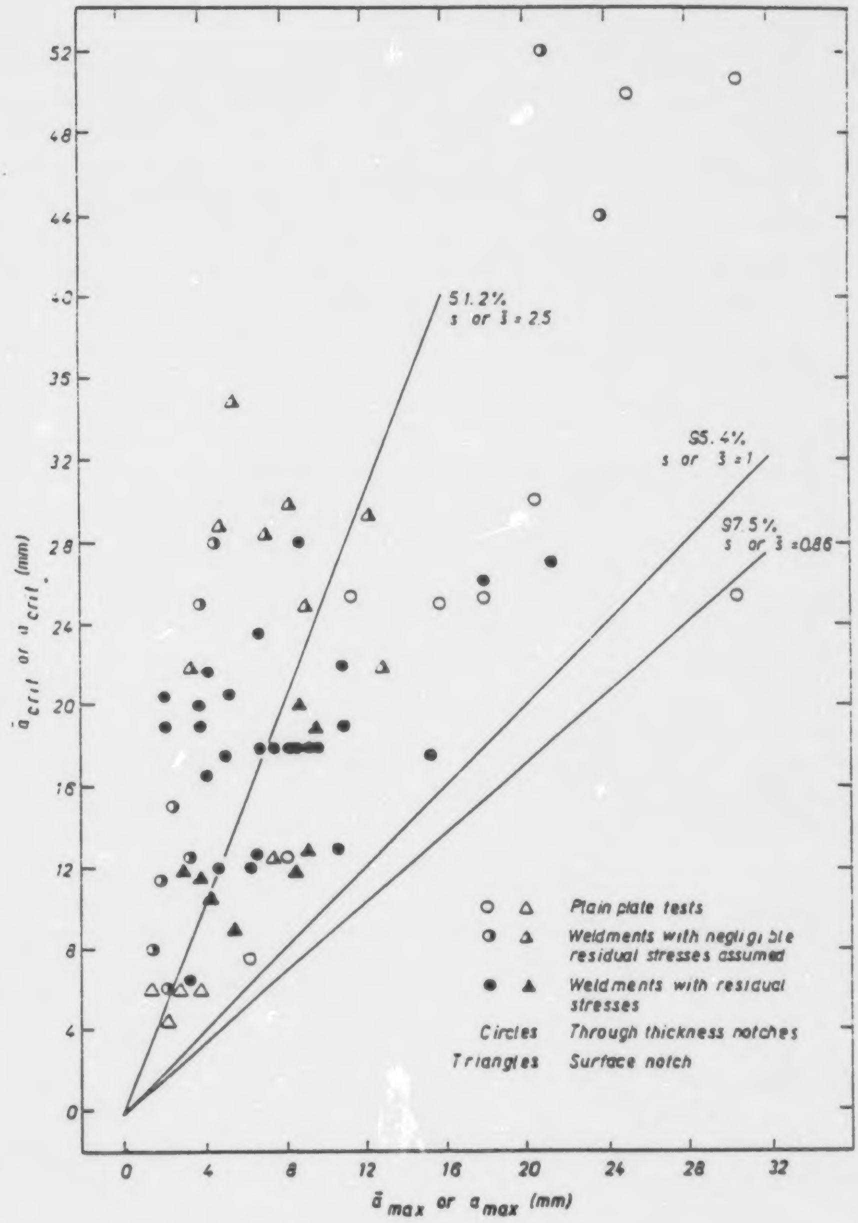

Figure 1: Correlation between Predicted Crack Size and Critical Crack Size from WPT (Dawes and Kamath, 1977)

4. NK WIDE PLATE TESTS

The Japanese Classification Society NK (Nippon Kaiji Kyokai) developed a fracture control plan based on wide plate test (WPT) results for ship steels. This fracture mechanics approach was presented by NK at the IACS (International Association of Classification Societies) Meeting in Oslo in 1979 (NK, 1979).

This approach is based on the correlation of the energy transition temperature estimated for the lower bound Charpy S-curve for individual ship steels.

The WPT formulae can be used to obtain the critical defect size as a function of steel grade and stress level (material utilization factor α). The material utilization factor is defined as the ratio of the maximum allowable stress to the yield strength of the steel. The following is assumed:

- The crack is oriented perpendicularly to the weld and to the far-field stress in the wide plate.
- Using linear elastic fracture mechanics, the maximum crack length at the point of unstable crack initiation is calculated as a function of the material utilization factor α, temperature, thickness and the steel grade.

The NK WPT approach consists of the following four steps:

1) The specified CVN energy at the test temperature is related through an empirical formula to the energy transition temperature.

2) The energy transition temperature is then used, together with the yield strength and thickness of the plate, to calculate the brittle fracture initiation temperature for an assumed crack length $2a=80$ mm and working stress equal to half of the yield strength ($\alpha=0.5$), using another experimental formula.

3) Finally, the fracture initiation temperature obtained in Step 2 is substituted into a third empirical equation to get fracture toughness of the steel as a function of temperature.

4) Linear fracture mechanics is then applied to analyze stability of an assumed defect.

Details of this approach can be found in the report to the CASPPR Subcommittee (Tomin, 1989). The algorithm of this approach is shown in the flowchart in Figure 2.

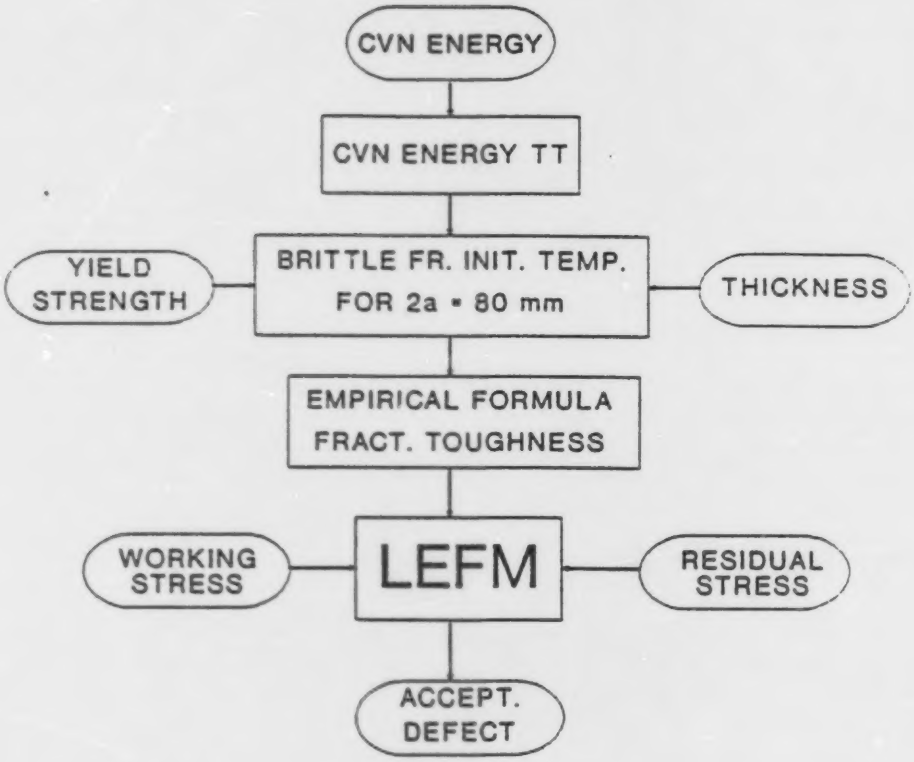
CVN ENERGY
CVN ENERGY TT
YIELD STRENGTH
BRITTLE FR. INIT. TEMP. FOR 2a = 80 mm
THICKNESS
EMPIRICAL FORMULA FRACT. TOUGHNESS
WORKING STRESS
LEFM
RESIDUAL STRESS
ACCEPT. DEFECT

Figure 2: Flowchart for WPT Fracture Mechanics Analysis of Fractures in Ships

The assumed configuration is that of a wide plate with a central crack, 2a = 250 mm for which the stress-intensity factor is given by

$$K=(\alpha+\beta)\sigma_y\sqrt{\pi a} \qquad (2)$$

where α is the material utilization factor σ/σ_y and β is the residual stress factor σ_{res}/σ_y.

The crack initiation criterion is then defined as

$$K\geq K_c \qquad (3)$$

where the fracture toughness, K_c, is defined using the NKK expression

$$K_c=cK_o\exp\left(-\frac{562}{T}\right) \qquad (4)$$

In the previous equation, factor c=1 for a machine notched plate specimen and c=0.68 for fatigue pre-cracked plate specimen (NKK, 1979).

The factor K_o is obtained using the fracture initiation temperature T_i for the assumed crack length 2a = 80 mm (a = 40 mm) as

$$K_o=\frac{1}{2}\sigma_y\sqrt{40\pi}\exp\left(\frac{562}{T_i}\right) \qquad (5)$$

Fracture toughness K_c can be related to CTOD (δ_c) through the Dugdale plastic strip model as

$$K_c=\sqrt{m\delta_c\sigma_y E} \qquad (6)$$

where the factor m is usually taken as 1 for plane-stress and 2 for plane-strain conditions respectively.

The residual stress assumed by NK was $\sigma_{res} = 0.6\sigma_y$ acting in the entire plate. For primary steel application, the applied stress (nominal) acting perpendicular to the crack was $\sigma_{app} = 0.4\sigma_y$. Thus, the combined stress acting on the crack was assumed to be equal to σ_y. Equation (2) is based on linear fracture mechanics and the NK approach does not assume any safety factor on the 250 mm long crack. In our view, this is justified since the wide test specimen configuration (see assumptions at the beginning of this section) is extremely conservative. In the actual hull design, the plates are reinforced by stiffeners and there is a multipass redistribution of stresses in the case of typical fractures.

5. EXPERIMENTAL PROGRAM

5.1 Selection and Characterization of Material

The plate (marked for traceability as 'WP') selected by MTC, was a high strength ship grade DH36, 1" thick.

The chemical analysis is given in Appendix A, Table A1. IACS (1979) requirements for chemical composition for Grade DH36 are also given in this table. It can be seen that the limitations on chemical composition of DH36 grade are fully met.

Table A2 shows the tensile properties in both longitudinal and tangential orientations. The 355 MPa minimum yield stress specified by IACS for DH36 steel is exceeded in both the tangential and longitudinal direction.

The specification for tensile strength (490-620 MPa) for grade DH36 is also met. The elongation requirement of 21% is highly exceeded in both directions.

5.2 CVN Toughness Results

Full Charpy-V-Notch (CVN) temperature transition curves in both longitudinal and tangential orientations were obtained, Tables A3 and A4. Furthermore, lateral expansion and % shear was measured at each temperature and this information is also listed in corresponding tables. The individual CVN results (longitudinal and transverse) are plotted in Figure 3. The averages at each temperature were splined in Figure 4 to see the trend of the transition curve.

The minimum CVN toughness is specified by IACS to be 34 J (L) and 24 J (T) at -20° C for Grade DH36. These requirements are shown also in Figure 4. It is apparent that this plate meets the DH36 CVN requirements in both longitudinal and transverse directions.

These results were also used to obtain the Weibull distribution of the transition curve, see Figure 5, using the Bishop method (Bishop et al 1982).

5.3 Nil Ductility Transition Temperatures (NDTT)

The NDTT results are presented in Table A5 and also shown in Figure 4. Two specimens were tested to yield NDTT equal to -10° and -15°C.

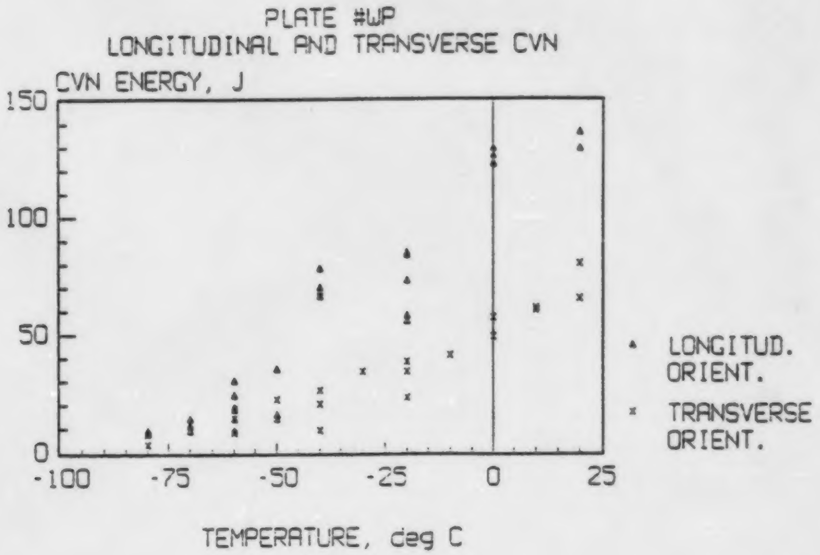

Figure 3: Longitudinal and Transverse CVN for Plate # WP (DH36)

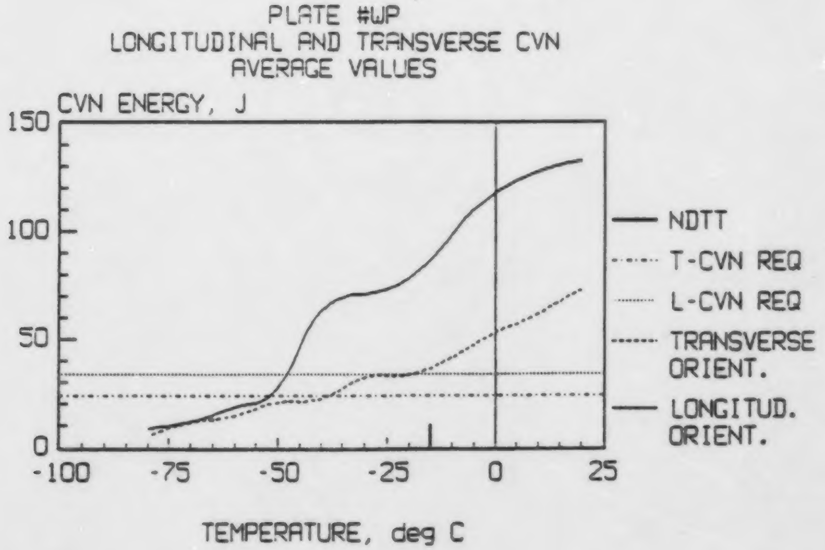

Figure 4: CVN Requirements, Average CVN-L and -T and NDTT for Plate # WP (DH36)

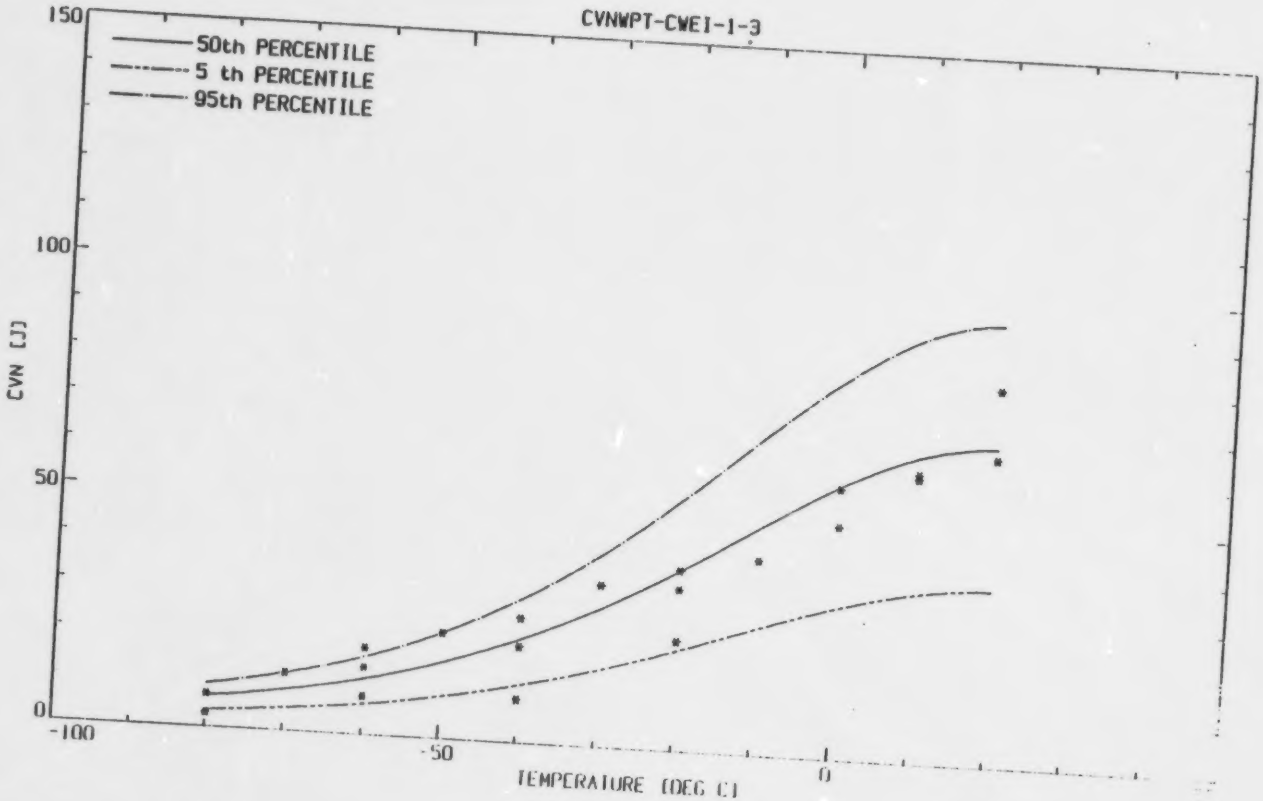

Figure 5: Weibull Distribution of CVN Toughness as a Function of Temperature

5.4 Fracture Toughness (CTOD)

The valid results of the crack tip opening displacement (CTOD) tests, measured at a quasi-static strain rate (10^{-5} s^{-8}) as per BSI BS 5762, are listed in Table A6. These results are denoted CTODcf to distinguish them CTOD values obtained from saw notched specimens, CTODcn, also presented in this table. Individual test results are plotted in Figure 6. Average values are shown shown in Figure 7.

The Weibull distribution of CTOD in the transition region is shown in Figure 8. Both the 5- and 95-%tile curves are shown. Similarly to the CVN Weibull distribution, the CTOD curves were obtained using the Bishop method (Bishop et al, 1982).

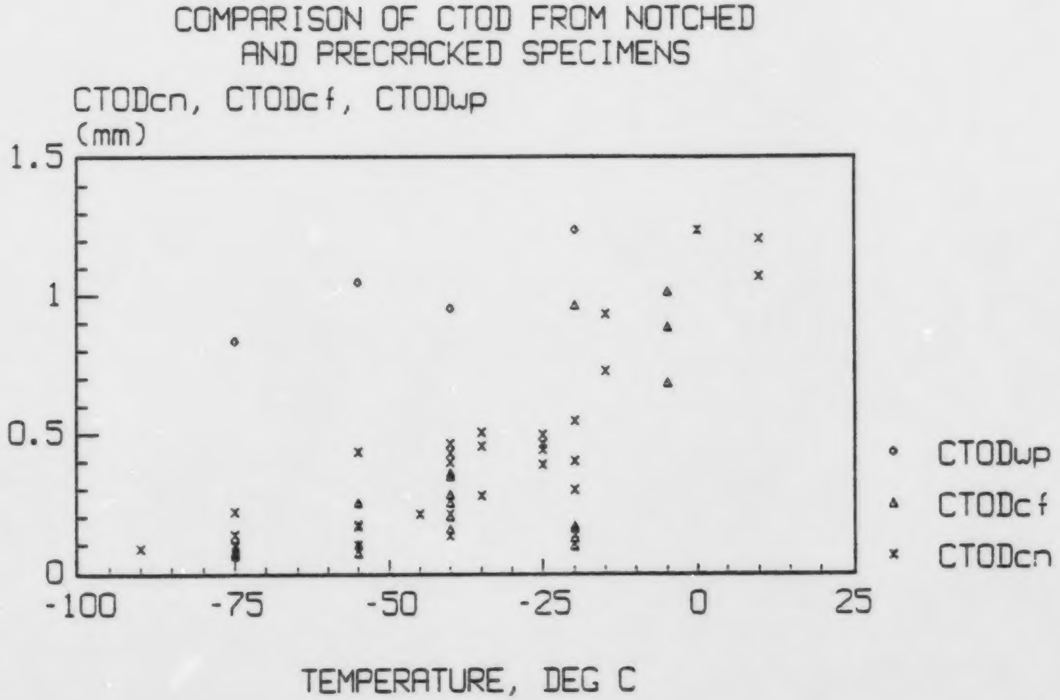

Figure 6: Single values of CTODcf, CTODcn and CTODwp as a Function of Temperature

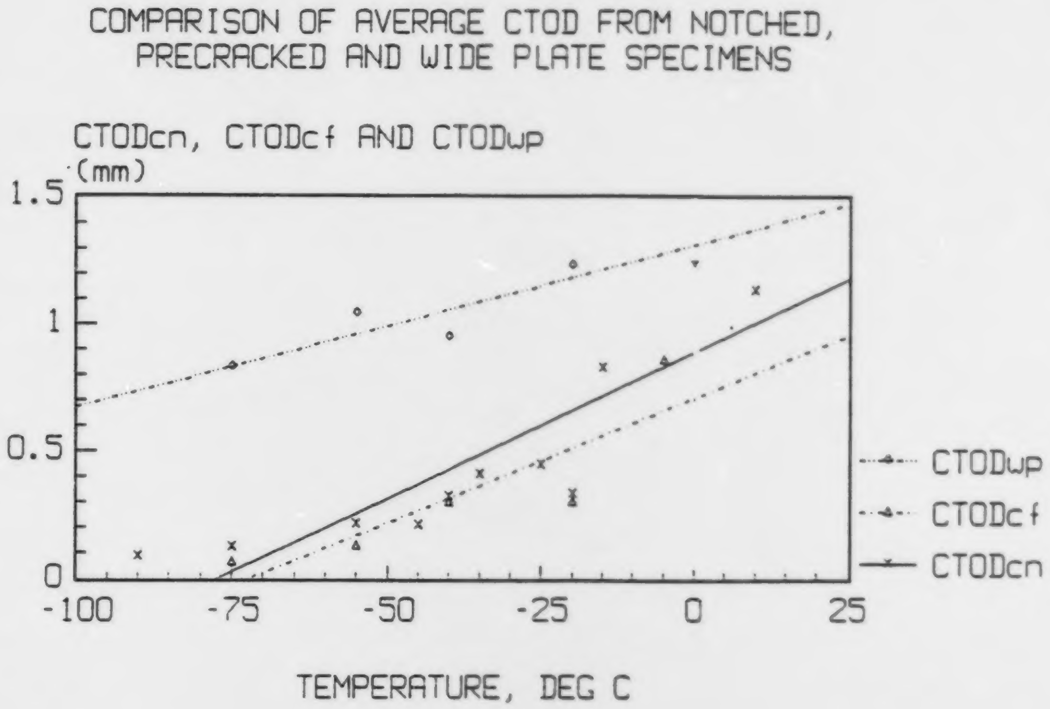

Figure 7: Average CTODcf, CTODcn and CTODwp as a Function of Temperature

The shift due to intermediate strain rates is shown in Figure 9. The effect of strain rate on fracture toughness of this steel is discussed in detail in the report by Malik and Tomin (1990).

5.5 Wide Plate Test Results

Four wide plate tests were pulled at the Canadian Welding Institute as a part of the current project. The tests were performed at -75°, -55°, -40° and -20°C. The test results are described in detail in the WIC Report RC 391/1/1990 (Bala, 1990). The CTODwp values measured at the point of incipient fracture of the wide plate specimens were added to Table A6 and are also shown in Figures 6 and 7.

The values of the fracture stress for the four wide plate tests are given in Table A7.

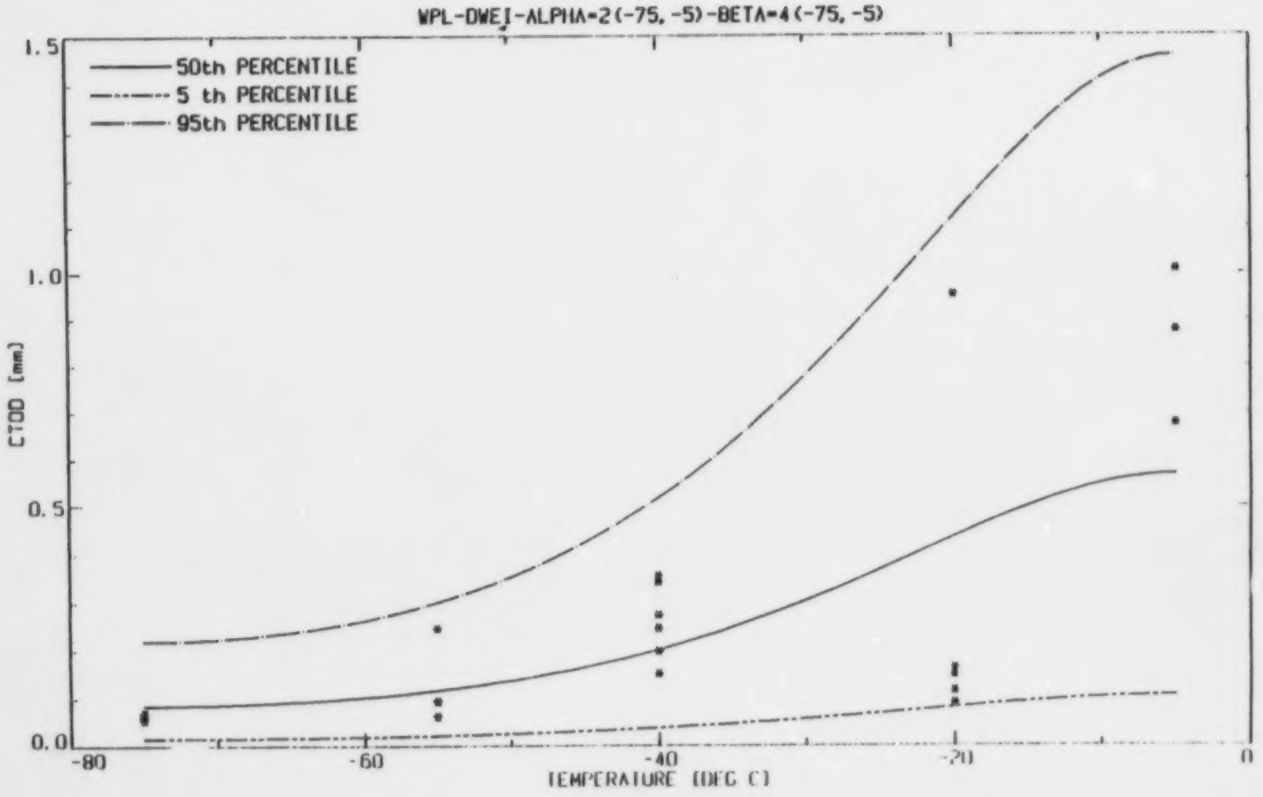

Figure 8: Weibull Distribution of Critical CTOD as a Function of Temperature

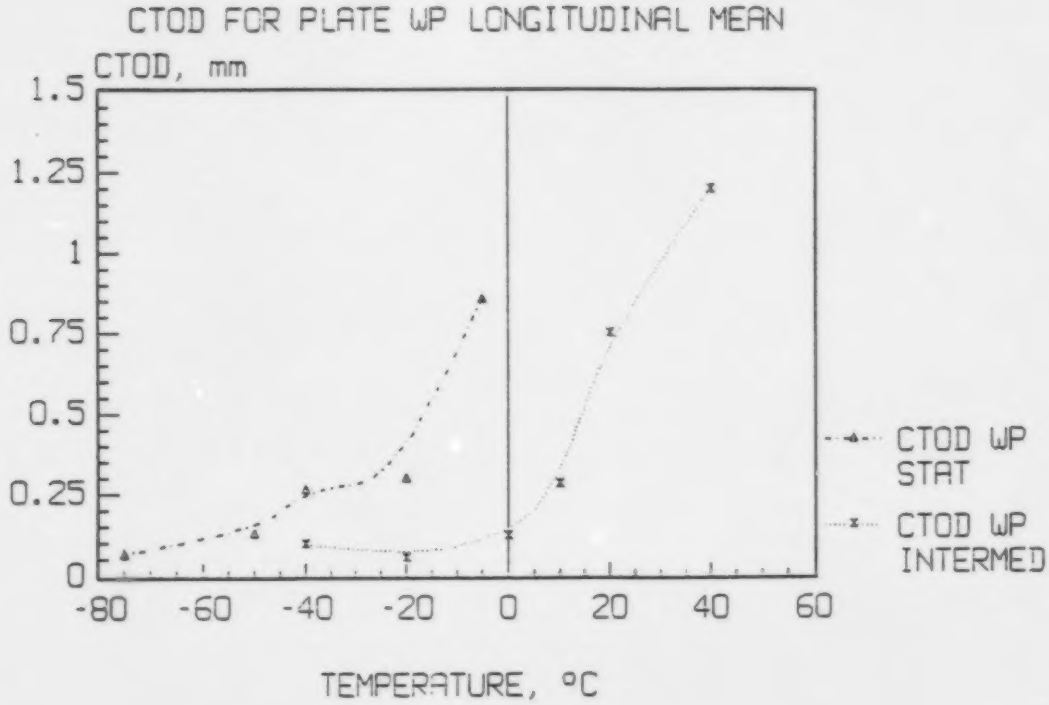

Figure 9: Temperature Shift of Critical CTOD due to Intermediate Strain Rate

6. DISCUSSION OF THE RESULTS

6.1 NK Wide Plate Test Criterion

The wide plate tests provide only four points on the fracture toughness - temperature curve. Nevertheless, the results provide an important information for 'calibration' of the NK approach which was used to verify the CASPPR steel selection requirements.

The relationship given by Equation (4) is plotted in Figures 10, 11 and 12. The fracture initiation temperature was taken for the DH36 steel from the report "Development of the Wide Plate Test Program", Tomin (1988), as T_i = -127.5°C. Since the studied steel satisfies requirements for EH36 grade, the NK curves for this grade (T_i = -137.6°C) are also included.

In Figure 10, fracture toughness points show Kc, where Kc was obtained from Equation (6) for m=2. To obtain the NK line, factor c=0.68 for sharp crack was used in Equation (4), since a comparison

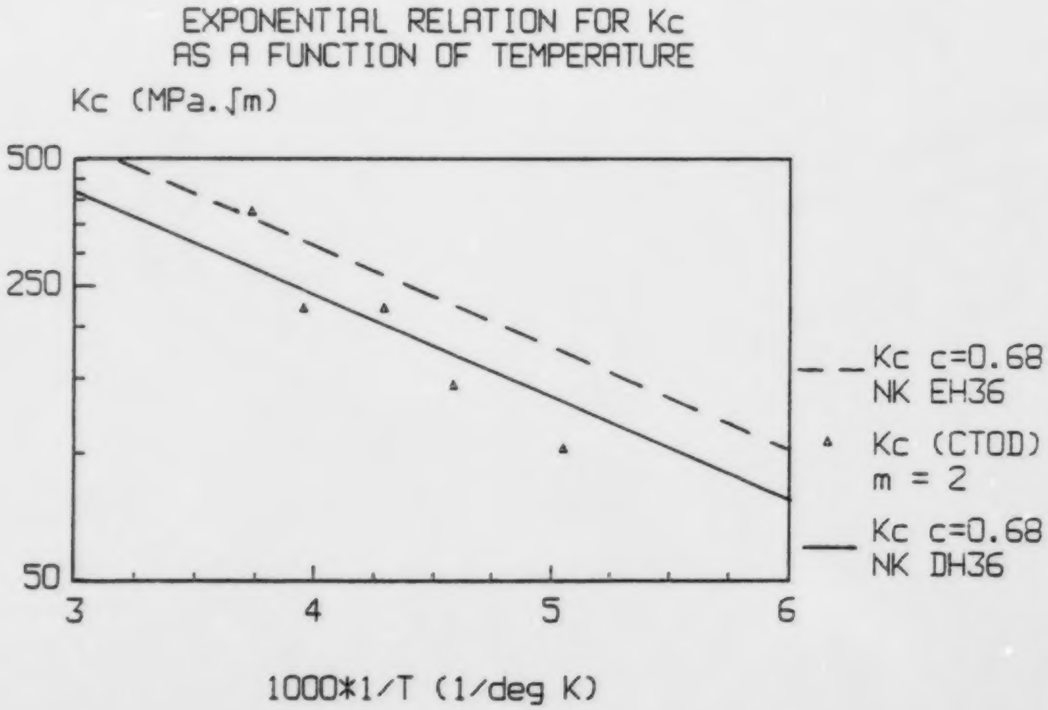

Figure 10: NK Line versus ln(Kc) Points from the CTODcf Data for m=2

is being made with fracture toughness corresponding to the sharp CTOD specimens. The CTOD results used for calculation of Kc were the average values obtained at temperatures -5°, -20°, -55° and -75°C (see CTODcf, Table A6). It can be seen that the values obtained from CTOD are scattered closely to the NK DH36 line. The results are more unconservative against the NK EH36 line.

Figure 11 shows the same as Figure 10 except that m=3 was used in Equation (6). The experimental points from CTOD are all above the NK DH36 line (conservative) except one point (-75°C) is just below this line. However, only two points are conservative against the NK EH36 line (0° and -40°C).

Even though it was mentioned previously that m is usually taken equal to 1 for plane-stress and 2 for plane-strain conditions, Malik (1990) found experimentally that for high yield stress

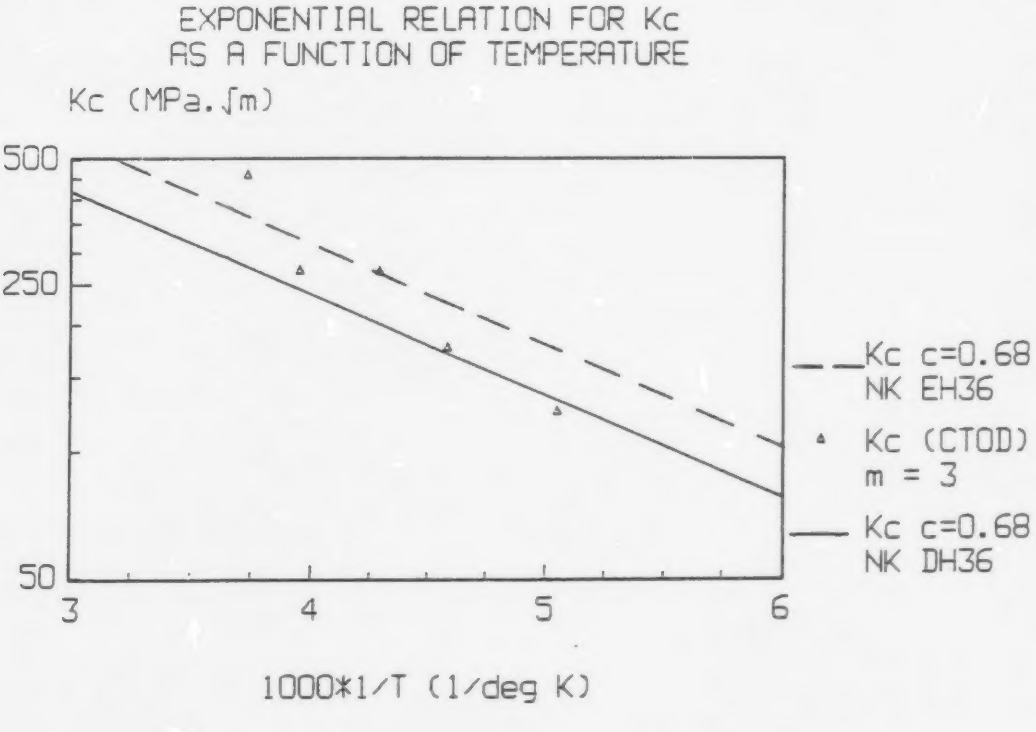

Figure 11: NK Line versus ln(Kc) Points from the CTODcf Data for m=3

material (320 MPa), factor m ranged from 2.5 to 5.2. This shows that using m=3 in Figure 11 provides adequate comparison. Figure 12 shows the NK lines for c=1 (mechanically notched plate) and c=0.68 (fatigue precracked plate) for both DH36 and EH36 grades. The points shown are those obtained from the actual fracture data: σ_{nom}, a_{actual} and δ_{wp}, linear fracture mechanics relationship, Equation (2) and the fracture criterion, Equation (3). The actual nominal fracture stress, σ_{nom}, see Table A7, was substituted for $(\alpha + \beta)\sigma_y$ in Equation (2).

The points Kc are located between the two NK DH36 lines (c=1 and c=0.68 respectively) showing that the empirical relationships given by Equations (4) and (5) hold well for this ship steel. The points lie, however, below the EH36 band which makes the results unconservative when assuming this grade in the NK approach.

The WPT data and Kc for DH36 are listed in Table 1 below.

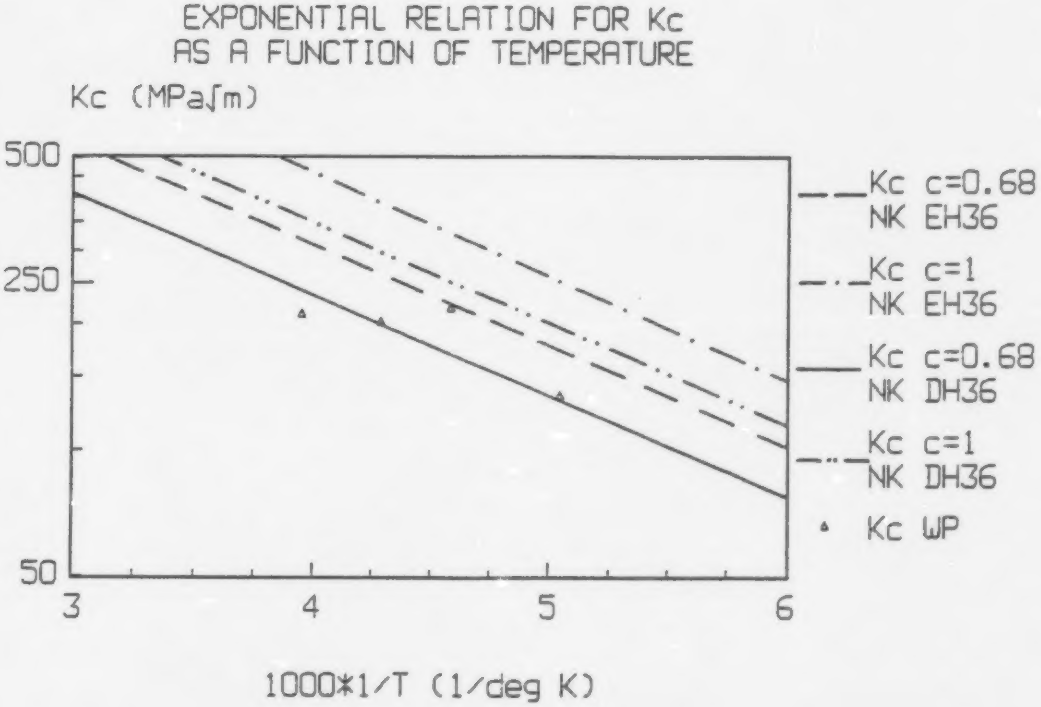

Figure 12: NK Lines for c=1 and c=0.68 together with Experimental Points

Since there were no means available at WIC to make fatigue pre-cracked plate specimens, it was not possible to establish the value c for this series of tests. However, as can be seen from Figure 12,this factor would be between 1 and 0.68. All fractures were brittle and there was no sign of noticeable plasticity in the vicinity of the notch.

TABLE 1

FRACTURE TOUGHNESS FROM WPT
USING EQUATIONS (2) AND (3)

Test #	Temp °C	σ_{nom} (MPa)	a_{wp} (mm)	Kc (MPa$\sqrt{m}$)
3	-20	335.5	251.2	210
2	-40	322.1	250.3	202
4	-55	347.6	250.1	217
1	-75	214.0	250.4	134

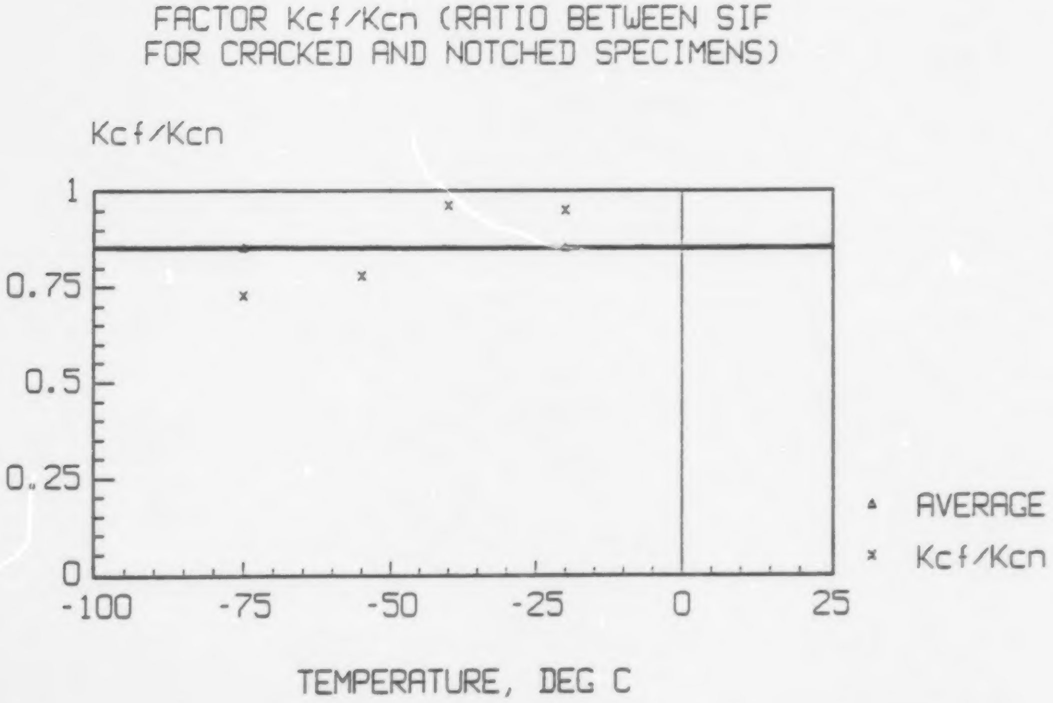

Figure 13: Kcf/Kcn Ratio Calculated from CTODcf and CTODcn

If Kcf and Kcn is calculated from CTODcf and CTODcn respectively using Equation (6), the ratio Kcf/Kcn is approximately 0.85, see Figure 13.

Also, the ratio between the allowable crack size from the CTOD criterion (using pre-cracked specimens) and the actual critical crack size is 2.6 for -20°, -55° and -55°C, see Table 2, which is in good agreement with the expected value between 2 and 3. This ratio is outside this range only for -75°C, the value 3.8 makes the allowable crack size more conservative.

6.2 Fracture Stress

The fracture stress for the wide plate tests is shown in Table A7. When divided by the yield stress, the factor ($\alpha + \beta$) is obtained. This combined factor is plotted in Figure 14 together with the value ($\alpha + \beta$)=0.6. This value corresponds to the stress for primary members (α=0.4) and the far-away residual stresses (β=0.2) assumed in the verification of the CASPPR requirements.

It can be seen that at -40°C (assumed MDT in CASPPR), the utilization of the material ($\alpha + \beta \approx 0.75$) in the wide plate tests provides a safety factor of 1.25 against the assumed factor for the primary members ($\alpha + \beta \approx 0.6$).

TABLE 2

RATIO BETWEEN THE ALLOWABLE AND CRITICAL CRACK SIZE

Test #	Temp. °C	σ_{nom} (MPa)	a_{wp} (mm)	CTODcf$_{av}$ (mm)	a_{al} (mm)	a_{al}/a_{wp}
3	-20	335.5	251.2	0.296	96.6	2.6
2	-40	322.1	250.3	0.263	94.8	2.6
4	-55	347.6	250.1	0.126	95.5	2.6
1	-75	214.0	250.4	0.063	65.9	3.8

6.3 Comparison with Sumpter 125 MPa√m Fracture Toughness Criterion

Sumpter et al (1988) studied fracture toughness of BS4360 Grade 43A, 43D and Admiralty B grade. The tests were conducted in both static and dynamic loading regimes. Based on the strain rates which occur in ship hulls due to various loading conditions, the authors concluded that steels which exhibit unacceptable CVN energies, may still provide acceptable resistance against brittle fracture initiation at low and intermediate strain rates.

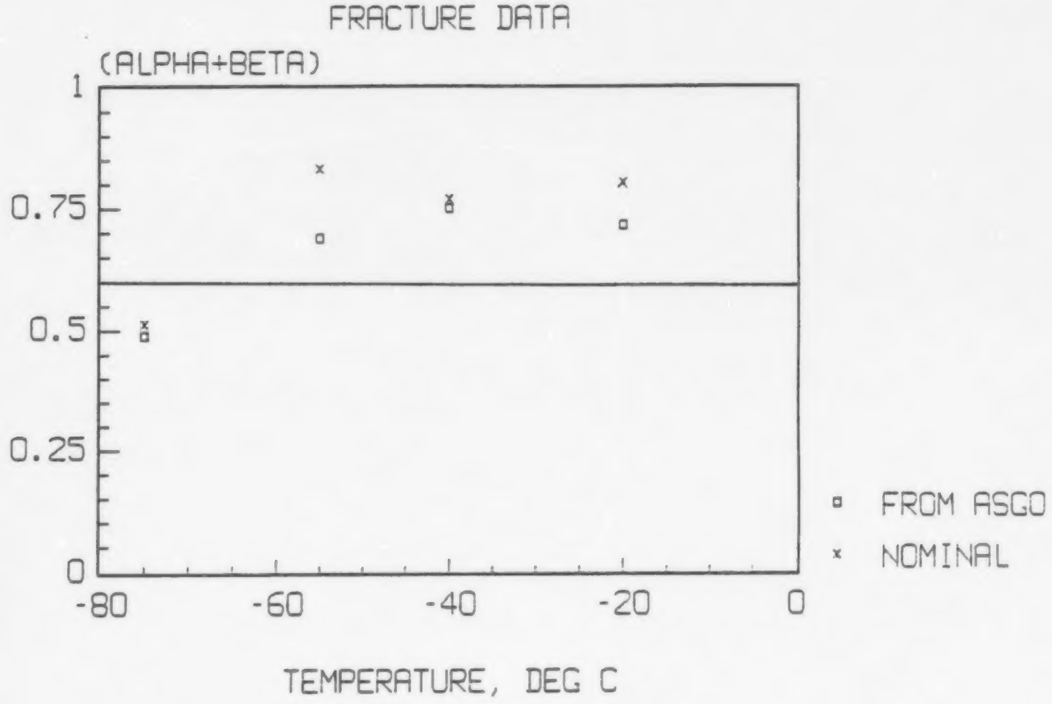

Figure 14: Utilization of the Material - Factor (α + ß)

Their fracture mechanics analysis, based on infinite plate with centre through thickness crack, showed that fracture toughness of 112 MPa√m would provide sufficient resistance against fracture initiation from short (50 mm) cracks, assuming full residual stresses (300 MPa) and applied stress of 100 MPa. Fracture toughness of 125 MPa√m should provide good resistance against unstable crack initiation from long cracks (1 m).

They concluded that "fracture toughness K_c = 125 MPa√m determined at appropriate minimum service temperature, material thickness and strain rate, would provide high assurance that brittle fracture initiation could be avoided during the course of a ship's life".

Kcf was calculated from CTODcf using Equation (6) with c=2. Figure 15 shows that this criterion is comfortably met for this steel at -40°C. The average Kcf at this temperature is close to 200 MPa.√m.

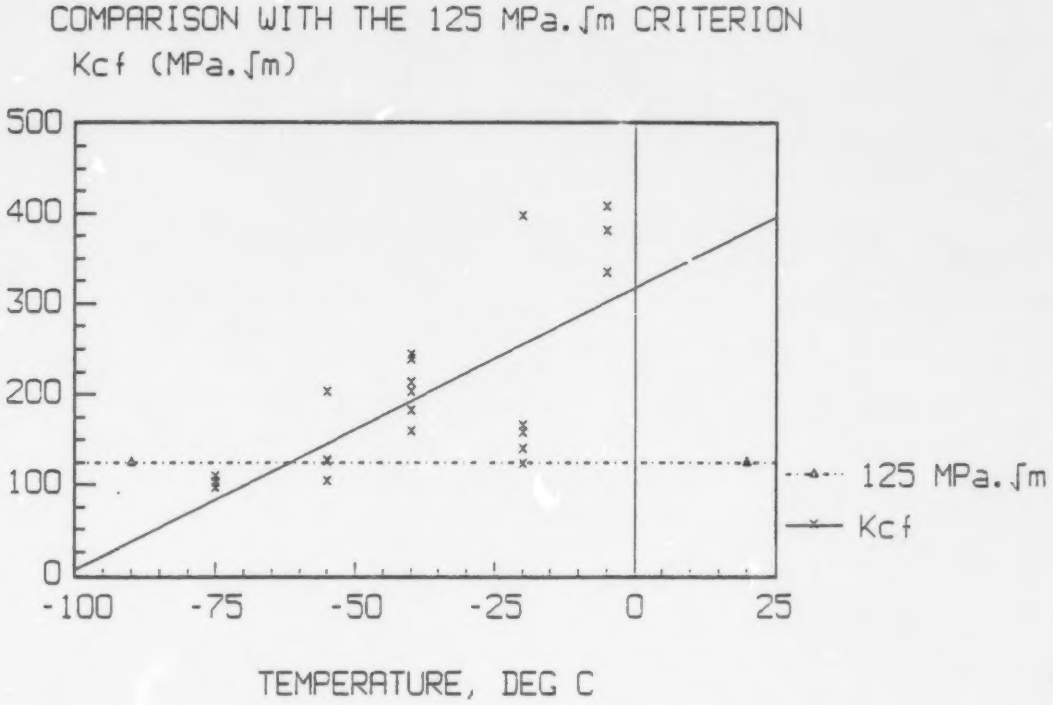

Figure 16: Comparison of Kcf for DH36 with the Sumpter Criterion

6.4 Other Fracture Criteria

Even though the fracture criteria below are not directly linked to the analysis of the wide plate tests performed in this project, they help to understand and interpret the CASPPR steel selection requirements vis-a-vis the fracture behaviour of the studied high strength steel DH36.

6.4.1 Fracture Appearance Criterion

Hodgson and Boyd (1958) investigated 180 ship fractures which occurred in ships built between 1945 and 1956.

Their criterion stated that brittle fractures in ships could be largely avoided if at critical locations, steels are used with a minimum Charpy V-Notch (CVN) energy of 47 J and maximum Charpy crystallinity (fracture appearance) of 70% at 0°C.

Application of this dual requirement (energy and appearance) would prevent, in general, the lower ship steel grades (A and B) from the use in ships for world-wide navigation. This criterion never found large application.

The investigated plate (DH36) meets this criterion consistently at -20°C in the longitudinal direction (Table A16) and at 0°C in the transverse direction (Table A17).

6.4.2 21 J Charpy Energy Criterion

A simple toughness criterion evolved from the fracture failures of all-welded Liberty ships and T-2 Tankers constructed during the Second World War. The plates of the fractured ships were tested for Charpy V-Notch impact toughness and grouped in three categories (e.g. Boyd, 1969):

a) plates in which unstable cracks initiated (source plates);
b) plates through which cracks propagated (through plates); and
c) plates in which cracks arrested (end plates).

The end plates showed the lowest average 21 J (15 ft-lb) transition temperature of about 10°C.

This grouping was done purely on the material (plate) basis without any weight being given to the stress state of the plates at the time of crack initiation or crack arrest.

This 21 J (15 ft-lb) toughness criterion was adopted for many other structures even though it was based on very specific data with respect to group of steels, fabrication quality, inspection and structural complexity. This criterion lost its significance with introduction of new families of ship steels and fabrication practices currently used in shipyards. Also, extrapolation of this criterion to low temperatures, prevailing in arctic shipping, is questionable.

The requirement of CVN_{21} transition temperature is met usually about 10° C above the minimum design temperature for world-wide shipping (0° C). For higher grade steels, the CVN energy curve drops faster in the transition range than is characteristic for those steels which were used for the development of this criterion. If this criterion is used, then it should be applied at the minimum design temperature.

The studied plate exceeds this criterion at -40°C in the longitudinal direction and at -20°C in the transverse direction (there is only one value measured at -30°C and even though it exceeds 21 J, it does not allow to make a conclusive statement).

6.4.3 Rolfe and Barsom NDTT Criterion

Rolfe and Barsom (1977) proposed a fracture control plan based on fully dynamic (impact) loading with strain rate approximately $10s^{-1}$. The resulting toughness requirement is no-break Drop Weight Nil Ductility Transition Temperature (NDTT) 18°C below the service temperature for critical areas midships. It seems that the assumption of fully dynamic strain rate is too conservative and it is not justified since the maximum strain rate measured during wave slamming or ice ramming is around $2x10^{-2}$ s^{-1}.

A detailed discussion of the effect of strain rate on this (WP) plate can be found in the report by Malik and Tomin (1991).

6.4.4 Approach Used by Classification Societies

The current approach taken by IACS is largely based on consensus between individual Classification Societies and was achieved through numerous discussions (such as the Meeting in Oslo in 1979). It reflects inevitably the conservatism reached by such consensus where each party promoted their experience and their own degree of conservatism. Table 3 (IACS, 1980) shows the limitation of application of ship steels as a function of joint category (special, primary and secondary), thickness and service temperature.

For example, using the above table, it can be seen that at -40 °C, Grade DH36 cannot be used in any primary areas in thickness over 10 mm. This would exclude this steel from practical usage for arctic shipping in midship area.

TABLE 3

IACS SELECTION OF SHIP STEEL GRADES

CATEGORY	GRADE	MINIMUM DESIGN TEMPERATURE 0	 -20	 -10	 -30	 -40	 -50
SECONDARY	A	30	20	10	X	X	X
	B	40	30	20	10	X	X
	D	50	40	30	20	10	X
	E	50	50	50	50	45	35
	AH	40	30	20	10	X	X
	DH	50	50	45	35	25	15
	EH	50	50	50	50	45	35
PRIMARY	A	20	10	X	X	X	X
	B	25	20	10	X	X	X
	D	35	25	20	10	X	X
	E	50	50	50	40	30	20
	AH	25	20	10	X	X	X
	DH	45	40	30	20	10	X
	EH	50	50	50	40	30	20
SPECIAL	A	X	X	X	X	X	X
	B	15	X	X	X	X	X
	D	20	10	X	X	X	X
	E	50	45	35	25	10	X
	AH	15	X	X	X	X	X
	DH	30	20	10	X	X	X
	EH	50	45	35	25	10	X

6.5 Probability of Fracture

Fracture initiation is a function of random variables such as stress, crack size and fracture toughness. Fracture toughness depends itself on other random quantities, for example, temperature, microstructure of the material and strain rate. Fracture is a random event which depends on simultaneous incidence of the presence of a crack, low toughness (low temperature, high loading rate) and sufficient stress to propagate the crack.

This stochastic phenomenon can be taken into account only in a full probabilistic fracture analysis. Canadian Coast Guard and CANMET sponsored several studies in this area (e.g. Tomin and Lantos, 1986; Tomin et al, 1988; or the current HAZ program by Fleet Technology Limited 1990).

Only through probabilistic analysis can the weight of individual variables be assessed in view of the contribution of other variables to fracture.

To show an example of such probabilistic analysis, some of the experimental data obtained for fracture toughness (CTOD) was used together with probability density functions (PDF) for crack size and assumed PDF for stress (applied, residual) in a simple crack initiation model. Monte Carlo simulation technique was used to obtain probability of failure.

In the following sections, the input data in the probabilistic model is briefly described.

6.5.1 Fracture Toughness

Fracture toughness is a random variable which exhibits a transition behaviour as a function of temperature. Bishop et al (1982) technique was used to obtain Weibull two-parametric distribution for CTOD, Figure 8, which was then used in the probabilistic model.

6.5.2 Crack Size

To assess the probability of brittle fracture from a large (250 mm) crack, a distribution for large cracks obtained by Antoniu (1977) was used. He collated data on 25,652 cracks detected over eight year period in 233 tankers. Lognormal distribution, Figure 17, fits well the data. Lognormal distribution is commonly used for crack size because it does not allow for negative values. The parameters for the three-parametric lognormal distribution were: $\varepsilon = 0.55$, $\alpha = 5.44$ and $\Theta = 40.5$ mm.

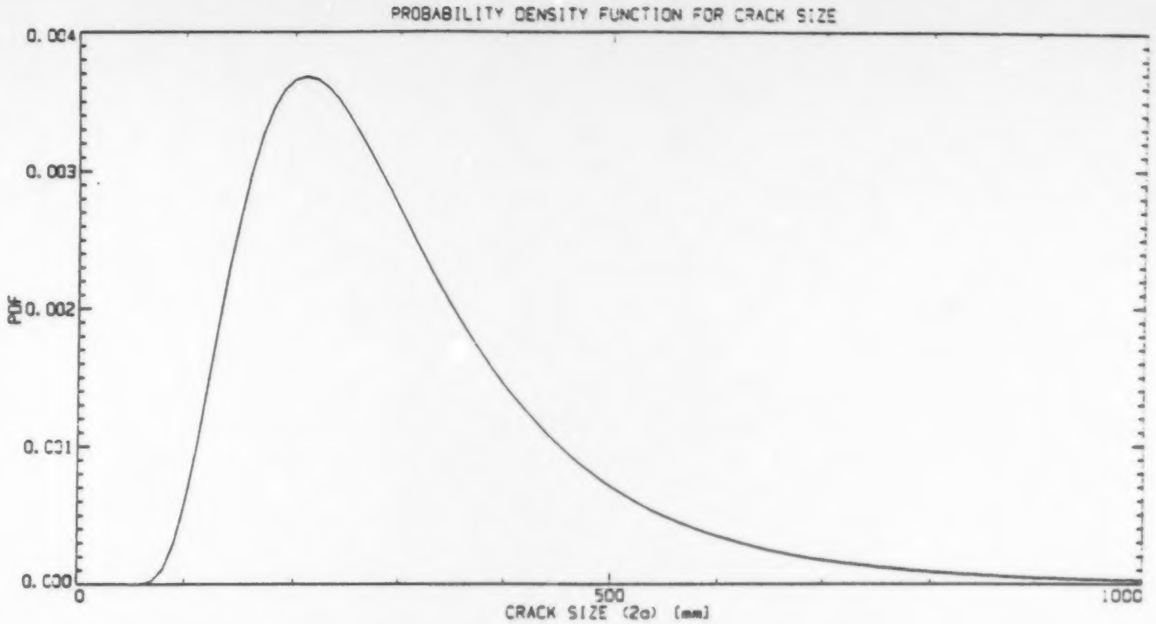

Figure 17: Lognormal Probability Distribution for Large Cracks

6.5.3 Applied and Residual Stress

Applied stress was assumed to follow normal distribution with $\sigma_{mean} = 0.4\sigma_y$ and coefficient of variation 20%. For large cracks, it was assumed that the residual stress is small, $\sigma_{res} = 0.2\sigma_y$, and constant.

6.5.4 Wide Plate Correlation (Safety) Factor

The correlation data between the crack size predicted from CTOD and the critical crack size obtained from Wide Plate Tests (Dawes and Kamath, 1977), Figure 1, was used in the analysis. The safety factor, s, between the critical crack size (from WPT) and predicted crack size (from CTOD) was obtained from the data shown in Figure 1 (s = 2.5 at 51.2%-tile and s = 1 at 95.4%-tile). Normal distribution was used to fit the data with $s_{mean} = 2.53$ and standard deviation std = 0.85.

6.5.5 Fracture Criterion

Crack initiation criterion (limit state function) based on CTOD/WPT correlation was used to calculate probabilities of failure. The probability of failure was defined as follows

$$P_f = Prob[a - sa_c > 0] \tag{10}$$

where 'a' is the crack depth for small cracks or half the through-thickness crack length for large cracks. a_c is the crack size obtained from the Burdekin and Dawes CTOD relationship, Equation (1).

Probability of failure was obtained from the Monte Carlo simulations for three temperatures: -5°, -20° and -40°C, see Figure 18. Semi-logarithmic plot (Log P_f vs. Temperature) was used.

Even though the probability of failure is relatively very high ($>10^{-1}$) due to the fact that we assumed the most unfavourable case (infinite plate with large crack subject to tensile stresses perpendicular to the crack and the crack distribution includes very large cracks, Figure 17), the relative magnitude of the probability of failure at each temperature is much more important. It can be seen from this figure that the difference between the probabilities is very small (less than one order of magnitude). This may be due to the fact that even though fracture toughness (CTOD) rises considerably with temperature in the upper bound (Figure 8), the increase in the lower bound of fracture toughness is negligible. The scatter in CTOD at -40°C is small compared with the scatter at -20° and -5°C.

This is an important conclusion which respects the variability of individual quantities which affect the propensity to fracture under the assumed configuration.

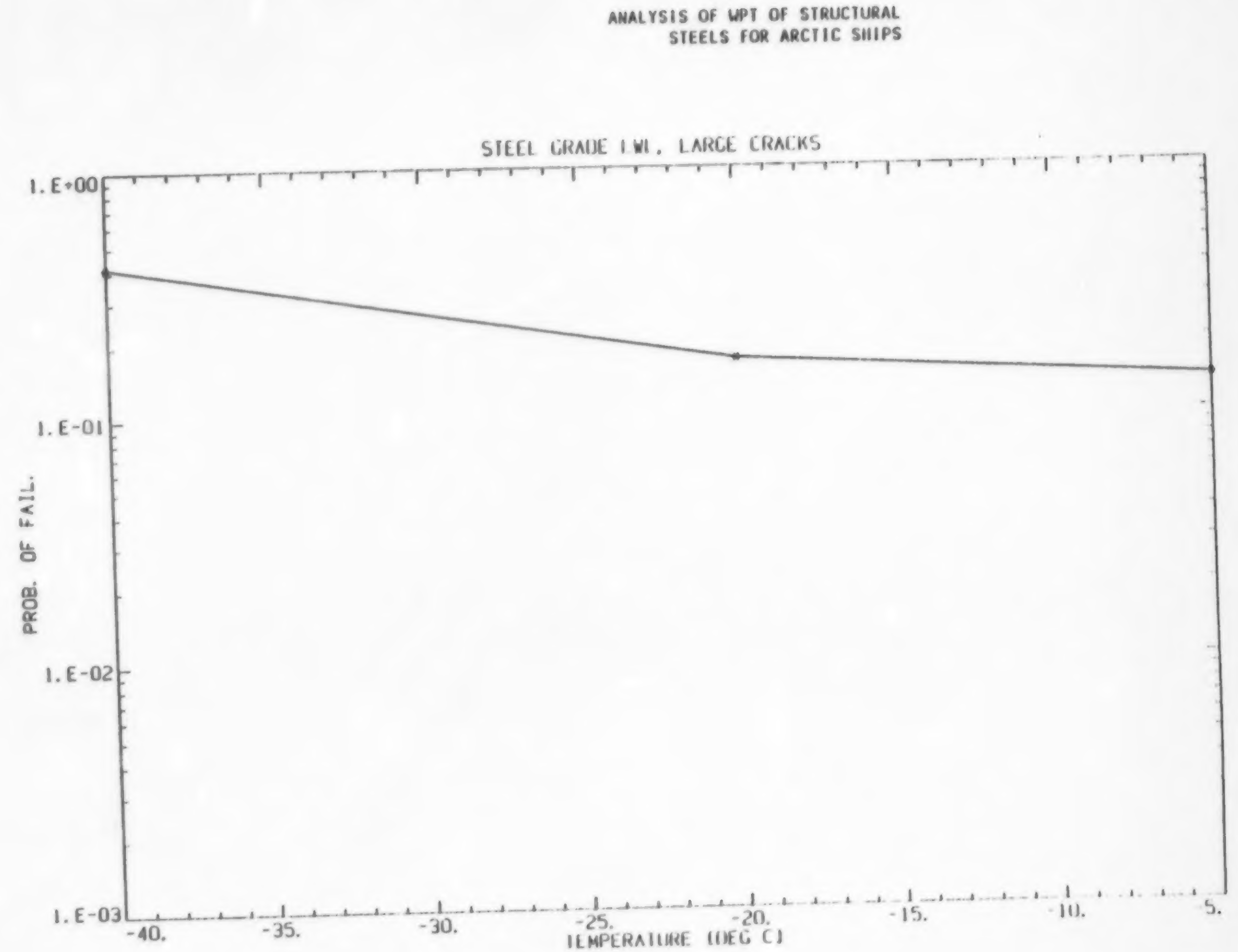

Figure 18: Probability of Failure as a Function of Temperature

7. SIGNIFICANCE OF THE RESULTS WITH RESPECT TO CASPPR

The CASPPR steel selection requirements are presented for reference in Appendix B. These requirements were previously assessed on the basis of the NK WPT approach (Tomin, 1989; and Tomin, 1990). The conclusions of this verification work are repeated in Appendix C. They show that, if the NK approach can be used with confidence for developing a fracture control plan for ships, the CASPPR requirements provide an acceptably low risk of brittle fracture.

An extensive discussion of the CASPPR requirements was presented in the report by Malik and Tomin (1991) in view of the experimental evidence on fracture toughness of the ship steels (Grades B, DH32, EH36, EH36 Mod and DH36 - the steel plate discussed in this report) studied in the project "Evaluation of Toughness of Conventional Ship Steels at Intermediate Loading Rate and its Implications". Without repeating this discussion here, it should be noted that this experimental evidence gives credence to the CASPPR steel selection requirements. However, it must be pointed out that this experimental evidence is limited in its extent and that its statistical significance does not allow to make all conclusive judgements.

The four wide plate tests, performed by WIC as a part of the current project, further corroborate the above conclusions. It was shown in Section 6 that the four WPT points, when plotted together with the NK DH36 line, support the NK approach postulated for verification of the CASPPR requirements.

The fact that the results appear unconservative against EH36 lines (Figure 12) should be noticed. If the steel was graded as EH36, the NK lines would not provide a safe lower bound. In this experimental program only one plate was tested, giving only a few experimental points. To be able to improve our judgement in this respect, more points would be needed.

The fracture stress at -40°C (and higher temperatures) shows that the combined utilization of the material $(\alpha+\beta)\sigma_y$ in the presence of large cracks exceeds that assumed for primary joints $(\alpha+\beta = 0.6)$. Caution is needed in concluding this, since the cracks were machine notched. Even though the results show that the plate would resist satisfactorily applied stresses assumed for primary joints $(\alpha = 0.4)$ without fracture initiation, the fact that all four plates broke in brittle manner suggest that the plate would not provide a notable resistance against dynamic crack propagation. Such fracture resistance, however, was neither assumed nor required.

Further, it was shown that the Sumpter et al criterion of 125 $\text{MPa}\sqrt{\text{m}}$ was exceeded for the studied plate DH36. All the other fracture criteria reviewed in Section 6.4 also show adequate fracture resistance except the Rolfe and Barsom NDTT criterion which was regarded as overconservative even before this experimental work started, due to the assumption of dynamic strain rates.

Even though the steel grades (B, DH32, EH36, EH36 Mod and DH36) in Malik and Tomin (1991) show that these steels may not have sufficient toughness at intermediate strain rates at -40°C, it was pointed out that the highest strain rate will be generated through impacts under the water (ice impacts or wave slamming) and the strain rates will decay rapidly with distance.

Furthermore, the conservatism inherent in both the NK and Sumpter approaches should be highlighted. It is evident from fracture mechanics analysis that the conditions conducive to brittle fracture require simultaneous occurrence of low fracture toughness, sufficient defect size as well as high stress. The WPT results are based on the assumption that the principal tensile stresses act normal to the crack plane. Also, wide plate tests use a uniform far-field fracture stress. Both these assumptions are very conservative when compared to real ship structural situations where cracks could be oriented at an angle to the principal stresses different from 90° and would often propagate in a stress field characterized by a decreasing gradient.

Also, the 'infinite' plate assumption is extremely conservative. In real, the plates are stiffened, thus reducing considerably the propensity of defects to fracture (crack initiation). It was shown (Tomin, Nessim and Cormeau, 1988) that the stiffening effect reduces the probability of fracture by one to two orders of magnitude and that ships can operate at probabilities of failure $\approx 10^{-1}$ due to their inherent structural redundancy.

It is obvious that probability of fracture will be highly dependent on the time of exposure to low temperatures (temperature distribution). A significant improvement of the probabilistic model would follow from inclusion of the temperature distribution of the operating temperatures. The probabilities of failure would be lowered if shown that the mean operating temperature is above those minimum design temperatures assumed by CASPPR (-5°C for submerged parts of the hull and -40°C for exposed areas). The recent projects, funded by the Coast Guard (Tomin and Edgecombe, 1989; Tomin, Edgecombe and Cormeau, 1990; and Tomin and Edgecombe ,1991), aim at obtaining more information on temperature distribution in the Canadian Arctic relevant to arctic shipping.

It must be noted that all this discussion applies to 25 mm (1") thick plates or less (conservatively). For the studied plate DH36, the CASPPR require its usage in this thickness at two locations (see Appendix B): a) 0.2L aft to 0.3L forward of midships, DH plate ≤ 25.5 mm is to be used for the shell side plating except the sheerstrake and stringer. Further, it may be used for the lower strake of longitudinal bulkhead at the bottom shell; b) outside this area, DH plate ≤ 25.5 mm may be used at any location.

The experimental results obtained from the WPT program and from the intermediate strain rate research improve our confidence in CASPPR steel selection requirements within the limitations of these results.

These positive conclusions should be seen in the light of statistical significance of the limited amount of experimental data and their thickness limitation (≤ 25.5 mm). It was shown, for example, that the fact that the CTOD values at -40°C show lower mean but small variability and the CTOD values at -20°C show higher average value but also much greater variability (see Figure 8) lead to probabilities of fracture which are very close. The same is true of the probability of fracture at -5°C which is largely affected by the CTOD variability.

It is felt that more data is needed to fill the gaps left after the current experimental programs are completed.

8. REFERENCES

Antoniu, A.C. (1977): "A Survey on Cracks in Tankers Under Repairs", PRADS - Int. Symp. on Practical Design in Shipbuilding, Tokyo, October.

Bala, S.R. (1990): see WIC (1990).

Barsom, J.M. (1976): In Proc. Int. Conf. on Dynamic Fracture Toughness, WI and ASM, London, July, pp. 281-302.

Bishop, T.A., Markworth, A.J., and Rosenfield, A.R. (1983): "Analyzing Statistical Variability of Fracture Properties", Metallurgical Transactions A, Volume 14A, April 1983, pp. 687-693.

Boyd, G.M. (1969): "Fracture Design Practices for Ship Structures", FRACTURE An Advanced Treatise, Vol. V, Fracture Design of Structures, Ch. 6, pp. 383-470.

Dawes, M.G., and Kamath, M.S. (1977): "The Crack Opening Displacement (COD) Design Curve Approach to Crack Tolerance", Institute of Mechanical Eng. Conference 1978, Paper C82/78, pp. 21-36.

Hodgson, J., and Boyd, G.M. (1958): "Brittle Fracture in Welded Ships: An Empirical Approach from Recent Experience", Institute of Naval Architects, Vol. 100, No. 3, p. 141, July.

IACS (1979): "Normal and High Strength Structural Steels", Requirements Concerning Materials and Welding, International Association of Classification Societies.

IACS (1990): "Guide for the Use of Hull Structural Steels for Prolonged Exposure to Low Service Temperatures", Recommendation No. 7, International Association of Classification Societies.

Malik, L. (1990): Experimental results submitted to RELTEC for analysis and interpretation.

Malik, L., and Tomin, M. (1991): "Evaluation of Conventional Ship Steels at Intermediate Loading Rate, and its Implications", Fleet Technology Report E73331C to DSS under Contract No. 23440-7-9227/01-SQ, January 1991.

NK (1979): "A Study Report on the Material Selection by Wide Plate Test Approach", Paper presented at the IACS Working Party on Materials and Welding, Oslo, 1979.

Rolf, S.T., and Barsom, J.M. (1977): Fracture and Fatigue Control in Structures, Prentice-Hall Inc.

Sumpter, J.D.G., Bird, J., Clarke, J.D., and Caudrey, A.J. (1988): "Fracture Toughness of Ship Steels", Paper No. 2, Spring Meeting, Royal Institute of Naval Architects, London.

Tomin, M., and Lantos, S.L. (1986): "Evaluation of Fracture Toughness Data with Respect to Reliability of Subarctic and Arctic Structures", VERITAS Report No. 86-CGY-042.

Tomin, M. (1988): "Development of Wide Plate Test Program", RELTEC Report to Det norske Veritas (Canada) Ltd., December 1988

Tomin, M., Nessim, M., and Cormeau, A. (1988): "Fracture Control for Arctic Structures: A Model for Analyzing Structural Details", Veritas Report to CANMET.

Tomin, M. (1989): "CASPPR Subcommittee Report Chapter 7: Steel Selection", RELTEC Report to Canadian Coast Guard, January 1989.

Tomin, M., and Edgecombe, M. (1989): "Experimental Design Temperature Database for Arctic Shipping", RELTEC Report REL-03-89 to Transport Canada.

Tomin, M. (1990): "Implementation of ASPPR Materials Requirements", RELTEC Report to Canadian Coast Guard Northern, Transport Canada Report No. TP 10434.

Tomin, M., Edgecombe, M., and Cormeau, A. (1990): "Analysis of a Design Temperature Database for Arctic Shipping", RELTEC Report to Canadian Coast Guard Northern, Transport Canada Report No. TP 10408E.

Tomin, M., and Edgecombe, M. (1991): "Hull Steel Temperature Measurement on an Operating Arctic Class Vessel", Draft Report to Canarctic Shipping Company Ltd., January.

WIC (1990): "Study of Wide Plate Testing of Structural Steels for Arctic Ships", Task 4, WIC Report No. RC 391/1/1990, prepared by S.R. Bala, June 1990.

APPENDIX A

APPENDIX A

TABLE A1

CHEMICAL COMPOSITION OF PLATE WP (WT %) AND COMPARISON WITH AIACS REQUIREMENT

	STEEL GRADE	C	Mn	Si	P	S	Cr	Ni	Mo	Cu	Al	V	Nb	N_2
Plate WP	DH36	0.17	1.07	0.23	0.018	0.012	0.13	0.10		0.20	0.043	0.055	<0.01	0.0066
AIACS Req.		<0.18	0.90-1.60	0.10-0.50	<0.040	<0.040	<0.20	<0.40	<0.08	<0.35	>0.015	0.05-0.10	0.02-0.05	

TABLE A2

TENSILE PROPERTIES OF STEEL WP
(AT ROOM TEMP., CROSS HEAD SPEED 0.125 IN/MIN)

PLATE NO.	ORIENTATION	σys upper N/mm2	σys lower N/mm2	σts N/mm2	ELONG. %
WP	Longitudinal	401	373	543	31.0
	Transverse	386	376	544	29.0

TABLE A3

PLATE WP LONGITUDINAL CVN

Test Temp. C	Absorbed Energy, J	Lat. Expan. (mm)	% Shear
20	136	2.00	80
20	129	2.20	NB
0	122	1.68	60
0	123	1.78	60
0	129	1.70	70
0	126	1.68	60
-20	85	1.50	30
-20	58	1.00	20
-20	84	1.33	40
-20	56	0.88	30
-20	73	1.25	30
-40	70	1.25	30
-40	66	1.15	30
-40	78	1.38	20
-40	68	1.08	20
-50	14	0.33	0
-50	35	0.30	10
-50	16	0.30	0
-60	30	0.63	10
-60	14	0.30	0
-60	18	0.40	0
-60	24	0.53	0
-60	19	0.33	0
-60	9	0.25	0
-70	9	0.28	0
-70	11	0.23	0
-70	9	0.25	0
-70	14	0.40	0
-80	8	0.23	0
-80	9	0.25	0

TABLE A4

PLATE WP TRANSVERSE CVN

Test Temp. °C	Absorbed Energy, J	Lat. Expan. (mm)	% Shear
20	65	1.20	60
20	80	1.50	80
10	60	1.18	40
10	61	1.25	50
0	49	1.05	40
0	57	1.25	50
-10	41	0.93	30
-20	38	0.80	30
-20	34	0.75	30
-20	23	0.58	20
-30	34	0.65	20
-40	9	0.20	10
-40	26	0.53	20
-40	20	0.55	10
-40	26	0.55	10
-50	22	0.43	10
-50	8	0.20	10
-60	18	0.38	10
-60	14	0.33	5
-70	12	0.30	0
-80	3	0.18	0
-80	7	0.23	0

TABLE A5

RESULTS OF NDT DROP WEIGHT TEST

	PLATE WP1		PLATE WP2	
	Test Temp. °C	B/NB	Test Temp. °C	B/NB
	-20	B	-10	B
	-15	B	- 5	NB
	-10	NB	- 5	NB
	-10	NB		
NDTT	-15°C		-10°C	

TABLE A6

CTOD OBTAINED FROM FATIGUE CRACKED SPECIMENS (CTODcf), SAW NOTCHED SPECIMENS (CTODcn) AND WIDE PLATE SPECIMENS (CTODwp)

Temperature (°C)	CTODcf (mm)	CTODcn (mm)	CTODwp (mm)
0		1.231	
10		1.200	
10		1.062	
- 5	0.878		
- 5	1.009		
- 5	0.678		
-15		0.722	
-15		0.924	
-20	0.091	0.396	1.232
-20	0.151	0.295	
-20	0.165	0.295	
-20	0.956	0.129	
-20	0.117	0.542	
-25		0.439	
-25		0.492	
-25		0.459	
-25		0.383	
-35		0.271	
-35		0.501	
-35		0.449	
-40	0.357	0.205	0.945
-40	0.247	0.125	
-40	0.199	0.393	
-40	0.275	0.427	
-40	0.153	0.459	
-40	0.344		
-45		0.206	
-55	0.095	0.432	1.040
-55	0.064	0.095	
-55	0.247	0.170	
-55	0.096	0.161	
-75	0.071	0.055	0.827
-75	0.056	0.099	
-75	0.063	0.212	
-75	0.131		
-75	0.091		
-90	0.083		

APPENDIX B

STEEL SELECTION REQUIREMENTS SPECIFIED IN CASPPR

The proposed CASPPR steel selection requirements within the hull for ships navigating in the Arctic are schematically shown in Figure B1 and also in Table B1 (Proposed Revision to CASPPR, Schedule 3, 9/8/89).

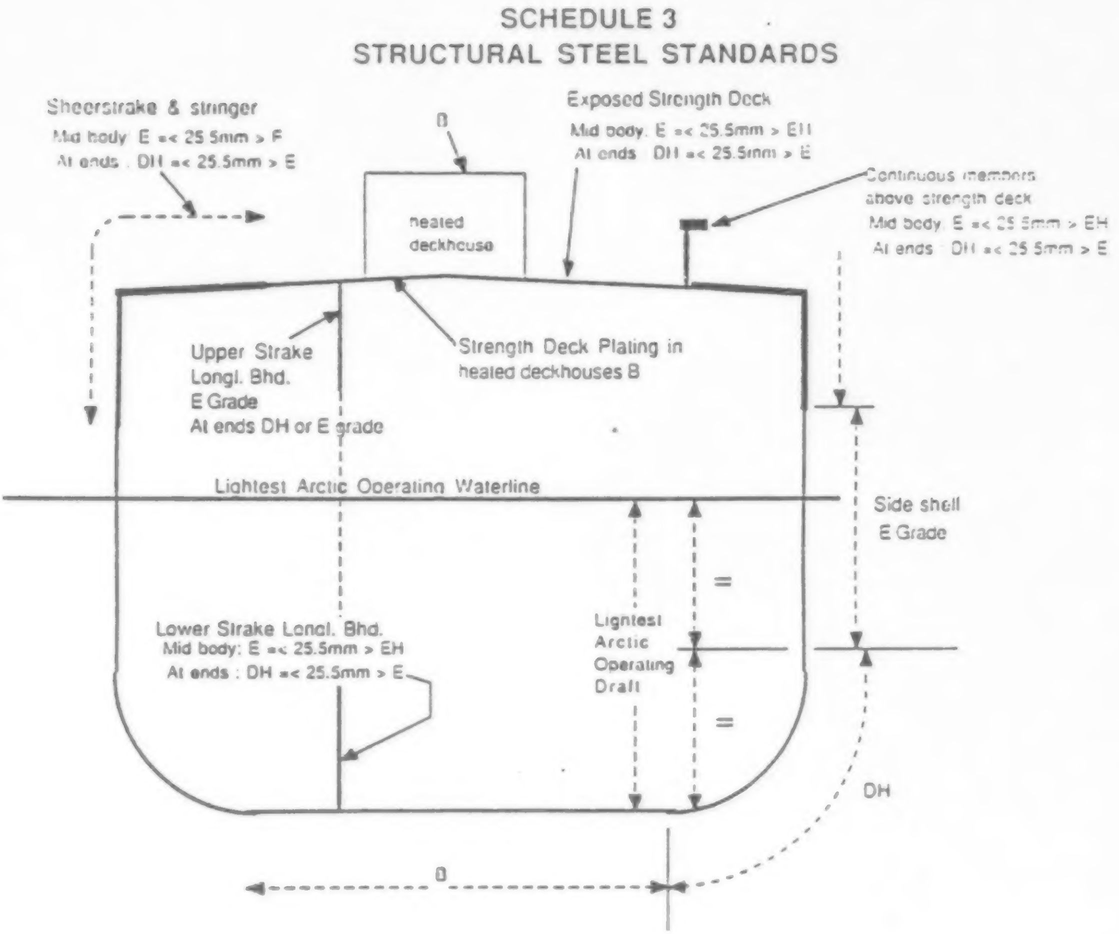
SCHEDULE 3
STRUCTURAL STEEL STANDARDS
Sheerstrake & stringer
Mid body: E =< 25.5mm > F
At ends : DH =< 25.5mm > E
B
heated deckhouse
Exposed Strength Deck
Mid body. E =< 25.5mm > EH
At ends : DH =< 25.5mm > E
Continuous members above strength deck
Mid body. E =< 25.5mm > EH
At ends : DH =< 25.5mm > E
Upper Strake Longl. Bhd.
E Grade
At ends DH or E grade
Strength Deck Plating in heated deckhouses B
Lightest Arctic Operating Waterline
Side shell
E Grade
=
Lightest Arctic Operating Draft
=
Lower Strake Longl. Bhd.
Mid body: E =< 25.5mm > EH
At ends : DH =< 25.5mm > E
DH
B

Figure B1: Distribution of Steels in Ship Hulls (after the Proposed Rev. CASPPR, Schedule 3)

TABLE B1

MINIMUM STEEL GRADES FOR STRUCTURAL MEMBERS OF ARCTIC CLASS SHIPS

ITEM	STRUCTURAL MEMBER INCLUDING ANY ATTACHED STRUCTURE FOR A DEPTH OF 740 mm	STEEL GRADES			
		FROM 0.2L AFT TO 0.3L FORWARD OF MIDSHIPS	FROM 0.2L AFT TO 0.3L FORWARD OF MIDSHIPS	OUTSIDE 0.2L AFT TO 0.3L FORWARD OF MIDSHIPS	OUTSIDE 0.2L AFT TO 0.3L FORWARD OF MIDSHIPS
	THICKNESS--------->	<=25.5 mm	>25.5 mm	<=25.5 mm	>25.5 mm
1	Sheerstrake at strength deck	E	F	D H	E
2	Strength deck plating exposed or in unheated deckhouses	E	E H	D H	E
3	Strength deck plating in heated deckhouses	B	B	B	B
4	Side shell plating from lower edge sheerstrake to waterline at half the lightest operating draft.	E	E	E	E
5	Remainder of side shell to flat of bottom.	D H	D H	D H	D H
6	Flat of bottom and keel	B	B	B	B
7	Exposed non-strength deck plating	B	B	B	B
8	Continuous longitudinal members above strength deck	E	E H	D H	E
9	Upper strake of longitudinal bulkhead at strength deck	E	E	D H	E
10	Upper strake of top wing tank longitudinal bulkhead	E	E	D H	E
11	Lower strake of longitudinal bulkhead at bottom shell	D H	D H	D H	D H
12	Sternframes, rudder horns, rudders, ice horns, shaft brackets,bossings			D H	D H

APPENDIX C

VERIFICATION OF CASPPR REQUIREMENTS USING NK WPT APPROACH

The NK WPT approach to defining fracture plan for ships was described in Section 4. It was used for preliminary verification of CASPPR steel selection requirements with respect to prevention of unstable fracture from long (fatigue) cracks in the field of low residual (reaction) stresses and from short cracks in the field of high residual stresses.

In the approach taken to verify CASPPR requirements, it was assumed that residual stresses for long cracks (far-field residual and reaction stresses) are equal to 20% of the yield strength ($\beta=0.2$) and the residual stresses for short cracks in the weld or HAZ are equal to the yield strength ($\beta=1.0$).

To assess the CASPPR requirements, the maximum allowable defect size was calculated for two design temperatures: -5°C for submerged parts of the hull and -40°C for the exposed areas. It was further assumed that the allowable defect length is 250 mm in the parent plate (long cracks) and 15% of the plate thickness for short cracks for $t \leq 50$mm and 7.5 mm for $t > 50$mm (see e.g. Tomin and Rengaard, 1984).

Using the NK WPT approach, the following was concluded:

Bottom Plating and Side Shell below LAOD

The proposed CASPPR steel selection requirements are satisfied for both thickness ranges $t \leq 25$ mm and $t > 25$ mm ($t < 70$ mm) for long cracks and applied stresses exceeding 90% of yield strength ($\alpha=0.9$).

Similarly, it was shown be shown that the CASPPR requirements are satisfied for short cracks in the weld metal or HAZ.

Strength Deck

The CASPPR steel selection requirements are satisfied for Grade E and applied stresses up to 90% of the yield strength for $t \leq 25$ mm from 0.2L aft to 0.3L forward of midships and outside 0.2L aft to 0.3L forward of midships for both $t \leq 25$ mm as well as for $t > 25$ mm (long and short cracks).

The requirement for $t > 25$ mm ($t \leq 50$ mm)is satisfied for long cracks up to 70% of the yield strength for both EH32 and EH36.

Reference:

Tomin, M., and Rengaard, O. (1984): "Development of Steel Plate Requirements for Fixed Offshore Structures", Veritas Rep. No. 84-CGY-023.